

UNIVERSITÀ DELLA CALABRIA



UNIVERSITA' DELLA CALABRIA

Dipartimento di CHIMICA e TECNOLOGIE CHIMICHE

Dottorato di Ricerca in
MEDICINA TRASLAZIONALE

CICLO
XXXI

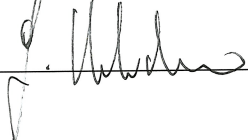
**REMEDICATION OF POLLUTED WATERS BY MEANS OF SURFACE MODIFIED
NATURAL CELLULOSE FIBERS**

Settore Scientifico Disciplinare CHIM/02

Coordinatore: Ch.mo Prof. Sebastiano Andò

Firma 

Supervisore/Tutor: Ch.mo Prof. Giuseppe Chidichimo

Firma 

Dottorando: Dott. Antonio Tursi

Firma 

TABLE OF CONTENTS

Table of contents	I
List of figures	IV
List of tables	VI
Acknowledgements	VIII
Abstract	IX
CHAPTER 1	1
INTRODUCTION	2
1.1 Water pollution	2
1.1 Types of water	3
1.2 Sources of water pollution	4
1.3 Effect of water pollution on the environment and human health	5
1.4 Types of contaminants	6
1.4.1 Organic Compounds and HOCs	7
1.4.2 Marine debris and plastic in the environment	8
1.4.3 Metals and Metalloids	10
1.4.4 Bacterial contamination and other water pathogens	12
1.4.5 Other pollutants	13
CHAPTER 2	14
2 Pollutants of interest and remediation treatments	15
2.1 HOCs and TPHs pollution	15
2.1.1 Effects of petroleum hydrocarbons on living matter	18
2.1.2 Remediation technologies for TPHs contamination	20
2.1.2.1 Physical methods	21
2.1.2.1.1 Booming	21
2.1.2.1.2 Skimmers	23
2.1.2.2 Chemical methods	24
2.1.2.2.1 Dispersants	25
2.1.2.2.2 Solidifiers	26
2.1.2.2.3 Sorbents	26
2.1.2.2.4 Thermal remediation	27
2.1.2.3 Biological methods	28
2.1.2.3.1 Bioremediation	28
2.1.2.3.2 Phytoremediation	30
2.1.2.5. Groundwater remediation	31
2.2 Endocrine Disrupting Chemicals and Bisphenol-A in water	33

2.3 Bisphenol A	34
2.3.1 BPA exposure and human health	35
2.3.2 BPA contamination	37
2.3.3 Remediation technologies for BPA pollution	39
2.3.3.1 Physical and chemical treatment	39
2.3.3.2 Biodegradation of BPA	39
2.3.3.3 Integrated systems for the removal of BPA from water	39
2.3 Mercury pollution	40
2.3.1 Mercury toxicity and carcinogenicity	40
2.3.2 Mercury in the environment	41
2.3.3 Remediation technologies for Mercury polluted water	42
2.3.3.1 Precipitation treatment processes	43
2.3.3.1.1 Coagulation/co-precipitation	43
2.3.3.1.2 Sulfide precipitation	43
2.3.3.2 Adsorption processes	44
2.3.3.2.1 Activated Carbon adsorption	44
2.3.3.3 Ion exchange processes	45
2.3.3.3.1 Ion exchange resin	45
2.3.3.4 Other adsorption processes	45
2.3.3.4.1 Chemical reduction	46
2.3.3.4.2 Membrane separation	46
2.3.3.4.3. Bioremediation	46
2.3.3.5 Other remediation technologies	47
2.4 Escherichia coli contamination	47
2.4.1 Effects of Escherichia coli on human health	48
2.4.2 Escherichia coli in the environment	50
2.4.3 Water pathogens decontamination methods	51
2.4.2.1 Disinfection treatments	52
2.4.2.1.1 Chlorination	53
2.4.2.1.2 Ozonation	53
2.4.2.1.3 Ultraviolet applications	54
2.4.2.2 Physical and chemical treatments	55
2.4.2.2.1 Coagulation and flocculation	55
2.4.2.2.2 Sedimentation or flotation	55
2.4.2.2.3 Filtration	56
CHAPTER 3	57
3 Pollutants and environment	58
3.1 Interactions between contaminants and environment	58

3.1.1 Adsorption mechanism	58
3.1.2 Absorption	60
3.1.3 Biodegradation	61
3.2 Kinetic and Equilibrium models of adsorption	63
3.2.1 Langmuir Isotherm Model	63
3.2.2 Freundlich Isotherm Model	64
3.2.3 Sips Isotherm Model	65
3.2.4 Liu Isotherm Model	65
3.2.5 Redlich–Peterson Isotherm Model	66
3.2.6 Other Unusual Isotherm Models	67
3.3 Natural materials as potential adsorbents for polluted water remediation	67
3.3.1 Typical natural biosorbents for TPHs and HOCs remediation processes	69
3.3.2 BPA remediation by means of natural adsorbent materials	73
3.3.3 Remediation of mercury polluted water using natural adsorbents	75
CHAPTER 4	90
4 INTRODUCTION TO THE EXPERIMENTAL STUDIES PERFORMED DURING THIS Ph.D. THESIS	91
CHAPTER 5. Remediation of hydrocarbons polluted water by hydrophobic functionalized cellulose	94
CHAPTER 6. Removal of endocrine disrupting chemicals from water: adsorption of bisphenol-A by biobased hydrophobic functionalized cellulose	105
CHAPTER 7. Low pressure plasma functionalized cellulose fiber for the remediation of petroleum hydrocarbons polluted water	119
CHAPTER 8. Preliminary studies of the adsorption of mercury (II) in water by means of cellulosic fibers	148
CHAPTER 9. Photocatalytic inactivation of Escherichia coli bacteria in water using low pressure plasma deposited TiO₂ cellulose fabric	155
CONCLUSION	177

List of figures

CHAPTER 1

Figure 1. Percentage of population using unimproved drinking water source.....	2
Figure 2. The great Pacific garbage patch.....	10

CHAPTER 2

Figure 3. Common hydrocarbons.....	16
Figure 4. Mechanical booms	22
Figure 5. Containment Booms for oil spills.....	23
Figure 6. Oleophilic skimmers.....	24
Figure 7. In situ burning.....	27
Figure 8. In situ bioremediation.....	28
Figure 9. Ex situ bioremediation.....	29
Figure 10. Phytoremediation	30
Figure 11. Pump and Treat method.....	32
Figure 12. PRB barriers.....	33
Figure 13. Scheme reaction for BPA production.....	35
Figure 14. Endocrine perturbation.....	36
Figure 15. BPA sources and consequences.....	37
Figure 16. Mercury cycling in the environment.....	42
Figure 17. Escherichia coli bacteria.....	49
Figure 18. Sources of E. coli contamination.....	50
Figure 19. UV apparatus.....	55
Figure 20. Physical and chemical treatments.....	56
Figure 21. Ultrafiltration system.....	56

CHAPTER 3

Figure 22. Adsorption mechanism.....	59
Figure 23. Absorption phenomena.....	61
Figure 24. Biodegradation mechanism.....	62

CHAPTER 5

Figure 1. Chemical structure of MDI, cellulose and the possible structure [...]	97
Figure 2. XPS survey spectra of the raw a) and functionalized fiber [...]	100
Figure 3. FTIR spectra of the raw fiber (RF) and of the MDI-functionalized fiber (FF)	100
Figure 4. a) Total petroleum hydrocarbons content and b) removal efficiency [...]	101
Figure 5. a) First order kinetic plots for the raw fiber and (b) for the functionalized fiber	102

CHAPTER 6

Figure 1. Effect of pH on the removal of Bisphenol A (BPA) by raw (RF)	110
Figure 2. BPA equilibrium adsorption capacity q_e as a function of pH	111
Figure 3. Bisphenol A removal efficiency, RE%, during regeneration and reuse of FF	112
Figure 4. Removal efficiency, RE%, in various water matrices	112
Figure 5. Process efficiency (%) in terms of BPA removal at various C_0/W ratios	113
Figure 6. (a) Fitting of the experimental data by the pseudo-second order kinetics model	113
Figure 7. Bisphenol A adsorption isotherm at 20 °C onto biobased FF [...]	114

CHAPTER 7

Figure 1. Scheme of the low pressure plasma apparatus	125
Figure 2. High resolution C1s spectra of pristine (a) and plasma treated at 10 W SB fibers (b)	130
Figure 3. (a) High resolution C1s spectra of SB fibers treated at different RF powers	131
Figure 4. High resolution F1s spectra of fibers treated at 10 W and 70 W	132
Figure 5. FTIR spectrum of the raw SB fiber and functionalized SB fiber	133
Figure 6. SEM pictures of pristine (a) and plasma treated fibers at 10 W (b) and 70 W (c)	134
Figure 7. Surface fibers chemical elemental spatial distribution	135
Figure 8. Time variation of the TPHs content in polluted water	136
Figure 9. Equilibrium adsorption capacity, as a function of the water contact angle	137
Figure 10. Raw and Functionalized SB fiber batch experiments	138
Figure 11. Adsorption kinetic data fitted by the pseudo second order model	139
Figure 12. Experimental adsorption isotherm and nonlinear curve fitting [...]	140
Figure 13. Removal Efficiency as a function of the adsorption/regeneration cycles	141

CHAPTER 8

- Figure 1.** Hg (II) concentration (a) and removal efficiency (b) as a function of time.....151
Figure 2. Hg (II) adsorption isotherm at 20 °C for the cellulose fiber [...].....152

CHAPTER 9

- Figure 1.** Scheme of the low pressure plasma reactor employed for the sputtering processes.....160
Figure 2. (a) XPS survey spectra of pristine SB fabric and (b) plasma-treated SB fabric.....161
Figure 3. (a) XPS high resolution O1s spectrum for sample A and (b) Ti2p spectra.....164
Figure 4. Kinetics of photocatalytic inactivation by different TiO₂-cellulose fabrics.....165
Figure 5. Effect of initial bacterial concentration.....167
Figure 6. Kinetics of photocatalytic bacterial degradation in different water matrices.....168
Figure 7. Bacterial degradation experiments for reuse purposes.....170
Figure 8: Ti2p XPS high resolution spectra acquired after SB plasma modified fiber use.....171
Figure 9. C1s spectra of as deposited and after recycle sample A.....172

List of tables

CHAPTER 1

- Table 1.** The main catastrophic events of recent times.....17
Table 2. The most common remediation techniques for oil spill.....21

CHAPTER 2

- Table 3.** The main conventional treatment techniques for mercury removal.....42
Table 4. The most common techniques for the decontamination of water from pathogens.....52

CHAPTER 3

- Table 5.** Other Isotherm Models.....67
Table 6. Lignocellulosic-based sorbent and ACs, used for the removal [...].....69
Table 7. Modified lignocellulosic sorbent, used for the removal of hydrophobic [...].....72
Table 8. ACs and biobased materials, used for BPA removal in water.....74
Table 9. ACs and biobased materials, used for Hg(II) removal in water.....76

CHAPTER 5

Table 1. First order kinetic parameters.....102

Table 2. Pseudo-second order kinetic data.....102

CHAPTER 6

Table 1. Pseudo-second order kinetic data for experimental runs shown in Figures 5 and 6.....114

Table 2. Comparison of FF adsorption performances with other adsorbents.....115

CHAPTER 7

Table 1. Curve-fit data for C1s spectra of raw and plasma treated SB fibers.....127

Table 2. WCA values measured on plasma treated SB fibers at different input power.....134

Table 3. B.E.T. surface area for pristine and plasma functionalized SB fibers.....136

Table 4. Kinetic values of plasma functionalized SB fibers at different C_0/w ratio.....139

CHAPTER 9

Table 1. Low pressure plasma sputtering processes experimental conditions.....161

Table 2. WCA values measured on untreated and plasma treated SB fabric.....165

Table 3. First order kinetic rate constant of the photocatalytic bactericidal activity.....166

Table 4. E. coli photoreactivation experiments, under natural light and dark.....169

Table 5. First order kinetic rate constant of the photocatalytic bactericidal activity.....170

Table 6. XPS atomic percent of plasma coated SB fiber.....171

ACKNOWLEDGMENTS

I would like to express my deep appreciation and gratitude to Prof. Giuseppe Chidichimo, who gave me the unique opportunity to participate in this PhD programme. He followed me step by step and always suggested me the best way to improve my work. Their constant presence in these years was fundamental to turn a “raw” PhD student into a more aware researcher.

In addition, I am very thankful to Dr. Amerigo Beneduci for their academic support, useful advice and organizational aid. This thesis would not have been possible without his scientific advice, patience and unconditional support. I am truly fortunate to have had the opportunity to work with him.

I also would like to thank Dr. Thalia Chatzisyneon (University of Edinburgh) that supervised me during my period in Scotland. Her willingness and suggestions were very important for my work improvement.

Last, but by no means least, thanks to my parents Salvatore and Caterina, my brother Davide, and my uncle Rosa, who have given me their unequivocal support and encouragement throughout and made me feel emotionally close when we were physically apart.

As individual work, pursuing a PhD can be a solitary road. Therefore, many special thanks go to all the kind people around me that made me feel accompanied all the way through.

ABSTRACT

The thesis concerns the development of natural materials for the remediation of water bodies from several types of pollutants, such as Hydrophobic Organic Compounds, Endocrine Disrupting Chemicals, Heavy metals and Bacteria, which can enter into the food chain and cause health risks, related to high toxicity, mutagenicity and carcinogenicity.

In this work a new approach to water remediation was introduced, which uses modified cellulose fibers to adsorb or degrade pollutants with high efficiency. The cellulose fiber used in this thesis was extracted from Spanish Broom: a spontaneously growing vegetable species in the Mediterranean area. The surface modification of the fibers has been projected for case to case, in order to create a good affinity between the fiber surface and the pollutants taking into consideration.

The pollutants chosen to evaluate the remediation capacities of the synthesized cellulosic fibers, has been:

- 1) Total Petroleum Hydrocarbons (for the class of Hydrophobic Organic Compounds), because include a large family of hundreds of hydrocarbon compounds, which are highly contaminating, persistent and carcinogenic;
- 2) Bisphenol-A (for the class of Endocrine Disrupting Chemicals), for its enormous diffusion, due to its use in the production of products for daily use;
- 3) Escherichia coli (for the class of bacteria), because it represents the most widespread fecal coliform bacteria.
- 4) Mercury (for the class of Heavy Metals), for its high diffusion, the strong bioaccumulative persistence and the high toxicity;

In the case of Total Petroleum Hydrocarbons, the leading parameter taking into account was the surface hydrophobicity, while in the case of Bisphenol-A, the functionalization processes consider the similarity of the molecular structure of the pollutant, with respect to that of the molecule used to grafted the fiber surface.

In the case of Escherichia coli, a TiO₂ deposition was considered appropriate for the photochemical activation of the fiber surface.

Finally, for mercury water purification, the chelating properties of the cellulose himself has been taken in consideration.

The approach presented in this thesis has proved to be very effective in water reclamation, since the functionalized fibers collect many important properties, which make it an ideal system for water remediation. In fact, the purification systems present:

- a) high chemical and mechanical stability;
- b) high specific surface area;
- c) low cost preparation methods.

The experiments demonstrated that the fibers, modified as above mentioned, have an excellent absorption capacity with respect to the pollutants and the kinetics of absorption are very fast. Furthermore, the photocatalytic approach, making use of TiO₂ layer on the fiber surface, are very promising feature for bacteria degradation in water.

For this reason, the results open the field to novel technologies for water remediation.

ABSTRACT

Il presente lavoro di tesi riguarda lo sviluppo di materiali naturali per la bonifica di corpi idrici contaminati da diverse classi di inquinanti, come composti organici idrofobici, endocrine disrupting chemicals, metalli pesanti e batteri, che possono entrare nella catena alimentare e causare rischi per la salute, correlati ad alta tossicità, mutagenicità e cancerogenicità.

In questo lavoro è stato introdotto un nuovo approccio per la bonifica delle acque, che vede l'impiego fibre di cellulosa modificate per adsorbire o degradare con alta efficienza gli inquinanti. La fibra di cellulosa utilizzata in questo lavoro è stata estratta dalla Spanish Broom, specie vegetale spontanea che cresce nell'area mediterranea.

La modifica superficiale delle fibre è stata progettata caso per caso, al fine di creare una buona affinità tra la superficie della fibra e gli inquinanti presi in considerazione.

Gli inquinanti scelti per valutare le capacità di bonifica delle fibre cellulosiche sintetizzate, sono stati:

- 1) Idrocarburi totali di petrolio (per la classe di composti organici idrofobici) in quanto comprendono una grande famiglia di centinaia di composti idrocarburici, altamente inquinanti, persistenti e cancerogeni;
- 2) Bisfenolo-A (per la classe degli endocrine disrupting chemicals), per la sua enorme diffusione, a causa del suo utilizzo nella produzione di oggetti di uso quotidiano;
- 3) Escherichia coli (per la classe di batteri), poiché rappresenta il più diffuso batterio fecale coliforme.
- 4) Mercurio (per la classe dei metalli pesanti) per la sua alta diffusione, la forte persistenza bioaccumulativa e l'elevata tossicità;

Nel caso degli idrocarburi totali del petrolio, il parametro principale preso in considerazione è stata la idrofobicità superficiale, mentre nel caso del Bisfenolo-A, i processi di funzionalizzazione hanno considerato la similarità della struttura molecolare dell'inquinante, rispetto a quella della molecola funzionalizzante, innestata sulla superficie della fibra.

Nel caso di Escherichia coli, una deposizione di TiO_2 è stata considerata appropriata per l'attivazione fotochimica della superficie della fibra.

Infine, per la purificazione dell'acqua dal mercurio, sono state prese in considerazione le proprietà chelanti della cellulosa stessa.

Le tecniche presentate in questo lavoro di tesi risultano essere molto efficaci nella purificazione dell'acqua inquinata, poiché le fibre funzionalizzate raggruppano molte proprietà importanti, che le rendono un sistema ideale per la bonifica delle acque contaminate. Infatti, i sistemi di depurazione presentano:

- a) elevata stabilità chimica e meccanica;
- b) alta superficie specifica;
- c) metodi di preparazione di basso costo.

Le prove sperimentali hanno dimostrato che le fibre, modificate come menzionato precedentemente, hanno un'eccellente capacità di assorbimento nei confronti degli inquinanti e che la cinetica di assorbimento è molto rapida. Inoltre, l'approccio fotocatalitico, facendo uso dello strato di TiO_2 sulla superficie della fibra, è una applicazione molto promettente per la degradazione dei batteri in acqua.

In definitiva i risultati risultano essere molto positivi ed incoraggiati e aprono il campo a nuove tecnologie per la bonifica dell'acqua.

CHAPTER 1

INTRODUCTION

1.1 Water pollution

Water is the fundamental natural resource for living beings. About 70% of the earth's surface is covered with water and only 2.5% is fresh water. Of this quantity, a part is unavailable for human activities, therefore only a very small amount, equal to 0.01% between lakes, rivers and slopes, is accessible to humans, who use it for domestic, agricultural and industrial purposes [1]. In the last hundred years, water consumption has increased dramatically compared to the resources available and, at the same time, environmental pollution has contributed to worsening its quality [2].

For this reason, water quality issues are a major challenge that humanity is facing in the twenty-first century.

Currently, more than 40 countries in the world, such as Africa, Latin America, the East and Australia, lack drinking water shortages. Data indicate that more than a quarter of the world's population drinks contaminated water (Fig.1).

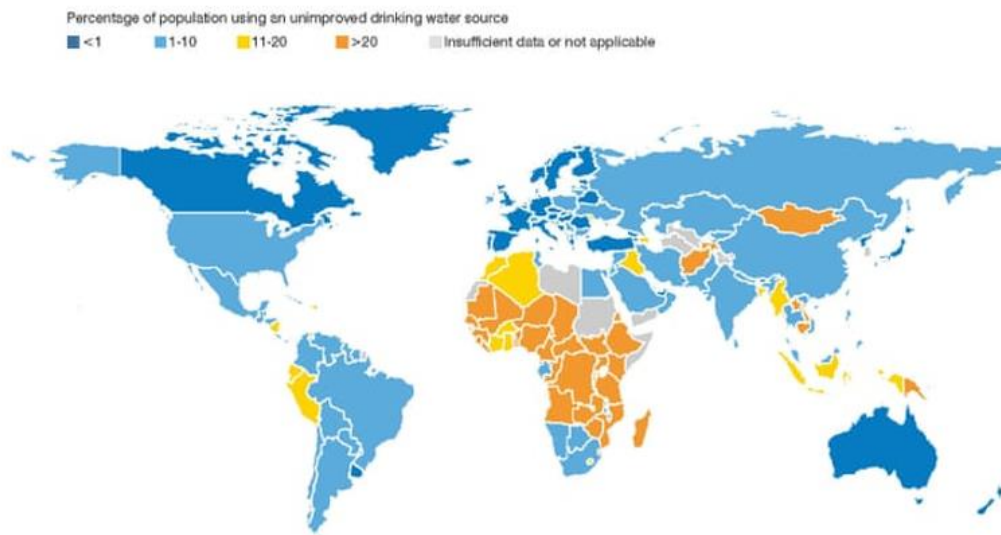


Figure 1. Percentage of population using unimproved drinking water source
Source: WHO/Unicef Joint Monitoring Programme

According to the World Health Organization (WHO), 80% of diseases derive from the consumption of water that is not perfectly decontaminated [3, 4].

However, most of these activities lead to the contamination of water, due to the presence of various industrial and natural chemical compounds, particularly harmful to ecosystems and to human health. The natural water purification cycle, very often, is not able to remedy the anthropic pollution, and the result is the production of polluted waters, which require reclamation activities to restore them [2].

Water is defined as polluted when there are components that compromise its use. The level of contamination varies according to the compromised body of water. Not always a contaminated water is not suitable, for example when the contamination conditions are limited, it may not be suitable for human consumption, but may be used for irrigation [5]. In fact, water is considered polluted if the substances present limit or prevent its use for a specific purpose. Olaniran (1995) has defined water pollution as the presence of excessive amounts of a pollutant in the water in such a way as not to be suitable for drinking, bathing, cooking or other uses [6].

The sources of water pollution can derive from spontaneous environmental events or from anthropogenic pollution, which is caused by human activities [5].

1.1 Types of water

Natural water is generally divided in surface water and groundwater.

Water is defined as superficial when is contained in identifiable water bodies such as lakes, reservoirs, rivers and streams, which are in direct contact with the atmosphere. Surface waters are an invaluable resource for their extraordinary biodiversity, but they are also subjected to unconditional exploitation by becoming receptors of discharges deriving from human activities [7].

Groundwater is the largest freshwater reserve in the world, accounting for over 97% of all freshwater available on earth (excluding glaciers and polar ice caps). The remaining 3% is mainly composed of surface waters (lakes, rivers, wetlands) [2, 8]. Groundwater is contained in the subsoil in "hidden" water bodies, whose characteristics and dimensions may vary depending on the type of subsoil present. Like in a river, even the groundwater flows from upstream to the valley, below the earth's surface and with much lower speed (of the order of at most 1-2 meters per day) since the motion of the water takes place in this case inside the subsoil itself, in pores or cracks of microscopic dimensions [9].

As groundwater flows slowly underground into the aquifers, the impact of human activities can remain for long periods of time: the pollution that occurred some decades ago, from agricultural,

industrial or other human activities, can still be a threat to the quality of groundwater and persist for many generations to come [7, 9].

Since surface water systems receive a continuous supply of water from groundwater flows, a poor quality of the latter is reflected in the quality of surface water. In practice, the effect of human activities on groundwater quality will have an impact on the quality of the associated aquatic ecosystems and terrestrial ecosystems that directly depend on it, if the natural self-purification response such as underground biodegradation is not sufficient to contain contaminants [5]. The large scale contaminated sites are the result of anthropic impacts of the past that still persist today, such as industrial sites and port areas, where it can be difficult if not impossible to restore the natural state of the affected areas with current technologies or with a waste of sustainable resources and energy [2].

1.2 Sources of water pollution

The sources of pollution are classified in point sources and nonpoint sources. Point sources indicate localized areas of contaminants and derive from pollutants emitted from power plants, refineries, factories, wastewater treatment plants, etc. The location of nonpoint sources is imprecise and distributed over an extended geographical area. Normally nonpoint sources include mobile sources as means of urban transport. Although each of these represents a small point source, the contaminants emanating are added, spreading over an extended geographical area [2, 7].

According to Haseena et al. (2017), the main sources that generate water pollution are [10]:

1. Industrial activities
2. Domestic waste
3. Pesticides and fertilizers
4. High population density
5. Animal waste
6. Oil spillage
7. Water treatment plants (WTPs)
8. Toxic waste disposal
9. Sediments degradation

Therefore humans and their activities, aimed at greater well-being, cause water pollution. At the same time, population growth and overcrowding of metropolitan areas generate more water pollution, due to different industrial and agricultural activities [11]. In fact waste from industrial, agricultural and domestic sectors are the main pollutants of ecosystems. The most polluting sources are untreated wastewater from industries and poured into nearby water basins. The unhealthy and irregular management leads to a substantial and immediate drop in the amount of oxygen dissolved in the water, as the bacteria immediately attack the organic matter in the waste water, consuming dissolved oxygen (O₂). The flora and fauna present in the water body, due to the lack of oxygen and the presence of toxic pollutants, undergo a change or death by suffocation [5].

1.3 Effect of water pollution on the environment and human health

Water pollution generates negative effects on the environment, on human health and on aquatic populations.

One fifth of the world's population does not have access to safe sources of drinking water [3]; more than 99% takes place in developing countries. Currently, 1.1 billion people do not have access to safe drinking water and 2.6 billion people lack adequate sanitation, especially in developing countries. A huge difference between rural and urban areas in access to both toilets is manifested [12].

Recent estimates have indicated that contamination of aquatic systems causes 14.000 deaths per day, mainly caused by untreated sewage that contaminates drinking water [3].

Large quantities of toxic waste are released into the environment accidentally or without treatment. The various industrial activities developed in the last decades have led to an increase in aquatic pollution. Most of the water pollution comes from sewage with a high organic content. Under these conditions the equilibrium of a water body receiving pollutants is altered. Significant damage is recorded to the flora and fauna, which directly fall on human health. [12]

Poor quality water compromises agricultural production and infects food, disturbing the food chain [13, 14]. In particular, heavy metals bioaccumulate and affect the respiratory system of fish. In fact, the main problems of human health derive from the consumption of fish that represent a fundamental element in the human food chain [15].

Therefore, a direct dependence between pollution and health problems is real, also due to the microorganisms contained in water considered as drinking but contaminated. They are known as

pathogens [16], which spread diseases to humanity and which are then spread by man to man by contact.

Many diseases such as neurological, neoplastic and cardiovascular diseases are related to the contamination of drinking water, as well as infectious diseases contracted due to fecal-oral infection [17]. Contaminated water has harmful effects on women exposed to chemicals during pregnancy and the subsequent health of the fetus [18]. Water contaminated with metals leads to renal failure and neural disorders [5].

The main risk of acute illness caused by the ingestion of drinking water in developing and transition countries is due to well known viruses, bacteria and protozoa, which spread through the fecal path [19]. Nine out of ten diseases affect children and 50% of child deaths occur in sub-Saharan Africa [20]. Easily preventable diarrheal diseases caused by unsafe water and lack of sanitation and hygiene contribute to 6.1% of all deaths due to health reasons; a report estimates that unsafe water is responsible for 15% to 30% of gastrointestinal diseases [12, 21].

According to the WHO estimates, concerning the sources of infectious diseases in 132 countries (from 1998 to 2001), outbreaks of diseases transmitted by water are at the top of the list; cholera is the most common disease, followed by acute diarrhea, legionellosis and typhoid fever [22].

In industrialized countries with a high-income, the modernization of sanitation and optimal water management entails greater protection of health, while in developing countries, where the safe water supply, the management of waters and improvements in sanitation are missing or scarce, the consequences on human health are negative and of primary importance [23].

1.4 Types of contaminants

Contamination of fresh water can occur by waste and wastewater from human activities, and by natural processes such as rainfall, forest fires, decomposition of organisms, etc., through which numerous substances of various origins, soluble and insoluble, are transported in fresh water flows [24].

But the most widespread and harmful contaminants, which alter ecosystems, are anthropogenic and can be classified as follows:

1. organic compounds and hydrophobic organic compounds (HOCs)
2. plastic products and their by-products

3. heavy metals and metalloids
4. bacteria and microorganisms
5. other contaminants (radionuclides, fertilizers ...)

1.4.1 Organic compounds and HOCs

The major concerns for the environment and for human health derive from organic compounds produced by human activities such as petroleum hydrocarbons, pesticides, herbicides, chemicals from industrial processes and energy production.

Organic contaminants are mainly composed of hydrocarbons, deriving from both natural sources and anthropogenic sources. There are many contaminating hydrocarbons in the environment, but the most monitored ones are among the carcinogens, mutagens and teratogens [15].

These contaminants enter the freshwater system from point sources such as effluents from wastewater treatment plants, industrial waste, sewage systems, mining and construction sites, etc., and from non-timely sources, such as agricultural runoff, urban run-off and atmospheric depositions [17].

Depending on the type of source or process, organic contaminants can belong to two categories: natural (sugars, alkaloids and terpenoids) and synthetic (produced by the reaction of different chemical species), which include TPHs, PAHs, POPs, VOCs, polychlorobiphenyls (PCBs), chlordane and dieldrin , etc. [18].

Particularly monitored are the so-called "Persistent Organic Pollutants" (POPs), because of their high resistance to decomposition to considerable toxic properties [10, 25]

Due to their characteristics of persistence and toxicity, they are particularly harmful to human health and the environment (even deadly for fauna). Their accumulation in organisms, due to their high lipoaffinity, has been found [26].

POPs are present in the atmosphere, in the air and in water and their propagation is also due to climatic events with the danger of their increasing accumulation in terrestrial and aquatic ecosystems.

The Stockholm Convention, in force since 2004, has highlighted and classified some potential POPs for the damage they can cause to the environment and to human health. These organic pollutants contaminate the water and persist for a long time in the environment. They tend to accumulate in nature reserves such as aquifers, soil, sediments, etc. to then move into the environment, through

various processes, and become available for the organic food chain. In this way, these contaminants tend to bioaccumulate and expose toxicity, mutagenicity, carcinogenicity and teratogenicity and acute disorders for living beings with prolonged contact [27].

The most harmful and problematic contaminants for all living systems are the so-called organic hydrophobic compounds (HOCs) due to their hydrophobicity. In aquatic ecosystems, HOCs are often stored in sediments, due to their hydrophobic interactions with the humic substances contained in the sediment particles [28]. These pollutants include Total petroleum hydrocarbons (TPHs), such as aliphatic and aromatic hydrocarbons, polychlorobiphenyls (PCBs), polycyclic aromatic hydrocarbons (PAHs), polychlorinated di-benzodioxins and others. Even if these compounds are very low soluble in water, they can explicate high toxicity, mutagenicity, and carcinogenicity because of their entering into the food chain [29].

Other organic chemicals included in HOCs classification is the category of chemicals called volatile organic chemicals (VOCs), which derive from petroleum. These pollutants are volatile, having low boiling points and high vapor pressures at room temperature and include BTEX (benzene, toluene, ethylbenzene, and xylenes) present in petroleum products, chloroform and bromoform as well as other low-molecular weight chlorinated aliphatic and aromatic hydrocarbons, and lower-molecular-weight aliphatic and aromatic compounds including some PAHs [30].

1.4.2 Marine debris and plastic in the environment

One of the biggest problems for the environment and human health is the increasing amount of plastic that spreads in the oceans and in the world's basins. Plastics represent a great resource for humanity from the point of view of benefits of packaging, availability and processing but, at the same time, there are multiple drawbacks [31]. Indeed, resistance to degradation, unsustainable use and inadequate waste management cause the accumulation of plastics in natural habitats. For example, in the marine environment, plastics, coming from various production processes and of various sizes, influence the life of marine species that ingest plastics or remain trapped in them [32].

Waste of natural origin can biodegrade quickly, while plastics take hundreds of years and, during their stay in the environment, sunlight and atmospheric agents can reduce plastic waste into smaller pieces. Very dangerous are the fragments, called microplastic (MPs), which are smaller than 5 mm in diameter, due to their high mobility [33]. In addition, large ocean currents have collected huge

amounts of floating plastic debris at points defined, causing "islands" to appear (garbage patches). In these areas, the plastic quantity exceeds that of the zooplankton [31, 34].

MPs are particularly troubling due to their tendency to bioaccumulate, which increases with decreasing size. They are generally ingested by aquatic organisms, fish, birds and mammals, and accumulated through the aquatic food chain. A collateral problem associated with the presence of plastics in the sea is their degradation: in fact, the release of a multitude of chemical additives and by-products is of great concern for the health of the ecosystem [35].

Therefore plastics and microplastics represent a vector for other contaminants due to their chemical composition: MPs accumulate contaminants such as metals and persistent, bioaccumulative and toxic compounds (PBTs, PCBs) [36]. So when an organism ingests plastic, it is also ingesting the contaminants it has absorbed.

However, the most released contaminants are the endocrine disrupting compounds (EDCs) as they are the main degradation products of plastics. Numerous studies have shown the release of Nonylphenol and Bisphenol A from MPs [31, 37]. Furthermore, Wagner and Oehlmann (2009) have shown that plastic leaches EDCs [38].

Currently, estimates state that plastics, coming from anthropogenic sources and emitted from rivers to the oceans, represent 70% - 80% of marine waste. Potential sources of such pollution include waste water treatment plants (WWTPs), abandoned waste on beaches, accidental releases of cargo ships and ports [31].

One of the most alarming concerns for the environment is the increasing amount of plastic and other waste in the oceans and lakes of the world. Waste is sometimes illegally or accidentally dumped into the ocean, for example from ships and offshore platforms, but more often it is transported by rivers and streams, washed over land by rainwater runoff or sewage discharge, or blown by the wind. In addition, personal care products such as facial scrubs, different cosmetics and toothpastes, are a further source as they contain tiny microplastic pearls [39].

The United States, due to the growing environmental contamination of microplastics, ingested by marine biota and available in the food chain, have banned microplastics in personal care products, starting in 2017. Canada and the European Union have adapted and seem to follow the intentions of the United States. With the Netherlands leading this campaign, they are also trying to tackle the problem of waste in ocean routes. Nevertheless, improper waste management takes place in all countries, however, and is a global problem [31, 39].

Millions of tons of plastic and other marine debris cluster in the ocean and are held together by circular currents, generated by the winds and by the effect of Coriolis from the rotation of the Earth. The largest accumulation of garbage is called the Great Pacific Garbage Patch and extends from California to Japan, in the vortex of the Subtropical Convergence Zone of the North Pacific (Fig. 2). But currently five major agglomerations of plastic and garbage waste are counted in the globe: they are found in the North Pacific, in the South Pacific, in the North Atlantic, in the South Atlantic and in the Indian Ocean [42].

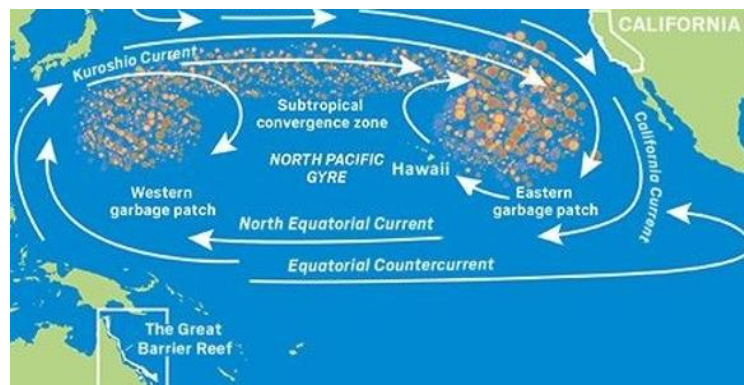


Figure 2. The great Pacific garbage patch
Source: <https://oceancruisingclub.org>

1.4.3 Metals and metalloids

Metals and metalloids represent the essential nutrients necessary for various biochemical and physiological functions of humans, animals and plants; metals such as cobalt (Co), copper (Cu), chromium (Cr), iron (Fe), magnesium (Mg), manganese (Mn), nickel (Ni), selenium (Se) and zinc (Zn) are essential at very low concentrations, but the inadequate supply of these micronutrients causes extreme toxicity and danger to living beings, with a variety of diseases and dysfunctions [42].

Heavy metals are defined “heavy” because they have a higher water density and “trace elements” due to their presence in trace concentrations (ppb interval less than 10ppm) in various environmental matrices [43].

In recent decades, human and environmental health has been threatened by high heavy metal contamination. Human exposure has increased exponentially due to the increased use of these contaminants for different sectors [44]. Environmental contamination and human exposure is mainly caused by anthropogenic point sources as industrial sources that include metalworking in foundries, coal combustion in power plants, oil combustion, nuclear power plants, plastics, textiles,

microelectronics, wood preservation and paper processing plants, mining operations, domestic and agricultural use of metal-containing compounds [45].

Environmental contamination can also occur through natural sources such as soil erosion, metal corrosion, atmospheric deposition, and the evaporation of metals from water resources to the soil [8]. It has also been reported that natural phenomena such as weathering and volcanic eruptions contribute significantly to heavy metal pollution [42, 46].

Their bioavailability depends on physical parameters such as temperature, adsorption and association, and on chemical parameters such as thermodynamic equilibrium, complex kinetics, octanol / water partition coefficients and liposolubility.

An important role is also played by biological factors such as trophic interactions and the biochemical/physiological behavior of the species [47].

Essential heavy metals exert biochemical and physiological functions in plants and animals. They are important constituents of several key enzymes and play important roles in various oxidation-reduction reactions [44].

Metals like copper are cofactors essential for different enzymes, including catalase, superoxide dismutase, peroxidase, ferroxidase, dopamine beta-monooxygenase, etc. as they are involved in the formation of different molecules such as hemoglobin, carbohydrate metabolism, catecholamine biosynthesis and cross-linking of collagen, elastin and hair keratin.

The ability of metals to pass from an oxidized to a reduced state (for example Cu (II) passes to the Cu (I) state) is used by cuproenzymes involved in redox reactions [48]. However, this property makes metals potentially toxic, if in excess, since the redox transitions generate superoxide and hydroxyl radical formation [42].

Many elements are essential for biological functioning, however, an excessive amount of these metals produces cellular and tissue damages that generate various human, disease and collateral dysfunctions. Several studies show that thinking metals influence the biological cycles of cell membranes, including their components as endoplasmic reticulum and mitochondria, in addition to inactivating the detoxification enzymes from the same metals [49].

The greatest damage is found by the interactions of metal ions with DNA, causing conformational changes that affect cell cycles, generating carcinogenic and toxic effects [50]. According to the United States Environmental Protection Agency (US EPA) and the International Agency for Research on Cancer (IARC), metals such as arsenic, chromium, lead, cadmium and mercury [42] are mainly responsible for these changes even at low levels of exposure, due to their high toxicity. Experimental studies have shown a direct link between the onset of cancer in living beings and exposure to these pollutants, being classified as "known" carcinogens.

Heavy metal-induced toxicity and carcinogenicity involves many mechanistic aspects, some of which are not clearly elucidated or understood. However, each metal is known to have unique features and physico-chemical properties that confer to its specific toxicological mechanisms of action.

The toxicity of metals depends strongly on their speciation and the form in which they exist in a given aquatic system. The most toxic form is represented by a dissolved free-form metal [49].

For example, Mercury in the free inorganic form has lower toxicity compared to its organic forms due to differences in bioavailability. In aquatic environments mercury is transformed into methylmercury, generating rapid bioaccumulation in the tissues of aquatic organisms like fish and a biomagnification in the food chain, up to humans. The daily allowable mercury dose through fish consumption is 0.1 mg/kg, beyond which health effects are known [42].

1.4.4 Bacterial contamination and other water pathogens

According to the World Health Organization (WHO) estimates, the mortality associated with diseases resulting from the consumption of contaminated water is around 5 million people per year. More than half of these diseases derive from microbial intestinal infections caused by the ingestion of water contaminated by human or animal faeces. The sources of pollution from faecal microorganisms are mainly wastewater discharges into freshwater streams and coastal marine waters [50, 51].

The most widespread disease is microbial diarrhea, which mainly affects populations in developing countries, with limited financial resources and absent or inadequate sanitation.

These problems are found in Asian and African countries, and the part of the population most affected by microbial diseases, transmitted through water, are children under the age of 5 years [52]. Globally, waterborne diseases have been and continue to be a major source of mortality. The problem of open defecation concerns about one billion people in the world. In 2010, around 60% of the world's population had access to adequate sanitation [53]. Even developed countries such as the United States, each year account for over half a million patients suffering from diseases transmitted by contaminated water intake, with an estimated annual mortality rate of over 10,000 people [50, 53].

Microorganisms such as bacteria, fungi and viruses naturally populate aquatic systems. However, an excessive concentration of pathogenic microorganisms can cause the compromise of a body of water that will no longer be suitable as a source of drinking water, irrigation or for industrial uses, due to the present pollution. In fact, many pathogenic microorganisms are able to compromise and cause serious damage to human health or crops.

The identification of polluting pathogenic organisms in an aquatic system has always been a difficult practice, for this reason, since 1920s, so-called fecal indicator bacteria (FIB) are used to monitor water quality. In fact, the most worrying source of pathogenic pollution derives from faecal contamination of coliform bacteria coming mainly from the intestine of mammals [50, 55].

The finding of these FIBs in water indicates the presence of pathogenic enteric bacteria. At the same time, their absence establishes a good level of safety of water quality, as faecal coliforms are more persistent than pathogenic organisms. The most used FIBs as indicators of water quality are total coliforms, i.e. *Escherichia coli* and *Enterococcus* sp. Their concentrations can be measured by simple laboratory procedures [55].

Although the number of wastewater and potable water treatment plants and the use of better technologies are constantly increasing, the percentages of mortality and inadequacy of disinfection processes belie the progress made in this field.

1.4.5 Other pollutants

Other contaminants of natural origin present in the water may be radioactive elements such as potassium-40, polonium-210 and uranium-238. They can be found in drinking water and results in a dose of radiation when it is consumed. While, traces of artificial radioactive material, such as cesium 137, can also be found in water, following discharges (often authorized), near nuclear-producing industries or as a result of radiological activities [56]. Other types of substances that contaminate the waters are the nutrients such as nitrate, ammonia, total nitrogen, orthophosphate and total phosphorus. Nutrients are naturally found in water, but high concentrations usually come from artificial sources, such as artificial fertilizers, manure and septic system effluents [57].

CHAPTER 2

2 Pollutants of interest and remediation treatments

2.1 HOCs and TPHs pollution

Hydrocarbons deriving from oil are nowadays one of the main sources of energy. Their use in industry, and the products derived from them, has increased tenfold compared to the first 50 years of the last century. The enormous exploitation and use has generated collateral problems, through pollution, which has inexorably poured into the environment and human health. Currently, contamination by hydrocarbons, both of soil and water, is one of the most important and damaging environmental problems [30].

Every year about 3×10^{10} barrels of oil (BP Statistical Review of World Energy) are extracted and a large amount of these are transported through oceans, pipelines and other means, making the terrestrial and aquatic environment prone to pollution caused by accidental oil spills, both in the extraction processes and both in the transport processes [58, 59].

Pollution incidents or accidental spillages of petroleum compounds both in the soil and in water are becoming increasingly frequent. The main problem is due to the toxic nature of most of the hydrocarbon components of petroleum and to the high persistence in the environment, often decades. Furthermore, the accumulation of these toxic pollutants in living systems can cause highly harmful and fatal effects on humans and animals [59].

The term petroleum hydrocarbons refers to an extremely complex mixture of a wide variety of low and high molecular weight hydrocarbons. This complex mixture contains saturated alkanes, branched alkanes, alkenes, aromatics (including aromatics containing heteroatoms such as sulfur, oxygen, nitrogen and other heavy metal complexes), and aromatic molecules such as resins, asphaltenes and hydrocarbons containing different functional groups such as carboxylic acids, ethers, etc. [60].

Figure 3 shows some common hydrocarbons compounds.

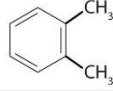
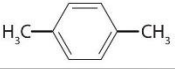

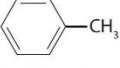
Name	Condensed Structural Formula	Octane Rating	Name	Condensed Structural Formula	Octane Rating
<i>n</i> -heptane	CH ₃ CH ₂ CH ₂ CH ₂ CH ₂ CH ₂ CH ₃	0	<i>o</i> -xylene		107
<i>n</i> -hexane	CH ₃ CH ₂ CH ₂ CH ₂ CH ₂ CH ₃	25	ethanol	CH ₃ CH ₂ OH	108
<i>n</i> -pentane	CH ₃ CH ₂ CH ₂ CH ₂ CH ₃	62	<i>t</i> -butyl alcohol	(CH ₃) ₃ COH	113
isooctane	(CH ₃) ₃ CCH ₂ CH(CH ₃) ₂	100	<i>p</i> -xylene		116
benzene		106	methyl <i>t</i> -butyl ether	H ₃ COC(CH ₃) ₃	116
methanol	CH ₃ OH	107	toluene		118

Figure 3. Common hydrocarbons

Source: https://saylordotorg.github.io/text_general-chemistry-principles-patterns-and-applications-v1.0/s06-06-industrially-important-chemicals.html

From an analytical point of view, the identification of these compounds in the environment occurs by monitoring the so-called Total Petroleum Hydrocarbons.

Total petroleum hydrocarbons (TPHs) are a term used to describe a large family of hundreds of chemical compounds that come from crude oil. Because of the wide variety of chemicals in crude oil and other petroleum products, it is not practical to measure them separately, so it is useful to measure the total amount of TPHs in a contaminated site.

TPHs are a mixture of chemicals, consisting primarily of hydrogen and carbon, called hydrocarbons. Scientists divide TPHs into oil hydrocarbon groups that have the same behavior in soil or water. These groups are called fractions of petroleum hydrocarbons. Each fraction contains many individual chemicals [29, 61].

The most abundant chemicals in TPHs are hexane, jet fuel, mineral oils, benzene, toluene, xylenes, naphthalene and fluorene, as well as other petroleum products and petrol components. However, it is not obvious that all samples of TPHs will contain all the compounds listed above but only some or a mixture of these [62].

The distribution of a chemical in the various environmental media depends on the solubility of the chemical in each phase (water, air, fat, soil).

Oil contamination is relatively common because of its widespread use and its associated disposal operations and accidental spills. Point sources of pollution of petroleum compounds derive from leaks

and discharges of oil tankers, oil pipelines and wells. Also, the emissions due to catastrophes in the last decades have caused a huge environmental contamination and in a short time [63].

Table 1 shows the main catastrophic events of recent times.

Table 1. The main catastrophic events of recent times

Incident	Date	Location	Oil spilt (T)
Torrey Canyon	1967	West Cornwall, UK	117,000
Amoco Cadiz	1978	West Brittany, France	223,000
Exxon Valdez	1989	Alaska, USA	38,000
Arabian Gulf installations	1991	Kuwait	>1 million
Braer	1993	Shetland Islands, UK	85,000
Sea Empress	1996	Pembrokeshire, UK	72,000
Erika	1999	Bay of Biscay, France	20,000 ^a
Prestige	2002	Cape Finisterre, Spain	63,000 ^a
Hebei Spirit	2007	Tae-an, South Korea	11,000
Deep Water Horizon installation	2010	Gulf of Mexico, USA	~7 million

^a Heavy fuel oil.

Source: Marine Pollution Bulletin 124(2) DOI: 10.1016/j.marpolbul.2017.01.068

However, most of the oil pollution comes from non-point sources, which generate a small amount of emissions into the environment over a long period of time, in fact 70% of the oil present in water bodies, basins and oceans, it is released by small spills of anthropogenic activity [59].

The main non-point sources are discharges and fuel leaks from commercial or pleasure boats, industrial plant effluents and human activities. Atmospheric agents and rainwater runoff, spread petroleum pollutants (as by-products of lubricants, solvents, oil-based paints and, above all, petrol) into the environment. Pollutants normally flow into watercourses and aquifers and spread slowly in all ecosystems. Wastewater from these sources also enter the marine environment through estuaries, which are the most pollution-critical habitats for a wide variety of plants and animals. In general, urban sources account for more than half of world oil pollution [59, 60, 63].

The main problem with the remediation of the environmental matrices involved by these pollutants is that generally they persist as a separate phase, because of their low solubility, so they can be found as free floating, emulsified, dissolved, or adsorbed to soil grains. The occurrence of these scenarios gives rise to what is known as secondary source of contamination. A source is the location from which a contaminant has entered a physical system. A primary source, such as a drum or a reservoir leaking onto a water body or surface soils, may produce a secondary source, such as a contamination plume or contaminated soils. While primary sources are easier to identify and to deal with, secondary sources

are very hard to manage. The situation becomes even worse if the cleaning procedures concern groundwater systems. Subsurface water-soil environments do not allow to directly observe and act on the processes occurring in their inside, resulting, in most cases, in very expensive and not very effective operations [29].

2.1.1 Effects of petroleum hydrocarbons on living matter

In large concentrations, the hydrocarbon molecules that make up crude oil and petroleum products are highly toxic to many organisms, including humans.

The environment and the living beings are exposed to the pollution of the oil in a direct or indirect way, due to the continuous release of by-products formed during the extraction, refining and processing of the oil for the synthesis of new products. Petroleum hydrocarbons can rapidly migrate from the site of contamination and adversely affect terrestrial and aquatic ecosystems and humans.

The majority of by-products, released from human activities or accidental spills, are highly toxic and only a relatively small number of all petroleum hydrocarbons are well characterized for toxicity damages. In fact, the hydrocarbon molecules have a wide distribution of molecular weights and boiling points, each of which corresponds to a different degree of toxicity to the environment and to living beings. Their toxicity depends on their chemical and physical nature, exposure modes and exposure time [30].

The degree of absorption and diffusion of a given contaminant in an environmental medium depends mainly on properties such as volatility and solubility. A hydrocarbon with high solubility and volatility has higher penetration capacity in aquifers or in the air, compared to one with lower solubility and volatility. Following the diffusion process, living organisms can be exposed to these fractions by ingesting contaminated water or breathing polluted air [30, 64].

TPHs cause serious effects on the health of people and wildlife and damage any system of organs in the human body such as the nervous system, the respiratory system, the circulatory system, the immune system, the reproductive system, the sensory system, the system endocrine, liver, kidneys, etc. For each type of exposure and effect corresponds a wide range of diseases and disorders [65]. The individuals most exposed to the toxic effects of oil pollution are infants, children, pregnant women and people with pre-existing serious health problems.

Smaller compounds belonging to the class of TPHs such as benzene, toluene and xylene, can damage the human central nervous system and when the exposures are very high, death can occur.

Exposure to toluene at concentrations above 100 ppm for several hours may cause fatigue, headache, nausea and drowsiness. Symptoms disappear when exposure ceases. However, prolonged exposure can cause permanent damage to the central nervous system [66].

Exposure to benzene is strongly associated with disorders of the haematopoietic system such as aplastic anemia [66-69]. Countless studies have shown that it causes cancer (leukemia) in humans. The International Agency for Research on Cancer (IARC) has classified benzene as a human carcinogen (group 1 classification).

Chronic exposure to VOCs and polycyclic aromatic hydrocarbons (PAHs) may compromise the immune system, leading to a decrease in the number of white blood cells and high oxidative stress [70] and the central nervous system, with symptoms such as headaches and dizziness [66, 71]. Acute exposure to polycyclic aromatic hydrocarbons causes symptoms such as nausea, irritation of the skin and eyes [72]. For pregnant women, PAH exposures have been linked to weight reduction and incomplete development of the newborn [73]. While chronic exposure causes an increased risk of contracting certain types of cancer, including lung, skin and bladder cancer [74]. In particular, naphthalene, a low molecular weight PAH, negatively affects the haematopoietic system, damaging the red blood cells [75]. Although studies concerning alkylated PAHs are limited, research suggests that their toxicity and carcinogenicity may be greater than the corresponding non-alkylated compounds [66, 76].

Another compound belonging to the TPHs, such as n-hexane, can fall ill in the central nervous system through a pathology called "peripheral neuropathy" which can lead to paralysis in the most severe cases. These disturbances were found in workers exposed to 500 ppm n-hexane in the air [66]. In general, the swallowing of some petroleum products such as petrol and kerosene causes irritation of the respiratory and digestive system, as well as disturbances of the central nervous system.

Some other compounds of TPH, such as benzo(a)pyrene and petrol, are considered carcinogenic to humans based on cancer studies in humans and animals. IARC classified them in groups 2A and 2B, respectively. Most of the other TPH compounds are considered not classifiable (Group 3) by IARC. [60].

2.1.2 Remediation technologies for TPHs contamination

Polluted aquatic ecosystems are currently one of the greatest threats to the health of living beings. Based on this problem, the global community aims to reduce polluting emissions and to develop better methods to safeguard the environment and human health. Over 50% of crude produced worldwide comes from the Persian Gulf area (onshore and offshore oil fields). Over the period 1995-1999, more than 500 oil spill incidents were recorded in the Persian Gulf area, resulting in a total loss of 14.000 barrels in the environment; while more than 10.000 barrels of oil were spilled in the early 21st century. Spills are mainly recorded in crude oil storage and transport systems during oil production operations [77].

The greatest efforts are focused on the search for effective remediation methods for polluted sites.

However, the remediation of oil-contaminated environments is a difficult issue due to the complex nature of chemical compounds and their great resistance to chemical and biological degradation. The degradation of oil pollutants in the natural environment depends on various factors such as pH, the chemical-physical characteristics of the medium in which the pollutant is dispersed, the diffusion phenomena, etc.

Oil released into the environment is affected by a series of physical, chemical and biological changes. In water bodies or in the sea, the hydrocarbon pollutant, lighter than water, spreads on the surface generating a thin film of less than 1 mm [77, 78].

The diffusion of the oil on the surface of the water depends on its chemical-physical characteristics, on the atmospheric conditions, on the temperature and on the flows of the reservoir. About 40% of the oil can evaporate in a short time, leading to an increase in the viscosity of the pollutant, while the remaining part will remain present in the water, since some components such as benzene, toluene and xylenes have a high solubility, which varies in the range of 150-1800 mg/L [79].

To remove pollutants from the contaminated soil and water site, several methods have been developed. But some of these methods are very expensive and inefficient, with the risk of worsening the pollution situation inside the site [80].

In general, the remediation of oil-contaminated sites can take place through biological, mechanical, chemical, and thermal treatments, both in situ and in ex situ [81, 82].

The most common remediation techniques for oil spill are shown in Table 2 and described in detail in the following paragraphs.

Table 2. The most common remediation techniques for oil spill

Method	Treatment
Physical	Skimming and booming
	Mechanical removal
Chemical	Dispersants
	Solidifiers
	In situ burning
Biological	Bioremediation
	Phytoremediation

2.1.2.1 Physical methods

The mechanical recovery of pollutants from aquatic environments is one of the most respectful methods of the ecosystem and the most used, since chemical agents are not used. Recovery techniques employ a wide variety of skimmers, collection containers and mechanical booms and do not require government permissions. The mechanical oil recovery systems are placed in areas of pollutant leakage or in areas that have suffered contamination following an event [83].

2.1.2.1.1 Booming

The booms are used in aquatic areas as a technology to contain the leakage and / or dispersion of oil on the surface of the water, in order to facilitate subsequent cleaning operations. Therefore, the purpose of the booms is to collect and circumscribe the oil on the surface of the water avoiding the dispersion.

The mechanical booms, different by type, always have the same general design, consisting of a floatation device filled with air or rigid, which remains above the surface of the water, a skirt (panel) dipped under the surface of the water, connected to the float, which retains the oil under the floating device and a ballast perpendicular to the surface (normally made of steel or lead) which has the

purpose of stabilizing the whole apparatus (Fig. 4) [83]. It is often believed that the effectiveness of the skirt depends on its depth. An optimal panel depth exists for every application [84].



Figure 4. Mechanical booms

Source: <http://www.abbcoboom.com/products/oil-boom/>

The dimensions of the containment arm are calculated according to the requirements of the polluted area and the quantity of dispersed pollutant; the construction of the equipment respects the following formula: $B = 1.25 \times H$, where B is the length in meters of booms, required to contain the free floating oil; H is the amount of oil spilled in m^3 [83].

The containment booms are divided into two categories: curtain booms and fence booms. Curtain booms consist of a lower foundation supported by a floating chamber (air or filled with foam), usually with a circular cross-section. The fence booms, on the other hand, have a flat cross section, which allows vertical floatation in the water.

In addition, a category of special booms is included in this technology: ice booms for light ice conditions, adsorption booms, tidal holding booms and fire booms. The latter, for example, are specifically built to withstand very high temperatures generated by oil combustion [84].

The use of the booms is strongly influenced by the conditions of the currents and the wind (Figure 5). For example, rough seas can prevent these technologies from functioning properly by transporting oil to the top of the containment boom (a). In addition, low viscosity oils tend to separate from the accumulated oil and flow under the arm skirt (b). This problem also occurs when the critical thickness of the skirt reaches the limit (c). Another negative aspect of this method is the speed of application, in fact even if the equipment is quick to organize and locate, the oil will have had ample time to spread over several square kilometers (2) [85].

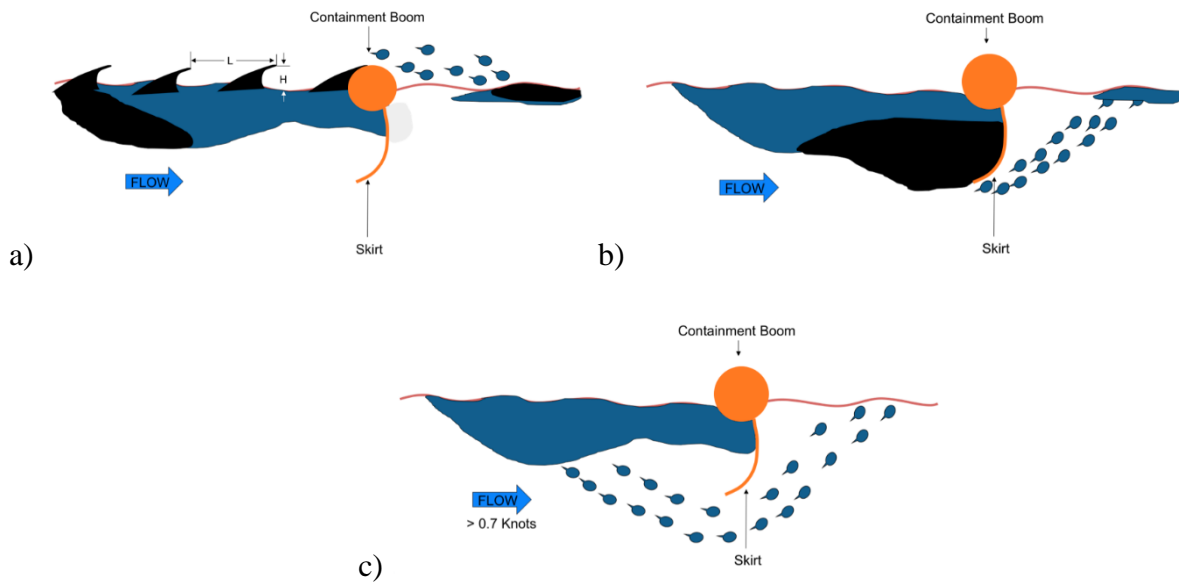


Figure 5. Containment Booms for oil spills

Source: <http://www.acmeboom.com/resources/oil-spill-containment-boom-boom-failure-methods>

2.1.2.1.2 Skimmers

The skimmer is a device for recovering the oil leaked from the surface of the water, transferring it to the collecting tanks on board the ship to which it is connected, without causing chemical-physical changes to its properties. It has the purpose of mechanically separating the floating oil on the surface of the water. Usually, the skimmers work in a complementary way with the booms.

The skimmers can be self-operating or connected to recovery ships. Its efficiency depends on the conditions of the basin/sea, in fact in very agitated waters, the skimmers tend to recover more water than oil. The skimmers, despite having a design that can be different, are based on the phenomenon of specific gravity and on the surface tension of the oil, in order to remove it from a moving medium. The different skimmers' designs allow to operate efficiently in different weather conditions.

Normally, they are classified into two classes: oleophilous and not oleophilous [84].

Oleophilic skimmers use materials with high affinity for oils rather than for water. The oil is adsorbed on the surface of the material that rotates inside the skimmer body and lifts the oil from the surface of the water. Once separated from the water surface, the oil is separated from the hydrophobic material and collected in a well to be transferred to the storage container.

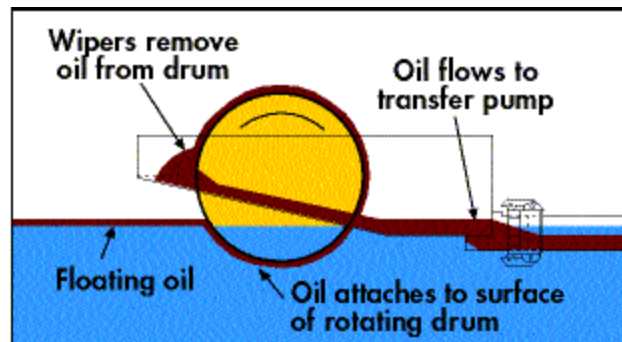


Figure 6. Oleophilic skimmers
Source:koldacorporation.com

Oleophilic materials are made of polymers or, more rarely, of metal surfaces. The shapes are many: disc, drum, belt, brush or rope-mop [85].

Many skimmer models have improved to perform their function despite the waves and situations of strong turbulence. The best technique is the skimmer with rotating belts, because it can be partially lowered under the oil-water interface to reduce the influence of the waves.

Non-oleophilic skimmers are used more rarely. The best type is the suction skimmer, although its performance is more inefficient than the oleophilic one, especially in marine waters, since even small marine turbulence involves the collection of large quantities of water [84, 86].

The skimmers are also classified according to the operating principle: selective (stationary and self-propelled), crane or integrated into the ship. In environments with large volumes of ice in the water (such as in the Arctic Ocean), the crane-driven or built-in skimmers are more used because the ice can prevent them from floating [83].

The choice of type of skimmer, in addition to weather conditions, depends on the viscosity of the leaked oil and the amount of debris. In fact, the high viscosity skimmer suction pump has a very low efficiency for transferring the oil to the storage tank on the ship [86].

Currently, the most reliable technology is the use of skimmers connected to ships, because of their ability to handle large volumes of inflow to be treated with a minimal negative impact on the environment.

2.1.2.2 Chemical methods

In this section, the description of chemical methods for removing hydrocarbon pollutants from water is provided.

2.1.2.2.1 Dispersants

The use of dispersants is a chemical method for removing oil from the aqueous medium. The purpose of this technique is to resize the oil patches in small drops, which dilute and degrade rapidly due to microorganisms present in the aquatic ecosystem. The technique prevents the oil from expanding further on the surface and reaching the mainland [83].

The dispersing agents consist of a hydrophobic part (attracted to petroleum) and a hydrophilic part (attracted by water). When the dispersants are dispersed on the surface of the water, the molecules are repositioned in such a way that the hydrophobic part comes into contact with the oil and the hydrophilic part with the water. This phenomenon reduces the surface tension of the oil / water interface; the motions of the aqueous medium, at this point, disperse the oil patch forming smaller droplets. To obtain an effective dispersion, the drops of oil must have a dimension between 1 μm and 70 μm [85].

The dispersants are generally classified into three groups according to their chemical nature: the first and second class of dispersants are no longer used due to environmental toxicity, while the third-generation dispersants are divided into classes 1 and 2. Dispersants belonging to the second class, in general, are diluted with sea water before use and must be used in large quantities to have a high efficacy. However, both classes consist of a concentrated mixture of two or three non-ionic surfactants (having a neutral charge, such as esters of fatty acids and esters of ethoxylated fatty acids) or anionics (having a negative charge, such as sodium alkylsulfosuccinate). The solvents used with surfactants are based on glycol and light petroleum distillate [83, 84].

The parameter that mainly influences the effectiveness of the dispersants is the temperature, in fact the density of the oil increases with the decrease of the temperature, therefore the dispersants are not effective with very high density oils [86], on the contrary, in the warm regions, the high temperatures allow better dispersion. Also the wave motion, the currents and the winds greatly influence the dispersion process, since the higher mixing energy corresponds to the greater ability to overcome the surface tension at the oil / water interface. For example, storm conditions, when Braer tanker sank in 1993, in Shetland, UK, improved the natural dispersion of low viscosity oil, reducing the impact of oil spill on nature.

The use of dispersants, however, also has disadvantages: when the oil is dispersed in the aqueous medium can reach marine organisms that otherwise would not come into contact with it. Furthermore, the application of dispersants must be carried out between 24-72 hours, since the oil comes into

contact with water, due to the degradation of oil [85]. Dispersants can be distributed to the place needed by ships or aircraft [86].

2.1.2.2.2 Solidifiers

Normally, the solidifying technique is used for limited polluted areas, in order to prevent the dispersion of the oil. The solidifying agents are hydrophobic polymers that interact by means of Van der Waals forces with the polluting hydrocarbon mass. The polymers are designed to increase the viscosity of the oil up to the formation of a solid mass [87]. If the polluting oil already possesses a high viscosity in itself then the solidifying agents may not penetrate the oil / water interface and drastically reduce the solidification efficiency [86, 87]. Subsequent mechanical methods allow to recover the solidified oil, which otherwise would sink.

There are three types of solidifying agents with unique characteristics:

- polymeric sorbents that absorb oil in their cavities through weak interactions;
- cross-linking agents and polymers with cross-linking agents which form chemical bonds between the hydrocarbon molecules; the bonds that are formed allow the formation of a solid mass, while the solidification can be incomplete and disadvantageous if the application is slow [87].

However, current studies do not allow complete information on their toxicity to the environment and their dependence on weather conditions. Furthermore, solidifiers have the disadvantage of costs if used on a large scale [84].

2.1.2.2.3 Sorbents

Sorbents are materials that have the ability to retain oil from water. There are two types of absorbers: adsorbents and absorbents. The adsorbent "captures" the particles of oil on the surface of the material, while the absorbent retains the oil because it penetrates into the pores of the material.

The sorbents, in general, to be effective must be hydrophobic (repelling water). They can be natural organic substrates (derived from plants), natural inorganic (deriving from inert materials) or synthetic (such as polyethylene) [86]. Sorbents perform their function following preliminary purification processes. Normally, sorbents have the ability to be re-used many times, which gives them the

characteristic of being environmentally friendly and low cost materials. Despite these reasons, the sorbing technology still has many limitations: difficulty in using the open sea, inefficiency with heavy oil and cumbersome for transport [86, 87].

2.1.2.2.4 Thermal remediation

Thermal remediation consists in the in situ combustion of the oil, following its containment with fireproof barriers (Figure 7). This technique is used when other methods can not be applied. The removal efficiency in this case is very high, over 90%: the oil is removed economically and quickly from the surface of the water with the consequent absence of the recovery and storage of the collected oil [86]. Although the method is very efficient from the point of view of remediation, it is very harmful to the ecosystem. In fact, by-products of combustion are ashes, which pollute the aquatic environment and high amounts of carbon dioxide in the atmosphere, up to 10% of the volume of the oil burned, that moves pollution into air. Among the pollutants that pass in the gaseous phase, there are carbon monoxide and nitrogen oxides, sulfur dioxide and some polynuclear aromatic hydrocarbons (PAH) [88].

However, this technology has difficulties in application caused by adverse weather conditions as containment barriers can not circumscribe pollution and formed emulsions. To solve these limitations, thickening agents can be used in such a way as to concentrate the pollutants more and reduce the emulsions [89].



Figure 7. In situ burning

Source: <http://ragingpelican.com/against-the-wind-t-mayheart-dardar/>

2.1.2.3 Biological methods

The biological remediation method is a secondary treatment, following mechanical or chemical processes, when the oil layer on the surface is not less than 0.1 mm.

The microorganisms capable of digesting petroleum hydrocarbons are mainly bacteria of the *Pseudomonas* family and some species of fungi and yeasts.

The effectiveness of bioremediation is related to the size of the oil particles: efficiency increases as the size of the hydrocarbon particles decreases. Furthermore, micro-organisms require the presence of nutrients such as nitrogen and phosphorus to perform their function; nutrient supply is one of the main problems of this method [86]. Even the external environment greatly influences the efficiency of the bioremediation process, in fact the microorganisms need temperatures around 15 °C (2 g/m surface). On the contrary, in cold and warm climatic conditions, the process is extremely slow and ineffective.

2.1.2.3.1 *Bioremediation*

Bioremediation is based on the ability of a microorganism to degrade hydrocarbons in compounds that are not toxic to the environment and living species, and which can be used by other microorganisms as a source of nutrients [59]. The degradation of hydrocarbon compounds returns harmless products such as water, carbon dioxide and other inorganic compounds through enzymatic attacks [90]. Degradation processes are normally aerobic but in recent decades anaerobic degradation processes have been developed [91].

Some classes of hydrocarbons, such as chlorinated hydrocarbons or high molecular weight aromatic hydrocarbons, are resistant to microbial degradation or are degraded very slowly. These limitations affect bioremediation applications for certain heavy pollution cases. But the limited costs and the possibility of advanced developments represent the main advantages of such bioremediation techniques [59].

There are two types of bioremediation:

1. In-situ Bioremediation:

The methods in-situ are mainly used to solve the problem of soil and water contamination by hydrocarbon compounds deriving from petroleum. In-Situ bioremediation treats contaminated

matrices in the location where it was found. Usually, selected microorganisms are pumped into the soil or groundwater (Figure 8). Normally, microorganisms can work up to 30-60 cm deep in the soil and at different depths in water. Therefore, the major limitations are due to the depth of penetration of the pollutants in contaminated medium [59].

Several methods are included in this category [86]:

- Bioventing/biosparging: this method represents the most effective bioremediation technique, in particular for light hydrocarbon contamination. It provides for the insufflation of oxygen and other nutrients within the polluted site to stimulate the degrading action of microorganisms. The simple installation of oxygen and nutrient injectors makes this process feasible and flexible for the treatment of a variety of contaminated sites.
- Biodegradation: oxygen and nutrients (oxygen and electron acceptors) are dispersed inside the contaminated area by means of an aqueous solution that circulates through the solid or liquid medium to stimulate the microorganisms responsible for degradation. This method is used to reclaim contaminated soils and aquifers.

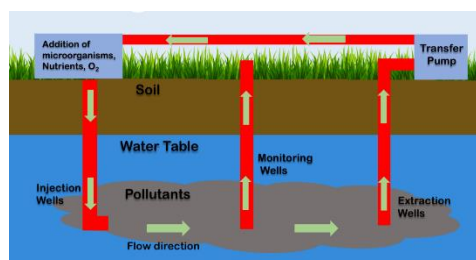


Figure 8. In situ bioremediation

Source: https://en.wikipedia.org/wiki/In_situ_bioremediation

2. Ex situ Bioremediation

Ex-situ degradation processes are not carried out at the site of contamination, but in separate and more monitored area. The contaminated water is pumped out while the contaminated soil is removed [86, 90]. After pollution degradations, the water and the soil are placed in the origin or other areas. The main techniques are:

- Biopiles: the process involves a sort of composting of the polluted matrix inside engineered and well-ventilated cells. This technique is used to decontaminate both soil and water polluted by petroleum products mainly. Biopiles allow the growth of indigenous aerobic and anaerobic

microorganisms. The technique is improved by the landfarming method in order to control the spread of the pollutant through volatilization and leaching [90].

- Bioreactors: the technique is used for ex situ bioremediation of contaminated water or soil. Suspension reactors or aqueous reactors are used as containment vessels. Three-phase mixing devices (solid, liquid and gas) are used to keep the solid or liquid matrix homogeneous and to allow the biodegradation of pollutants by the micro-organisms contained in the biomass [92].

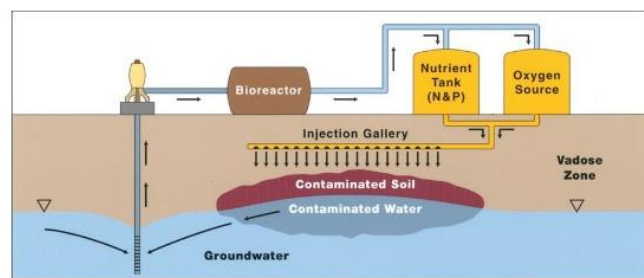


Figure 9. Ex situ bioremediation

Source: <https://slideplayer.com/slide/686417/>

Both In-Situ and Ex-Situ methods of bioremediation are effective. The bioreactor technique, however, provides better results in safety and control, as the conditions of the process are always monitored and the pollutants, microorganisms and nutrients are not leached and removed from the system.

2.1.2.3.2 Phytoremediation

The term "phytoremediation" was coined in 1991 and represents a new method of removal, degradation and containment of pollutants in soil, sediments and water. Plants act as filters and metabolize polluting compounds, using them for its growth [59].

The technique is eco-friendly and economical, in fact green plants and selected vegetation is used to limit a polluted area. The advantages of the phytoremediation are different: long times of persistence of the purification process, aesthetic advantages and low economic expenditure. In addition, the plants have a great capacity for accumulation and transformation of persistent pollutants such as hydrocarbons. The technique is normally used following primary treatment [59, 86].

Phytopurification techniques are divided according to the type of pollutants to be treated:

- Phytoextraction or phytoaccumulation: the plants retain the contaminant inside the roots, the leaves and the shoots. Usually, the sites that need this treatment are polluted by metals.

- Phytotransformation or Phytodegradation or phytostabilization: the process exploits the ability of some plants to absorb organic pollutants from water, soil or sediments and immobilize them in its cavities. The aim of the treatment is to transform a contaminant into a less toxic and less mobile molecule, in order to avoid its diffusion into the environment.
- Rhizodegradation or phytodegradation: the process involves the degradation of contaminants through activity in the rhizosphere, by enzymes or microorganisms such as bacteria, yeasts, fungi secreted by plants, which improve the degradation of contaminants present. During the process a symbiotic relationship is established between plants and microorganisms: the plant provides nutrients to microorganisms that have the task of degrading complex compounds in the contaminated medium.

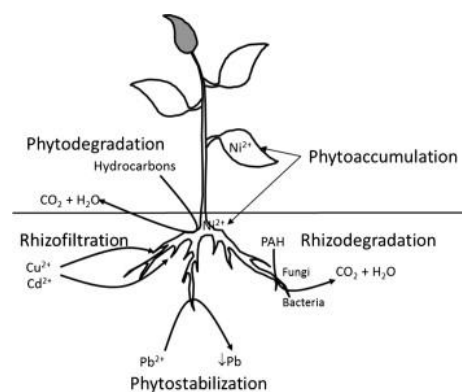


Figure 10. Phytoremediation

Source: <https://www.semanticscholar.org/paper/Electrokinetic-enhanced-phytoremediation-of-soils%3A-Cameselle-Chirakkara/cdd65a786bec013b8c33d9e0c7d31d3a83d8fd1d>

2.1.2.5. Groundwater remediation

Other remediation options are used for contaminated groundwater: as geotechnical techniques to contain the spread of contaminants, mechanical techniques that involve the removal of pollution by excavation and subsequent soil washing, or by pump and treat system, or the treatment of groundwater in situ through the installation of permeable reactive barriers (PRB) for a more selective remediation [93, 94].

The most used techniques for groundwater remediation are:

- Pump-and-treat: these system have been used for decades to remove contamination. The pump and treat technique is an in situ remediation process. The process involves the formation of a hydraulic barrier, in order to pump the water from the water table on the surface, and their

subsequent treatment. After the treatment process, the decontaminated water can be poured into a surface water basin or place of origin (Fig. 11).

One of the main disadvantages of these systems is represented by long operating times for optimal reclamation. In fact, the concentration of the contaminants decreases slowly. When pumping is stopped because the concentration of pumped contaminants has reached low levels, it can often be observed that their concentration increases again, due to the dissolution of the contaminants desorbed by the walls of the water table; these phenomena are called tailing and rebounding [95].

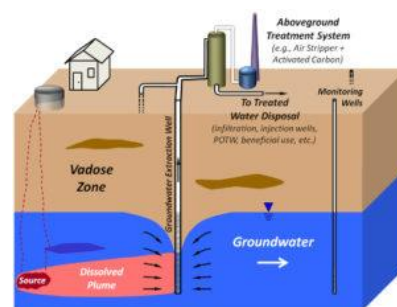


Figure 11. Pump and Treat method

Source: <http://hazmatmag.com/2017/10/performance-assessment-of-pump-and-treat-systems/>

- PRB barriers: this technology is an innovative method of groundwater reclamation. The contaminants are removed through the physical, chemical or biological in situ treatment of contaminated groundwater. The innovation lies in the reactive materials that encountered the contaminated flow and perform redox reactions, precipitation, adsorption, ion exchange and biodegradation (Fig. 12).

The reactive materials are placed inside underground trenches, inside which the flow of polluted water passes. This process allows the removal of contaminants without soil excavation or water pumping [96].

Several processes are used in PRBs, but the most commonly used reactive materials are iron particles which act as a reducing agent through the redox reaction



An important advantage lies in the containment of costs, 50% lower than the pump and treat methods [97].

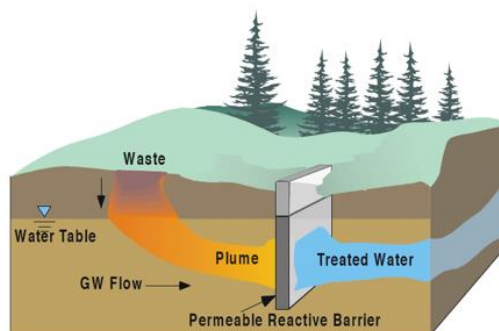


Figure 12. PRB barriers

Source: <http://www.powellassociates.com/PAservices/PAservices/PRBillustration/PRBillustration.html>

2.2 Endocrine Disrupting Chemicals and Bisphenol-A in water

Since the 1990s, concern over the harmful effects of certain chemicals on human health has increased significantly. In particular, the Endocrine Disrupting Chemicals (EDCs) have gained a lot of attention from the scientific community because of the interferences they can cause to the hormonal apparatuses of living organisms [98].

The first studies, to investigate the potential effects of endocrine toxicity of different compounds on living systems [99], were conducted at the University of Florida, led by Professor Emeritus Theo Colborn [100]. Initial epidemiological studies have shown negative health effects for exposure to EDCs, since a large number of chemical compounds have been banned from trade. The damage to health mainly concerns young children, wildlife and the effects are poured on the reproduction of the species and on the proper functioning of the body glands [101, 102].

Endocrine systems perform key functions in all mammals, birds, fish and other types of living organisms. It is constituted by glands, located throughout the body, hormones produced by the glands and released into the bloodstream (or cells) and receptors in various organs and tissues that bind to the hormones to perform a certain function. The female ovaries, the hypophysis, the thyroid and the adrenal glands, the male testes are main constituents of the endocrine system [103].

A generic endocrine cycle starts from the hormones, released by the glands, which transport chemical "information" into the body; hormones reach, through the circulatory system, the receptors, contained in the target cells.

When the hormone has reached the target receptor, the latter executes the hormone's instructions, generating the proteins needed by the cell or activating the genes that allow the construction of a new protein. Thus, the endocrine system regulates all biological processes that occur from birth until death. For this reason, the hormonal alteration of the endocrine system can generate serious dysfunctions in living organisms, mainly in mammals, with serious repercussions on health. EDCs have been defined by the US Environmental Protection Agency (EPA) as an exogenous agent responsible for the interference in secretion, transport, metabolism, functioning of hormones in the body that alter homeostasis, reproduction and the development process [103].

One of the most identified emerging EDCs is bisphenol A (BPA), a fundamental organic chemical used as a monomer in the production of polycarbonate plastics, epoxy resins and flame retardants [104].

2.3 Bisphenol A

Bisphenol A (BPA) is a monomer widely used in the industrial production of food packaging, electronic components, building materials and more. As demand for these products has increased, BPA production has also increased [105].

Around 8 billion tonnes of BPA are produced in the world each year, so its presence in the environment is inevitable [106]. Its release can take place during production processes, transportation and industrial use. Emissions sources are primarily derived from the discharge of contaminated water from production plants, municipal wastewater treatment plants, burning of waste, leaching into landfills and degradation of plastics into the environment [107]. Therefore, the potential risks to human health and the environment are real [105, 108].

BPA is synthesized by the condensation of phenol with acetone (Fig. 13), has a low vapor pressure, a high melting point and a moderate water solubility [109]. BPA has a low or moderate hydrophobicity [110] and a modest bioaccumulation capacity, as suggested by the KOW log values in a range from about 2 to 4. It is estimated that the major environmental ecosystems that contain BPA contamination is associated with basins and aquifers (53%), soil (25%) and sediment (23%) [105, 111].

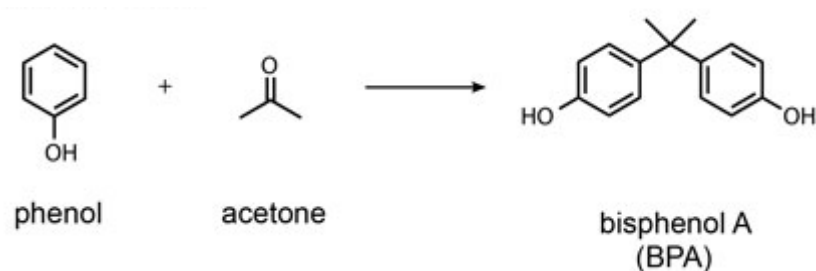


Figure 13. Scheme reaction for BPA production

BPA can also derive from foods and products contained in polycarbonate containers such as baby bottles, cans, etc. from which, undoubtedly, the greatest human exposure derives. Estimated human ingestion of BPA by epoxy resin containers is approximately 7 $\mu\text{g}/\text{person per day}$ [112]. Furthermore, the heating of plastics, in microwave ovens or from heat sources in general, increases the transfer of BPA into liquids and food. Many countries have restricted or prohibited the use of BPA for the manufacture of objects and containers, in contact with food and liquids: the European Union and China have banned the use of BPA in baby bottles in 2011. In 2008, Canada reported BPA as a toxic chemical and prohibited its use in baby bottles. Indeed, France, since 2005, has banned the use of BPA for the production of containers and in all objects used for food [104].

2.3.1 BPA exposure and human health

BPA is classified as an endocrine disruptor. The mechanization of endocrine perturbation/interference involves the generation of toxicity at various physiological levels (Fig. 14). The dysfunction is caused by alterations in hormone secretion or the change from the usual hormone-receptor interaction with related changes in metabolism and hormone production [104].

BPA, even at concentrations below 1 $\mu\text{g}/\text{m}^3$, performs endocrine disruption. Exposure to BPA sources is particularly harmful to the fetus and newborns.

Numerous studies have been performed to investigate the correlation between BPA exposure and effects on health. Krishnan et al. 1993 [113] investigated for the first time the endocrine-disruptive effect of BPA. Currently, it is evident that BPA is able to interfere with the action of estrogens, generating an endocrine disruption in the organism.

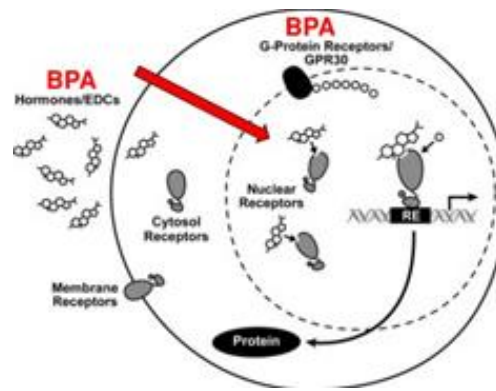


Figure 14. Endocrine perturbation

Source: <https://desdaughter.com/tag/bisphenol-a/page/10/?iframe=true&preview=true%2Ffeed%2F>

Several toxicological studies show that BPA negatively influences the hormonal activity linked to growth, development and reproduction in animals and humans. This compound is able to increase risk for cancers, in particular ovarian, breast and prostate cancer [114, 115] as well as various metabolic disorders such as obesity, endometrial hyperplasia, recurrent miscarriages and polycystic ovary syndrome (Fig. 15) [116, 117].

In fact, BPA can modify the activity of sex hormones, generating mutations and carcinogenicity, immunotoxicity and hepatotoxicity. Other studies have shown that exposure to BPA could lead to the risk of obesity, diabetes and heart disease, especially in infants or children. In particular, Welshons et al. (2006) have correlated serious health disorders to limited exposure of BPA to the fetus, such as congenital dysfunction and malformations before and after birth, which cause functional and structural disorders, and in some cases even death for newborns [118].

Other epidemiological studies have correlated the onset of different types of cancer at BPA exposures. This evidence was confirmed by in vitro studies, demonstrating that low doses of BPA can contribute significantly to the development of mammary tumors and metastases in mice, with increasing aggressiveness in cells potentially exposed to this type of tumor [117, 118]

Furthermore, recent endocrinological research has correlated human reproductive system dysfunctions to chronic BPA exposures. Epidemiological data associate these exposures with an increase in erectile difficulty and a decrease in sexual desire.

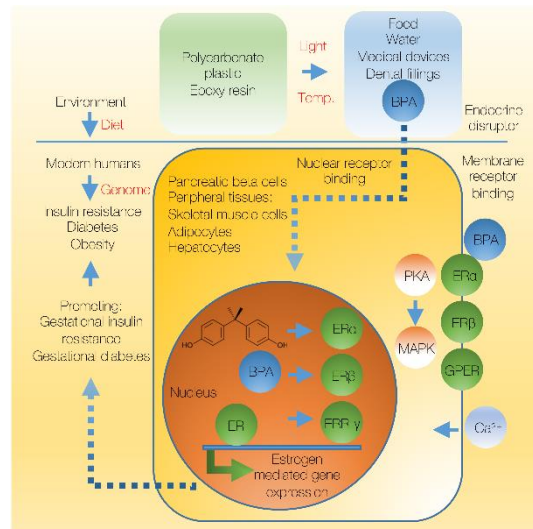


Figure 15. BPA sources and consequences

Source: <https://peerj.com/articles/3809/>

The major source of BPA exposure to humans is through ingestion of contaminated food, while workers who are involved in the production of BPA have high risks of chronic exposure through epithelial contact and inhalation. USEPA has established a reference dose (RfD) for humans equal to 50 µg of BPA/kg/day [119].

2.3.2 BPA contamination

The scientific interest in monitoring the concentrations of BPA in different environments (water, soil and air) has increased enormously in recent years [120].

The most worrying situation concerns the contamination of water, in fact high concentrations of BPA in groundwater have been detected, particularly in the vicinity of agricultural areas and landfills [121]

The main source of BPA contamination in the aquatic environment comes from industrial activities, discharges from wastewater treatment plants and landfills.

The concentrations of BPA in the sea basins are lower than those of freshwater. However, the degradation of plastic products, especially in marine basins, where large quantities of plastic waste are accumulated, could release significant amounts of BPA and its bioavailability in marine environments is favoured by its greater compatibility with salty rather than fresh water [112].

The concentration values of BPA in waters show a widespread contamination all over the globe.

Huang et al. [122] found that the concentration of BPA is higher in industrial areas than in other areas less subject to sources of pollution. USEPA estimates [119] show BPA concentrations in groundwater in the United States ranging from 0.001 to 2 mg/L. In England, the BPA concentration reaches up to 2.2 mg/L [123]; Yamamoto et al. [124] found that BPA can reach values up to 17.2 mg/L in landfill leachate, probably due to the degradation of plastic waste. Basheer et al. [125] collected superficial samples of seawater in several coastal areas of Singapore with concentrations ranging between 0.001 and 0.3 mg/L. Lacorte et al. [126] and Latorre et al. [127] found concentrations of BPA in groundwater, in several agricultural areas of Spain, of 0.1 mg/L and >0.2 mg/L, respectively. While, Godejohann et al. [128] have analyzed groundwater close to a site of ammunition destruction in Switzerland, finding BPA concentrations of 1.5 mg/L. High concentrations of BPA were also found near wastewater treatment plants (up to 370 µg/L) [129], in river waters in Germany (up to 0.8 µg/L) [130], in bottled water in France (0.07 - 4.21 µg/L) [131], to name just a few. Azevedo et al. [132] found values above 0.2 mg/L at some points near industrial areas in Portugal; Patrolecco et al. [133] found BPA concentrations in the Tiber river (Italy) up to 0.02 mg/L. Loos et al. [134] monitored river water in Belgium and Italy with maximum concentrations of 0.01 mg/L and 0.02 mg/L, respectively. Pojana et al. [135] found similar concentrations in water samples in the Venice Lagoon, with values between 0.01 and 0.015 mg/L.

Studies that have monitored both the water and the sediments below report much higher concentrations of BPA in sediments than in the upper water column. Funakoshi and Kasuya [136] determined an important dependence between the BPA levels of the aquifer (or upper water column) and those in the sediment.

Contamination of bisphenol can generate serious interference with nitrogen fixation at the roots of plants, with growth of some harmful bacteria. Despite the half-life in the soil of a few days, its chemical-physical characteristics make it a harmful pollutant.

The primary source of BPA in soils is the presence of sewage sludge or polluting waste on the ground [137]. The reported levels of BPA vary by many orders of magnitude, with concentrations ranging from 0.10 to 3×10^7 mg/kg of dry weight [118].

The average BPA concentration in soils is 150 µg/kg dry weight (p.w.). Agricultural fields added with biosolides or irrigated with contaminated water present the highest concentrations.

2.3.3 Remediation technologies for BPA pollution

2.3.3.1 Physical and chemical treatments

In recent years, numerous studies have been made to develop efficient adsorption methods for the removal of chemical substances interacting with the endocrine system, such as BPA, in aqueous matrices. The most used techniques for the degradation of BPA are ozonization, application of ultrasound, oxidation with phosphorus and electrochemical oxidation [138].

Furthermore, the use of membrane filtration for the removal of BPA from water and wastewater is increasingly widespread. Although these physico-chemical methods are very effective in eliminating endocrine disrupting compounds (EDCs), their high costs and the risk of generating toxic by-products represent obstacles to large-scale application [139].

2.3.3.2 Biodegradation of BPA

Biodegradation methods by microorganisms play an important role in the degradation of BPA molecules. In fact, the use of the metabolic potential of microorganisms to mineralize pollutants is considered a safer and more economical alternative to the widely used physical-chemical processes.

The molecule can be metabolised by many microbial families and numerous BPA-degrading strains have been isolated from water, soil and biomass from wastewater treatment systems. In the environment, the degradation of BPA occurs thanks to the metabolic action of these bacteria, but also the degrading abilities of fungi and algae are used [139].

2.3.3.3 Integrated systems for the removal of BPA from water

In recent years, the interest in combined methods of BPA removal from wastewater is an alternative to the conventional processes described above. Integrated technologies involve the integration of chemical and biological approaches, where conventional biological treatment is supported by Advanced Oxidation Processes (AOP) such as photocatalysis, ozone oxidation, Fenton and wet air oxidation (WAO). Normally, these combined methods have been applied to increase biodegradability and improve water quality, with the aim of maintaining low costs and high efficiency [138, 139].

2.3 Mercury pollution

Mercury (Hg) is a heavy metal present in nature in three different chemical forms: elementary form, which evaporates in contact with the air; the inorganic form which is in the form of mercuric oxide (HgO), mercuric chloride (HgCl₂) and mercuric sulfide (HgS); and finally the organic form, such as methylmercuric chloride, dimethylmercury and phenylmercuric acetate, formed by the combination of mercury with carbon and other elements [139]. Methylmercury is the most common in the environment, produced by the methylation of inorganic (mercury) forms of mercury by microorganisms present in soil and water [140]. In the environment it can also be in cation form as Hg¹⁺ and Hg²⁺ [141].

The strong environmental persistence of mercury in its various forms, involves a high degree of human exposure to these polluting sources, and a consequent risk to human health.

2.3.1 Mercury toxicity and carcinogenicity

Mercury exerts its toxicity by involving oxidative stress and interfering with the body's chemical and biological functions. At the cellular level, the Hg (II) and MeHg species interact and bind with protein residues, reducing cellular antioxidants and causing the accumulation of reactive oxygen species (ROS), normally eliminated by antioxidant species [139]. The absence or decrease of antioxidant enzymes generates defects in oxidative phosphorylation and in the transport of electrons between coenzymes and proteins that allow cellular respiration [142] and inducing the high diffusion of electrons in molecular oxygen with the consequent increase in radical species of oxygen. Both organic and inorganic mercury have been shown to alter calcium homeostasis through different mechanisms: organic mercury compounds (MeHg) increase intracellular calcium by mobilizing intracellular reserves, while inorganic mercury compounds (Hg²⁺) increase intracellular calcium reserves through the influx of calcium from the extracellular medium [139, 143].

Although, until recently, it was thought that the onset of oncogenesis or tumor inhibition was not related to DNA mutations, several studies have shown the opposite and that mercury affects cellular organelles and their biological functions, causing defects in transcription, signal transduction and amplification of oncogenesis [139, 145]. Thus, mercury has been shown to induce ROS formation causing DNA damage in cells and trigger cancerous processes. Furthermore, the direct action of these free radicals on nucleic acids can generate genetic mutations [146].

2.3.2 Mercury in the environment

Mercury is a toxic pollutant, very persistent in the environment that induces serious alterations in human and animal tissues following direct and indirect exposure [147].

This metal is widely used in various industrial processes, in electrical and electronic equipment, in numerous household products, in dental fillings materials, in industrial processes, in barometers, diffusion pumps, batteries and many other laboratory instruments. Even today, it is used in medical equipment, data transmission equipment, telecommunications, mobile phones, mercury vapor lamps and advertising posters [139].

After 1980s, the industrial demand for mercury began to decline, up to 1994, with the introduction of prohibitions on uses in products in contact with humans, such as pesticides, paints and more.

Natural sources such as volcanoes and erosion of the crust represent one of the main sources of the spread of mercury in the environment, while anthropogenic sources are responsible for one third of mercury emissions [148].

The main source of mercury comes from mines, refineries, medical products and particular types of industries that work metals.

Among anthropogenic sources, 65% come from combustion phenomena and occur mainly in coal-fired power plants. The 11% derives from mining and more than 20% from production processes and waste. Several estimates show that the quantities of mercury released into the environment from anthropogenic sources are equal to about 6×10^3 tons per year [139].

Although the use of mercury has decreased in recent decades, high concentrations of residual metal are still present in sediments and in aquifers and groundwater.

Human exposure to different sources of mercury mainly occurs through environmental pollution, industrial emissions and food contamination [149].

Following the degradation of the earth's crust and anthropogenic emissions, mercury enters the water. Mercury in water undergoes a methylation process by algae and bacteria that transform it into methylmercury (Fig. 16). Subsequently, it accumulates in the food chain starting from fish and reaching human being [139, 150].

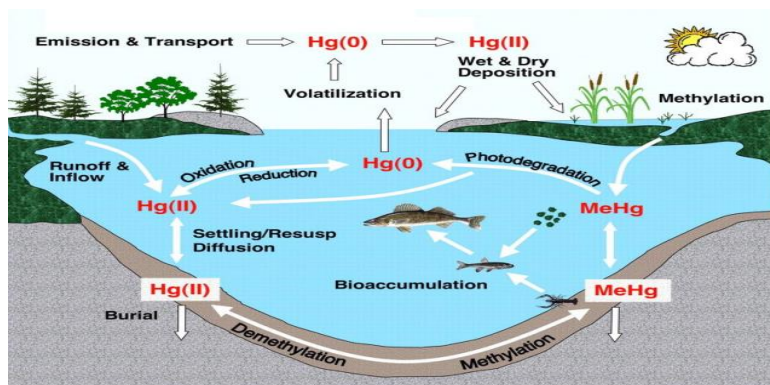


Figure 16. Mercury cycling in the environment

Source: <https://sites.tufts.edu/sciencediplomacy/files/2017/07/MercuryGame-International-Mercury-Assessment.pdf>

When it enters the blood, Hg (0) is able to overcome cell membranes and is oxidized to highly reactive Hg²⁺. While, methylmercury is absorbed in the gastrointestinal tract and accumulated in lipid tissues due to the very low excretion rate [139].

The greater quantity accumulates in the kidneys, in the neurological tissue and in the liver. In light of these considerations, all forms of mercury are toxic to humans and their effects include widespread toxicity [151].

2.3.3 Remediation technologies for mercury polluted water

Mercury can enter water and drinking water in various ways, through rain, by transport with air, by erosion of the earth's crust and subsequent contact with surface water reserves such as lakes, rivers and water basins. In addition, mercury can infiltrate underground water reserves from industrial waste. Currently, there are several decontamination techniques for mercury-contaminated waters. The following Table 3 summarizes the main conventional treatment techniques [152].

Table 3. The main conventional treatment techniques for mercury removal

Processes	Method
<i>Precipitation Treatment Processes</i>	Coagulation/co-precipitation
	Sulfide precipitation
<i>Adsorption processes</i>	Activated carbons adsorption
	Other adsorption processes

<i>Ion exchange treatment</i>	Ion exchange resin
<i>Other processes</i>	Chemical reduction
	Membrane separation
	Bioremediation

2.3.3.1 Precipitation treatment processes

Precipitation and coagulation techniques are among the most established approaches to remove mercury from polluted waters.

2.3.3.1.1 Coagulation/co-precipitation

The removal of inorganic and organic mercury by coagulation/co-precipitation is the most used technology for the decontamination of polluted water.

The effectiveness of mercury removal for this technology strongly depends on the chemical-physical characteristics of the water and the presence of other contaminants in the aqueous phase [153].

The coagulants that are normally used are aluminum sulphate (alum), iron salts and lime. The mechanism of mercury removal through the use of alum and iron is most likely due to the adsorbing co-precipitation, in which an ion is adsorbed on the surface of another solid, formed by addition of alum and precipitation of aluminum hydroxide or by addition of an iron salt (ferrous or ferric) and precipitation of iron hydroxide [154].

The adsorption process is isothermal and the treatment performance can be improved by acting on the characteristics of the solids and on the pH, in order to obtain a solid surface ideal for mercury speciation.

2.3.3.1.2 Sulfide precipitation

Sulfide precipitation is one of the most commonly reported precipitation methods for the removal of inorganic mercury from wastewater. In this process, the sulfide (e.g., as sodium sulfide or another sulfide salt) is added to the water stream to convert the soluble mercury (Hg^{2+}) in the form of relatively insoluble mercury sulfide (HgS).

As with other precipitation treatments, the process is usually combined with pH regulation, flocculation and subsequent separation of solids through sedimentation or filtration processes. Flocculation, with or without a chemical coagulant, can be used to improve the removal of precipitated solids. The most effective precipitation with the use of the minimum dosage of sulfide, is obtained in a neutral pH range. Mercury removal efficiency decreases significantly for pH values above 9 [152, 153]. The methods of sulfide precipitation represent the most used practice for the removal of mercury in plants that need to treat this type of polluted water. The removal efficiencies are in a range between 95% and 99% when the processes are respecting the stoichiometric relationships between mercury and sulphides [152].

2.3.3.2 Adsorption processes

Adsorption processes have high mercury removal efficiencies, especially when pollutant concentrations are around 100 mg/L. The activated carbons are preferentially used with respect to other types of adsorbent material. Other adsorbents may be materials of vegetable or mineral origin, which undergo pretreatment before being used.

The materials used, albeit marginally, are activated carbons from peanuts and treated with bicarbonate, modified lignin materials, coal ash and agricultural waste [153].

Also some metal hydroxides are used as adsorbents and, in this case, the process is commonly called coagulation or co-precipitation when metal hydroxides are used.

2.3.3.2.1 Activated carbon adsorption

Granular activated charcoal (GAC) is the most commonly used adsorbent system for the treatment of industrial wastewater containing mercury [152]. The process involves the passage of contaminated water through columns in series until the contaminant is no longer detected or its concentration is so low that it can be discharged into an effluent.

The use of multiple columns makes it possible to fill the first column with a greater capacity of adsorbent, in order to remove the greater pollutant load, while the steps in the subsequent columns allow to break down the residues of the contaminant. Furthermore, when the activated carbon of a column reaches saturation, then the adsorbent material can be regenerated or replaced [154].

An alternative method of treatment involves the use of activated carbon powder (PAC). The PAC is usually added to a contact reactor and the PAC solids are subsequently removed in a subsequent separation step. Normally, the PAC is not regenerated for re-use, due to the high costs of the process.

2.3.3.3 Ion exchange processes

Ionic exchange processes are carried out inside packed columns. The process involves four operations per single removal cycle: assistance, backwashing, regeneration and rinsing.

2.3.3.3.1 Ion exchange resin

During the working phase, the ion-exchange resin in the packed column is contacted with the water containing the mercury to be removed. The resin is considered to be exhausted when a mercury bound concentration at the column outlet is reached. A subsequent backwashing process is carried out by washing the ion-exchange material, then a backwashing step is started to extend the bed and remove the particles that could clog the packed bed. The spent resin is then regenerated through contact with the concentrated solution in order to obtain a material having the same concentration as the original exchange ion, so that a reverse exchange process occurs [154].

Advantages

- It also works in case of variability of the water composition;
- It can reach a zero contaminant concentration at the end of the process;
- It is available in a wide variety of specific resins;
- It can normally obtain an inversion of advantageous selectivity after regeneration.

Disadvantages:

- It has a maximum peak of contaminant removal;
- It can give a variable quality of the effluents;
- It generally can not be used for waters with a high level of total dissolved solids content.

2.3.3.4 Other adsorption processes

In addition to the treatment technologies of precipitation, adsorption and ion exchange, other processes can be used for the removal of mercury from water, such as chemical reduction, separation membranes and bioremediation [153].

2.3.3.4.1 Chemical reduction

Metals have their own standard electrical potential that determines their location in the electrochemical series, which is a series of elements in decreasing order of their standard potential. These characteristics have been exploited in order to remove the ionic mercury from the solution by reduction with another metal higher up in the electrochemical series and then separated by filtration or other solids separation technique. The reducing agents include aluminum, zinc, iron, hydrazine, stannous chloride and sodium borohydride [153].

2.3.3.4.2 Membrane separation

Membrane filtration processes for the removal of mercury from water are effective but poorly used due to the high costs and higher volume of final residues compared to other treatment processes. Furthermore, the effectiveness of the process is influenced by the presence of contaminants in untreated water such as suspended solids, organic compounds, and other contaminants that can cause membrane clogging.

Several membrane processes have been applied for the treatment of water and wastewater mercury. These include ultrafiltration, loaded filtration, cross-flow microfiltration, magnetic filtration and reverse osmosis. The ultrafiltration processes represent the most used techniques: they occur through the introduction of a pressure and the use of porous membranes [152]. These systems differ from reverse osmosis systems for working pressures that are less than 150 psi.

In recent times, chelation combined with ultrafiltration has spread more to heavy metal removal processes, including mercury. This concept is based on the reaction of ligands with cationic metal components to form a complex containing the chelated metal, and then remove it later by ultrafiltration [154].

2.3.3.4.3 Bioremediation

Bioremediation techniques (in situ or ex situ) have been shown to be effective in several studies. The mechanisms that allow bioremediation to reduce the concentration of mercury exploit the conversion of mercury into species that are retained in biomass or converted into species that are more easily removed from water by another technology, such as precipitation or adsorption [152, 153].

Bioremediation of mercury can also occur with the use of microbes with reduction of costs and increase in the effectiveness of degradation. Mercury-resistant bacteria are a promising solution

because they passively release the non-toxic forms of Hg into the environment. Furthermore, they do not pose the problem of the accumulation of contaminated biomass [154].

2.3.3.5 Other remediation technologies

When mercury pollution hits a groundwater reserve, emerging in-situ procedures, such as permeable reactive walls and leaching, have been developed. These technologies are similar to those used for the removal of hydrocarbons, but in some situations, the efficiency of removal is low or economically disadvantageous [154].

2.4 Escherichia coli contamination

Currently, one of the major objectives that humanity must achieve is global access to safe drinking water. The contamination of water from faecal coliform bacteria is the biggest problem that afflicts the whole world, especially the underdeveloped countries [155, 156].

In fact, faecal coliform bacteria are a group of bacteria that come from faecal droppings of humans, livestock and wildlife. The most widespread member of this category is *Escherichia coli*.

These organisms have the ability to grow at high temperatures, mainly in warm, dark and wet environments [157], unlike other microorganisms belonging to the total colonic group. Under favourable conditions, these bacteria reproduce rapidly and multiply to form colonies.

The main contaminations derive, mainly, from wastewater treatment plants, from the agricultural leaching that collects the outflow from the areas contaminated by the manure of the fauna. In addition, the rains cause the leaching of these microorganisms that are poured into aquifers and reservoirs [158].

When the *E. coli* is found in water, it is clear indication that the water supply has been contaminated by microorganisms such as animal waste. Indeed, the *E. coli* can live outside its host for long periods and this makes it possible to consider it as an indicator organism of contaminated water.

Around 1880s, Von Fritsch used bacteria for the first time as indicators of water quality, isolating some microorganisms deriving from human feces and correlating them with different types of pneumonia. Subsequently, several scientists began to carry out bacteriological tests of the waters and in 1885, Escherich isolated and described the *Bacillus coli* and renamed it *Escherichia coli* [156].

From that moment on, scientists concluded that in the waters must be identified organisms characteristic and dangerous to human health, such as *Escherichia coli*, to prove a contamination [155].

From the late 1800s, several methods were developed and adopted for the enumeration of *E. coli* and bacteria by direct plating of water samples onto agar plates [156]. However, the counting of bacteria colonies in the water was recognized by bacteriologists in the early twentieth century, and the research of *E. coli* has become the universal indicator for monitoring water quality.

In general, the presence of *E. coli* microorganism is not of great concern for human health, in fact most of the strains are harmless and live in the intestine of healthy men and animals. However, there are some strains that cause serious illness in humans such as *E. coli* O157: H7 (Ee KOE-lye), which can contaminate water, foods like meat and green leafy vegetables. This strain produces a powerful toxin that can cause serious illness [159].

E. coli O157: H7 bacteria are found mainly in limited groups of livestock farms where they can live in the intestine of healthy cattle. The release or spread of these germs occurs because of intestinal movements of human or animal infected with water, such as private wells or aquifers [156].

2.4.1 Effects of Escherichia coli on human health

E. coli is genotypically and phenotypically different. Classification is based on the reaction of antibodies to different types of antigens (Kauffman classification): the somatic (O), capsular (K) and flagella (H) antigens. Currently, *E. coli* has been shown to possess 173 O, 103 K and 56 H antigens. Serotypes consisting of the combination of O and H antigens have been identified, in particular the serotype O157: H7 represents the most dangerous for human health, as mentioned above [160].

Pathogenic *E. coli* can cause a large number of human diseases that start from the gastrointestinal tract and then spread to extraintestinal areas such as the urinary tract and the nervous system. In the countries of sub-Saharan Africa and South Asia, diseases deriving from *E. coli*, mainly hemorrhagic diarrhea, can cause mortality worldwide, especially in children in the first years of life [159, 160].

E. coli is transmitted to other animals and humans via contaminated feed and food, and drinking water. Infection occurs by mouth or by inhalation of contaminated dust. *E. coli* bacteria can also be transmitted by direct contact from animals to humans.

The sources of contamination have been mainly associated with the consumption of contaminated food, such as meat and vegetables, and not perfectly drinking water [156].

The severities of dysfunctions differ among the different pathogenic types, classified into six major diarrheagenic *E. coli* pathotypes: enteropathogenic *E. coli* (EPEC), Shiga toxin-producing *E. coli* (STEC) (eg, enterohemorrhagic *E. coli* [EHEC]), Shigella/enteroinvasive *E. coli* (EIEC), enteroaggregative *E. coli* (EAEC), diffusely adherent *E. coli* (DAEC), and enterotoxigenic *E. coli* (ETEC) [50, 160].

In most of the world, as previously mentioned, the *E. coli* O157: H7, belonging to the STEC pathotype, is the most harmful serotype that causes human diseases.

After ingestion, *E. coli* survives the acidic conditions of the stomach, succeeding in colonizing the intestinal mucosa, to bind to the epithelial cells, by means of numerous filaments (Fig. 17) that escape from the pathogenic bacterium, and to generate virulence through Shiga toxin production [160].



Figure 17. Escherichia coli bacteria

Source: <https://wickhamlabs.co.uk/technical-resource-centre/fact-sheet-escherichia-coli/>

Related infections can range from mild diarrhea to hemorrhagic diarrhea. After this initial symptom, fever, abdominal cramps and vomiting are recorded. The incubation period occurs in a few days and the symptoms remain 10 days. On average 5% of *E. coli* O157: H7 infections lead to acute renal failure [161].

Patients who contract the infection undergo the onset of hemorrhagic colitis in the following days after the initial onset of diarrhea. While 30% of patients come to suffer from hemolytic uremic syndrome (HUS), which includes heart failure, severe gastrointestinal problems, chronic renal dysfunction, diabetes and neurological problems [50].

Ultimately, despite the intestinal and extraintestinal dysfunctions are different in severity and symptoms, the *E. coli* appears to be an important public health problem. Furthermore, the pathogen continues to evolve, as witnessed by the epidemic throughout Europe, in 2011. This also indicates the ease of transmissibility of pathogenic *E. coli* and the numerous potential sources of contamination and transmission.

2.4.2 *Escherichia coli* in the environment

Recent studies have shown that *E. coli* can survive and reproduce outside the intestinal tract, even for long periods, especially if the weather is warm or mild, causing widespread pollution [160]. Potentially pathogenic *E. coli* strains can also survive and grow in natural environments and potentially affect water quality.

Potential sources of environmental bacterial contamination derive mainly from sewage, faeces and waste of the animals, farms, landfill leachate, wastewater treatment plants.

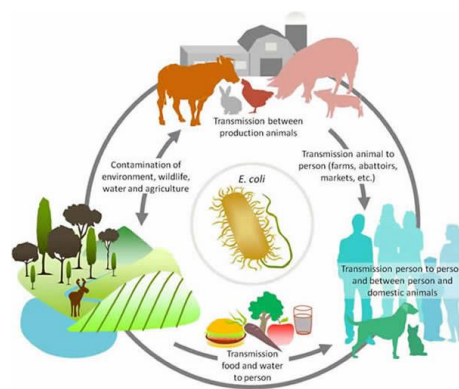


Figure 18. Sources of *E. coli* contamination

Source: https://www.tankonyvtar.hu/en/tartalom/tamop425/0032_vizkeszletgazdalkodas_es_vizminoseg/ch14s04.html

Unfortunately, the most important issue is related to the ability of *E. coli* to survive and migrate between one habitat and another, moving from soil to groundwater and vice versa [162].

Escherichia coli O157: H7 represents a serious contamination, coming from different agricultural and industrial sectors, and it is poured directly on the environment (Fig. 18). The concentrations of *E. coli* O157: H7 from animal waste range from 10^2 to 10^5 CFU/g of faeces and spread in the agricultural, soil and water [164].

Soil factors such as structure, porosity and density cover crucial roles for their adsorption and gravitational movement with water [163]. While, the determinant diffusion factors in water, are

related to pH, available nutrients and moisture, temperature and the presence of other toxic contaminants for E. coli. However, for organic media such as manure and sewage, the absorption and spread of bacteria is also linked to its biophysical characteristics [162].

Escherichia coli O157: H7 and other pathogenic E. coli strains are also known to be very persistent on the surface of green leafy vegetables (e.g. lettuce and spinach) and can cause food poisoning outbreaks. Some E. coli can become naturalized (i.e. become part of the indigenous microflora) in these environments [160].

Some strains of E. coli, coming from irrigation water, manure and percolates, produce filamentous structures that allow cells to bind to organic surfaces, such as those of lettuce plants or other vegetables, or to roots and spread [165]. This capacity gives the pathogenic bacterium enormous resistance against washing and disinfectants. Therefore, contamination can also move into the food chain.

Infections transmitted by food are constantly growing; some estimates show worrying values: the diseases transmitted by contaminated food are about 80 million. In the US more than 5.000 deaths are recorded each year for this cause. High percentage is caused by E. coli O157: H7 [166].

Moreover, E. coli O157:H7 infections were related to the consumption of contaminated water or use of surface water for recreational purposes [165]. Several cases of sick people have been reported in North America after drinking polluted water or swimming in contaminated water; in May 2000, in Canada, more than 2000 cases of infection and 7 deaths, due to bacterial contamination of E. coli O157:H7, were recorded due to consumption of drinking water contaminated by feces (Walkerton epidemic) [167].

2.4.3 Water pathogens decontamination methods

Currently, many water pathogen decontamination techniques are used in order to ensure safe and hygienic drinking water. Pathogenic contamination affects surface and groundwater, due to effluent from sewage treatment plants, agricultural runoff and leaching of animal feces.

Depending on the degree of contamination, the waters require different treatments, single or multiple, to provide drinking water for the human population [168, 169].

Normally, a single treatment process is not able to remove the different types of pathogens from the water, for this reason the use of multiple stages is necessary to make available water with a high level of hygiene [170].

Disinfection treatment methods include chlorination (and its derivatives), ozonation and ultraviolet light. These techniques are integrated with other treatments (multiple treatments), such as coagulation/flocculation, sedimentation and filtration.

Groundwater and surface water can undergo these treatments. The effectiveness of disinfection is judged by researching the indicator microorganism (total coliform bacteria or E.coli)

The most common techniques for the decontamination of water from pathogens are reported in Table 4 and described in the following paragraphs [168].

Table 4. The most common techniques for the decontamination of water from pathogens

Treatment	Method
<i>Disinfection treatments</i>	Chlorination
	Ozonation
	UV radiation
<i>Chemical and physical treatments</i>	Coagulation and flocculation
	Sedimentation or flotation
	Filtration
	Membrane technologies

2.4.2.1 Disinfection treatments

The factors that determine the choice of the methodology to be used to disinfect water for human consumption are [171]:

- the efficiency of removal / degradation of pathogens in the water (bacteria, viruses, and protozoa);
- the ability to limit the by-products that are formed in the water following the treatment;
- the final quality of the decontaminated water;
- the feasibility of using the technology based on the type of water and the volume to be treated;
- the ability to control the process.

The fundamental chemical-physical factors that regulate disinfection kinetics are:

- type of disinfectant and its concentration;
- type of micro-organism to be removed;

- temperature, pH, suspended solids content and water turbidity;
- time of application of the disinfectant.

Furthermore, if the temperature exceeds 14-16 °C, the ability of microorganisms to multiply and form resistant biofilms on the surface increases [172].

2.4.2.1.1 Chlorination

Chlorination is currently the main method of treatment of water contaminated by pathogenic microorganisms. Chlorine compounds have been used for disinfection processes for almost a century [169]. Chlorination occurs by means of chemicals such as gaseous chlorine, chlorine dioxide, hypochlorite, chloramines, and other disinfectant chemicals.

The chlorination process exploits the oxidizing power of the chlorinated products, which acts on the cell membranes and inactivates the microorganisms. This method of treatment showed a high degree of disinfection against microbial pathogens, in particular for enteric bacteria [168, 169].

Some pathogenic bacterial strains, as in the case of E.coli, developed phenotypic resistance and adaptation to disinfection with chlorine.

Both for this reason and for the production of toxic and carcinogenic disinfection by-products, the use of chlorination is in the process of being abandoned [168, 173].

2.4.2.1.2 Ozonation

Ozone is a powerful oxidizing agent that causes inactivation of vegetative bacteria. It is widely used in wastewater treatment plants.

Ozone is generated by a source of gas that contains oxygen (or liquid compressed air). The gas pass through a chamber, in which the oxygen molecules are dissociated in atomic form, from an electron source. Then, they collide with each other, forming unstable ozone molecules (O₃) [174].

When ozone is introduced into the water for remediation, free radicals are decomposed and formed, such as hydrogen peroxide (·OOH) and hydroxyl (·OH). These free radicals are highly reactive and have a high disinfecting capacity, thus contact times are lower than that of other disinfectants.

In addition, ozone leaves no toxic residues and quickly turns into oxygen.

Ozonation is also used in combination with hydrogen peroxide in photocatalytic reactions and ultraviolet radiation to increase the efficiency of inactivation and degradation of pathogens and pollutants [175]. This combination of oxidation techniques is known as Advanced Oxidation Processes (AOP).

2.4.2.1.3 Ultraviolet applications

In recent years, the Ultraviolet (UV) application has been used in the disinfection processes of contaminated water, in particular from pathogenic strains.

UV disinfection systems consist of just a few necessary components: UV lamp, treatment chamber and control panel, which makes it an easy-to-use technology. These advantages make it possible to use the system in existing treatment plants (Fig. 19) [168, 176].

This technology exploits the ability of DNA to absorb the photonic energy of UV light, causing degradation of target microorganisms.

Inactivation involves the breaking and / or damaging of DNA, preventing replication and related processes, and generating rapid destruction of bacteria [177]. The inactivation of microbial pathogens, using UV radiation is much studied, for the application improvements.

The UV light is classified according to the wavelength: UV-C (100-280 nm), UV-B (280-315 nm) and UV-A (315-400 nm).

The UV wavelengths between 200 and 300 nm are considered germicidal, due to the fact that are absorbed directly by the DNA. In particular, the wavelengths of 254 nm and 280 nm may potentially be the best for eliminating microorganisms, since at these values there is the highest rate of absorption of photons by the DNA, above all, when the chlorination techniques do not are able to inactivate pathogenic bacteria [178].

While, UV-B and UV-C wavelengths have less germicidal power and, consequently, less use.

The most important factors, on which the effectiveness of UV rays depend, are: the design of the apparatus, the physico-chemical characteristics of the medium, the type of contaminating microorganism and the characteristics of the UV source (e.g., wavelength, power, etc.).

Conventional disinfection using UV mercury vapor lamps: monochromatic low pressure lamps, and polychromatic medium pressure lamps, emitting radiation at 253.7 nm and between 700 nm – 200 nm, respectively. But in the last few decades, UV-LEDs have played an important role as an alternative to mercury vapor lamps, in fact, lamps are made of not toxic compounds, such as aluminum nitride (AlN) or gallium and aluminum nitride (AlGAN) [179]. Another advantage of LEDs lamps is the high energy transmission efficiency with less emission of heat [168].

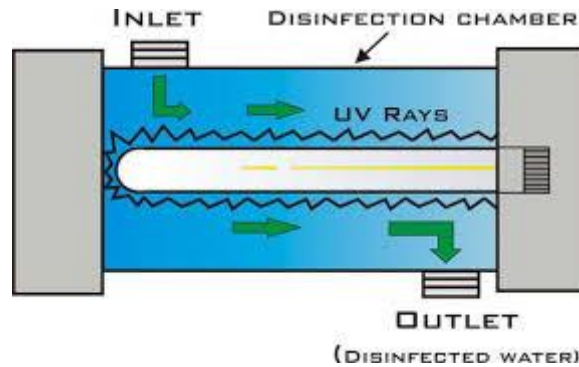


Figure 19. UV apparatus

Source: <https://www.kent.co.in/blog/a-brief-note-on-uv-water-filtration/>

2.4.2.2 Physical and chemical treatments

Contaminated water requires additional treatments, before and/or after disinfection processes, to remedy undesirable characteristics such as color, odor and turbidity, which can affect the final water quality.

Therefore, the water contaminated by microorganisms can undergo other chemical or physical treatments, also to avoid the consumption of excessive doses of disinfectants: for example, the pre-sedimentation to remove suspended solids, filtration and coagulation to reduce organic matter in the raw waters [168].

2.4.2.2.1 Coagulation and flocculation

The conventional techniques used initially are coagulation and flocculation.

Normally, coagulants are made up of inorganic compounds with a positive charge. When added to the water, their charge interacts with the negative charge of the waste and with the other particles in the water. This behavior allows the formation of flakes, which aggregate the suspended organic particles such as algae, bacteria and particles of organic and inorganic material (flocculation). The most common coagulants used are aluminum sulfate, ferric sulfate and ferric chloride [180].

2.4.2.2.2 Sedimentation or flotation

The sedimentation step is subsequent to the coagulation process: the flakes decant at the bottom of the treatment tank due to gravity [181].

Injection of air bubbles are carried out in the tank if the flakes are very light, in such a way as to favor the floatation and the subsequent mechanical removal (floatation dissolved in the air) (Fig. 20).

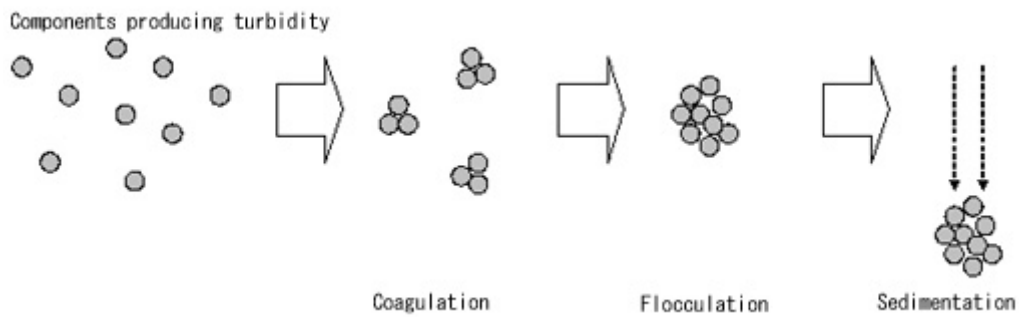


Figure 20. Physical and chemical treatments

Source: <https://www.safewater.org/fact-sheets-1/2017/1/23/conventional-water-treatment>

2.4.2.2.3 Filtration

The filtration process allows to retain suspended organisms and particles, which have escaped previous steps. After the flakes have settled on the bottom of the chamber or treatment tank, the overlying water is passed through filters, consisting of different filter materials such as sand, activated carbon, etc. to remove particles, such as dust, parasites, bacteria, viruses and chemicals.

A particular type of filtration is membrane filtration (Fig. 21).

Membrane filters can remove particles larger than 0.2 μm , for drinking water, including E.coli, Giardia and Cryptosporidium. Microfiltration (MF) and ultrafiltration (UF) [170] are the most used membrane processes for the removal of microbiological charge in drinking water treatment.

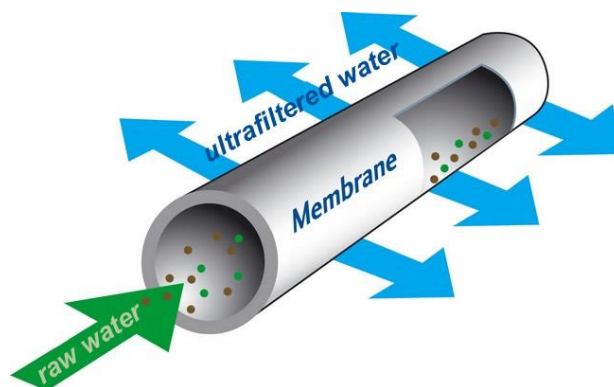


Figure 21. Ultrafiltration system

Source: <http://legmannews.com/global-ultrafiltration-membrane-filtration-market-growth-and-regional-analysis-by-2022/>

CHAPTER 3

3 Pollutants and environment

3.1 Interactions between contaminants and environment

Normally, organic and inorganic chemical contaminants interact with the environment (soil, water, air) in different ways. They can remain in the environment and undergo various processes of diffusion or degradation or change of form, or can be retained by a material, following the establishment of interactions. Factors that play key roles in the retention phenomena are:

- chemical structure of the pollutant;
- characteristics of the medium in which they are widespread;
- solubility of the contaminant in the aqueous or solvent medium.

Adsorption and absorption are the most frequent phenomena occurring in the environment. The evaluation of two phenomena can be carried out by studying the correlations between sorbent material and pollutant and their chemical-physical characteristics.

Adsorption is a process that involves the surface properties of the adsorbent, while absorption involves the entire volume of the material.

3.1.1 Adsorption mechanism

Adsorption is the ability of a material to retain on its surface ions or molecules (gaseous or liquid). Normally, in an adsorption process, the solutes are removed from the liquids, through surface interactions: the phenomenon generates a film of adsorbed on the surface of the adsorbent [182, 183].

The ability of an adsorbent to adsorb a solid will depend on several factors:

- specific surface (m^2/g) of the adsorbent.

Some types of clays, such as Montmorillonite, have an accessible surface ranging from 40 to 100 m^2/g , conferring high adsorption capacity and versatility. While active carbons (industrially modified) exhibit larger specific surface areas (up to 3000 m^2/g), which give an extremely high microporosity. Finally, adsorbents such as metal salts, mainly used in coagulation and flocculation processes, reach larger surface areas.

- Nature of the adsorbed-adsorbent bond,

that means, the energy necessary to allow the adsorption interaction between the part of the reactive molecule and the affine surface area of the material. In an aqueous medium, the thermodynamic models allow to measure the differential enthalpy of adsorption between the adsorption energy and the desorption energy of the molecule in water, associated to the interface. Ultimately, the interactions that govern the adsorption are the Van der Waals forces and the Coulomb electrostatic forces. For example, aromatic molecules (such as benzene and derivatives) have a strong affinity with the analogous structure on carbonaceous surfaces while they tend to reject polar and non-aromatic molecules (Fig. 22).

- Contact time, the time necessary for the solutes or pollutants to migrate from solution to the surface of the adsorbent solid [182].

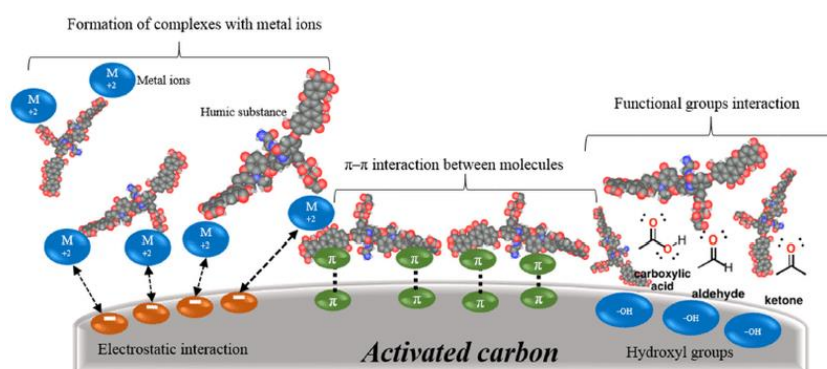


Figure 22. Adsorption mechanism

Source: <https://www.researchgate.net/publication/314262646>

In the environmental field, adsorption processes are used to remove certain components from a mobile phase, such as water. The adsorbents are characterized by the high presence of functional sites or micropores, on the surface, capable of retaining a certain chemical compound and adapting to molecular species with different chemical and dimensional characteristics. The most common adsorbing materials are active carbons, clayey materials, zeolites, etc.

The activated carbons have a hydrophobic character and are suitable for the removal of organic contaminants. Clay minerals also have good adsorbing properties against organic chemicals. The zeolites, defined molecular sieves, preferentially absorb polar materials, thanks to the fine distribution of micropores on the surface [182].

In the industrial field, adsorption applications can be used for production or abatement processes, such as the removal of water from natural gas, the removal of organic compounds from combustion mixtures (refining processes) [184]

The mass of adsorbed compounds per unit of adsorbent mass (g/g or g/m²) depends on the concentration of the compounds in the liquid phase. This dependence determines the achievement of a state of equilibrium, in which a dynamic exchange between the molecules adsorbed on the surface and those that remain in solution takes place.

The ratio between the concentration of the substance adsorbed on the surface of the solid material (C_{solid} , expressed in mol/Kg) and the concentration of the substance in the liquid (C_{liquid} , expressed in mol/L) (usually water) is called the partition coefficient (K_D , expressed in L/Kg) and is represented by the following equation:

$$K_D = \frac{C_{solid}}{C_{water}}$$

The molecules are considered adsorbed, when the washing of the surface, with the same medium of the solvent, in which the adsorbent material is immersed, does not release them in solution.

Finally, the adsorption process is generally classified as *physisorption* when the forces of interactions between the adsorbent and the adsorbate are weak forces of van der Waals, while it is called *chemisorption* when covalent bonds are established [182].

3.1.2 Absorption

Absorption is a phenomenon that affects many environmental processes.

This phenomenon consists in the absorption of atoms, molecules or ions in the internal structure of an absorbent (gas, liquid or solid) (Fig. 23). Unlike adsorption, the molecules are absorbed within the volume, rather than on the surface [182, 183].

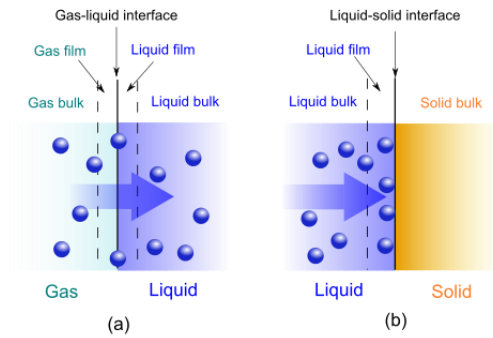


Figure 23. Absorption phenomena
 Source: <https://en.wikipedia.org/wiki/Sorption>

The absorption interactions between the absorbent material and the absorbed solute can be of a chemical and physical nature.

Physical absorption or non-reactive absorption (also called *physisorption*) occurs between two different phases of matter, liquid that absorbs a gas or solid that absorbs a liquid. The molecules that must be absorbed, change their physical characteristics (polarized), while the chemical characteristics remain unchanged [184].

Mass transfer rate occurs at the absorbent-absorbed interface, and depends on parameters such as gas or liquid solubility, temperature and pressure; whereas, in the case of the absorbent material, contact time and surface [184].

Instead, chemical absorption or reactive absorption, also referred to as *chemisorption*, is a chemical reaction that occurs between the absorbent material and the absorbed material. Normally, the absorbed material is converted into a different product from the original one, changing its chemical structure. The concentration and stoichiometry of the reagents govern this phenomenon.

Sometimes, the two absorption phenomena, reactive and non-reactive, can occur in a complementary manner. In general, absorption is a unitary phenomenon that is used for the production and / or purification of chemicals and for the protection of the environment in the reduction of polluting emissions [184].

3.1.3 Biodegradation

Biodegradation is one of the most important environmental processes. The process is based on the decomposition of chemical substances present in a medium, in other less harmful substances, through the action of microorganisms (Fig. 24). In fact, the latter use chemicals as food sources for their

growth metabolism. The basic parameters of the process include nutrient availability, absorption, solubility, pH, temperature, and dissolved oxygen [182].



Figure 24. Biodegradation mechanism

Source: <https://www.slideshare.net/IrwanEffendi3/biodegradation-of-pollutant-1>

When microorganisms degrade compounds, but can not use them as a growth substance, biodegradation is called cometabolism. Subsequently, it may happen that microorganisms begin to adapt to the material to be absorbed.

The factors that influence the adaptation of microorganisms are:

- prolonged contact between microorganisms and degradable solute;
- sufficient number of micro-organisms;
- presence of carbon sources;
- concentration of the pollutant in the water.

In some cases, when the degradation reaction products maintain the same structure as the toxic mother molecule, they often retain their toxicity of the starting compounds.

Degradation processes can also occur through the action of other events or treatments. An example can be the degradation due to environmental factors such as temperature, solar rays, pressure variations. Some degradation studies are based on the use of a suitable energy source that operates at a specific wavelength sensitive for a given compound or system (such as the photocatalytic degradation of bacteria or chemical compounds) [182, 184]

3.2 Kinetic and Equilibrium models of adsorption

The increasing diffusion of pollutants in the aqueous media and the subsequent development of remediation methods and techniques, based mainly on adsorption, require the use of models that effectively explain the various phenomena that occurred [185, 186].

In fact, the understanding of the data concerning a certain phenomenon on the adsorption equilibrium are fundamental information to understand the mechanisms and other parameters of the process. Therefore, the design and experimental developments of an adsorption process are based on kinetic and equilibrium models. More information, obtained from the adsorption isotherms, derive from linear and nonlinear regression analysis [185].

The kinetic models analyze the behavior of the adsorbent and adsorbates, define an adsorption model and monitor the distribution of the adsorbates, in solution and on the surface of the adsorbent.

Whereas, other parameters deriving from the equilibrium models describe the superficial properties of the adsorbent, the relations between adsorbent and adsorbate, such as the equilibrium adsorption capacity (q_e), which describes the relationship between the amount of adsorbed adsorbate by adsorbent and equilibrium concentration (C_e), that is the concentration of adsorbate that remains in solution after equilibrium is reached [187]. Other basic information extrapolated from the kinetic models are intrinsic constants of kinetic adsorption (k) and the order of chemical reaction, which can be of pseudo-first order, of pseudo-second, of general order [188], etc.

The statistical parameters deriving from the development and application of kinetic models are the coefficient of determination (R^2) and the standard deviation. The thermodynamic enthalpy and entropy data are associated with the kinetic models in order to understand the type of adsorption process.

The equilibrium isotherm models most used in literature, for the treatment of adsorption phenomena, are the following: model of Langmuir, Freundlich, Sips, Liu, Redlich-Peterson [185].

3.2.1 Langmuir Isotherm Model

The Langmuir isotherm describes and quantifies the adsorption capacity of a specific adsorbent material, evaluating the dynamic equilibrium, which is the adsorption and desorption fractions of the solute on the surface of the material [189].

The Langmuir isotherm is based on the following assumptions:

- the adsorbates/solutes are chemically adsorbed on well defined and fixed superficial sites;
- under saturation conditions, a monolayer of the adsorbate forms on the surface of the adsorbent;
- each site adsorbs only one species/molecule of adsorbate;
- all sites are energy-equivalent;
- interactions between the adsorbed species are absent.

The Langmuir equation is reported in the following linear form [185]:

$$\frac{C_e}{q_e} = \frac{1}{q_m K_e} + \frac{C_e}{q_m},$$

where, q_e is the amount of adsorbed adsorbate at equilibrium (mg/g), C_e is the concentration of adsorbate at equilibrium (mg/L), K_L is the equilibrium constant of Langmuir (L/mg), and q_m is the maximum adsorption capacity of the adsorbent (mg/g).

Furthermore, for the Langmuir isotherm, the additional parameter R_L can be defined by the following equation:

$$R_L = \frac{1}{1 + K_L C_o},$$

where, K_L is constant of Langmuir (mg/g) and C_o is initial concentration of adsorbate (mg/g). The value R_L irreversible adsorption when $R_L = 0$, favorable when $0 < R_L < 1$, unfavorable when $R_L > 1$, linear when $R_L = 1$ [185].

3.2.2 Freundlich Isotherm Model

The Freundlich isotherm model can be applied to adsorption processes that occur on heterogeneous surfaces and assumes that the concentration of adsorbate on the surface of the adsorbent material increases as the concentration of adsorbate increases, implying an exponential distribution of active sites. The model suggests adsorption process through the formation of several layers rather than a single layer.

The Freundlich's isotherm linear form is defined as follows [185]:

$$\log q_e = \log K_F + \frac{1}{n} \log C_e,$$

where, q_e is the amount of solute adsorbed at equilibrium (mg/g), K_F is the Freundlich equilibrium constant (L/mg), n is the Freundlich exponent (dimensionless), C_e is the concentration of adsorbate at equilibrium (mg/L).

3.2.3 Sips Isotherm Model

The Sips model is an empirical model, which combines the isothermal models of Langmuir and Freundlich.

The Sips model [189] has the following form:

$$q_e = \frac{K_s C_e^{\beta_s}}{1 + a_s C_e^{\beta_s}},$$

where, q_e is the amount of solute adsorbed at equilibrium (g/g), K_s is the Sips equilibrium constant (L/g), C_e is the concentration of adsorbate at equilibrium (g/L), β_s is the Sips isotherm exponent, and a_s is the Sips model constant (L/g).

This model is indicated to treat adsorption phenomena that occur on heterogeneous surfaces. The SIPS model allows to overcome the limiting assumption of the direct dependence between adsorption concentration increase and exponential adsorption increase, associated with the Freundlich model [185]. For low concentrations of adsorbate, the model is reduced to the Freundlich model, while for high concentrations it follows the characteristics of the single layer Langmuir model.

3.2.4 Liu Isotherm Model

The Liu isotherm model is a 3-parameter empirical model. It represents a combination of the Langmuir and Freundlich isothermal models, according to which the active sites of the adsorbent

material have different energy, so the adsorbate can have preferences for certain active sites rather than for others [190].

The equation below describes the Liu model:

$$q_e = \frac{Q_{\max} \cdot (K_g \cdot C_e)^{n_L}}{1 + (K_g \cdot C_e)^{n_L}}$$

where, q_e is the amount of solute adsorbed at equilibrium (mg/g), Q_{\max} is the maximum adsorption capacity of the adsorbent (mg/g), K_g is the Liu equilibrium constant (L/mg); n_L is dimensionless exponent of the Liu equation.

The infinite adsorption of the Freundlich model and the monolayer covering of the Langmuir model are not accepted.

3.2.5 Redlich–Peterson Isotherm Model

Redlich–Peterson Isotherm Model is a further combination of the Freundlich and Langmuir models. The advantage of the method lies in its ability to interpret both homogeneous and heterogeneous systems [185].

The equation describing the Redlich–Peterson Isotherm Model is shown below:

$$q_e = \frac{K_{RP} \cdot C_e}{1 + a_{RP} \cdot C_e^g}$$

where, q_e is the amount of solute loading on the adsorbent at equilibrium (mg/g), C_e is the liquid-phase concentration of adsorbate at equilibrium (mg/L), K_{RP} is Redlich–Peterson constants (L/g), a_{RP} is a constant ((L m)/g), g is the Redlich–Peterson exponent between 0 and 1 (dimensionless). When $g = 1$, equation becomes linear and correspond to Langmuir equation, while at high liquid-phase concentration of adsorbate, the Redlich–Peterson equation reduces to the Freundlich equation.

3.2.6 Other Unusual Isotherm Models

Other models can be adopted to describe the behavior in solution of an adsorbent material against a solute (adsorbed). The most popular secondary models are the models of Hill, Khan, Radke-Prausnitz and Toth. The corresponding equations are shown in the following Table 5 [185]:

Table 5. Other Isotherm Models [185]

Isotherm	Equation
Hill	$q_e = \frac{Q_{\max} \cdot C_e^n H}{KH + C_e^n H}$
Khan	$q_e = \frac{Q_{\max} \cdot K_K \cdot C_e}{(1 + K_K \cdot C_e)^{n_K}}$
Radke–Prausnitz	$q_e = \frac{Q_{\max} \cdot K_{RAP} \cdot C_e}{(1 + K_{RAP} \cdot C_e)^{1/n_{RP}}}$
Toth	$q_e = \frac{Q_{\max} \cdot K_T \cdot C_e}{[1 + (K_T \cdot C_e)^{1/n_T}]^{n_T}}$

3.3 Natural materials as potential adsorbents for polluted water remediation

Nowadays, various technologies with different levels of success and practicality are available in order to solve or minimize the problem of water pollution [191]. However, conventional treatment methods for the removal of pollutants from water have many limitations, mainly due to the high costs, the limited selectivity towards particular pollutants and the final production of large quantities of by-products, which require further treatment [192].

For this reason, the scientific community is perennially looking for sustainable, low cost and respectful processes for human health for the decontamination of polluted waters [193].

Adsorption processes represent the real alternative to existing methods, manifesting the following advantages:

- it is economically advantageous, thanks to the use of low-cost materials,
- it has a high efficiency for the high specific surface and high selectivity for the great variety of materials and functional groups that can be used in the processes,
- it has a lower environmental impact, due to the absence of by-products,
- normally, the materials used can be reused easily. [193]

Activated carbons (deriving from agricultural, industrial and domestic waste), sludge, mineral materials, natural products and a wide variety of plant species, are the most commonly used adsorbents. They are versatile for the removal of different classes of pollutants from water, such as hydrophobic organic compounds (HOCs, PAHs, EDCs, dyes, fertilizer, etc.), heavy metals, etc. [192, 193].

Moreover, due to the advantages listed above, scientific studies of pollutant adsorption focus on improving the absorption capacity and the stability of biomaterials, through physical and chemical modifications: through heating processes (pyrolysis and drying), through functionalization reactions using inorganic/organic compounds (eg acids, such as HNO₃, HCl, H₂SO₄, bases, such as NaOH, and numerous organic compounds, such as acetates, isocyanates, silanes, acrylates, etc.) [194 - 196]

Lignocellulosic substrates are the most available materials for surface modifications, for their high environmental retrieval and for the lignin and cellulose reactivity, due to the presence of reactive functional groups, such as hydroxyl groups [195]

Moreover, the advantage offered by lignocellulosic materials, in addition to the reasons described above, is the possibility of grafting selectable functional groups (representing active sites during adsorption), based on the contaminant that wants to be removed from an aqueous medium.

At the base of these considerations, in the last decades, many scientific works have investigated the use of low-cost adsorbents for wastewater treatment. The greatest attention was paid to the following classes of pollutants, which also represent the most widespread and most dangerous contaminants for human health:

- Hydrophobic compounds of petroleum derivation (such as TPHs, PAHs, BTEX),
- Endocrine disrupting compounds (such as BPA),

- heavy metals, in particular, mercury.

The following subparagraphs describe the most recent and innovative research concerning the remediation of water from these classes of pollutants [194].

3.3.1 Typical natural biosorbents for TPHs and HOCs remediation processes

TPHs and oil, in general, consist mainly of non-polar hydrocarbons and molecules with the presence of one or more cyclic rings of an aromatic or aliphatic nature. Their adsorption is attributed to non-covalent physical interactions such as van der Waals forces [197].

In recent years, several authors have investigated the possibility of using low-cost natural materials to retain hydrocarbon compounds from water.

The most investigated natural materials for the reclamation of water from oil are sugar cane bagasse, fruit scraps, cotton, lignocellulose residues such as rice husk and barley residues, and various plant materials. These types of adsorbents have good adsorption capacity when compared to synthetic adsorbents. They have been used in some studies roughly or after carbonization processes. During carbonization, the pyrolytic decomposition of the material and the elimination of many species such as H, N, O and S occurs [197].

This process allows to obtain a material in the form of fixed carbonaceous char. Subsequently, in order to remove the amorphous carbon parts from the pores and make the internal surface accessible (increasing the porosity), chemical treatments, with activators such as $ZnCl_2$, H_3PO_4 , H_2SO_4 , KOH , K_2S or physical activation processes, with the use steam, CO_2 and air, are performed [197]

Khan et al. [198] studied the adsorbing capacity towards hydrocarbon pollutants of seven natural plants: Kapok fiber, cattail fiber, *Salvinia* sp., Wood chips, rice husk, coconut peel and bagasse. All the adsorbent materials were dried at 60 °C for 24h and used in adsorption tests. The adsorption capacities range from 0.02 to 1 g of oil per g of adsorbent. Sorbents that are more hydrophobic like kapok fiber, typhus fiber, and *Salvinia* sp., and remove more oil than other adsorbents.

Brandao et al. [199] conducted studies, in which the adsorption capacity of the bagasse sugarcane was monitored, to remove the oil contaminants from the aqueous medium. The adsorption capacities in different conditions range from 8 to 10 mg/g, exhibiting not excessively fast kinetics. Other

adsorption studies were conducted on Coconut peel, Barley straw, Walnut shell, Kapok fiber, Sugarcane bagasse, Rice husks after carbonization or heating processes [197, 198].

The most important applications are shown in the following Table 6:

Table 6. Lignocellulosic-based sorbent and ACs, used for the removal of hydrophobic organic compounds.

Adsorbent	Treatment	Adsorbate/ pollutant	Sorbate and sorption capacity (g oil/g fibre)	Reference
Rice Husks	Alkaline treatment	Marine diesel	1.9 g/g	[200]
Potato peel	Drying and crushing	Lubricating oil	2.2 g/g	[201]
Kapok fiber	Drying at 60°C for 24h	Oil	0.8 g/g	[198]
Cattail fiber	Drying at 60°C for 24h	Oil	1.1 g/g	[198]
Salvinia sp.	Drying at 60°C for 24h	Oil	0.9 g/g	[198]
Wood chips	Drying at 60°C for 24h	Oil	0.3 g/g	[198]
Rice husk	Drying at 60°C for 24h	Oil	0.3 g/g	[198]
Coconut peel	Drying at 60°C for 24h	Oil	0.06 g/g	[198]
Bagasse	Drying at 60°C for 24h	Oil	0.02 g/g	[198]
Barley straw	Carbonisation (T: 400 °C, 0.5–3 h)	Gas oil	9.0 g/g	[202]
Walnut shell	Drying at 105°C for 16h	Standard mineral oil	0.3 g/g	[203]
Kapok fibre	Dried	Diesel oil	19.4 g/g	[204]
Sugarcane bagasse	Dried	Diesel oil	10.5 g/g	[204]
Rice husks	Dried	Diesel oil	2.6 g/g	[204]
Fir fibres	Delignification, carbonisation at 380 or 900 °C, 1 h	Heavy oil	10-80 g/g	[204]
Rice husk	Carbonization at 480°C	Different oils	3.7 – 9.2 g/g	[205]

The use of activated carbons as adsorbent material is practiced starting from the first half of the last century [206]. Nevertheless, the production processes are energetically and economically disadvantageous. For this reason, scientists have undertaken new studies, with the aim to development low-cost adsorbents and less waste production.

However, natural materials, if not subject to the carbonization processes mentioned above, exhibit low hydrophobicity and adsorption capacity. To overcome these limitations, several studies explore the possibility of increasing hydrophobicity of natural plant materials and fibers, by reacting their surface with hydrophobic groups. The changes, mainly, improve the properties such as hydrophobicity and adsorption capacity, leaving unchanged those that do not influence the adsorption processes and the biocompatibility of the material.

Deschamps et al. [207], studied the efficiency of modified cotton fibers for the purification of water contaminated by fuel, mineral oil and vegetable, showing an adsorption capacity of around 20 g/g. The hydrophobization of the filter material was obtained by acylation of cellulose with fatty acid by microwave radiation. Yang et al. [208], studied the possibility of using superhydrophobic lignin, modified with diisocyanated groups, by organogel formation in THF. The natural fiber showed a water contact angle of about 150°. The material was used for adsorption studies on gasoline. Hydrophobically modified Kapok fibers, with polymerized butyl methacrylate (PBMA) and silica nanoparticles, have been studied by Wang et al. as adsorbent for oil, showing a maximum adsorbing capacity of 90 g/g. In another study, concerning the same starting material, other methods of surface functionalization, with silica nanoparticles and silanization, were carried out. The materials showed an adsorption capacity of various oils up to 85 g/g. Other natural materials, such as cotton have been hydrophobized superficially by grafting with silica nanoparticles and silane groups, reaching a water contact angle of 156° and a high adsorbent capacity between 30 and 50 g/g of different oils [209]. Other adsorption studies with different modified processes were conducted on Kapok fibers, lignin, cellulose foam, cotton, etc [208-214].

The most important studies are shown in the following table:

Table 7. Modified lignocellulosic sorbent, used for the removal of hydrophobic organic compounds.

Adsorbent	Modifying process	Adsorbate/ pollutant	Sorbate and sorption capacity (g oil/g fibre)	Reference
Cotton fibers	grafting with silica nanoparticles and silane groups	Oils	30 – 50 g/g	[209]
Kapok fibers	Polymerization with PBMA and silica nanoparticles	Petrol	90 g/g	[210]
Kapok fibers	Functionalization with silica nanoparticles and silanization	Oils	85 g/g	[210]
Lignin	modified with disiocyanated groups	Gasoline	2 – 4 g/g	[208]
Cotton fibers	acylation of cellulose with fatty acid by microwave radiation	Fuel	20 g/g	[207]
Cotton fibers	Functionalization with silica nanoparticles	n-hexane	25-50 g/g	[211]
Sugarcane bagasse	Esterification with stearic acid	Engine oil	1-3 g/g	[213]
Barley straw	surfactant-modification	Mineral oil	0.5 g/g	[214]

In conclusion, the adsorption capacity of natural materials depends on several factors, such as hydrophobicity, porosity, surface area, etc. Certainly, activated carbons have a good adsorption capacity, higher than raw materials of origin, but functionalized biosorbents, allowing to achieve greater adsorption capacity, without the use of production processes that require a lot of energy.

3.3.2 BPA remediation by means of natural adsorbent materials

BPA removal from water by natural adsorbent materials has been widely considered in many studies [215-222].

The use of natural fibers has gained a lot of visibility over time, due to the enormous resources available and the advantages concerning reuse and environmental impact. Nevertheless, the most important advantage of natural fibers is the presence of a variety of functional groups and basic chemical structures, which have potential absorption capacity for these polluting compounds.

Also in this case, the activated carbon (ACs) are excellent adsorbent materials in the process of adsorption of BPA in water, thanks to their high surface area and adsorption capacity;

Materials derived from empty fruit shells, rice straw, agricultural waste, and so on, were developed.

Kumar et al. [223] used sulfuric acid to produce activated carbon from the coconut marrow. The adsorption capacity at an initial pH of 2 to 35 ° C particle size of 250-500 μm, provided a value of 55 mg/g. Chang et al. [224] used pretreatment with potassium hydroxide (KOH) to transform rice straw into activated carbon. The high surface area of the material provided an adsorption capacity of 181.19 mg/g.

Nakanishi et al. [225] developed activated carbons adsorbing from the Sugi chip, Sugi sawdust, from the Hinoki chip, Kenaf raffia, Kenaf fiber and Kenaf sawdust, through an electric furnace at temperatures between 873 and 1073 K, in a stream of nitrogen. The adsorbent capacities of the materials against BPA are between 1.0 and 18 mg/g.

Tsai et al. [227] studied mineral wastes, exhibiting adsorbent capacities equal to or greater than 200 mg/g.

Activated carbons prepared from the bunch of empty palm oil residue fruits to remove Bisphenol A from aqueous media has been studied by Wirasnita et al. [228]. The maximum absorption capacity of the activated carbon mono-layer was 41.98 mg/g. While, Bautista-Toledo et al. (2005) studied almond shells, prepared by carbonization in N₂ steam at 1273 K for 1 h, and steam-activated at 1123 K for 5 h, with adsorption capacity of 188.9 mg/g.

However, the preparation of activated carbons is expensive and high energy expenditure.

Therefore, some studies have examined the use of natural materials, such as treated coconut fiber, coconut shell and durian peel, in an original way, as an alternative adsorbent for BPA [229]. Instead, studies concerning surface modifications of biosorbent, by specific functional groups, are limited or almost absent.

The most significant studies are shown in the following Table 8.

Table 8. ACs and biobased materials, used for BPA removal in water

Adsorbent	Modifying process	Adsorption capacity (mg/g)	Reference
<i>Activated Carbons (ACs)</i>			
Coconut marrow	Sulfuric acid	55.0 mg/g	[223]
Rice straw	Potassium hydroxide	181.2 mg/g	[224]
Sugi chip		11.5 mg/g	
Sugi sawdust		12.1 mg/g	
Hinoki chip	Carbonization at temperatures between	18.0 mg/g	[225]
Kenaf	873 and 1073 K, in a stream of nitrogen	2.6 mg/g	
Defibred Kenaf		4.7 mg/g	
Kenaf sawdust		1.0 mg/g	
Palm oil residues	Carbonization at 500 °C for 1 h, under nitrogen gas	41.98 mg/g	[227]
Almond shell	Carbonization at 1273 K for 1 h and steam-activated at 1123 K for 5 h	188.9 mg/g	[228]

<i>Raw natural materials</i>			
Coconut fiber		4.3 mg/g	
Coconut shell	Raw	4.2 mg/g	[229]
Durian peel		4.2 mg/g	

Also in this case, as for the hydrophobic organic compounds, the activated carbons exhibit greater adsorbing capacities with respect to the biosorbents used in a raw or functionalized manner. However, the advantages of the latter are considerable and convenient.

3.3.3 Remediation of mercury polluted water using natural adsorbents

In recent decades, the search for unconventional methods, low cost and efficient, for the removal of mercury from aqueous solutions, has attracted the interest of many scholars. Adsorption is a convenient technique for this purpose and the use of activated carbons deriving from natural materials has allowed the achievement of important scientific results.

Zhang et al. [230], used activated carbons, carbonizing organic purification sludge at 650 °C for 1 h, and using different acids and ZnCl₂, for chemical activation.

Zabihi et al. [231], obtained activated carbons in powder form (PAC), deriving from the nutshell for the sequences of Hg (II) in water. The adsorption capacity is between 100 and 150 mg/g.

Activated adsorbents, prepared from *Ceiba pentandra*, *Phaseolus aureus* shells and *Cicer arietinum* waste have shown a removal capacity of more than 20 mg/g for an initial Hg (II) concentration of 40 mg/L [232].

While, Namasivayam [233], has carried out adsorption studies of mercury (II) from aqueous solutions, using coconut, which showed adsorption capacity of 154 mg/g.

Although activated carbons have effective adsorption properties, they are expensive for large-scale application. Since the absorption depends on conditions such as pH, metal concentration, particle size

and functional groups involved, the modification of sorbents can also improve the adsorption capacity, avoiding the use of expensive methods of activation of the carbon substrates.

Potentially low-cost adsorbent materials are lignocellulose materials such as natural fibers, bark, chitosan, xanthate, clay, moss, algae, and other biomasses.

In this regard, Arias Arias et al. [234], have studied the adsorbent capacities of lignocellulosic material derived from the Spanish broom plant. A maximum adsorption capacity of 20 mg/L at pH 5 was obtained in Hg (II) polluted aqueous solutions.

Instead, Santhana et al. [235] prepared cellulose grafted with glycidyl methacrylate (GlyMA), through the microwave technique. The resulting material showed adsorption capacity of 37.03 mg/g. Singh et al. [236], have also adopted the same method to modify the *Cassia javanica* with polymers of acrylic acid. In this case, the mercury adsorption capacity was 12.5 mg/g

Bicak et al. [237] have obtained cellulose with polyacrylamide groups, from cotton, using ammonium sulphate as initiator, for water contaminated by Hg (II), while, for the same purpose, Shibi and Anirudhan [238] using ferric ammonium/H₂O₂ redox initiator for grafting the acrylamide groups onto the banana stem.

Other reagents adopted for functionalization processes are o-benzeneditol [239] and polyethylenimine [240] for cellulose, and polyacrylamide for the coconut bark [241].

The most important studies are shown in the following Table 9.

Table 9. ACs and biobased materials, used for Hg(II) removal in water

Adsorbent	Modifying process	Adsorption capacity (mg/g)	Reference
<i>Activated Carbons (ACs)</i>			
Organic purification sludge	Carbonization at 650 °C for 1 h; acids and ZnCl ₂	-	[230]
Nutshell	Carbonization	100.9-151.5 mg/g	[231]
Ceiba pentandra		25.88 mg/g	

Phaseolus shells	Carbonization	23.66 mg/g	[232]
Cicer arietinum		22.88 mg/g	
Coconut	Carbonization	154 mg/g	[233]
<i>Raw and functionalized natural materials</i>			
Spanish broom	Raw	20 mg/g	[234]
Cellulose	Grafting with glycidyl methacrylate	37.03 mg/g	[235]
Cassia javanica	Grafting with acrylic acid	12.5 mg/g	[236]
Cellulose	Grafting with polyacrylamide	6.9 mg/g	[237]
Cellulose	Functionalization with o-benzeneditol	23 mg/g	[239]

Activated carbons in most cases have higher adsorption values compared to Hg (II), but, at the same time, the processes are extremely drastic, with the use of concentrated acids in subsequent treatments, which worsen the possibility of large-scale applications.

References

- [1] Sulaiman A. Alrumman, Attalla F. El-kott, Sherif M. A. S. Keshk, Water Pollution: Source & Treatment, American Journal of Environmental Engineering, Vol. 6 No. 3, 2016, pp. 88-98. doi: 10.5923/j.ajee.20160603.02.
- [2] Water Contamination and Pollution. Linda Schweitzer, James Noblet. CHAPTER 3.6
- [3] World Health Organ. (WHO)/UN Child. Fund (UNICEF). 2008. Progress on Drinking-Water and Sanitation: Special Focus on Sanitation. Geneva, Switz./New York: WHO/UNICEF. 58 pp.
- [4] V.V. Goncharuk. Drinking water. Physics, chemistry and Biology. In Chapter 1: Role of water in human life. Springer Cham Heidelberg New York Dordrecht London. DOI 10.1007/978-3-319-04334-0
- [5] F. W. Owa. Water pollution: sources, effects, control and management.. International Letters of Natural Sciences, 3 (2014) 1-6.
- [6] Olaniran N.S. (1995). Environment and Health: An Introduction, in Olaniran, N.S. et. al (Ed) Environment and Health. Lagos. Micmillan Nig. Pub. Co for NCF, 34-151.
- [7] Groundwater and Human Security. Chapter 1: INTRODUCTION TO THE GROUNDWATER AND HUMAN SECURITY – CASE STUDIES PROJECT. Editors: Renaud, Fabrice and Schuster-Wallace, Corinne ISBN: 978-92-808-6082-5
- [8] A. du Plessis, Freshwater Challenges of South Africa and its Upper Vaal River, Springer Water, DOI 10.1007/978-3-319-49502-6_1
- [9] Singh S.K. Water Pollution: Sources, Effects, and Control Measures. Journal of Agroecology and Natural Resource Management. (2006), 3 (1), pp. 64-66
- [10] Haseena M, Malik MF. Water pollution and human health. Environ Risk Assess Remediat. 2017;1(3) pp. 16-19
- [11] Eguabor V., STAN Journal Environmental Education series (2) (1998) 49
- [12] Global Water Pollution and Human Health. R. P. Schwarzenbach, T. Egli, T. B. Hofstetter, U. von Gunten, and B. Wehrli. Annu. Rev. Environ. Resour. 2010. 35:109–36
- [13] Khan MA, Ghouri AM. Environmental Pollution: Its effects on life and its remedies. Journal of arts, science and commerce. 2011;2(2):276-85.
- [14] Halder JN, Islam MN. Water pollution and its impact on the human health. Journal of environment and human. 2015;2(1):36-46.
- [15] Ahmed T, Scholz F, Al-Faraj W, et al. Water-related impacts of climate change on agriculture and subsequently on public health: A review for generalists with particular reference to Pakistan. International journal of environmental research and public health. 2013;13:1-16.
- [16] Halder JN, Islam MN. Water pollution and its impact on the human health. Journal of environment and human. 2015;2(1):36-46.
- [17] Ullah S, Javed MW, Shafique M, et al. An integrated approach for quality assessment of drinking water using GIS: A case study of Lower Dir. Journal of Himalayan Earth Sciences. 2014;47(2):163-74.
- [18] Currie J, Joshua GZ, Katherine M, et al. Something in the water: contaminated drinking water and infant health. Canadian journal of economics. 2013;46(3): 791-810.
- [19] Ashbolt NJ. 2004. Microbial contamination of drinking water and disease outcomes in developing regions. Toxicology 198:229–38
- [20] World Health Organ. (WHO)/UN Child. Fund (UNICEF). 2006. Meeting the MDG Drinking Water and Sanitation Target: The Urban and Rural Challenge of the Decade. Geneva, Switz./New York: WHO/UNICEF
- [21] Ashbolt NJ. 2004. Microbial contamination of drinking water and disease outcomes in developing regions. Toxicology 198:229–38

- [22] World Health Organ. (WHO). 2002. Global defense against the infectious disease threat. In *Emerging and Epidemic-Prone Diseases*, ed. MK Kindhauser, pp. 56–103. Geneva, Switz.: WHO
- [23] Alley WM, Reilly TE, Franke OL. *Sustainability of Groundwater Resources*. U.S. Geological Survey (U.S.GS), Denver, CO; 1999.
- [24] M. Mosharraf Hossain, K. M. Nazmul Islam and Ismail M. M. Rahman (2012). *An Overview of the Persistent Organic Pollutants in the Freshwater System, Ecological Water Quality - Water Treatment and Reuse*, Dr. Voudouris (Ed.), ISBN: 978-953-51-0508-4, InTech
- [25] T. Navratil and L. Minarik, Trace elements and contaminants, In: V. Cilek and R. H. Smith (Eds.), *Encyclopedia of Life Support System*, Vol. IV, pp. 1184–1213, 2005.
- [26] A. Pal, K.Y.-H. Gin, A.Y.-C. Lin and M. Reinhard, "Impacts of emerging organic contaminants on freshwater resources: Review of recent occurrences, sources, fate and effects", *Science of the Total Environment*, Vol. 408, pp. 6062–6069, 2010.
- [27] K.K. Barnes, D.W. Kolpin, E.T. Furlong, S.D. Zaugg, M.T. Meyer and L.B. Barber, "A national reconnaissance of pharmaceuticals and other organic wastewater contaminants in the United States–I) Groundwater", *Science of the Total Environment*, Vol. 402, pp. 192–200, 2008.
- [28] K.A. Kidd, R.H. Hesslein, B.J. Ross, K. Koczanski, G.R. Stephens and D.C.G. Muir, "Bioaccumulation of organochlorines through a remote freshwater food web in the Canadian Arctic", *Environmental Pollution*, Vol. 102, pp. 91–103, 1998.
- [29] Tursi A, Beneduci A, Chidichimo F, De Vietro N, Chidichimo G. Remediation of hydrocarbons polluted water by hydrophobic functionalized cellulose. *Chemosphere*, 2018; 201:530-539.
- [30] S. Abha and C.S. Singh (2012). *Hydrocarbon Pollution: Effects on Living Organisms, Remediation of Contaminated Environments, and Effects of Heavy Metals Co-Contamination on Bioremediation, Introduction to Enhanced Oil Recovery (EOR) Processes and Bioremediation of Oil- Contaminated Sites*, Dr. Laura Romero-Zerón (Ed.), ISBN: 978-953-51-0629-6, InTech,
- [31] M. Wagner, C. Scherer, D. Alvarez-Muñoz, N. Brennholt, X. Bourrain, S. Buchinger, E. Fries, C. Grosbois, J. Klasmeier, T. Marti, S.R. Mozaz, R. Urbatzka, A.D. Vethaak, M.W. Nielsen, G. Reifferscheid. Microplastics in freshwater ecosystems: What we know and what we need to know. *Environmental Sciences Europe* 2014, 26:12
- [32] Barnes DK, Galgani F, Thompson RC, Barlaz M: Accumulation and fragmentation of plastic debris in global environments. *Philos Trans R Soc Lond B Biol Sci* 2009, 364:1985–1998.
- [33] Andrady AL, Neal MA: Applications and societal benefits of plastics. *Philos Trans R Soc Lond B Biol Sci* 2009, 364:1977–1984
- [33] Wright SL, Thompson RC, Galloway TS: The physical impacts of microplastics on marine organisms: a review. *Environ Pollut* 2013, 178:483–492
- [34] Eriksen M, Maximenko N, Thiel M, Cummins A, Lattin G, Wilson S, Hafner J, Zellers A, Rifman S: Plastic pollution in the South Pacific subtropical gyre. *Mar Pollut Bull* 2013, 68:71–76.
- [35] Dekiff JH, Remy D, Klasmeier J, Fries E: Occurrence and spatial distribution of microplastics in sediments from Norderney. *Environ Pollut* 2014, 186:248–256.
- [36] Koelmans AA, Besseling E, Wegner A, Foekema EM: Plastic as a carrier of POPs to aquatic organisms: a model analysis. *Environ Sci Technol* 2013, 47:7812–7820
- [37] Hirai H, Takada H, Ogata Y, Yamashita R, Mizukawa K, Saha M, Kwan C, Moore C, Gray H, Laursen D, Zettler ER, Farrington JW, Reddy CM, Peacock EE, Ward MW: Organic micropollutants in marine plastics debris from the open ocean and remote and urban beaches. *Mar Pollut Bull* 2011, 62:1683–1692
- [38] Wagner M, Oehlmann J: Endocrine disruptors in bottled mineral water: total estrogenic burden and migration from plastic bottles. *Environ Sci Pollut Res* 2009, 16:278–286.
- [39] Browne MA, Crump P, Niven SJ, Teuten E, Tonkin A, Galloway T, Thompson R: Accumulation of microplastic on shorelines worldwide: sources and sinks. *Environ Sci Technol* 2011, 45:9175–9179

- [40] Hidalgo-Ruz V, Gutow L, Thompson RC, Thiel M: Microplastics in the marine environment: a review of the methods used for identification and quantification. *Environ Sci Technol* 2012, 46:3060–3075.
- [41] Law KL, Moret-Ferguson S, Maximenko NA, Proskurowski G, Peacock EE, Hafner J, Reddy CM: Plastic accumulation in the North Atlantic subtropical gyre. *Science* 2010, 329:1185–1188.
- [42] PB Tchounwou, CG Yedjou, AK Patlolla, and DJ Sutton. *Heavy Metals Toxicity and the Environment*. NIH Public Access. EXS 2014
- [43] WHO/FAO/IAEA. World Health Organization. Switzerland: Geneva; 1996. *Trace Elements in Human Nutrition and Health*.
- [44] Bradl, H., editor. *Heavy Metals in the Environment: Origin, Interaction and Remediation Volume 6*. London: Academic Press; 2002.
- [45] Pacyna, JM. Monitoring and assessment of metal contaminants in the air. In: Chang, LW.; Magos, L.; Suzuli, T., editors. *Toxicology of Metals*. Boca Raton, FL: CRC Press; 1996. p. 9-28.
- [46] Nriagu JO. A global assessment of natural sources of atmospheric trace metals. *Nature*. 1989 338:47–49.
- [47] Verkleji, JAS. The effects of heavy metals stress on higher plants and their use as biomonitors In *Plant as Bioindicators: Indicators of Heavy Metals in the Terrestrial Environment*. Markert, B., editor. New York: VCH; 1993. p. 415-424.
- [48] Stern BR. Essentiality and toxicity in copper health risk assessment: overview, update and regulatory considerations. *Toxicol Environ Health A*. 2010; 73(2):114–127.
- [49] Chang, LW.; Magos, L.; Suzuki, T., editors. *Toxicology of Metals*. Boca Raton. FL, USA: CRC Press; 1996.
- [50] J. P. S. Cabral. *Water Microbiology. Bacterial Pathogens and Water*. *Int. J. Environ. Res. Public Health* 2010, 7, 3657-3703; doi:10.3390/ijerph7103657
- [51] Fenwick, A. Waterborne Diseases—Could they be Consigned to History? *Science* 2006, 313, 1077–1081.
- [52] Seas, C.; Alarcon, M.; Aragon, J.C.; Beneit, S.; Quiñonez, M.; Guerra, H.; Gotuzzo, E. Surveillance of Bacterial Pathogens Associated with Acute Diarrhea in Lima, Peru. *Int. J. Infect. Dis.* 2000, 4, 96–99.
- [53] Enteroinvasive *Escherichia coli* (EIEC); US Department of Health & Human Services, U.S. Food and Drug Administration.
- [54] Medema, G.J.; Payment, P.; Dufour, A.; Robertson, W.; Waite, M.; Hunter, P.; Kirby, R.; Anderson, Y. Safe drinking water: an ongoing challenge. In *Assessing Microbial Safety of Drinking Water. Improving Approaches and Method*; WHO & OECD, IWA Publishing: London, UK, 2003; pp. 11–45.
- [55] Regmi C, Joshi B, Ray SK, Gyawali G and Pandey RP (2018) Understanding Mechanism of Photocatalytic Microbial Decontamination of Environmental Wastewater. *Front. Chem.* 6:33. doi: 10.3389/fchem.2018.00033
- [56] Radiation Protection and Safety of Radiation Sources: International Basic Safety Standards, No.GSR Part3
- [57] https://www.doi.gov/oc/1/hearings/112/NutrientPollution_100411
- [58] Macaulay, B.M. (2015). Understanding the behaviour of oil degrading microorganisms to enhance the microbial remediation of spilled petroleum. *Appl. Ecol. Environ. Res.*, 13(1): 247- 262
- [59] A Banerjee, A Roy, S Dutta, and S Mondal. BIOREMEDIATION OF HYDROCARBON - Review. *International Journal of Advanced Research* (2016), Volume 4, Issue 6, 1303-1313
- [60] Agency for Toxic Substances and Disease Registry (ATSDR). 1999. *Toxicological Profile for total petroleum hydrocarbons (TPH)*. Atlanta, GA: U.S. Department of Health and Human Services, Public Health Service.
- [61] Burris DR, Macintyre WG. 1984. Water solubility behavior of hydrocarbon mixtures -- Implications for petroleum dissolution. In: Vandermeulen JH, Hiudey SE, eds. *Oil in freshwater: Chemistry, biology, countermeasure technology*. New York,NY: Pergamon Press, 85-94.
- [62] Mercer, J.W., Cohen, R.M., 1990. A review of immiscible fluids in the subsurface: properties, models, characterization and remediation. *J. Contam. Hydrol.* 6 (2), 107-163.

- [63] ASTM, E1689-95(2014), 2014. Standard Guide for Developing Conceptual Site Models for Contaminated Sites. ASTM International, West Conshohocken, PA. www.astm.org.
- [64] Welch F., Murray V. S. G., Robins A. G., Derwent R. G., Ryall D. B., Williams M. L., Elliott A. J., Analysis of a petrol plume over England: 18–19 January 1997, *Occup Environ Med* 1999;56:649–656
- [65] Costello J., Morbidity and Mortality Study of Shale Oil Workers in the United States, *Environmental Health Perspectives*, Vol. 30, pp. 205-208, 1979
- [66] KZ Kponee, A Chiger, II Kakulu, D Vorhees and WH Bernays. Petroleum contaminated water and health symptoms: a cross-sectional pilot study in a rural Nigerian community. *Environmental Health* (2015) 14:86
- [67] Smith MT. Advances in understanding benzene health effects and susceptibility. *Annu Rev Publ Health*. 2010;31:133–48.
- [68] Collins JF. Benzene Reference Exposure Levels: Technical Support Document for the Derivation of Noncancer Reference Exposure Levels. Cal OEHHA. 2014.
- [69] Khalade A, Jaakkola MS, Pukkala E, Jaakkola JJ. Exposure to benzene at work and the risk of leukemia: a systematic review and meta-analysis. *Environ Health*. 2010;9:31–9.
- [70] Bahadar H, Mostafalou S, Abdollahi M. Current understandings and perspectives on non-cancer health effects of benzene: a global concern. *Toxicol Appl Pharm*. 2014;276(2):83–94.
- [71] Greenberg MM. The central nervous system and exposure to toluene: a risk characterization. *Environ Res*. 1997;72(1):1–7.
- [72] ATSDR. Toxicological profile for Polycyclic Aromatic Hydrocarbons. 1995. <http://www.atsdr.cdc.gov/toxprofiles/tp69.pdf>. Accessed January 27 2015.
- [73] Kim KH, Jahan SA, Kabir E, Brown RJ. A review of airborne polycyclic aromatic hydrocarbons (PAHs) and their human health effects. *Environ Int*. 2013;60:71–80.
- [74] Mastrangelo G, Fadda E, Marzia V. Polycyclic aromatic hydrocarbons and cancer in man. *Environ Health Perspect*. 1996;104(11):1166–70.
- [75] Sudakin DL, Stone DL, Power L. Naphthalene mothballs: emerging and recurring issues and their relevance to environmental health. *Curr Top Toxicol*. 2011;7:13–9.
- [76] Wickliffe J, Overton E, Frickel S, Howard J, Wilson M, Simon B, et al. Evaluation of polycyclic aromatic hydrocarbons using analytical methods, toxicology, and risk assessment research: seafood safety after a petroleum spill as an example. *Environ Health Perspect*. 2014;122(1):6–9.
- [77] N Al-Jammal, T Juzsakova. Review on the effectiveness of adsorbent materials in oil spills clean up. 7th International Conference of ICEEE, 17-19 of November 2016, Budapest, Hungary
- [78] Daugherty SJ. 1991. Regulatory approaches to hydrocarbon contamination and underground storage tanks. In: *Hydrocarbon contaminated soils and groundwater: analysis, fate, environmental and public health effects, and remediation*. Vol. 1. Chelsea MI: Lewis Publishers, Inc., 23-53.
- [79] ATSDR. 1997a. Toxicological profile for benzene (update). Agency for Toxic Substances and Disease Registry, Public Health Service, U.S. Department of Health and Human Services, Atlanta, GA.
- [80] Salleh, A.B., Ghazali, F.M., Rahman, R. and Basri, M. (2003). Bioremediation of petroleum hydrocarbon pollution . *Indian J. Biotech*. 2: 411-425.
- [81] I. Ivshina, et al., “Oil spill problems and sustainable response strategies through new technologies” , *Environ. Sci.: Processes Impacts*, 17, 1201-1219, 2015.
- [82] M., Amro, “Treatment Techniques of Oil-Contaminated Soil and Water Aquifers”, *International Conf. on Water Resources & Arid Environment*, (2004).
- [83] A Muizis. Evaluation of the Methods for the Oil Spill Response in the Off-shore Arctic Region. Helsinki Bachelor’s Thesis. Bachelor of Engineering. Metropolia University of Applied Sciences. 15 May 2013
- [84] Ventikos, N.P., Vergetis, E., Psaraftis, H.N., Triantafyllou, G. “A High-Level Synthesis of Oil Spill Response Equipment and Countermeasures” *Journal of Hazardous Materials*. 107 (2004): 51-58
- [85] <https://sharkresearch.rsmas.miami.edu/a-review-of-different-methods-for-responding-to-an-oil-spill/>

- [86] John C. Reis. Environmental Control in Petroleum Engineering. ELSEVIER SCIENCE & TECHNOLOGY, United Kingdom (1996)
- [87] National Response Team Science & Technology Committee, NRT-RRT Factsheet: Application of Sorbents and Solidifiers for Oil Spills, 2007
- [88] Allen, Alan A. and Ronald J. Ferek. Advantages and disadvantages of burning spilled oil. Presented at the 1993 International Oil Spill Conference, Tampa, Florida, March 1993.
- [89] Allen, A. A. and E.M. Fischer. 1988. Test and evaluation of a new and unique fire containment boom. Presented at the Eleventh Annual Arctic and Marine Oilspill Program Technical Seminar, June 7-9, 1988, Vancouver, British Columbia. Environment Canada, Ottawa, Ontario.
- [90] de la Cueva, S. C., Rodríguez, C. H., Cruz, N. O. S., Contreras, J. A. R., & Miranda, J. L. (2016). Changes in Bacterial Populations During Bioremediation of Soil Contaminated with Petroleum Hydrocarbons. *Water, Air, & Soil Pollution*, 227(3): 1-12.
- [91] Franchi, E., Agazzi, G., Rolli, E., Borin, S., Marasco, R., Chiaberge, S. and Barbafieri, M. (2016). Exploiting hydrocarbon-degrader indigenous bacteria for bioremediation and phytoremediation of a multi-contaminated soil. *Chemical Engineering & Technology*.
- [92] Vidali M. (2001). Bioremediation. An overview. *Pure Appl. chem.* 73(7):1163-1172.
- [93] F.-G. Simon, T. Meggyes and T. Tünnermeier. Groundwater remediation using active and passive processes. Federal Institute for Materials Research and Testing (BAM), Unter den Eichen 87, D-12205 Berlin, Germany
- [94] Suthersan, S. (1996). Remediation Engineering: Design Concepts. Environmental Science and Engineering Series. Lewis, Boca Raton, Florida.
- [95] Eastern Research Group (1996). Pump-and-Treat Ground-water Remediation, A Guide for Decision Makers and Practitioners, EPA/625/R-95/005. US Environmental Protection Agency, Washington DC.
- [96] Smyth, D. A., Shikaze, S. G. and Cherry, J. A. (1997). Hydraulic performance of permeable barriers for the in situ treatment of contaminated groundwater. *Land Contamination and Reclamation* 5(3), 131–137.
- [97] Schad, H. and Gratwohl, P. (1998). Funnel and gate systems for in-situ treatment of contaminated groundwater at former manufactured gas plant sites. In: H. Burmeier (ed.), *Treatment Walls and Permeable Reactive Barriers*, NATO CCMS Series, Vol. 229, pp. 56–65. NATO, Vienna.
- [98] Hester, R.E. Harrison, R.M. (Eds). *Endocrine Disrupting Chemicals*. Royal Society of Chemistry, Cambridge, 1999.
- [99] Carson, R. *Silent Spring*. Houghton Mifflin, New York, 1962.
- [100] Colborn T., Clement C. *Advances in Modern Toxicology. Volume XXI. Chemically-Induced Alterations in Sexual and Functional Development: The Wildlife/Human Connection*. Princeton Scientific, New Jersey, 1992 4. Colborn T. From Silent Spring (1962) to Wingspread (1991). *Comments on Toxicology* 4(4-5):319–328, 1996
- [101] Colborn T, Dumanoski D, Myers J. P. 1996. *Our Stolen Future: Are We Threatening our Fertility, Intelligence and Survival? A Scientific Detective Story*. Dutton, New York, NY, 1996, and Plume Books/Penguin USA, New York, 1997.
- [102] Ankley G.T., Johnson RD, Toth, G., Folman L.C., Detenbeck N.E., et al. Development of a research strategy for assessing the ecological risk of endocrine disruptors. *Review. Toxicology* 1:71-106, 1997
- [103] Hester, R.E. Harrison, R.M. (Eds). *Endocrine Disrupting Chemicals*. Royal Society of Chemistry, Cambridge, 1999, pp. 14-15
- [104] Z Lin, L Wang, Y Jia, Y Zhang, Q Dong, C Huang. A Study on Environmental Bisphenol A Pollution in Plastics Industry Areas. *Water Air Soil Pollut* (2017) 228: 98
- [105] N Sangai, H A Pandya, R Singh. Critical Review on Bisphenol A: Invisible Pollution. *International Journal of Pharma Research and Health Sciences* (2016), 4(2), 1043-49
- [106] Tsai WT. Human health risk on environmental exposure to bisphenol-A: a review. *J Environ Sci Health C* 2006; 24: 225-255

- [107] Oehlmann J, Schulte-Oehlmann U, Kloas W, Jagnytsch O, Lutz I, Kusk KO et al. A critical analysis of the biological impacts of plasticizers on wildlife. *Phil. Trans. R. Soc. B* 2009; 364: 2047- 2062.
- [108] Greiner E, Kaelin T, Nakamura K, 2007. Bisphenol A. CEH Report by SRI Consulting. *Environ Res* 2007; 103(1):9–20.
- [109] Shareef A, Angove MJ, Wells JD, Johnson BB. Aqueous solubilities of estrone, 17 β -estradiol, 17 α -ethynylestradiol, and bisphenol A. *J ChemEng Data* 2006; 51:879-881.
- [110] Cousins IT, Staples CA, Klecka GM, Mackay D. A multimedia assessment of the environmental fate of bisphenol A. *Hum Ecol Risk Assess* 2002; 8:1107-1135.
- [111] Heinonen J, Honkanen J, Kukkonen VK, Holopainen IJ. Bisphenol A accumulation in the freshwater clam *Pisidiumammnicum* at low temperatures. *Arch Environ Contam Toxicol* 2002; 43:50-55
- [112] Careghini A, Mastorgio AF, Saponaro S, Sezenna E. Bisphenol A, nonylphenols, benzophenones, and benzotriazoles in soils, groundwater, surface water, sediments, and food: a review. *Environ Sci Pollut Res Int.* 2015 Apr;22(8):5711-41.
- [113] Krishnan, A. V., Stathis, P., Permeth, S. F., Tokes, L., and Feldman, D. (1993). Bisphenol-A: An estrogenic substance is released from polycarbonate flasks during autoclaving. *Endocrinology* 132, 2279–2286.
- [114] Rochester, J.R., (2013) Bisphenol A and Human Health: A review of the literature, *Reproductive Toxicology*, 42, 132-155.
- [115] Castoria, G., Giovannelli, P., Lombardi, M., De Rosa, C., Giraldi, T., de Falco, A., Barone, M.V., Abbondanza, C., Migliaccio, A., Auricchio, F., (2012) Tyrosine phosphorylation of estradiol receptor by -Src regulates its hormone-dependent nuclear export and cell cycle progression in breast cancer cells. *Oncogene*, 31(46), 4868-4877.
- [116] Di Donato, M., Cerneria, G., Giovannelli, P., Galasso, G., Bilancio, A., Migliaccio, A., Castoria, G., (2017) Recent advances on bisphenol-A and endocrine disruptor effects on human prostate cancer. *Mol Cell Endocrinol.*, 457, 35-42.
- [117] Braun, J.M., Kalkbrenner, A.E., Calafat, A.M., Yolton, K., Ye, X., Dietrich, K.N., Lanphear, B.P., (2011) Impact of early-life bisphenol A exposure on behavior and executive function in children. *Pediatrics*, 128, 873-882.
- [118] Careghini A, Mastorgio AF, Saponaro S, Sezenna E. Bisphenol A, nonylphenols, benzophenones, and benzotriazoles in soils, groundwater, surface water, sediments, and food: a review. *Environ Sci Pollut Res Int.* 2015 Apr;22(8):5711-41.
- [119] USEPA (2010a) Bisphenol A action plan. U.S. Environmental Protection Agency, Washington
- [120] Michałowicz J (2014) Bisphenol A—sources, toxicity and biotransformation. *Env Toxicol Pharma* 37:738–758
- [121] Kawahata H, Ohta H, Inoue M, Suzuki A (2004) Endocrine disruptor nonylphenol and bisphenol A contamination in Okinawa and Ishigaki Islands, Japan—within coral reefs and adjacent river mouths. *Chemosphere* 55:1519–1527
- [122] Hu X, Peng J, Jiang G, Jonsson JA.. Evaluating the impacts of some environmentally relevant factors on the availability of bisphenol-A with negligible- depletion SPME. *Chemosphere* 2006; 65:1935- 1941
- [122] Huang YQ, Wong CKC, Zheng JS, Bouwman H, Barra R, Walhlstrom B, Neretin L, Wong MH (2012) Bisphenol A (BPA) in China: a review of sources, environmental levels, and potential human health impacts. *Environ Int* 42:91–99
- [123] Stuart ME, Manamsa K, Talbot JC, Crane EJ (2011) Emerging contaminants in groundwater. OR/11/013. British Geological Survey Open Report. Keyworth, Nottingham (UK), 123 pp
- [124] Yamamoto H, Liljestrand HM (2003) The fate of estrogenic compounds in the aquatic environment: sorption onto organic colloids. *Water Sci Technol* 47(9):77–84
- [125] Basheer C, Lee HK, Tan KS (2004) Endocrine disrupting alkylphenols and bisphenol-A in coastal waters and supermarket seafood from Singapore. *Mar Pollut Bull* 48:1145–1167

- [126] Lacorte S, Latorre A, Guillamon M, Barcelò D (2002) Nonylphenol, octylphenol, and bisphenol A in groundwaters as a result of agronomic practices. *Sci World J* 2:1095–1100
- [127] Latorre A, Lacorte S, Barcelo D (2003) Presence of nonylphenol, octylphenol and bisphenol-A in two aquifers close to agricultural, industrial and urban areas. *Chemosphere* 57:111–116
- [128] Godejohann M, Heintz L, Daolio C, Berset J, Muff D (2009) Comprehensive non-targeted analysis of contaminated groundwater of a former ammunition destruction site using ¹H-NMR and HPLC-SPE-NMR/TOF-MS. *Environ Sci Technol* 43:7055–7061
- [129] Fukazawa, H., Watanabe, M., Shiraishi, F., Shiraishi, H., Shiozawa, T., Matsushita, H., et al. (2002) Formation of Chlorinated Derivatives of Bisphenol A in Waste Paper Recycling Plants and Their Estrogenic Activities. *J Health Sci.*, 48(3), 242–9.
- [130] Heemken, O.P., Reincke, H., Stachel, B., Theobald, N., (2001) The occurrence of xenoestrogens in the Elbe river and the North Sea. *Chemosphere*, 45(3), 245–59.
- [131] Colin, A., Bach, C., Rosin, C., Munoz, J-F., Dauchy, X., (2014) Is drinking water a major route of human exposure to alkylphenol and bisphenol contaminants in France? *Arch Environ Contam Toxicol.*, 66(1), 86–99.
- [132] Azevedo DA, Lacorte S, Viana P, Barcelo D (2001) Occurrence of nonylphenol and bisphenol A in surface waters from Portugal. *J Brazil Chem Soc* 12:532–537
- [133] Patrolecco L, Capri S, De Angelis S, Pagnotta R, Polesello S, Valsecchi S (2006) Partition of nonylphenol and related compounds among different aquatic compartments in Timber River (Central Italy). *Water Air Soil Poll* 172:151–166
- [134] Loos R, Hanke G, Umlauf G, Eisenreich SJ (2007) LC-MS-MS analysis and occurrence of octyl- and nonylphenol, their ethoxylates and their carboxylates in Belgian and Italian textile industry, waste water treatment plant effluents and surface waters. *Chemosphere* 66:690–699
- [135] Pojana G, Jonkers N, Marcomini A (2007) Natural and synthetic endocrine disrupting compounds (EDCs) in water, sediment and biota of a coastal lagoon. *Environ Int* 33:929–936
- [136] Funakoshi G, Kasuya S. Influence of an estuary dam on the dynamics of bisphenol A and alkylphenols. *Chemosphere* 2009; 75: 491-497.
- [137] Loffredo E, Senesi N. Fate of anthropogenic organic pollutants in soils with emphasis on adsorption/desorption processes of endocrine disruptor compounds. *Pure Appl Chem* 2006; 78: 947-961.
- [138] Zielinska, M.; Wojnowska-Baryla, I.; Cydzik-Kwiatkowska, A. (2019) Bisphenol A Removal from Water and Wastewater. Springer International Publishing
- [139] Zielińska M., Bułkowska K., Cydzik-Kwiatkowska A., Bernat K., Wojnowska-Baryła I., Removal of bisphenol A (BPA) from biologically treated wastewater by microfiltration and nanofiltration, *International Journal of Environmental Science and Technology* 13: 2239-2248, 2016
- [140] Heavy Metals Toxicity and the Environment. Paul B Tchounwou, Clement G Yedjou, Anita K Patlolla, and Dwayne J Sutton. *EXS*. 2012 ; 101: 133–164. doi:10.1007/978-3-7643-8340-4_6.
- [141] Dopp E, Hartmann LM, Florea AM, Rettenmier AW, Hirner AV. Environmental distribution, analysis, and toxicity of organometal (loid) compounds. *Crit Rev Toxicol*. 2004;34:301–333
- [142] Guzzi G, LaPorta CAM. Molecular mechanisms triggered by mercury. *Toxicol*. 2008;244:1–12.
- [143] Palmeira CM, Madeira VMC. Mercuric chloride toxicity in rat liver mitochondria and isolated hepatocytes. *Environ Toxicol Pharmacol*. 1997;3:229–235
- [144] Sunja Kim S, Dayani L, Rosenberg PA, Li J. RIP1 kinase mediates arachidonic acid-induced oxidative death of oligodendrocyte precursors. *Intl Physiol Pathophysiol Pharmacol*. 2010;2(2):137–147.
- [145] Marnett LJ. Oxyradicals and DNA damage. *Carcinogenesis*. 2000;21(3):361–370.
- [146] Crespo-Lopez MR, Macedo GL, Pereira SID, Arrifano GPF, Picano-Dinc DLW, doNascimento JLM, Herculano AM. Mercury and human genotoxicity: Critical considerations and possible molecular mechanisms. *Pharmacol Res*. 2009;60:212–220.
- [147] Sarkar BA. Mercury in the environment: Effects on health and reproduction. *Rev Environ Health*. 2005;20:39–56

- [148] U.S. EPA (Environmental Protection Agency) Mercury Study Report to Congress. 1997 Available at: <http://www.epa.gov/mercury/report.htm>.
- [149] Sarkar BA. Mercury in the environment: Effects on health and reproduction. *Rev Environ Health*. 2005;20:39–56
- [150] Sanfeliu C, Sebastia J, Cristofol R, Rodriquez-Farre E. Neurotoxicity of organomercurial compounds. *Neurotox. Res*. 2003;5:283–305
- [151] Tchounwou PB, Ayensu WK, Ninashvilli N, Sutton D. Environmental exposures to mercury and its toxicopathologic implications for public health. *Environ Toxicol*. 2003;18:149–175.
- [152] U.S. Environmental Protection Agency (2007) Treatment Technologies for Mercury in Soil, Waste, and Water
- [153] U.S. Environmental Protection Agency. Capsule Report (1997) Aqueous Mercury Treatment.
- [154] Mercury Contaminated Sites: A Review of Remedial Solutions. Jennifer Hinton, Marcello Veiga. Proc. NIMD (National Institute for Minamata Disease) Forum 2001. Mar. 19-20, 2001, Minamata, Japan
- [155] Alley WM, Reilly TE, Franke OL: Sustainability of Groundwater Resources. U.S. Geological Survey (U.S.GS), Denver, CO; 1999.
- [156] PK Pandey, PH Kass, ML Soupir, S Biswas and VP Singh. Contamination of water resources by pathogenic bacteria. *AMB Express* 2014, 4:51
- [157] Arnone RD, Walling JP: Waterborne pathogens in urban watersheds. *J Water Health* 2007, 5(1):149–162.
- [158] Bai S, Lung WS: Modeling sediment impact on the transport of fecal bacteria. *Water Res* 2005, 39: 5232–5240.
- [159] Baker-Austin C, McArthur J, Lindell A, Wright M, Tuckfield R, Gooch J, Warner L, Oliver J, Stepanauskas R: Multi-site analysis reveals widespread antibiotic resistance in the marine pathogen: *Vibrio vulnificus*. *Microb Ecol* 2009, 57(1):151–159.
- [160] S.Ischii, MJ Sadowsky. *Escherichia coli* in the environmental: implication for water quality and human health. *Microber Environ* (2008) 23 (2) 101-108
- [161] World Health Organization. Enterotoxigenic *Escherichia coli* (ETEC). In *Diarrhoeal Diseases*; Available online: http://www.who.int/vaccine_research/diseases/diarrhoeal/en/index4.html (assessed on 4 September 2010).
- [162] Vital M, Hammes F, Egli T. (2008). *Escherichia coli* O157 can grow in natural freshwater at low carbon concentrations. *Environ Microbiol* 10: 2387–2396.
- [163] Van Elsas JD, Trevors JT, van Overbeek LS. (1991). Influence of soil properties on the vertical movement of genetically-marked *Pseudomonas fluorescens* through large soil microcosms. *Biol Fertil Soils* 10: 249–255.
- [164] Campbell GR, Prosser J, Glover A & Killham K (2001) Detection of *Escherichia coli* O157:H7 in soil and water using multiplex PCR. *J Appl Microbiol* 91: 1004–1010.
- [165] Solomon EB, Yaron S & Matthews KR (2002b) Transmission of *Escherichia coli* O157:H7 from contaminated manure and irrigation water to lettuce plant tissue and its subsequent internalization. *Appl Environ Microbiol* 68: 397–400.
- [166] Mead PS & Griffin PM (1998) *Escherichia coli* O157:H7. *Lancet* 352: 1207–1212.
- [167] Olsen SJ, Miller G, Breuer T, Kennedy M, Higgins C, Walford J, McKee G, Fox K, Bibb W & Mead P (2002) A waterborne outbreak of *Escherichia coli* O157:H7 infections and hemolytic uremic syndrome: implications for rural water systems. *Emerg Infect Dis* 8: 370–375.
- [168] MO Adeboye. Disinfection of *Escherichia coli* in Water Using Ultraviolet–Leds. M.Sc thesis. University of Eastern Finland, Department of Environmental Science. December 2014
- [169] Nelson K.Y., McMartin., Yost C.K., Runtz K.J. and Ono T. (2013). Point-of-use water disinfection using UV light-emitting diodes to reduce bacterial contamination. *Environmental Science Pollution Research* 20, 5441-5448.

- [170] LeChevallier M.W. and Au K.K. (2002). Water treatment for microbial control: A review document. World Health Organization.
- [171] Anastasi E.M., Wohlsen T.D., Stratton H.M. and Katouli M. (2013). Survival of *Escherichia coli* to sewage treatment plants using UV irradiation and chlorination for disinfection. *Water Research* 47, 6670-6679.
- [172] Ainsworth R. (2004). *Safe Piped water: Managing Microbial Water Quality in Piped Distribution Systems*. World Health Organization Drinking Water Quality Series. IWA publishing, London, UK.
- [173] Ashbolt N.J. (2004). Microbial contamination of drinking water and disease outcomes in developing regions. *Toxicology* 198, 229-238.
- [174] Wu D., Yang Z., Wang W., Tian G., Xu S. and Sims O. (2012). Ozonation as an advanced oxidant in treatment of bamboo industry wastewater, *Chemosphere* 88, 1108-1113.
- [175] Gimeno O., Rivas F.J., Beltran F.J. and Carbajo M. (2007). Photocatalytic Ozonation of Winery Wastewaters, *Journal of Agriculture and Food Chemistry*. 55, 9944-9950.
- [176] Ibrahim M.A.S., MacAdam J., Autin O. and Jefferson B. (2014). Evaluating the impact of LED bulb development on the economic viability of ultraviolet technology for disinfection. *Environmental Technology for Disinfection* 35(4), 400-406.
- [177] Soloshenko I.A., Bazhenov V.Y., Khomich V.A Tsiolko V.V. and Potapchenko N.G. (2006). Comparative research efficiency of water decontamination by UV radiation of cold hollow cathode discharge plasma versus that of low and medium-pressure lamps. *IEE Transactions on Plasma Science*. 34, 1365-1369.
- [178] Beck S.E., Rodriguez R.A., Linden K.G., Hargy T.M., Larason T.C. and Wright H.W. (2014). Wavelength Dependent UV inactivation and DNA Damage of Adenovirus as Measured by Cell Culture Infectivity and Long Range Quantitative PCR. *Environmental Science and Technology* 48, 591-598.
- [179] Vilhunen S., Särkkä H. and Sillanpää M. (2009). Ultraviolet light-emitting diodes in water disinfection. *Environmental Science and Pollution Research* 16, 439-442.
- [180] Gregory J. (2006). *Particles in water: properties and processes*. IWA publishing/CRC Press, London.
- [181] Liu D. and Liptak B. (1999). *Wastewater treatment*. CRC Press, BocaRaton, USA
- [182] JG Speight. *Environmental Organic Chemistry for Engineers*. In Chapter 7, *Chemical Transformations in the Environment*.
- [183] Calvet, R., 1989. Adsorption of organic chemicals in soils. *Environ. Health Perspect.* 83, 145–177.
- [184] Mokhatab, S., Poe, W.A., Speight, J.G., 2006. *Handbook of Natural Gas Transmission and Processing*. Elsevier, Amsterdam, Netherlands.
- [185] N Ayawei, AN Ebelegi, and D Wankasi. Modelling and Interpretation of Adsorption Isotherms. *Journal of Chemistry* Article ID 3039817, 11 pages
- [186] N. Ayawei, M. Horsfall Jnr, and I. Spiff, “Rhizophora mangle waste as adsorbent for metal ions removal from aqueous solution,” *European Journal of Scientific Research*, vol. 9, no. 1, p. 21, 2005.
- [187] M. I. El-Khaiary, “Least-squares regression of adsorption equilibrium data: comparing the options,” *Journal of Hazardous Materials*, vol. 158, no. 1, pp. 73–87, 2008
- [188] J. H. De Boer, *The Dynamical Character of Adsorption*, Oxford University Press, Oxford, England, 1953.
- [189] M. I. El-Khaiary, “Least-squares regression of adsorption equilibrium data: comparing the options,” *Journal of Hazardous Materials*, vol. 158, no. 1, pp. 73–87, 2008
- [190] S. D. Fost and M. O. Aly, *Adsorption Processes for Water Treatment*, Betterworth Publications, Stoneham, Massachusetts, Mass, USA, 1981.
- [191] S De Gisi, G Lofrano, M Grassi, M Notarnicola. Characteristics and adsorption capacities of low-cost sorbents for wastewater treatment: A review. *Sustainable Materials and Technologies* 9 (2016) 10–40
- [192] Wang J., Chen C. (2009) Biosorbents for heavy metals removal and their future, *Biotechnology Advances*, 27 , 195–226
- [193] M Stojanovic, Z Lopičić, J Milojković, Č Lačnjevac, M Mihajlović, M Petrović, A Kostić. Biomass waste material as potential adsorbent for sequestering pollutants. *Scientific paper UDC:504.054:631.872.874*

- [194] Tran, V.S., Ngo, H.H., Guo, W., Zhang, J., Liang, S., Ton-That, C., 2015. Typical low cost biosorbents for adsorptive removal of specific organic pollutants from water. *Bioresour. Technol.* 182, 353e363.
- [195] Abdeen Z., Mohammad S.G. 2013. Study of the Adsorption Efficiency of an EcoFriendly Carbohydrate Polymer for Contaminated Aqueous Solution by Organophosphorus Pesticide. *Open J. Org. Polym. Mater.*
- [196] Akhtar, M., Bhanger, M.I., Iqbal, S., Hasany, S.M., 2006. Sorption potential of rice husk for the removal of 2,4-dichlorophenol from aqueous solutions: Kinetic and thermodynamic investigations. *J. Hazard. Mater.* 128, 44-52.
- [197] R Wahi, LA Chuaha, TS Yaw, CZN Mohsen, M Nourouzia. *Separation and Purification Technology*. Volume 113, 24 July 2013, Pages 51-63
- [198] E Khan, W Virojnagud, T Ratpukdi. Use of biomass sorbents for oil removal from gas station runoff. *Chemosphere* 57 (2004) 681–689
- [199] P.C. Brandão, T.C. Souza, C.A. Ferreira, C.E. Hori, L.L. Romanielo. Removal of petroleum hydrocarbons from aqueous solution using sugarcane bagasse as adsorbent. *Separation and Purification Technology* 113 (2013) 51–63
- [200] Bazargan A, Tan J, Hui D, Mckay G. Utilization of rice husks for the production of oil sorbent materials (2014) *Cellulose* 21(3)
- [201] Alaa El-Din, G., Amer, A.A., Malsh, G., Husse, M. Study on the use of banana peels for oil spill removal. *Alexandria Eng. J.*, Article-In-Press.
- [202] M. Husseien, AA Amer, A El-Maghraby, NA Taha. Experimental Investigation of Thermal Modification Influence on Sorption Qualities of Barley Straw. *Journal of Applied Sciences Research*, 4(6): 652-657, 2008
- [203] A. Srinivasan, T. Viraraghavan. Removal of oil by walnut shell media. *Bioresour. Technol.* 99 (2008), pp.8217–8220
- [204] N Ali , M El-Harbawi , AA Jabal, CY Yin (2012) Characteristics and oil sorption effectiveness of kapok fibre, sugarcane bagasse and rice husks: oil removal suitability matrix, *Environmental Technology*, 33:4, 481-486, DOI: 10.1080/09593330.2011.579185
- [205] M. Inagaki, A. Kawahara, H. Konno. Sorption and recovery of heavy oils using carbonized fir fibers and recycling. *Carbon*, 40 (1) (2002), pp. 105-111
- [206] D. Angelova, I. Uzunov, S. Uzunova, A. Gigova, L. Minchev. Kinetics of oil and oil products adsorption by carbonized rice husks. *Chem. Eng. J.*, 172 (1) (2011), pp. 306-311
- [207] Deschamps, G., Caruel, H., Borredon, M-E., Bonnin, C., Vignoles, C., 2003. Oil removal from water by selective sorption on hydrophobic cotton fibers 1. Study of sorption properties and comparison with other cotton fiber-based sorbents. *Environmental Science and Technology* 37, 1013–1015.
- [208] Yang, Y., Deng, Y., Tong, Z., Wang, C., 2014. Renewable lignin-based xerogels with self-cleaning properties and superhydrophobicity. *ACS Sustain. Chem. Eng.* 2, 1729e1733.
- [209] Calcagnile, P., et al., 2017. A bio-based composite material for water remediation from oily contaminants. *Mater. Des.* 134, 374e382.
- [210] Wang, J., Zheng, Y., Kang, Y., Wang, A., 2013. Investigation of oil sorption capability of PBMA/SiO₂ coated kapok fiber. *Chem. Eng. J.* 223, 632e637.
- [211] Liu, H., Geng, B., Chen, Y., Wang, H., 2017. Review on the aerogel-type oil sorbents derived from nanocellulose. *ACS Sustainable Chem. Eng.* 5, 49e66.
- [212] A.E. Said, A.G. Ludwick, H.A. Aglan. Usefulness of raw bagasse for oil absorption: a comparison of raw and acylated bagasse and their components. *Bioresour. Technol.*, 100 (7) (2009), pp. 2219-2222
- [213] A.E. Said, A.G. Ludwick, H.A. Aglan. Usefulness of raw bagasse for oil absorption: a comparison of raw and acylated bagasse and their components. *Bioresour. Technol.*, 100 (7) (2009), pp. 2219-2222
- [214] S. Ibrahim, H. Ang, S. Wang. Removal of emulsified food and mineral oils from wastewater using surfactant modified barley straw. *Bioresour. Technol.*, 100 (23) (2009), pp. 5744-5749
- [215] Ahmaruzzaman, M. (2008). Adsorption of phenolic compounds on low-cost adsorbents: a review. *Advances in Colloid and Interface Science*, 143(1), 48–67

- [216] Bhatnagar, A., & Jain, A. (2005). A comparative adsorption study with different industrial wastes as adsorbents for the removal of cationic dyes from water. *Journal of Colloid and Interface Science*, 281(1), 49–55.
- [217] Bhatnagar, A., & Sillanpää, M. (2010). Utilization of agroindustrial and municipal waste materials as potential adsorbents for water treatment—a review. *Chemical Engineering Journal*, 157(2), 277–296.
- [218] Chun, L., Hongzhang, C., & Zuohu, L. (2004). Adsorptive removal of Cr(VI) by Fe-modified steam exploded wheat straw. *Process Biochemistry*, 39(5), 541–545.
- [219] Grassi, M., Kaykioglu, G., Belgiorno, V., & Lofrano, G. (2012). Removal of emerging contaminants from water and wastewater by adsorption process emerging compounds removal from wastewater (pp. 15–37): Springer
- [220] Khattri, S. D., & Singh, M. K. (2009). Removal of malachite green from dye wastewater using neem sawdust by adsorption. *Journal of Hazardous Materials*, 167(1–3), 1089–1094
- [221] Rossner, A., Snyder, S. A., & Knappe, D. R. U. (2009). Removal of emerging contaminants of concern by alternative adsorbents. *Water Research*, 43(15), 3787–3796.
- [222] Wan Ngah, W., & Hanafiah, M. (2008). Removal of heavy metal ions from wastewater by chemically modified plant wastes as adsorb
- [223] Kumar, A. J., & Namasivayam, C. (2014). Uptake of endocrine disruptor bisphenol-a onto sulphuric acid activated carbon developed from biomass: equilibrium and kinetic studies. *Sustainable Environment Research*, 24(1)
- [224] KL Chang, JF Hsieh, BM Ou, MH Chang, WY Hsieh, JH Lin, PJ Huang, KF Wong, ST Chen (2012) Adsorption Studies on the Removal of an Endocrine-Disrupting Compound (Bisphenol A) using Activated Carbon from Rice Straw Agricultural Waste, *Separation Science and Technology*, 47:10, 1514-1521, DOI: 10.1080/01496395.2011.647212
- [225] Nakanishi, A., Tamai, M., Kawasaki, N., Nakamura, T., & Tanada, S. (2002). Adsorption characteristics of bisphenol a onto carbonaceous materials produced from wood chips as organic waste. *Journal of Colloid and Interface Science*, 252(2), 393–396.
- [226] Tsai, W.-T., Lai, C.-W., & Su, T.-Y. (2006). Adsorption of bisphenol-a from aqueous solution onto minerals and carbon adsorbents. *Journal of Hazardous Materials*, 134(1–3), 169-175
- [227] Wirasnita, R., Hadibarata, T., Yusoff, A., & Yusop, Z. (2014). Removal of bisphenol a from aqueous solution by activated carbon derived from oil palm empty fruit bunch. *Water, Air, & Soil Pollution*, 225(10), 1–12
- [228] Bautista-Toledo, I., Ferro-García, M.A., Rivera-Utrilla, J., Moreno-Castilla, C., & Vegas Fernández, F.J. (2005). Bisphenol a removal from water by activated carbon. Effects of carbon characteristics and solution chemistry. *Environmental Science & Technology*, 39(16), 6246-6250
- [229] Lazim, Z.M.; Hadibarata, T.; Puteh, M.H.; Yusop, Z. Adsorption characteristics of bisphenol A onto low-cost modified phyto-waste material in aqueous solution. *Water Air Soil Pollut.* 2015, 226, 34–45.
- [230] Zhang, F.S., Nriagu, J.O., Itoh, H., 2005. Mercury removal from water using activated carbons derived from organic sewage sludge. *Water Res.* 39, 389-395
- [231] Zabihi, M., Haghghi Asl, A., Ahmadpour, A., 2010. Studies on adsorption of mercury from aqueous solution on activated carbons prepared from walnut shell. *J. Hazard. Mater.* 174, 251-256.
- [232] Rao, M.M., Reddy, D.H.K.K., Venkateswarlu, P., Seshaiyah, K., 2009. Removal of mercury from aqueous solutions using activated carbon prepared from agricultural by-product/waste. *J. Environ. Manag.* 90, 634-643, 2009.
- [233] Namasivayam C. Bicarbonate-treated peanut hull carbon for mercury (II) removal from aqueous solution. (2003) *Water Research* 27(11):1663-1668
- [234] Arias, F., Beneduci, A., Chidichimo, F., Furia, E., Straface, S., 2017. Study of the adsorption of mercury (II) on lignocellulosic materials under static and dynamic conditions. *Chemosphere* 180, 11-23.

- [235] Santhana A, Kumar K, Mniraj B, Puvvada S, Rajesh N. Microwave assisted preparation of glycidyl methacrylate grafted cellulose adsorbent for the effective adsorption of mercury from a coal fly ash sample. 2013 Journal of Environmental Chemical Engineering 1(4)
- [236] V. Singh, S. Kumar Singh, S. Maurya. Microwave induced poly(acrylic acid) modification of Cassia javanica seed gum for efficient Hg(II) removal from solution. Chem. Eng. J., 160 (2010), pp. 129-137
- [237] N. Bicak, D.C. Sherrington, B.F. Senkal. Graft copolymer of acrylamide onto cellulose as mercury selective sorbent. React. Funct. Polym., 41 (1999), pp. 69-76
- [238] G. Shibi, T.S. Anirudhan. Synthesis, characterisation, and application as a mercury(II) sorbent of banana stalk-polyacrylamide grafted copolymer bearing carboxyl groups. Ind. Eng. Chem. Res., 41 (2002), pp. 341-5352
- [239] Y. Takagai, A. Shibata, S. Kiyokawa, T. Takase. Synthesis and evaluation of different thio-modified cellulose resins for the removal of mercury(II) ion from highly acidic aqueous solutions. J. Colloid Interface Sci., 353 (2011), pp. 593-597
- [240] R. Navarro, K. Sumi, N. Fujii, M. Matsumura. Mercury removal from wastewater using porous cellulose carrier modified with polyethyleneimine. Water Res., 30 (1996), pp. 2488-2494
- [241] T.S. Anirudhan, M.R. Unnithan, L. Divya, P. Senan. Synthesis and characterization of polyacrylamide-grafted coconut coir pith having carboxylate functional group and adsorption ability for heavy metal ions. J. Appl. Polym. Sci., 104 (2007), pp. 3670-3681

CHAPTER 4

4 INTRODUCTION TO THE EXPERIMENTAL STUDIES PERFORMED DURING THIS Ph.D. THESIS

This thesis work concerned the development of purifying systems for water contaminated by various types of pollutants, in particular all developed systems have in common purifying materials derived from cellulose fibers, extracted from the *Spartium Junceum* plant variety. These fibers can be extracted from the vegetable by means of alkali digestion processes which dissolve the ligninic and pectinic components, which have the purpose of keeping the fibers adhered to the inner layers of the branches of the plant, in the form of fibrils, having a diameter of a few tens of microns and lengths varying between 5 and 20 cm.

For these morphological characteristics, they exhibit a high surface area and therefore represent the ideal basis for the development of filtering systems. In addition, other advantages should be added to those just mentioned, which are represented by the ease of finding the plant, which grows spontaneously and is widespread in all parts of the world, especially in the Mediterranean area and the simplicity and low cost of the processes extraction.

The surface of the cellulosic fibers exposes hydroxyl groups (3 for each glucosidic ring) outwards and therefore has a strongly hydrophilic nature. It has been shown in this thesis that the surface is strongly captive for heavy metals such as Hg (II). A part of the thesis work concerns precisely the study of the purifying power for waters polluted by heavy metals.

However, the same cellulose fibers are not suitable for the capture of organic hydrophobic pollutants, such as hydrocarbons or complex molecules containing hydrocarbon parts, such as TPHs and EDCs. In order to be able to use the fibers in the purification processes of waters polluted by hydrophobic substances, they must be treated in such a way that their surface becomes hydrophobic.

In order to hydrophobize the cellulosic fibers at the surface level, for use in the purification of waters polluted by TPHs and Bisphenol-A (pollutants selected in the initial phase for their high persistence in the environment and toxicity to living species), two different modes of functionalization were used.

A first method of functionalization has exploited the ease of reaction of the diisocyanates with the surface hydroxyl groups of the fiber itself. In particular, the 4,4'-Methylenebis (phenyl isocyanate) reagent was used. In this case, one of the isocyanic groups served to bind the hydrophobic molecule to the surface of the fiber, through the formation of a urethane bond, while the second isocyanate group was subsequently transformed into an amino group.

A second method of functionalization employed the use of a low pressure plasma technique, by which it was possible to graft the surface of the fibers with fluorinated groups which confer a superhydrophobic character.

A further purifying system based on the cellulose fibers of Spanish Broom, has been developed to purify the water from widely diffused bacteria such as *Escherichia coli*. In this case a photocatalytic approach was employed, covering the surface of the fibers with a thin layer of TiO₂. The fibers/fabrics thus functionalized, in the presence of UV-A radiation lamps at a wavelength of 365 nm, showed a good capacity for bacterial inactivation.

The research carried out, not only allowed to determine the purifying capacities of the systems developed, but, also, aimed at defining the thermodynamic and kinetic aspects of the adsorption processes involved. The variation of pollutant concentrations in function of time has been interpreted in terms of kinetic models that have allowed us to discover all the speed constants involved.

Most of the work performed during this Ph.D. thesis has been published or are under consideration for publication in peer review journals and have been attached to this manuscript as individual chapter.

Furthermore, the promising materials and water treatment technologies developed in these studies, will be the subject of patents.

The studies conducted in this thesis work are reported in the following chapters in this order:

CHAPTER 5. Remediation of hydrocarbons polluted water by hydrophobic functionalized cellulose

Published:

Tursi A, Beneduci A, Chidichimo F, De Vietro N, Chidichimo G. *Remediation of hydrocarbons polluted water by hydrophobic functionalized cellulose. **Chemosphere**, 2018; 201:530-539.*

CHAPTER 6. Removal of endocrine disrupting chemicals from water: adsorption of bisphenol-A by biobased hydrophobic functionalized cellulose

Published:

Tursi A, Chatzisyneon E, Chidichimo F, Beneduci A, Chidichimo G. *Removal of endocrine disrupting chemicals from water: adsorption of bisphenol-A by biobased hydrophobic functionalized cellulose. **International Journal of Environmental Research and Public Health** 2018, 15(11), 2419; <https://doi.org/10.3390/ijerph15112419>*

CHAPTER 7. Low pressure plasma functionalized cellulose fiber for the remediation of petroleum hydrocarbons polluted water

Under review:

Tursi A, De Vietro N, Beneduci A, Milella A, Chidichimo F, Fracassi F, Chidichimo G. *Low pressure plasma functionalized cellulose fiber for the remediation of petroleum hydrocarbons polluted water. Journal of Hazardous Materials*

CHAPTER 8. Preliminary studies of the adsorption of mercury (II) in water by means of cellulosic fibers

Preliminary studies

CHAPTER 9. Photocatalytic inactivation of Escherichia coli bacteria in water using low pressure plasma deposited TiO₂ cellulose fabric

Under review:

Tursi A, De Vietro N, Beneduci A, Chidichimo F, Dalena F, Fracassi F, Chatzisyneon E, Chidichimo G. *Photocatalytic inactivation of Escherichia Coli in water using grafted TiO₂ cellulose fabric obtained through the low plasma technique. Photochemical & Photobiological Sciences*

CHAPTER 5



Remediation of hydrocarbons polluted water by hydrophobic functionalized cellulose

Antonio Tursi^a, Amerigo Beneduci^{a, c, *}, Francesco Chidichimo^{b, c}, Nicoletta De Vietro^d, Giuseppe Chidichimo^{a, c}

^a Department of Chemistry and Chemical Technologies, University of Calabria, Via P. Bucci, Cubo 15D, 87036, Arcavacata di Rende, CS, Italy

^b Department of Environment and Chemical Engineering, University of Calabria, Via P. Bucci, Cubo 41B, 87036, Arcavacata di Rende, CS, Italy

^c SIRiA S.r.l. - Servizi Integrati e Ricerche per l'Ambiente, Spin-off of the University of Calabria, c/o Department of Chemistry and Chemical Technologies, Via P. Bucci, Cubo 15D, 87036, Arcavacata di Rende, CS, Italy

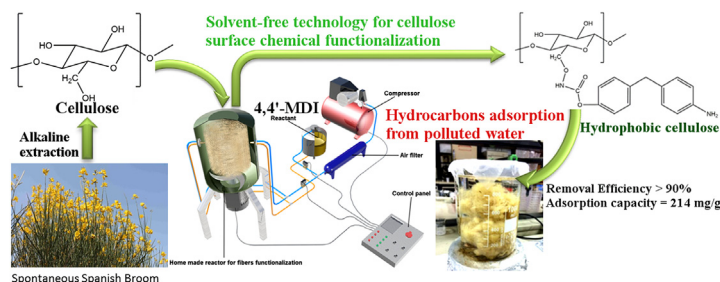
^d Institute of Nanotechnology (Nanotec), National Research Council (CNR), c/o Department of Chemistry, University of Bari "Aldo Moro", Italy



HIGHLIGHTS

- Hydrocarbons removal from water by adsorption on surface hydrophobized cellulose.
- Hydrophobization by a green, solvent free reaction process for large-scale production.
- Fast hydrocarbons adsorption kinetics with removal efficiency larger than 90%.
- Large surface/weight ratio with adsorption capacity as high as 214 mg/g.
- Roughly 0.5 kg of cellulose for removing 100 ppm of pollutants from a ton of water.

GRAPHICAL ABSTRACT



ARTICLE INFO

Article history:

Received 27 August 2017

Received in revised form

27 February 2018

Accepted 5 March 2018

Available online 7 March 2018

Handling Editor: Shane Snyder

Keywords:

Hydrocarbons polluted water

Surface modified cellulose

Hydrophobic cellulose

Hydrocarbons adsorption

ABSTRACT

Remediation of water bodies from petroleum hydrocarbons is of the utmost importance due to health risks related to the high toxicity, mutagenicity and carcinogenicity of the hydrocarbons components that may enter into the food chain. Though several methods were proposed to face up this challenge, they are generally not easily feasible at a contaminated site and quite costly. Here we propose a green, cost-effective technology based on hydrophobized Spanish Broom (SB) cellulose fiber. The natural cellulose fiber was extracted by alkaline digestion of the raw vegetable. The hydrophilic cellulose surface was transformed into a hydrophobic one by the reaction with 4,4'-diphenylmethane diisocyanate (MDI) forming a very stable urethane linkage with the hydroxyl groups of cellulose emerging from the fibers surface. Chemical functionalization was performed with a novel solvent-free technology based on a home-made still reactor where the fiber was kept under vortex stirring and the MDI reactant then spread onto the fiber surface by nebulizing it in form of micrometer-sized droplets.

* Corresponding author. Department of Chemistry and Chemical Technologies, University of Calabria, Via P. Bucci, Cubo 15D, 87036, Arcavacata di Rende, CS, Italy.

E-mail address: amerigo.beneduci@unical.it (A. Beneduci).

The functionalized fiber, characterized by means of WCA measurements, XPS and ATR-FTIR spectroscopy, shows fast adsorption kinetics adsorption capacity as high as 220 mg/g, among the highest ever reported so far in the literature for cellulosic materials.

© 2018 Elsevier Ltd. All rights reserved.

1. Introduction

One of the major environmental problem which need to be solved today is the recovering of water bodies such as sea, lakes, rivers and aquifers polluted by Hydrophobic Organic Compounds (HOCs). These pollutants include aliphatic and aromatic hydrocarbons, polychlorobiphenyls (PCBs), polycyclic aromatic hydrocarbons (PAHs), polychlorinated di-benzodioxins and some pesticides. Even if these compounds are very low soluble in water, they can explicate high toxicity, mutagenicity, and carcinogenicity because of their entering into the food chain (European Union, 2008; Van der Oost et al., 2003). Oil contamination is relatively common because of its widespread use and its associated disposal operations and accidental spills. The main problem with the remediation of the environmental matrices involved by these pollutants is that generally they persist as a separate phase, because of their low solubility, so they can be found as free floating, emulsified, dissolved, or adsorbed to soil grains. The occurrence of these scenarios gives rise to what is known as secondary source of contamination. A source is the location from which a contaminant has entered a physical system. A primary source, such as a drum or a reservoir leaking onto a water body or surface soils, may produce a secondary source, such as a contamination plume or contaminated soils (ASTM and E1689-95(2014), 2014). While primary sources are easier to identify and to deal with, secondary sources are very hard to manage. The situation becomes even worse if the cleaning procedures concern groundwater systems. Subsurface water-soil environments do not allow to directly observe and act on the processes occurring in their inside, resulting, in most cases, in very expensive and not very effective operations (Hardisty and Ozdemiroglu, 2005; Mercer and Cohen, 1990; Robinson and Angyal, 2008). Consequently, attention has been focused on the identification of measures to be taken to limit and control secondary contamination sources. Proposed techniques, to remove HOCs from water, may include heterogeneous photocatalysis, technologies based on Fenton reaction chemistry (including homogeneous photocatalysis such as photo-Fenton), ozonation, electrochemical processes (Trellu et al., 2016). However, these processes are not easily feasible at a contaminated site, and are generally quite costly. More traditional processes are thermal treatment (very perturbing and high costly), pump and treat (low efficiency), biodegradation (very long treatment times). Specifically, with regards to soil pollution, Soil Washing and Soil Flushing techniques, using extracting agents, are today under development (Mulligan et al., 2001; Mao et al., 2015; Mousset et al., 2014; Lau et al., 2014; Paria, 2008).

Here the term extracting agent is used to define additives which increases pollutants solubility in water, helping their extraction from the soil matrix, thus increasing the efficiency of the cleaning process and reducing the working time and relative costs. Of course, these extracting agents need to have some important peculiar characteristics: they must be not toxic and biodegradable in a reasonable time. It has been recently reported, that these additives, being somewhat polar, can also mobilize heavy metals (Mao et al., 2015). Anyway, when using soil washing techniques, the pollution is transferred from the soil to a, generally water based,

liquid phase. The methodology seems to be more efficient with respect to the others, but researchers are required to develop efficient processes to separate the pollutants from the liquid extracting phase, in order to recycle it continuously in the soil recovering process and to have a clean liquid phase at the end. This would lower the cost, reducing the amount of extracting reactants and allow to treat large amount of soil (Rosas et al., 2013; Navarro et al., 2008; Villa et al., 2010).

A recent study (Trellu et al., 2016) reviews the possible degradation process that can be applied to clean soil washing solutions, focusing mainly on photocatalysis based on Fenton reaction chemistry, ozonation, electrochemical processes and biological treatments. In other words, in the remediation from HOCs of both water bodies and soils, is of primary importance to find fast and low cost methods to clean aqueous phases from the hydrophobic pollutants.

In this paper, we present a study concerning the possibility to use hydrophobized cellulose fibers extracted from Spanish Broom (SB). This vegetable is a spontaneously growing shrub of the Mediterranean flora, largely diffuse even in other continents. It is an interesting Liberian plants, being constituted by many short branches, called "Vermene", containing a high content of easily removable cellulose fibers. The plant has been traditionally used in the ornamental trade, for yellow dye extraction, as well as for cellulose fibers production (Cerchiara et al., 2010a, 2010b, 2014; Gabriele et al., 2009).

Recently, it has been also shown its potential use as reinforcing agent in polyurethane composites (Chidichimo et al., 2016).

Several authors, in the last few years have taken into consideration the possibility to use natural fibers to remediate water polluted by HOCs (Wahi et al., 2013). Experiments have been done using sugarcane bagasse (removal efficiency up to 70%) (El-Gendy and Hussein, 2016), straw-peat composite (Paulauskienė and Jucikė, 2015), other agriculture wastes such as rice straw (Younis et al., 2014), activated rice husk (Yakout and Daifullah, 2013), naturally hydrophobic cellulose such as unprocessed cotton, kapok, or milkweed seed hair and, in addition, a wide assortment of activated cellulosic materials (Hubbe et al., 2013). Here the term activated cellulosic materials, means materials (peat, sawdust, wood shavings, wood chips, cotton, cotton cloth, etc.) heated in the presence of a limited quantity of air, at temperature of 180–210 °C for several hours, to increase their hydrophobic character.

The possibility to increase the hydrocarbon uptake by natural vegetable fibers, by reacting the cellulose fiber surface with hydrocarbon chemical groups has been recognized more than 10 years ago. Deschamps et al. (2003) pointed out that hydrophobic cotton fibers, obtained by acylation of cellulose with fatty acid using microwaves radiations, have a high selective affinity for vegetable or mineral oil, fuel, and petroleum, in aqueous medium. Their sorption capacity (mass of sorbate picked up by a given unit mass of sorbent) can be as high as 20 g/g. Similar absorbing capacity, of cotton-peat composites has been found by other authors (Sun et al., 2004).

As far as it is in our knowledge, this paper is a first example where SB surface hydrophobic cellulose fibers have been considered as a possible system for HOCs removal from polluted water.

Our interest for these fibers has been raised, due to new technologies developed in our University which allows to extract the SB cellulose fibers by a very fast, automated process. This process consists of an alkaline attack by NaOH water solution. Only 20 min at 80 °C are required to dissolve limited amounts of pectines and lignines which glues the cellulose fibers to the external cortex of the plant. The innovation, with respect to the past, is represented by the realization of a pilot plant which allows the complete automation of the full process (Gabriele et al., 2009), in such a way that the cost of the fibers is very competitive. Cellulose fibers are extracted with typical length ranging from 5 to 50 cm, and diameters of the order of about 10 μm . Since they have a very high surface extension they are suitable to be applied in filtering processes. Of course these fibers are strongly hydrophilic, being their surface covered by hydroxyl groups. For this reason they have been successfully applied to remediation of water from heavy metals, at least at laboratory scale (Arias et al., 2017).

The idea presented in this work is to use surface hydrophobized SB fibers to remediate water polluted by HOCs pollutants. Here the term hydrophobized means that the surface of the cellulose fibers has been reacted with chemical agents carrying an appropriate hydrophobic group thus removing the intrinsic hydrophilic character of the fibers. We have chosen to react the surface of the fibers with the 4,4'-diphenylmethane diisocyanate (MDI) (Fig. 1).

A very stable urethane linkage is established between the MDI and the hydroxyl groups emerging from the fibers surface (Fig. 1), as proved by X-ray photoelectron spectroscopy (XPS) analyses and attenuated total reflectance-fast Fourier transformed infrared (ATR-FTIR) measurements. On the other hand, the core of MDI is surely strongly hydrophobic, thus changing the character of fibers from hydrophilic to hydrophobic.

Another important innovation presented in this work is the technology used for the cellulose fiber chemical functionalization. Indeed, surface treatment has been made in a home-made reactor with a solvent-free method consisting in the nebulization of the

MDI on the surface of the fibers, in order to reduce the chemical impact of the process as well as its cost. Batch experiments of hydrocarbon removal from water show that the hydrophobized fibers has very efficient adsorption performances of the pollutants, exhibiting a maximum adsorption capacity as high as 220 mg/g, corresponding to removal efficiencies of about 99% and a relatively fast kinetics, in that the adsorption equilibrium is reached within 1 h of contact time.

2. Materials and methods

2.1. Materials

MDI (4,4'-diphenylmethane diisocyanate) (Fig. 1) used in this study has been provided by The Dow Chemical Company (Pisticci Scalo, MT, Italy); Aceton water free has been purchased from Sigma-Aldrich; gasoline has been used as pollutant. All materials were used as received.

SB fibers were extracted by treating the raw vegetable, grown into the botanic garden of the University of Calabria, with a 5% w/w NaOH/water solution for 20 min at 80 °C. The cellulosic fiber has been manually separated from the woody central part of the vegetable and further purified by a 30 min digestion at 80 °C in a 0.5% w/w NaOH/water solution, to remove lignin impurities that did not exceed 5% wt after the treatment (Gabriele et al., 2009). Photos of the fibers used are reported in Figure S1.

2.2. Cellulose fiber hydrophobization

About 0.5 kg of SB fiber, with an average diameter of 20 μm , obtained as described above, has been cut at a length of about 5 cm. The fiber has been inserted in a homemade 316 steel reactor having cylindrical shape and a volume of about 100 L. Propeller blades were mounted on an axis emerging centrally from the bottom of the cylinder. The blades could be rotated with a speed ranging from

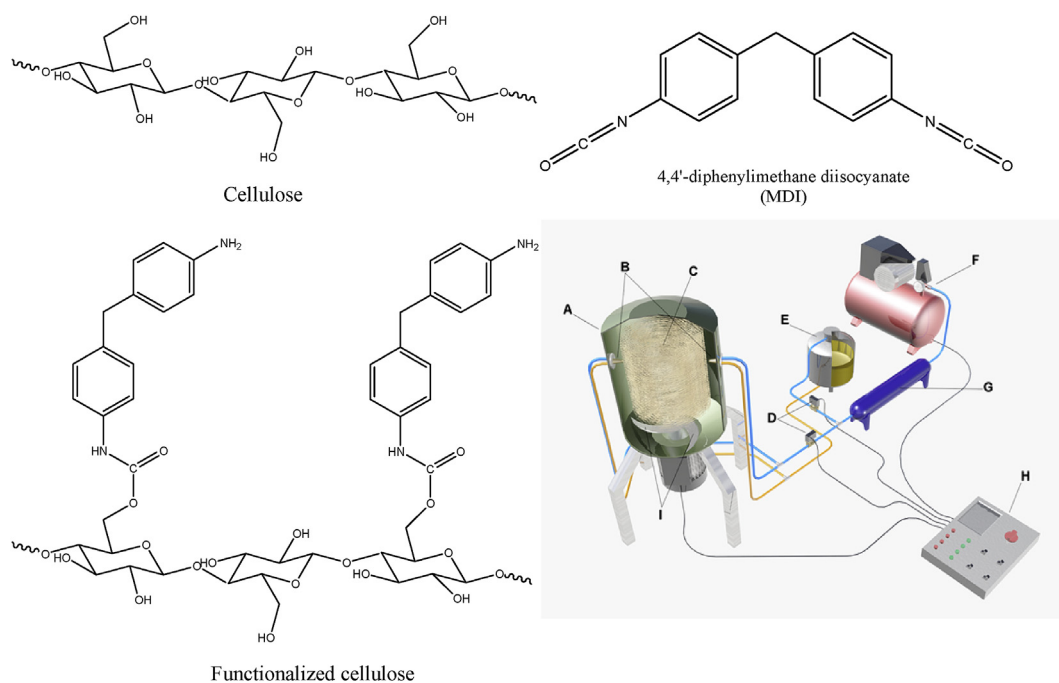


Fig. 1. Chemical structure of MDI, cellulose and the possible structure of the functionalized cellulose obtained by the reaction of MDI with the hydroxyl groups of cellulose and subsequent washing in 0.1 M HCl and NaOH. Home-made reactor for SB fibers functionalization (bottom right). A: Still vessel; B: nebulizer injectors; C: vortivating fibers; D: flux control electro valves; E: Compressed still vessel containing the reactant; F: compressor; G: Air dehydrating filter; H: Electric control panel; I: Rotating blades.

5 to 20 turns per sec., by means of an appropriate engine.

Two symmetric nebulizers IKAUCHI BIMJ04 were placed in the vertical walls of the reactor at a height of about 30 cm from the bottom. They could spread micron sized droplets of reactant on the fibers while these were vortically stirred by means of the rotating blades. A scheme of the home-made apparatus is reported in Fig. 1.

This device allows the functionalizing agent to bind the fiber without the use of solvents or using limited amount of solvent to adapt the viscosity of reactants. The reactant in this case consisted of 10 mL of 4,4'-diphenylmethane diisocyanate, mixed with 10 mL of dry acetone, used to decrease the viscosity of the reactant in such a way that it could be easily spread through the above described nebulizer. The reactant has been added on the fiber in about 5 min, using a nebulizer pressure of 2 bars. The temperature in the reactor has been maintained at about 100 °C for at least 1 h. Acetone evaporated very rapidly from the surface of the fiber at this temperature. The fiber has been then left to rest for 24 h in the reactor at room temperature. The fiber has been then washed with a 0.1 M HCl solution, to purify it from any excess of unbound MDI. The diisocyanate groups are transformed into amine groups and finally into ammonium cations, thus carrying the MDI excess into the water solution. Free terminal isocyanate group of MDI molecules tied on fiber surface are also transformed in an ammonium cation, thus reducing the hydrophobicity of fibers. To avoid these groups, the fibers are further washed with a 0.1 M NaOH/water solutions, and finally rinsed with clean water. We like to underline that the choice of using MDI, for the creation of a hydrophobic coating on the fiber surface, has been suggested by the possibility to adopt the above described experimentally strategy to clean the fibers without using organic solvents.

2.3. Scanning electron microscopy (SEM) analysis

SEM images of gold-coated raw and functionalized cellulose fibers were acquired by a LEO 420 microscope (LEO Electron Microscopy Ltd., Cambridge, England). Sputter-coating were performed with an Auto Sputter Coater, AGAR.

2.4. ATR-FTIR analysis of fibers

FTIR spectra of the cellulose SB fibers were acquired by a Bruker ALPHA FT-IR spectrometer equipped with a A241/D reflection module between 375 and 4000 cm^{-1} . Spectra were collected on dry samples of the fibers that were directly placed onto the instrument probe.

2.5. XPS surface characterization

XPS analyses of raw and functionalized SB fibers were conducted with a PHI-VersaProbe II X-ray spectrometer (Physical Electronics GMBH.) equipped with a monochromatic Al K α X-ray source, operating at 1486.6 eV, with a spot of 100 μm corresponding to a power of 24.8 W. Survey (0–1100 eV) and high resolution spectra were recorded in FAT (Fixed Analyzer Transmission) mode at pass energy of 187.85 and 46.95 eV, respectively. All spectra were acquired at a take-off angle of 45° with respect to the sample surface. Surface charging was neutralized with a flood gun (18 mA of emission current and 40 eV of electron energy) and the C1s signal of the hydrocarbon component (284.8 eV) was used as internal standard for charging correction.

High resolution spectra of detected elements (C1s, O1s, N1s and Ca2p) were acquired for quantitative and detailed binding energy (BE) chemical shift analysis. Atomic percentages were calculated using the Scofield sensitivity factors set in the MultiPak software (Ulvac phi-inc.) and a nonlinear Shirley background subtraction

algorithm. Measurements on repeated samples (three different spots for each sample) registered a maximum relative standard deviation (RSD) of about 3%. The full-width at half maximum (FWHM) of each C1s line-shape was fixed to 1.34 eV for the raw SB fiber and to 1.50 eV in the case of the functionalized one, while the maximum determined standard deviation in the peak position was ± 0.4 eV, for both samples.

2.6. WCA measurements

Sessile drop water contact angle values were measured with a manual goniometer (Ramé Hart, Inc.), utilizing a 2 μl bi-distilled water drop. The measurements, performed in order to verify whether the functionalization process has allowed the increase of the hydrophobic character of the considered cellulosic material, were conducted on functionalized SB fibers (100 min after reaction) and repeated 5 times for each sample. WCA value of the raw SB fibers was also acquired as reference.

2.7. Batch tests for water purification using functionalized SB fiber

The absorption capacity of the SB functionalized fibers has been evaluated by several batch tests. In each experiment, a certain amount of fiber ranging from 5 to 15 g have been added to 900 mL of polluted water obtained by mixing the gasoline petrol with ultrapure water (18.2 M Ω cm, Arioso-Human Corporation) at a loading ranging from 300 ppm up to 3600 ppm. The system has been maintained under gently stirring for all time by means of a magnetic stirrer. The total hydrocarbons content has been monitored as a function of time (the zero time represents the instant at which the fibers have been added to the polluted water) for several contact time intervals (1, 5, 10, 15, 30, 60 and 120 min).

Adsorption isotherm data have been collected at 20 °C by analogous batch tests experiments as described above. The equilibrium total hydrocarbons content has been measured after 4 h of contact time with 15 g of fiber by varying the initial total hydrocarbons load from 300 mg/L up to 3600 mg/L.

Measurement of total hydrocarbons content in the system, has been made by the ASTM D7678-11 procedure which is a Standard Test Method for Total Petroleum Hydrocarbons (TPH) in water and waste water (ASTM D7678-11) (ASTMD7678-11, 2011). This method consists in a solvent extraction of hydrocarbons followed by their quantification with Mid-IR Laser spectroscopy.

To analyze the results, the adsorption capacity, i.e., the amount of adsorbed hydrocarbons per unit mass of adsorbent (q_t), has been determined:

$$q_t = \frac{(C_0 - C_t)V}{W} \quad (1)$$

where, C_0 and C_t are the TPH loads (mg L^{-1}) at the initial time and at time t , respectively, V is the volume of the solution (L) and W is the adsorbent mass (g). When the adsorption equilibrium condition holds, $C_t = C_e$ and $q_t = q_e$ where, C_e is the equilibrium concentration and q_e is the equilibrium adsorption capacity.

The removal efficiency (RE%), defined by equation (2), has been also used to assess the adsorption performances of the fiber.

$$RE \% = \frac{(C_0 - C_t)}{C_0} \times 100 \quad (2)$$

2.8. Curve-fitting procedure and statistical analysis on adsorption data

The curve-fitting procedures have been performed by the Levenberg-Marquardt nonlinear least squares method. It involves an iterative improvement to parameter values in order to reduce the sum of the squares of the errors between the function and the measured data points. At each iteration, the parameters used in the model have been varied in order to minimize the chi-square (χ^2):

$$\chi^2 = \frac{1}{n_{\text{eff}} - p} \sum_i w_i [y_i - f(x_i; p_1, p_2, \dots)]^2 \quad (3)$$

$$\sigma_{i=} = \sqrt{C_{ii} \chi_i^2} \quad (4)$$

where, y is the dependent variable, the independent variables, is the total number of experimental points used in the fitting, p is the total number of adjustable parameters used in the fitting, p_1, p_2, \dots are the model parameters to be varied in order to minimize χ^2 .

The adjusted r -square (R^2) has been used as a measure to assess the goodness of fit. The closer the fit is to the data points, the closer the adjusted r -square will be to the value of 1.

Standard error on each fitted parameters has been calculated in the fitting procedure by equation (4) where, C_{ii} is the diagonal element of the variance-covariance matrix.

Each experiment has been replicated at least three times. The data points on each graph represent the average value calculated over the replicates and the error bars are the corresponding standard deviations.

3. Results and discussion

3.1. Fibers characterization

Figure S1 shows representative SEM images of the raw and functionalized fibers used in this study. At this zoom, neither morphological nor surface differences can be observed. While this indicates that the functionalization reaction does not affect the integrity of the fiber, it also tells us that surface changes occurring on a nanometer scale-length can not be detected by SEM. For this reason, we have performed a systematic characterization of the fiber by XPS and FTIR spectroscopy.

Results from XPS analysis indicated the presence mainly of carbon and oxygen and traces of calcium on the surface of the raw SB fiber, as evident observing the survey spectrum reported in Fig. 2a.

The cellulosic nature of the raw fiber surface has been confirmed by the fitting analysis of the C1s signal (Fig. 2b), which shows the peaks centered at 286.1 eV (C2) and at 287.8 eV (C3), due to C–C(H)/C–O and to O–C–O bonds, respectively, typical of cellulose (Beamson and Briggs, 1993). The peak centered at 285.0 eV (C1), is due to the presence of small percentage of contamination (about 2%), while the peak at 289.5 eV can be associated to the carboxyl groups of the small lignin fraction (~5%) still present after the alkaline extraction (Table S1). This surface chemical composition reflects the presence of the hydroxyl groups of cellulose which have the ability to absorb water molecules through hydrogen bonding, resulting in an overall hydrophilic material, as confirmed by the measured WCA value of $75^\circ \pm 2^\circ$.

According to the XPS results, the FTIR analysis of the raw fiber clearly shows its prevalently cellulosic nature. The FTIR spectra of the raw fiber (RF) (Fig. 3), is indeed characterized by the typical bands of cellulose, such as the hydrogen-bonded OH stretching at ca. 4000–2995 cm^{-1} , the C–H stretching at 2900 cm^{-1} , the H–C–H

and O–C–H in-plane bending vibrations at 1430 cm^{-1} , the CH deformation vibration at 1375 cm^{-1} , the C–O–C, C–C–O, and C–C–H deformation modes and stretching vibrations involving the motions of the C5 and C6 atoms of cellulose appear at 900 cm^{-1} . The C–O–H out-of-plane bending modes falls at 668 cm^{-1} (Siqueira et al., 2010).

XPS and ATR-FTIR measurements show significant change of the SB fibers due to the functionalization process. The XPS analysis shows that the surface composition of the functionalized fiber is composed mainly by carbon (about 92%) and, in a really equal small amount (about 4%), by oxygen and nitrogen (Fig. 2c). Thus, it shows a huge relative increase of the hydrocarbon component of the fiber surface and the introduction of the nitrogen atoms brought by the MDI functionalizing agent.

The fitting analysis of the C1s signal of the functionalized SB fibers, tell us that, in addition to the characteristic functional groups of cellulose, the C–N and O–C=N functional groups give a contribution to the C1s signal (Fig. 2d and Table S2).

On the other hand, the treatment with MDI introduced small, yet significant, modification in the FTIR spectrum of the functionalized fiber (FF) (Fig. 3). Small bands appear at 1618 and 1563 cm^{-1} that can be assigned to amide I and amide II vibrations due to the formation of ureic products. A small band at 1731 cm^{-1} , assigned to the CO double bond stretching vibration, indicates the presence of the urethane group. A further low intensity band at 2300 cm^{-1} corresponds to unreacted isocyanate groups (Siqueira et al., 2010). This band quite disappears after repetitive washing of the fiber sequentially in HCl and NaOH solutions (Fig. 3).

In conclusion, therefore, the surface of the functionalized SB fiber was essentially populated by pure hydrocarbons groups (about 90%) which justifies the high hydrophobic behavior showed by WCA measured value of $148^\circ \pm 5^\circ$ (Figure S1).

3.2. Adsorption properties of the raw and functionalized fibers

Initially, we compared the adsorption properties of the raw fiber with those of the functionalized one, in order to assess whether the surface fiber functionalization effectively achieved any improvement of the hydrocarbons adsorption capacity from polluted water. The raw and functionalized fibers have been placed in heavily contaminated aqueous/hydrocarbons dispersion (600 mg/L of gasoline hydrocarbons load) and the total hydrocarbons amount has been monitored as a function of the contact time (Fig. 4a).

In both cases, the total hydrocarbons content starts to decrease just after the addition of the fiber, and tends to a constant value after a few tens of minutes that, however, depends on the type of fiber (Fig. 4a). This is reflected in the opposite trend found for the removal efficiency, which increases with the contact time reaching a maximum value of about 96% and 52%, respectively for the FF and RF (Fig. 4b). Thus, both the fibers can capture the hydrocarbons but the functionalized fiber has a much higher removal efficiency than the raw one, supporting a successful chemical grafting of the fiber by means of the process described in Fig. 1, leading to an effective hydrophobization of its surface. It is noteworthy that the residual hydrocarbons content in the solution treated with the FF is close to the acceptable limit of total hydrocarbons in waste water (10 ppm for Italian Legislative Decree n. 152/2006).

With the aim to better understand the adsorption properties of the FF, we studied the removal efficiency as a function of the initial TPH load (Fig. 4c) and of the mass of fiber (Fig. 4d).

Fig. 4c shows that the RE% is almost constant to a value of about 96% for initial hydrocarbons loads of up to about 1000–1500 mg/L, while it starts to significantly decrease at higher loads, even if it is still as high as 80% when the initial load is 3600 mg/L. This trend is probably due to the saturation of the adsorption sites on the fiber

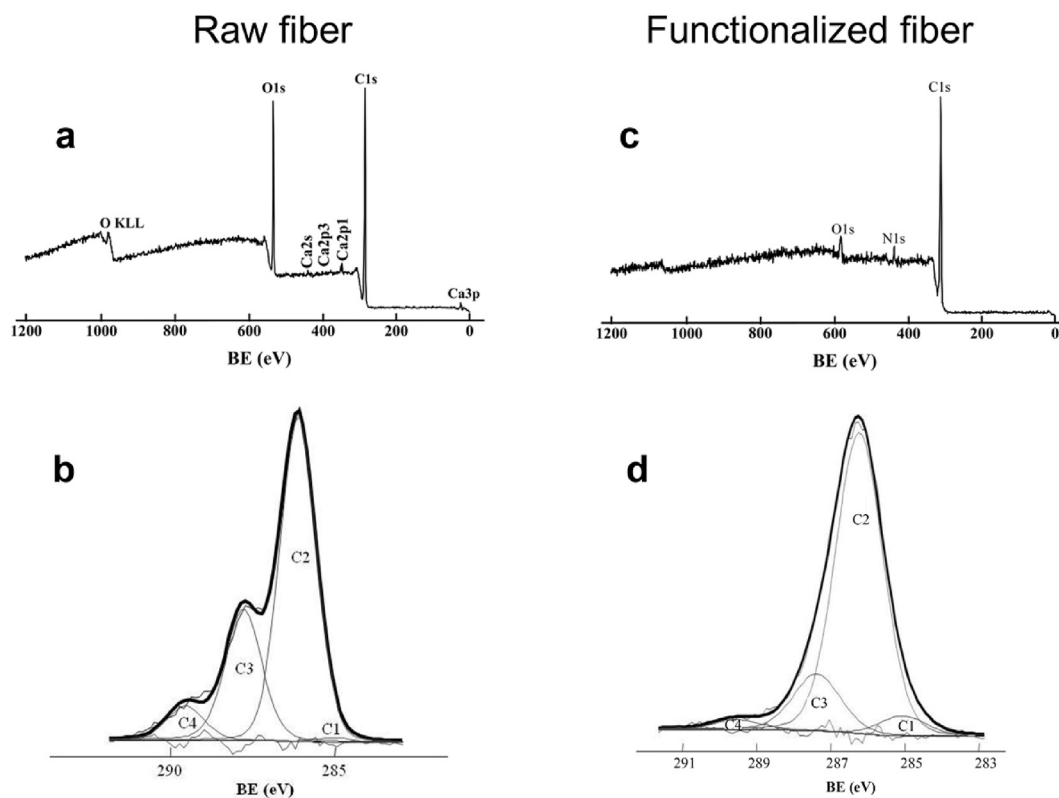


Fig. 2. XPS survey spectra of the raw a) and functionalized fibers c). Fitting of C1s XPS signal of the raw b) and of functionalized fiber d).

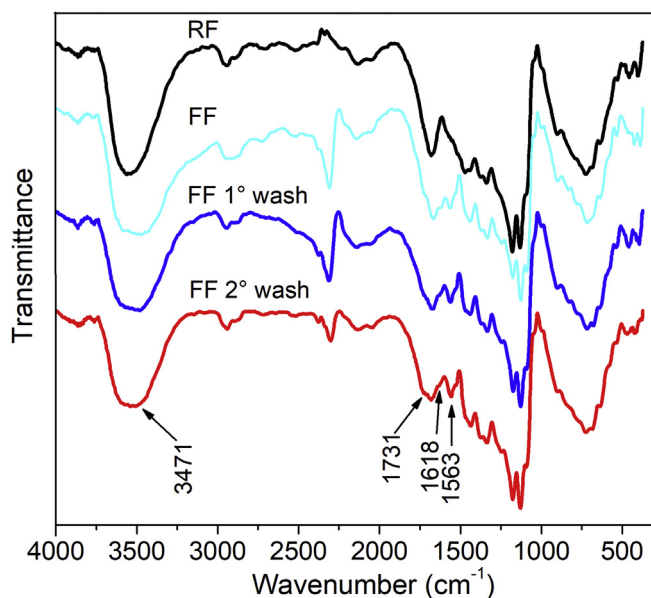


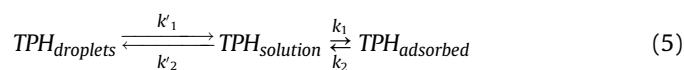
Fig. 3. FTIR spectra of the raw fiber (RF) and of the MDI-functionalized fiber (FF).

surface above a certain initial concentration. On the other hand, if we keep constant the initial hydrocarbons load and increase the amount of fiber, the RE% increases up to a plateau value, as shown in Fig. 4d. This further supports the existence of adsorption sites on the functionalized fiber that are prone to be occupied by the hydrocarbons as long as there is a significant concentration in solution. Of course, when the sites are overwhelming with respect to the initial hydrocarbons load, no further increase of the removal

efficiency occurs.

3.3. Kinetics of the adsorption process

The low miscibility of TPH in water leads to a system with three different phases: the organic phase, the aqueous phase and the solid one made of the cellulose fiber. Due to the low hydrocarbons solubility in water, the aqueous phase is a dilute solution. Under stirring conditions, a thoroughly dispersion of the organic phase occurs and the system appears to be perfectly transparent, indicating the absence of optically dispersive droplets. Of course, invisible nanodroplets of organic phase could be present. It is clear that the heterogeneous adsorption process, fundamentally occurs at the aqueous/fiber interface, being the aqueous phase the dispersive medium mostly in contact with the fiber. Therefore, the equilibrium processes occurring in the system could be described by the following equations:



where, the hydrocarbons forming the droplets ($TPH_{droplets}$) are in equilibrium with those dissolved in the aqueous phase ($TPH_{solution}$) which are, in turn, in equilibrium with those adsorbed onto the fiber surface ($TPH_{adsorbed}$). In order to apply kinetic and isotherm adsorption models generally used for describing the adsorption of solute from a solution on a solid surface, we need to assume that the first process is a rapid equilibrium and that the adsorption kinetics is determined by the second process, i.e., that the kinetic constants $k_1, k_2 \gg k_1, k_2$. This is a reasonable assumption if we consider that the first process is the repartition between two liquid phases while the other one involves the diffusion of the aqueous phase through the fiber and the adsorption of the organic

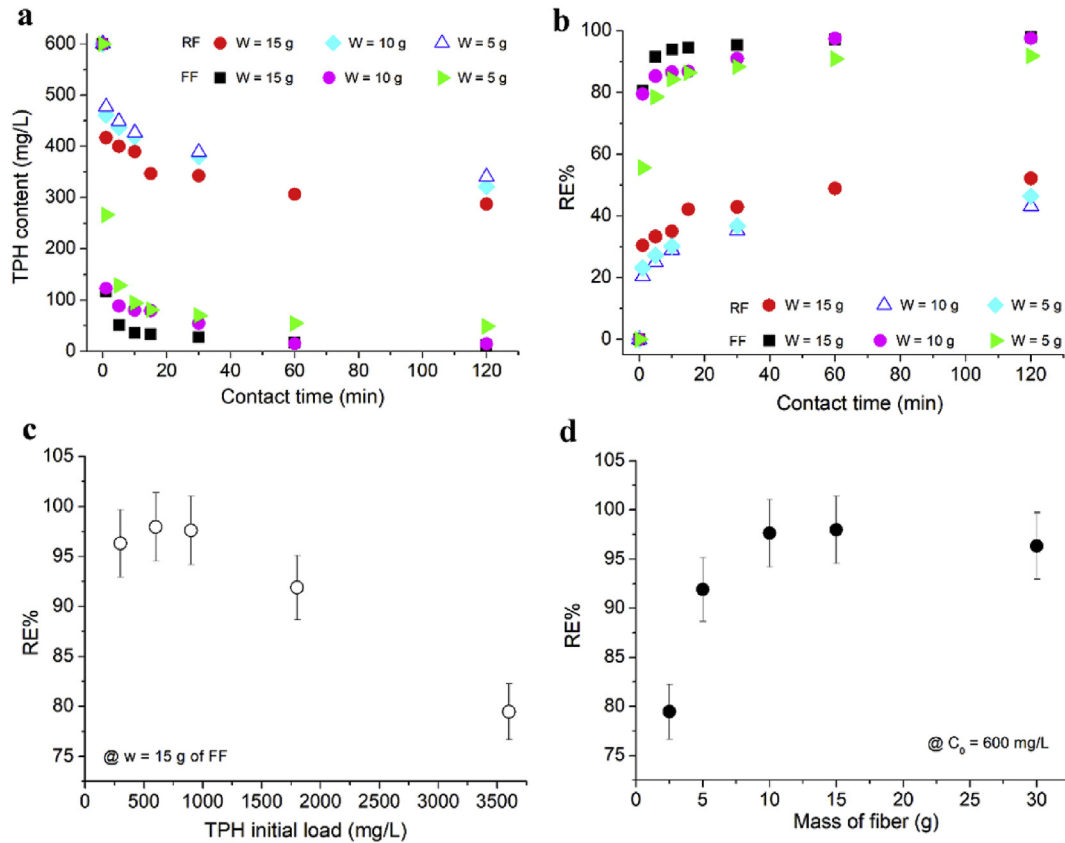


Fig. 4. a) Total petroleum hydrocarbons content and b) removal efficiency as a function of the contact time with the SB Functionalized Fiber and Raw Fiber. c) Removal efficiency as a function of the initial total petroleum hydrocarbons loads at $w = 15$ g and d) of the mass of functionalized cellulose fiber at an initial TPH load of 600 mg/L.

substances on the fiber surface. Under these assumptions, the concentration of TPH in the aqueous phase is directly proportional to the amount of TPH in the droplet and the total amount of TPH can be approximated to the that of the droplet, due to the low TPH solubility in water. Therefore, the kinetics of adsorption of TPH from the aqueous solution and the kinetics of removal of TPH from the system are the same.

The kinetic data have been therefore modeled by a first order model based on the fractional conversion of the TPH content according to the equilibrium (5) and defined by equation (6) (Bhattacharya and Venkobachar, 1984):

$$X_{TPH}(t) = C_{TPH}(0) - C_{TPH}(t) \quad (6)$$

$$\frac{dX_{TPH}(t)}{dt} = (k_1 + k_2)(X_{TPH}(\infty) - X_{TPH}(t)) \quad (7)$$

where, k_1 and k_2 are the first order kinetic constants for the adsorption and desorption process and $X_{TPH}(\infty) = C_{TPH}(0) - C_{TPH}(\infty)$ is the fractional conversion at equilibrium.

Integration of equation (7) leads to:

$$1 - \frac{X_{TPH}(t)}{X_{TPH}(\infty)} = e^{-(k_1+k_2)t} \quad (8)$$

where, the ratio $\frac{X_{TPH}(t)}{X_{TPH}(\infty)}$, is the fractional attainment of the equilibrium.

Equation (8) has been used to fit each set of kinetic data and the results are summarized in Figure S2-S3 and in Table S3. It can be

seen that the first order model fits fairly well the data on the FF fiber with R^2 as high as 0.99, while it is not as good as to fit the data on the raw fiber ($R^2 = 0.70$). As expected, the fitted value of $k_1 + k_2$ is almost constant over the entire set of experiments which differ for the initial conditions, i.e., either for the initial load and/or for the mass of fiber used. Due to this evidence, the fitting analysis has been performed on the average data for each type of fiber (Fig. 5). The first order kinetic constant k_1 and k_2 were then obtained by taking into account that the ratio between the two kinetic constants gives the thermodynamic equilibrium adsorption constant K_{ads} (equation (9)) and that this last can be calculated from the equilibrium adsorption data as the ratio between the amount of TPH adsorbed on the fiber and that remained in the liquid phase (equation (10)):

$$K_{ads} = \frac{k_1}{k_2} \quad (9)$$

$$K_{ads} = \frac{TPH_{adsorbed}(\infty)}{TPH_{solution}(\infty)} \quad (10)$$

The calculated parameters related to the first order kinetics are reported in Table 1.

The first order kinetic constant for the adsorption of TPH on the functionalized fiber is almost twenty times higher than that for the raw cellulosic fiber while the first order constant for the desorption process from the FF is about a half that of the raw fiber. This determines the larger adsorption equilibrium constant for the FF.

The kinetic data were also modeled by the pseudo first order and a pseudo second order kinetic models based on the adsorption

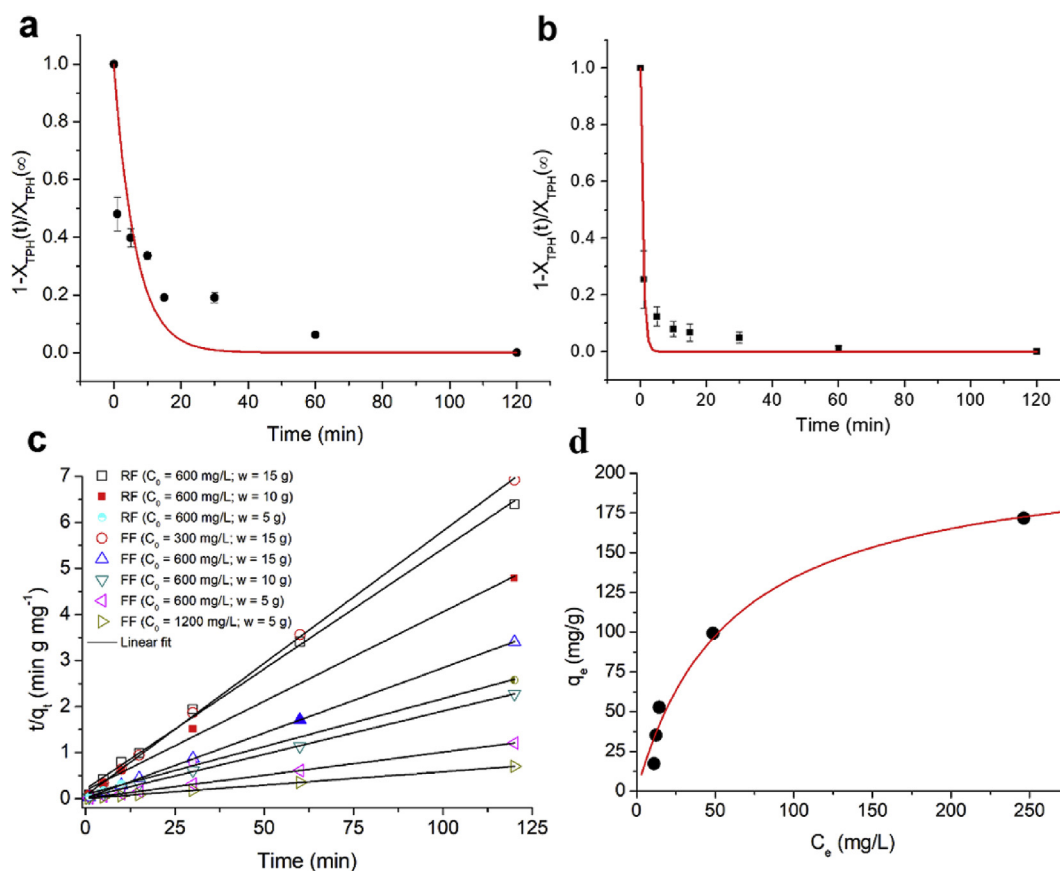


Fig. 5. a) First order kinetic plots for the raw fiber and (b) for the functionalized fiber. The continuous lines are the fit of the points with equation (8). c) Fitting of the kinetic adsorption data by the pseudo second order model (eq. (12)). d) Total petroleum hydrocarbons adsorption isotherm at 20 °C for the functionalized fiber (circles) and fitting with the Langmuir model (continuous line).

Table 1
First order kinetic parameters.^a

Fiber	$(k_1 + k_2)(\text{min}^{-1})$	R^2	$k_1(\text{min}^{-1})$	$k_2(\text{min}^{-1})$	K_{ads}
RF	0.16 (0.05)	0.70	0.08 (0.03)	0.084 (0.008)	0.9 (0.2)
FF	1.3 (0.4)	0.79	1.25 (0.04)	0.048 (0.009)	26 (19)

^a Values in parentheses are the standard deviations of the data.

capacity (Arias et al., 2017). The pseudo first order model failed to reproduce the experimental data (data not shown). In contrast, Fig. 5 shows that the TPH adsorption kinetics can be very well fitted by a pseudo second order model (Arias et al., 2017; Ho and McKay, 1999; Kumar, 2006), with R^2 values close to 1. The rate of change of the adsorption capacity is given by equation (11) (Ho, 2006):

$$\frac{dq_t}{dt} = k_2(q_e - q_t)^2 \quad (11)$$

where, k_2 is the pseudo-second order rate constant ($\text{g mg}^{-1}\text{min}^{-1}$) which is a function of the initial concentration, the forward (sorption) and back (desorption) kinetic constants. Integration of equation (11) and linearization leads to equation (12) which has been used to fit the data by plotting the t/q_t ratio as a function of t (Fig. 5c) (Arias et al., 2017; ASTM D7678-11, 2011; Beamson and Briggs, 1993; Siqueira et al., 2010; Ho and McKay, 1999; Kumar, 2006), from which the parameters k_2 and q_e have been calculated (Table 2):

Table 2
Pseudo-second order kinetic data.^a

Fiber	W (g)	C_0 (mg/L)	k_2 ($\text{g mg}^{-1}\text{min}^{-1}$)	q_e (mg g^{-1})	R^2
RF	15	600	0.013 (0.004)	19.2 (0.4)	0.99699
	10	600	0.008 (0.004)	25.8 (0.9)	0.99517
	5	600	0.005 (0.002)	48 (1)	0.99672
FF	15	300	0.05 (0.02)	17.4 (0.1)	0.99957
	15	600	0.06 (0.01)	35.36 (0.08)	0.99997
	10	600	0.015 (0.006)	53.2 (0.4)	0.99958
	5	600	0.010 (0.001)	99.9 (0.2)	0.99997
	5	1200	0.006 (0.001)	172.7 (0.6)	0.99993

^a Values in parentheses are the standard deviations of the data.

$$\frac{t}{q_t} = \frac{1}{K_2 q_e^2} + \frac{1}{q_e} t \quad (12)$$

The data reported in Table 2 show that the equilibrium adsorption capacity (q_e) of the functionalized fiber (FF) almost double with respect to that of the raw fiber (RF) under the same experimental conditions. Moreover, the kinetics of the adsorption process is faster with the FF fiber as indicated by the value of the kinetic constant that is about 5 times higher than that observed with the RF. It can be also seen that the adsorption capacity of the FF significantly increases with the increase of the C_0/W ratio while the rate constant decreases, in agreement with the hypothesis that the fiber surface has a high degree of chemical functionalization, i.e., a high number of adsorption sites.

3.4. Adsorption isotherm

The hydrocarbons adsorption capacity of the functionalized fiber has been assessed by the measurement of the adsorption isotherm for TPH removal from water. The isotherm is shown in Fig. 5d, where the equilibrium adsorption capacity has been plotted as a function of the equilibrium total hydrocarbons concentration at room temperature. The adsorption capacity shows a nonlinear increase with the equilibrium concentration and seems to approach a plateau value, corresponding to the maximum adsorption capacity (q_m) of the fiber. This important parameter used for sorbent's performance metrics, can be estimated by assuming that the trend just described can be modeled by a Langmuir model (equation (13)) for which the surface of the adsorbing material is covered by a monolayer of the adsorbate (Limousin et al., 2007; Atkins and De Paula, 2006).

$$q_e = \frac{q_m K_L C_e}{1 + K_L C_e} \quad (13)$$

where, K_L is the Langmuir adsorption constant. The nonlinear curve fitting of the data in Fig. 5d with the Langmuir model gives satisfactory results with an R^2 of 0.96521. The fitted values are $K_L = (0.017 \pm 0.004) \text{ L g}^{-1}$ and $q_m = (214 \pm 22) \text{ mg g}^{-1}$. The functionalized fiber shows a very high hydrocarbons uptake capacity if compared to that of other biosorbent materials toward a variety of organic pollutants such as TPHs, HOCs, PAHs, phenols, etc. (Tran et al., 2015).

The high affinity of the FF for hydrocarbons is also highlighted by the large value of the distribution coefficient, K_d given by equation (14), estimated to be $3 \times 10^4 \text{ mL g}^{-1}$:

$$K_d = \frac{q_e}{C_e} \quad (14)$$

4. Conclusion

In conclusion, this work reports the first application of MDI functionalized cellulose fiber to remove hydrocarbons pollution from water. A novel green technological process for cellulose grafting has been described, which consists in a solvent-free surface chemical functionalization of cellulose with MDI. It has been shown that this "green" method that allows the use of minimum amount of solvent, has been successful for achieving a high degree of surface functionalization by transforming the cellulose hydroxyls into urethane moieties, thus achieving fiber surface hydrophobization. The functionalized cellulose fiber exhibits notable adsorption properties for total petroleum hydrocarbons. Indeed, adsorption kinetics is fast and the pollutant can be removed with efficiencies larger than 90% in times of the order of 10 min, for fibers/pollutants weight ratio as low as 0.01, in samples having the volume of about 1 L. To be more clear, let us say that 0.5 kg of fibers could be sufficient to remove 100 ppm of pollutants from a ton of water in times of the order of some minute. In our opinion, this opens good possibility for practical application of this technology, due to the high availability of cellulose and the easily scalable process for cellulose functionalization.

Notes

The authors declare no competing financial interest.

Acknowledgments

The authors are grateful to the Ministero dell'Istruzione dell'Università e della Ricerca Italiano (MIUR) and the University of Calabria for supporting this project in the framework of the ex 60% budget grant.

Appendix A. Supplementary data

Supplementary data related to this article can be found at <https://doi.org/10.1016/j.chemosphere.2018.03.044>.

References

- Arias, F., Beneduci, A., Chidichimo, F., Furia, E., Straface, S., 2017. Study of the adsorption of mercury (II) on lignocellulosic materials under static and dynamic conditions. *Chemosphere* 180, 11–23.
- ASTM, E1689-95(2014), 2014. Standard Guide for Developing Conceptual Site Models for Contaminated Sites. ASTM International, West Conshohocken, PA. www.astm.org.
- ASTM D7678-11, 2011. Standard Test Method for Total Petroleum Hydrocarbons (TPH) in Water and Wastewater with Solvent Extraction Using Mid-IR Laser Spectroscopy. ASTM International, West Conshohocken, PA. www.astm.org.
- Atkins, P., De Paula, J., 2006. *Physical Chemistry*, eighth ed. W. H. Freeman and Company, New York.
- Beamson, G., Briggs, D., 1993. High resolution XPS of organic polymers: the scienta ESCA300 database. *J. Chem. Educ.* 70 (1), A25.
- Bhattacharya, A.K., Venkobachar, C., 1984. Removal of cadmium (II) by low cost adsorbents. *J. Environ. Eng.* 110 (1), 110–122.
- Cerchiara, T., Chidichimo, G., Gallucci, M.C., Vuono, D., 2010. Effects of extraction methods on the morphology and physico-chemical properties of Spanish Broom (*Spartium junceum* L.) fibres. *Fibres Text. East. Eur.* 18 (2), 13–16.
- Cerchiara, T., Chidichimo, G., Ragusa, M., Belsito, E., Liguori, A., Arioli, A., 2010. Characterization and utilization of Spanish Broom (*Spartium junceum* L.) seed oil. *Ind. Crop. Prod.* 31 (2), 423–426.
- Cerchiara, T., Chidichimo, G., Rondi, G., Gallucci, M.C., Gattuso, C., Luppi, B., Bigucci, F., 2014. Chemical composition, morphology and tensile properties of Spanish broom (*Spartium junceum* L.) fibres in comparison with flax (*Linum usitatissimum* L.). *Fibres Text. East. Eur.* 22, 25–28.
- Chidichimo, G., Aloise, A., Beneduci, A., De Rango, A., Pingitore, G., Furguele, F., Valentino, P., 2016. Polyurethanes reinforced with spartium junceum fibers. *Polym. Compos.* 37 (10), 3042–3049.
- Deschamps, G., Caruel, H., Borredon, M.E., Bonnin, C., Vignoles, C., 2003. Oil removal from water by selective sorption on hydrophobic cotton fibers. 1. Study of sorption properties and comparison with other cotton fiber-based sorbents. *Environ. Sci. Technol.* 37 (5), 1013–1015.
- El-Gendy, N.S., Hussein, N.N., 2016. Study on the effectiveness of spent waste sugarcane bagasse for adsorption of different petroleum hydrocarbons water pollutants: kinetic and equilibrium isotherm. *Desalin. Water Treat* 57 (12), 5514–5528.
- European Union, Directive 2008/98/CE, (2008); <http://eur-lex.europa.eu/legal-content/EN/TXT/PDF/?uri=CELEX:32008L0098&from=EN>.
- Gabriele, B., Cerchiara, T., Salerno, G., Chidichimo, G., Vetere, M.V., Alampi, C., Gallucci, M.C., Conidi, C., Cassano, A., 2009. A new physical-chemical process for the efficient production of cellulose fibers from Spanish broom (*Spartium junceum* L.). *Bioresour. Technol.* 101, 724–729.
- Hardisty, P.E., Ozdemiroglu, E., 2005. *The Economics of Groundwater Remediation and Protection*. CRC Press, New York.
- Ho, Y.S., 2006. Review of second-order models for adsorption systems. *J. Hazard Mater.* 136 (3), 681–689.
- Ho, Y.S., McKay, G., 1999. Pseudo-second order model for sorption processes. *J. Process. Biochem.* 34 (5), 451–465.
- Hubbe, M.A., Rojas, O.J., Fingas, M., Gupta, B.S., 2013. Cellulosic substrates for removal of pollutants from aqueous systems: a review. 3. Spilled oil and emulsified organic liquids. *Bio-Research* 8, 3038–3097.
- Kumar, K.V., 2006. Linear and non-linear regression analysis for the sorption kinetics of methylene blue onto activated carbon. *J. Hazard Mater.* B137, 1538–1544.
- Lau, E.V., Gan, S., Ng, H.K., Poh, P.E., 2014. Extraction agents for the removal of polycyclic aromatic hydrocarbons (PAHs) from soil in soil washing technologies. *Environ. Pollut.* 184, 640–649.
- Limousin, G., Gaudet, J.P., Charlet, L., Szenknect, S., Barthes, V., Krimissa, M., 2007. Sorption isotherms: a review on physical bases, modeling and measurement. *Appl. Geochem.* 22 (2), 249–275.
- Mao, X., Jiang, R., Xiao, W., Yu, J., 2015. Use of surfactants for the remediation of contaminated soils: a review. *J. Hazard Mater.* 285 (18), 419–435.
- Mercer, J.W., Cohen, R.M., 1990. A review of immiscible fluids in the subsurface: properties, models, characterization and remediation. *J. Contam. Hydrol.* 6 (2), 107–163.
- Mouset, E., Oturan, M.A., Van Hullebusch, E.D., Guibaud, G., Esposito, G., 2014. Soil


- washing/flushing treatments of organic pollutants enhanced by cyclodextrins and integrated treatments: state of the art. *Crit. Rev. Environ. Sci. Technol.* 44 (7), 705–795.
- Mulligan, C.N., Yong, R.N., Gibbs, B.F., 2001. Surfactant-enhanced remediation of contaminated soil: a review. *Eng. Geol.* 60 (1–4), 371–380.
- Navarro, R.R., Iimura, Y., Ichikawa, H., Tatsumi, K., 2008. Treatment of PAHs in contaminated soil by extraction with aqueous DNA followed by biodegradation with a pure culture of *Sphingomonas* sp. *Chemosphere* 73 (9), 1414–1419.
- Paria, S., 2008. Surfactant-enhanced remediation of organic contaminated soil and water. *Adv. Colloid Interface Sci.* 138 (1), 24–58.
- Paulauskienė, T., Jucikė, I., 2015. Aquatic oil spill cleanup using natural sorbents. *Environ. Sci. Pollut. Res.* 22, 14874–14881.
- Robinson, D., Angyal, G., 2008. Use of mixed technologies to remediate chlorinated DNAPL at a brownfields site. *Remed. J.* 18 (3), 41–53.
- Rosas, J.M., Vicente, F., Santos, A., Romero, A., 2013. Soil remediation using soil washing followed by Fenton oxidation. *Chem. Eng. J.* 220, 125–132.
- Siqueira, G., Bras, J., Dufresne, A., 2010. New process of chemical grafting of cellulose nanoparticles with a long chain isocyanate. *Langmuir* 26 (1), 402–411.
- Suni, S., Kosunen, A.L., Hautala, M., Pasila, A., Romantschuk, M., 2004. Use of a by-product of peat excavation, cotton grass fibre, as a sorbent for oil-spills. *Mar. Pollut. Bull.* 49 (11–12), 916–921.
- Tran, V.S., Ngo, H.H., Guo, W., Zhang, J., Liang, S., Ton-That, C., 2015. Typical low cost biosorbents for adsorptive removal of specific organic pollutants from water. *Bioresour. Technol.* 182, 353–363.
- Trellu, C., Mousset, E., Pechaud, Y., Huguenot, D., Van Hullebusch, E.D., Esposito, G., Oturan, M.A., 2016. Removal of hydrophobic organic pollutants from soil washing/flushing solutions: a critical review. *J. Hazard Mater.* 306, 149–174.
- Van der Oost, R., Beyer, J., Vermeulen, N., P.E., 2003. Fish bioaccumulation and biomarkers in environmental risk assessment: a review. *Environ. Toxicol. Pharmacol.* 13, 57–149.
- Villa, R.D., Trovó, A.G., Nogueira, R.F.P., 2010. Soil remediation using a coupled process: soil washing with surfactant followed by photo-Fenton oxidation. *J. Hazard Mater.* 174, 770–775.
- Wahi, R., Chuah, L.A., Choong, T.S.Y., Ngaini, Z., Nourouzi, M.M., 2013. Oil removal from aqueous state by natural fibrous sorbent: an overview. *Separ. Purif. Technol.* 113, 51–63.
- Yakout, S.M., Daifullah, A.A.M., 2013. Removal of selected polycyclic aromatic hydrocarbons from aqueous solution onto various adsorbent materials. *Desalin. Water Treat* 51, 6711–6718.
- Younis, S.A., El-Gendy, N.S., Waleed, I.E.A., Moustaf, Y.M., 2014. Kinetic, isotherm, and thermodynamic studies of polycyclic aromatic hydrocarbons biosorption from petroleum refinery wastewater using spent waste biomass. *Desalin. Water Treat* 56 (11), 3013–3023.

CHAPTER 6



Article

Removal of Endocrine Disrupting Chemicals from Water: Adsorption of Bisphenol-A by Biobased Hydrophobic Functionalized Cellulose

Antonio Tursi ^{1,2,*}, Efthalia Chatzisyneon ², Francesco Chidichimo ^{3,4}, Amerigo Beneduci ^{1,4} 
and Giuseppe Chidichimo ^{1,4}

¹ Department of Chemistry and Chemical Technologies, University of Calabria, Via P. Bucci, Cubo 15D, 87036 Arcavacata di Rende (CS), Italy; amerigo.beneduci@unical.it (A.B.); giuseppe.chidichimo@unical.it (G.C.)

² School of Engineering, Institute for Infrastructure and Environment, University of Edinburgh, The King's Buildings, Edinburgh EH9 3JL, UK; E.Chatzisyneon@ed.ac.uk

³ Department of Environment and Chemical Engineering, University of Calabria, Via P. Bucci, Cubo 41B, 87036 Arcavacata di Rende (CS), Italy; francesco.chidichimo@unical.it

⁴ SIRiA S.r.l.-Servizi Integrati e Ricerche per l'Ambiente, c/o Department of Chemistry and Chemical Technologies, Spin-Off of the University of Calabria, Via P. Bucci, Cubo 15D, 87036 Arcavacata di Rende (CS), Italy

* Correspondence: antonio.tursi@unical.it; Tel.: +39-34-0185-9667

Received: 26 September 2018; Accepted: 29 October 2018; Published: 31 October 2018



Abstract: The aim of this study is to examine the efficiency of biobased Spanish broom (SB) surface modified cellulose fibers to remove bisphenol A (BPA), a well-known endocrine disruptor, from water. Spanish brooms are flowering plants, which are native and abundant to Mediterranean regions. The functionalized fibers (FF) were found to have the best adsorption efficiency at pH 5, due to the optimal hydrophobic interaction between the FF fiber and BPA. Adsorption kinetics of BPA was found to fit well a pseudo-second order reaction. Equilibrium isotherm data were fitted by Langmuir and Freundlich models. A very fast and simple regeneration method was developed and it was observed that adsorption capacity of the fibers was kept almost unchanged after 3 consecutive uses. Bottled water and synthetic wastewater were also tested to assess the efficiency of the process under more realistic water and wastewater treatment conditions. It was found that BPA removal was slightly decreased from 77% in ultrapure water to 64% in synthetic wastewater matrix, indicating that FF has a high selectivity toward BPA, even in the presence of other organic compounds. Overall, it was observed that SB-modified fibers can be a new promising green biotechnology for water purification.

Keywords: endocrine disruptors; wastewater treatment; priority pollutants; surface modified cellulose; EDCs; Spanish broom

1. Introduction

Endocrine disrupting chemicals (EDCs) are natural or synthetic compounds that have the ability to generate alterations in endocrine functions within the body and to interact with several classes of nuclear receptors and hormone receptors associated with endocrine and steroid hormones [1]. One of the most identified emerging EDCs is bisphenol A (BPA), a fundamental organic chemical used as a monomer in the production of polycarbonate plastics, epoxy resins and flame retardants [2]. The global production of BPA is about 8 million tons per year. This huge BPA production and processing volumes are responsible of the high presence of this substance in the environment [3]. Wastewater treatment plants, for example, inadvertently release BPA in effluents since they are not initially designed to treat

such persistent and xenobiotic substances [4]. Huang et al. [5] found that the concentration of BPA is higher in industrial and commercial areas than in other regions, affecting water quality of rivers and lakes close to those areas. Moreover, recent studies by Yamamoto et al. [6] have shown that BPA can reach values up to 17.2 mg/L in landfill leachates, probably due to the presence of plastic debris. High BPA concentrations were also found in sewage treatment plant influents and in effluents of waste paper recycling plants (up to 370 µg/L) [7], in river water in Germany (up to 0.8 µg/L) [8], in wastewater in Ontario (up to 149 µg/L) [9], and in bottled water in France (0.07–4.21 µg/L) [10], to name but a few.

Drinking water treatment technologies are usually not able to remove the entire amount of BPA present in source waters [11], therefore there is a high risk of long-term exposure of humans to this compound. In this direction, numerous studies have been performed to investigate the correlation between BPA exposure and effects on health. These publications show the capability of this compound to increase risk for cancers, in particular ovarian, breast and prostate cancer [12,13], as well as various metabolic disorders such as obesity, endometrial hyperplasia, recurrent miscarriages and polycystic ovary syndrome [14,15]. Other different disorders associated with BPA exposure are cardiovascular disease, altered immune system activity, diabetes in adults, infertility and precocious puberty [16].

Several technologies, such as coagulation/flocculation/sedimentation/filtration [17,18], carbon nanomaterials (CNMs) (e.g., carbon nanotubes (CNTs) [19] and graphene oxides (GOs) [20]), membrane filtration [21,22], ultraviolet (UV) irradiation [23,24], biological processes [25,26], and advanced oxidation techniques [27–31] have been studied for BPA removal. Nevertheless, energy consumption, low process efficiency, production of toxic by-products, and addition of hazardous chemicals prevent the wider application of all these technologies at large-scale. Therefore, effective, more sustainable methods are sought to remove such contaminants from water and wastewater [32,33].

Physical adsorption is generally considered an effective method for the removal of these types of organic molecules in aqueous medium, provided that adsorbents have large accessible internal and/or external surfaces. In this regard, Nakanishi et al. [34] studied the adsorption characteristics of BPA on natural adsorbents produced from a variety of wood chips. Asada et al. [35] stressed that the porous carbon produced by bamboo could be an interesting adsorbent for the removal of BPA from aqueous solution. Yoon et al. [36] found out that adsorption efficiency of six types of activated charcoal powder (PAC), with respect to BPA, ranges from 31% to >99% with an activated carbon dosage of 5 and 15 mg/L. Also, Lazim et al. [37] observed that coir pith removed 72% of BPA reaching a maximum adsorption capacity of 4.308 mg/g, followed by durian peel (70%, 4.178 mg/g) and coconut shell (69%, 4.159 mg/g).

The development of an effective, simple, renewable and low-cost method to remove BPA from aqueous environment is therefore of great environmental importance and will safeguard public health. Based on these considerations, this work investigates the possibility to use hydrophobized cellulose fibers extracted from Spanish broom (SB) plants as a new biobased technology to remove BPA from water. Spanish brooms is a flowering plant, which is native and abundant to the Mediterranean regions in southern Europe, southwest Asia and northwest Africa. Spanish brooms cellulose fibers were successfully applied, by our research group, to remediate total petroleum hydrocarbons and heavy metals polluted water [38,39]. The interest for these fibers stemmed from the new techniques developed at the University of Calabria, which allows the extraction of the SB cellulose fibers through a fast and automated process, thus making the production costs extremely competitive. Cellulose fibers are extracted with a typical length ranging from 5 to 50 cm, and diameters of the order of about 10 µm. These fibers are suitable to be applied in filtering processes, since they have a very high specific surface area. The surface of the fibers was chemically modified in order to increase its hydrophobicity, using the reactivity of the cellulose hydroxyl groups with the 4,4'-diphenylmethane diisocyanate (MDI) [38]. One of the isocyanate groups of this molecule is bound on the cellulose surface through a urethane link, while the other one is transformed in an amine group by water washing. In this way the fiber surface is coated by a chemical group which is very similar to BPA, and thus an expected high chemical affinity

for this molecule is achieved. As previously reported [38], the SB fibers functionalization was carried out in a home-made reactor, by a direct nebulization of MDI on the surface of the fibers. This procedure avoids the use of solvents, reducing the chemical impact and the cost of the process.

In this study, batch experiments were performed in order to assess the remediation capacity of the modified SB fibers with respect to BPA polluted water. Kinetics and thermodynamics aspects of the adsorption process were studied. A method to regenerate the used fibers was developed and the removal efficiency of the regenerated fibers was studied.

2. Materials and Methods

2.1. Materials

All chemicals used in this study were of analytical grade and without further modification. Bisphenol A (CAS No: 80-05-7) was purchased from Sigma-Aldrich (Haverhill, Suffolk, UK); MDI (4,4' diphenylmethane diisocyanate) was provided by The Dow Chemical Company (Pisticci Scalo, MT, Italy); acetone water free was purchased from Sigma-Aldrich.

The fibers of the vegetable, which grows naturally in the Mediterranean area, were obtained by using a pulping process in a 5% *w/w* NaOH solution. The vegetable was macerated for 20 min at a temperature of 80 °C. After this treatment the cellulose fiber could be easily separated from the inner woody skeleton of the SB bushes. Lignin impurities were removed by further washing the cellulose fibers with a 5% *w/w* NaOH solution at a temperature of 80 °C [40].

Experiments were performed by spiking appropriate amounts of BPA into various water matrices, such as ultrapure and bottled (with TOC = 4.2 mg/L; COD = 10 mg/L; pH = 7.2) water as well as synthetic wastewater. Synthetic wastewater (with TOC = 160.1 mg/L; COD = 367 mg/L; pH = 7.7) was prepared by dissolving the following components in one liter of distilled water: peptone, 160 mg; meat extract, 110 mg; urea, 30 mg; anhydrous dipotassium hydrogen phosphate (K_2HPO_4), 28 mg; sodium chloride (NaCl), 7 mg; calcium chloride dihydrate ($CaCl_2 \cdot 2H_2O$), 4 mg; magnesium sulphate heptahydrate ($Mg_2SO_4 \cdot 7H_2O$), 2 mg. Total organic carbon (TOC) was determined by measuring the organic concentration by a TOC analyzer (Shimadzu TOC-VCPh). Chemical oxygen demand (COD) was determined colorimetrically by the dichromate method. Commercially available digestion solution containing potassium dichromate, sulfuric acid and mercuric sulfate (Palintest, Camlab, UK) was used.

Biochemical Oxygen Demand (BOD_5), total nitrogen (N) and total phosphorous (P) were determined according to the following standard methods: APAT IRSA CNR 5120 and 4060, respectively [41].

The measured $BOD_5/N/P$ ratios for synthetic wastewater are 100/22.7/2.3 which are close to typical values found for raw municipal wastewater [42]

2.2. Cellulose Fiber Hydrophobization

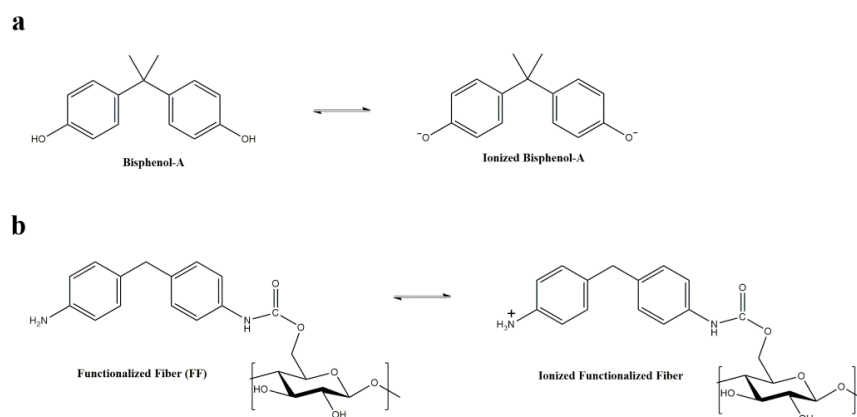
Hydrophobization of SB fibers was performed through a novel solvent-free technology based on a home-made steel reactor that keeps the fibers under vortex stirring by rotating blades, which were set at the bottom of the reactor. During this phase, the MDI reactant is spread onto the surface of the fibers in the form of micrometer-sized droplets, by two nebulizers, following the procedure described in Tursi et al. [38]. Both raw (RF) and functionalized (FF) fibers were chemically characterized by fast Fourier transform infrared spectroscopy (FT-IR) [38], confirming the presence of urethane bond in the FF fibers.

2.3. Cellulose Fiber Surface Characterization

Further support of the functionalization process comes from the Boehm titration analysis, which was used to measure the content of the acidic and basic functional groups on the fiber surface. This method measures the amount of NaOH, Na_2CO_3 , and $NaHCO_3$ neutralized by the acid groups

present on the surface of a material, corresponding to weak, moderate and strong acid fractions, respectively. Hydrogen chloride was instead used to measure the basic functional groups content [43].

The weak, moderate and strong acid fractions of the FF are (0.018 ± 0.002) mmol/g, (0.035 ± 0.004) mmol/g, (0.005 ± 0.001) mmol/g, respectively, while the basic groups content is (0.814 ± 0.003) mmol/g, due to the grafting of ammine groups on the cellulose fiber surface (Scheme 1).



Scheme 1. (a) Bisphenol-A (unionized and ionized forms), and (b) Functionalized cellulose fiber (unionized and ionized forms).

On the other hand, functionalization of the fiber does not significantly change the specific surface area (SSA) of the fiber as determined by the Brunauer–Emmett–Teller (BET-SSA) analysis of the raw (RF) and functionalized (FF) fibers which are 1.3 ± 0.4 m²/g and 1.4 ± 0.4 m²/g, respectively. The BET-SSA was measured with an Autosorb IQ Chemi TCD instrument (Quantachrome Instruments, Boynton Beach, FL, USA), utilizing adsorption–desorption N₂ isotherms at 77 K. The cellulosic fiber extracted from the Spanish broom has a very large specific surface area compared to other natural fibers such as hemp and flax whose BET-SSA ranges from 0.31 to 0.88 m²/g [44].

2.4. BPA Analytical Determination

Bisphenol A concentration in filtrate samples was measured by means of a high-performance liquid chromatography (HPLC) system (S200 Pump, S225 Autosampler, Perkin Elmer, Beaconsfield, UK) coupled with a diode array detector (S200 EP, Perkin Elmer Beaconsfield, UK). Samples were separated by reverse phase (RP) chromatography using a C18 Luna (Phenomenex) column (5u, 250 × 4.6 mm). The HPLC method was obtained by Davididou et al. [27]. The mobile phase was a mixture of water/acetonitrile (35/65, v/v) at a flow rate of 1 mL/min using UV wavelength at 225 nm. The solvents were eluted isocratically and the injection volume was kept at 40 μL.

2.5. Adsorption Tests

The adsorption capacity of the SB functionalized fibers was studied by carrying out several batch experimental runs. In each experiment, a certain amount of fiber ranging from 10 to 20 g/L was added to the polluted water, which was obtained by spiking BPA in distilled water at an initial concentration ranging from 10 mg/L to 30 mg/L. Experimental temperature was 20 °C.

The initial pH of the reactant mixture was varied in order to study the effect of this parameter on the adsorption capacity, by using appropriate amounts of NaOH or HCl solutions.

Experiments were also performed with bottled water and synthetic wastewater. The system was maintained under magnetic stirring for the whole duration of the experiment. Bisphenol A concentration was monitored as a function of time (zero time was defined as the time that fibers were added in the reactant mixture) and samples were withdrawn at specific time intervals.

The adsorption capacity, i.e., the amount of adsorbed BPA per unit mass of adsorbent (q_t), was defined as:

$$q_t = \frac{(C_0 - C_t)V}{W} \quad (1)$$

where C_0 is the initial BPA concentration (mg/L), C_t is the one observed at time t , V is the solution volume (L) and W is the adsorbent mass (g). Once the equilibrium condition of the adsorption process is reached, $C_t = C_e$ (equilibrium concentration) and $q_t = q_e$ (equilibrium adsorption capacity).

Alternatively, data were reported in terms of removal efficiency ($RE\%$), defined as the following Equation (2):

$$RE\% = \frac{(C_0 - C_t)}{C_0} 100 \quad (2)$$

3. Results and Discussion

3.1. Effect of pH

The effect of pH on the adsorption efficiency of RF and FF was studied. Experiments were conducted at different pH values (4, 5, 6, 7, 9) in the presence of 30 mg/L of BPA and 1 g of fiber in 100 mL of water. Figure 1 shows BPA concentration as a function of contact time between the BPA and the fibers. As a preamble, three important observations can be made: (a) concentration of BPA decreases with time and tends to reach a plateau after about 15 min, due to the limited number of active sorption sites on the fiber; (b) BPA adsorption onto FF changes as a function of pH, with the highest removal (50%) taking place at pH 5; (c) removal efficiency of FF is significantly higher than that of the RF (only about 6% BPA removal), at all pH values assayed.

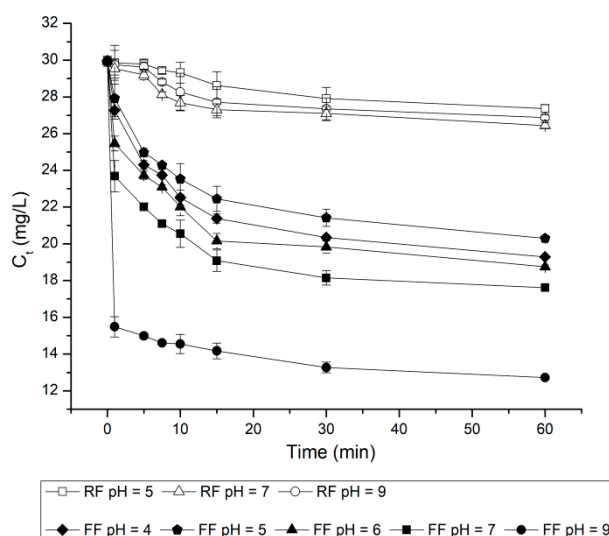


Figure 1. Effect of pH on the removal of Bisphenol A (BPA) by raw (RF) and functionalized (FF) fiber. Experimental conditions: fiber loading = 1 g; water volume = 100 mL; $C_0 = 30$ mg/L; water matrix = UP.

The variation of adsorption capacity with pH can be qualitatively explained by taking into consideration the acid/base equilibrium of the interacting species (Scheme 1). The pH of the solution determines the ionization state of both the adsorbent (FF) and adsorbed (BPA) functional groups and thereby their hydrophobicity, thus governing the adsorbent-adsorbed interactions. The BPA molecule has a $pK_a = 9.6$ [2], which means that the fraction between the ionized (BPA^{2-}) and unionized (BPA) forms increases with pH, reaching a considerable amount only at pH 9, at which roughly 1/4 molecules of BPA are ionized (at pH 9 it is about 0.25, at pH 7 is 0.0025 and at pH 5 is 0.000025). Therefore, at higher pH values the BPA solubility in water increases, i.e., it becomes more hydrophilic, thereby its tendency to be adsorbed onto hydrophobic surfaces decreases.

In contrast, the effect of altering the pH on the amine function (aniline like) of the FF is the opposite: since the pK_b of aniline is 9.6, about 70% of amine residues are in the ionized (protonated) form at pH 4, while at pH values above 5 only a small fraction of the amine terminal groups is protonated. In other words, the hydrophobicity of the absorbing fiber surface decreases abruptly when pH decreases from 5 to 4. Moreover, there is no doubt that any anion/cation binding interaction plays an important role, since, when BPA is in the anion form at high pH, the surface of the fiber is neutral and, vice versa, when the fiber surface is in the cation form at low pH, BPA is neutral.

The data reported in Figure 1 shows qualitatively that the hydrophobic interaction between the functional group of the cellulose and the BPA, as well as the hydrophilic interactions of the ionic forms of both MDI amine residue and BPA molecules with water molecules playing a role in the sorption efficiency of FF fibers. Data shown in Figure 1 can be better discussed when observing Figure 2, where the plot of equilibrium adsorption capacity (q_e) versus pH is presented. The maximum in q_e around pH 5 is due to the optimal hydrophobic interaction between the FF fiber and BPA. At lower pH values, FF fibers gradually lose their hydrophobicity, which also happens to BPA at pH above 5, thus lowering the adsorption efficiency of the fibers.

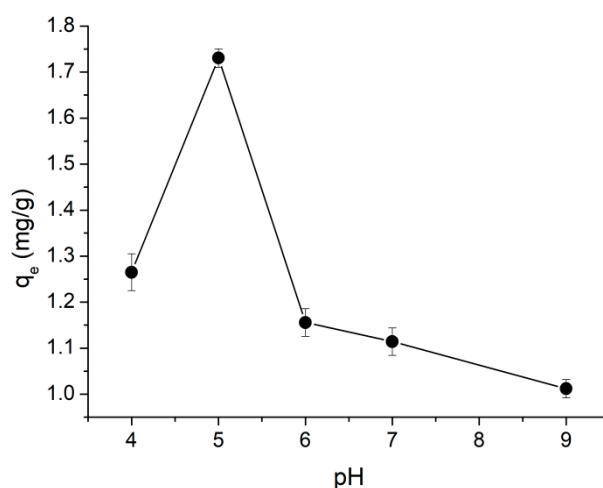


Figure 2. BPA equilibrium adsorption capacity q_e as a function of pH. Experimental conditions: fiber loading = 1 g; water volume = 100 mL; C_0 = 30 mg/L; water matrix = UP.

3.2. Regeneration and Reuse of Fiber

Recycling of the adsorbent material reduces the operational costs and the environmental footprint of the treatment process. Therefore, regeneration studies are important to assess the potential of applying this biobased treatment technology at large-scale. Regeneration of the fibers were performed with the aim to clean the adsorbent sites and use them again for BPA removal. The regeneration procedure was based on the ionic hydrophilic form that BPA takes when the pH increases, thus allowing pollutant desorption. For this reason, the used FF was washed for 2 min with a 0.1 M NaOH solution and then further washed with water to remove any possible NaOH residual on the fiber surface. After this very simple and quick treatment, the FF was used again for BPA removal, and the results are shown in Figure 3. It can be seen that the regenerated FF exhibits satisfactory reusability, since its adsorption capacity is very close to that of the original FF, which accounts for about 70% of BPA removal even after three consecutive regeneration cycles.

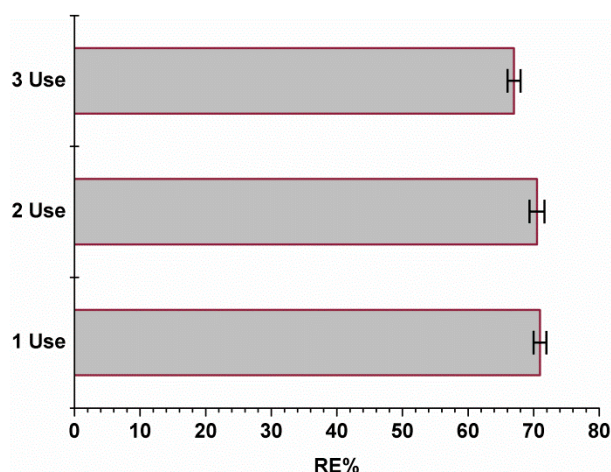


Figure 3. Bisphenol A removal efficiency, RE%, during regeneration and reuse of FF. Experimental conditions: fiber loading = 1 g; water volume = 50 mL; C_0 = 15 mg/L; pH = 5; contact time = 60 min.

3.3. Effect of Water Matrix

Further experiments were conducted in water matrices like ultrapure water (UP), bottled water (BW), synthetic wastewater (WW) and diluted WW in UP at a 50/50 ratio (WW/UP) in order to resemble more realistic water and wastewater treatment conditions. All water matrices were spiked with an initial BPA concentration of 15 mg/L and treated by 1 g of FF at a pH = 5 in a volume of 50 mL. Results are shown in Figure 4, where it can be observed that higher BPA removal (values shown in brackets) is achieved for experiments conducted in UP ($77 \pm 1\%$) followed by BW ($76 \pm 1\%$), WW/UP ($67 \pm 1\%$) and WW ($64 \pm 1\%$). This slight reduction in the RE% of BPA can be explained by the presence of other organic compounds such as urea, and those contained in peptone and meat extract in the WW/UP and WW, which interfere, to a lesser extent, with the adsorption of BPA, since they might compete with BPA for the active sites of the adsorbent. This is in agreement with the low COD and TOC removal efficiencies, which indicate that the FF does not have any specific preference for binding the organic components of WW other than BPA. In contrast, the fiber has a high selectivity toward BPA whose adsorption remains above about 64%, independently from the nature of the aqueous matrix in which it is dissolved.

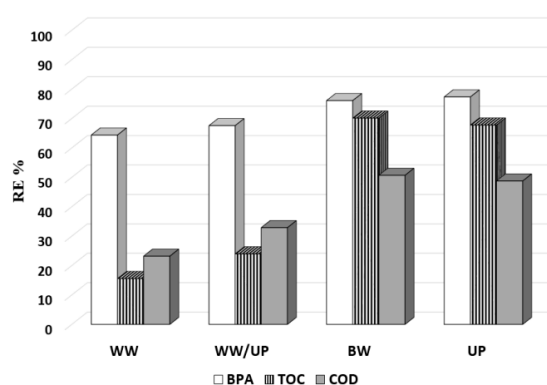


Figure 4. Removal efficiency, RE%, in various water matrices. Experimental conditions: fiber loading = 1 g; water volume = 50 mL; C_0 = 15 mg/L; pH = 5; contact time = 60 min. The errors in the calculated removal efficiency are 1% for BPA, 2% for TOC and 4% for COD.

These data highlight further the high affinity of FF surface for BPA, which is due to the functional group added, having a chemical structure very similar to that of the BPA molecules (Scheme 1). On the other hand, the low affinity of the FF surface for the other organic components of the WW is mainly due to their polar nature (amino acids, urea, etc.) having high affinity for water.

3.4. Adsorption Kinetics of BPA

Several experimental runs were performed in order to investigate the kinetics of the process. In Figure 5, process efficiency in terms of BPA removal is shown. It can be observed that in the presence of 5–30 ppm BPA/g of FF, BPA removal is at $70 \pm 1\%$ after 5 min of treatment and increases up to about $79 \pm 1\%$ after 60 min. At higher C_0/W ratios of 60, 90 and 120 ppm/g removal efficiency of BPA is substantially lower at $74 \pm 1\%$, $64 \pm 1\%$ and $55 \pm 1\%$ after 60 min of treatment.

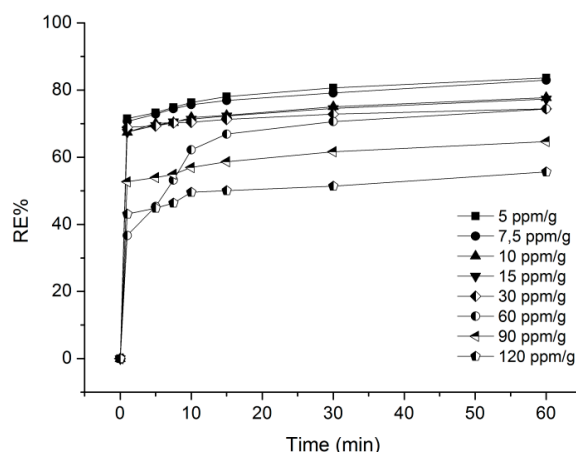


Figure 5. Process efficiency (%) in terms of BPA removal at various C_0/W (i.e., initial BPA concentration/fiber mass) ratios. Experimental conditions: water volume = 50 mL; pH = 5. The errors in the calculated removal efficiency are in the range from 0.11 to 1.17%.

Figure 6 shows that BPA adsorption kinetics were fitted very well by a pseudo-second order model, with excellent R^2 values. The rate of change of the adsorption capacity is given by Equation (3) [45]:

$$\frac{dq_t}{dt} = k_2(q_e - q_t)^2 \tag{3}$$

where k_2 and q_e are the pseudo-second order rate constant ($g/mg \text{ min}$) and the equilibrium absorption capacity (mg/g), respectively. Equation (4), obtained after integration and linearization of Equation (3), was used to estimate the parameters k_2 and q_e by fitting the t/q_t ratio as a function of time (Table 1):

$$\frac{t}{q_t} = \frac{1}{K_2 q_e^2} + \frac{1}{q_e} t \tag{4}$$

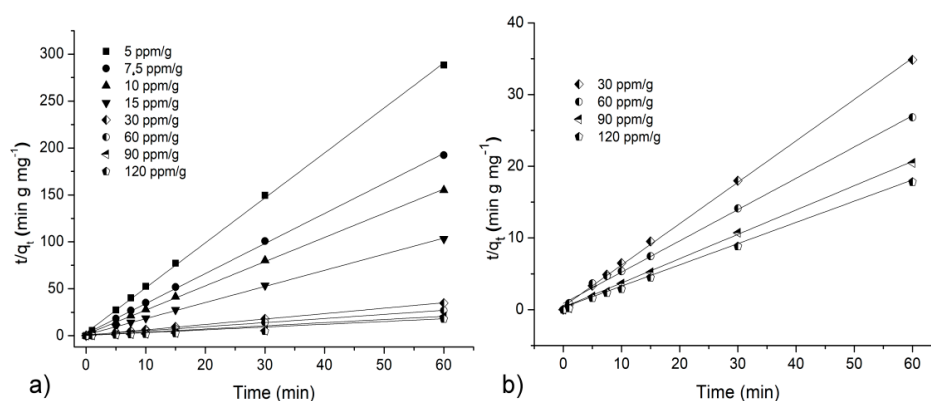


Figure 6. (a) Fitting of the experimental data by the pseudo-second order kinetics model. Experimental conditions: water volume = 50 mL; pH = 5. (b) Magnification of the data from 30 ppm/g to 120 ppm/g for a better visibility of the fitting. The errors in the t/q_t evaluations are in the range from 0.09 to 0.72%.

Table 1. Pseudo-second order kinetic data for experimental runs shown in Figures 5 and 6.

C_0/W (ppm/g)	k_2 ¹ ($\text{g mg}^{-1} \text{min}^{-1}$)	q_e ¹ (mg g^{-1})	R^2
5	7.175 (1.140)	0.21 (0.04)	0.99935
7.5	4.629 (0.885)	0.31 (0.03)	0.99913
10	4.311 (0.590)	0.39 (0.02)	0.99940
15	2.937 (0.393)	0.58 (0.02)	0.99940
30	0.757 (0.155)	1.73 (0.04)	0.99917
60	0.219 (0.123)	2.29 (0.05)	0.99637
90	0.353 (0.115)	2.95 (0.07)	0.99869
120	0.273 (0.101)	3.37 (0.04)	0.99775

¹ Values in parentheses are the standard deviations of the data.

The equilibrium adsorption capacity significantly increases with the C_0/W ratio while k_2 decreases in agreement with the hypothesis that the fiber surface has a high degree of chemical functionalization, i.e., a high number of adsorption sites.

3.5. Adsorption Isotherm

The adsorption capacity of the FF in terms of BPA removal has been assessed by plotting the adsorption isotherm data (q_e vs. C_e), which has been fitted with Langmuir and Freundlich models (Figure 7).

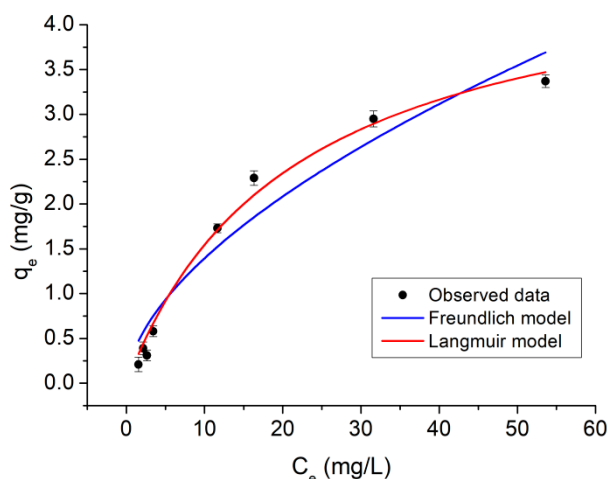


Figure 7. Bisphenol A adsorption isotherm at 20 °C onto biobased FF (black symbols) and fitting with the Langmuir (red line) and Freundlich (blue line) models.

As can be seen, the equilibrium adsorption capacity (q_e) increases nonlinearly with the equilibrium concentration of BPA (C_e) and almost reaches a plateau at $C_e > 30$ mg/L.

The Langmuir model, which assumes that the surface of the adsorbing material is covered by a monolayer of the adsorbate, that the adsorption sites are all equivalent and that the solute particles adsorbed do not interact with each other [46], is expressed by Equation (5):

$$q_e = \frac{q_m K_L C_e}{1 + K_L C_e} \quad (5)$$

where K_L is the Langmuir adsorption constant and q_m is the maximum adsorption capacity of the FF in terms of BPA removal. Figure 7 shows an excellent agreement between the experimental and calculated values, indicating the goodness ($R^2 = 0.99$) of the Langmuir model with estimated $K_L = (0.046 \pm 0.008)$ L/g and $q_m = (4.86 \pm 0.3)$ mg/g.

Worse results have been obtained by modeling the experimental data with the Freundlich model, according to Equation (6):

$$q_e = K_F C_e^{1/n} \quad (6)$$

where K_F is the Freundlich adsorption constant, related to the surface heterogeneity. Figure 7 shows that the fitting curve (blue line) obtained with the Freundlich model ($R^2 = 0.935$), to which correspond the following fitting parameters: $K_F = (0.4 \pm 0.1) \text{ L}^n/\text{g mg}^{(n-1)}$ and $n = (1.72 \pm 0.23)$.

Natural materials, whose adsorbing capacities have been improved through intensive treatments with high environmental impact (e.g., carbonization), have higher adsorption capacities than those materials treated with eco-friendly processes. Among these last adsorbents (Coir pitch, Coconut shell, Durian peel), the SB FF has the highest adsorption capacity, shows the fastest adsorption kinetics, and works in a relatively wide pH range (4–6) (Table 2).

Table 2. Comparison of FF adsorption performances with other adsorbents.

Adsorbent	q_{\max} (mg g ⁻¹)	Contact Time	pH	Isotherm Model	Reference
Coir pitch	4.31	24 h	3	Langmuir	[37]
Coconut shell	4.16	24 h	3	Langmuir	[37]
Durian peel	4.18	24 h	3	Langmuir	[37]
SB Functionalized fiber (FF)	4.86	1 h	5	Langmuir	This study
ACs from Rice Straw	181.19	1.5 h	2.35	Langmuir	[47]
ACs from Almond shell	188.90	—	2–8	Langmuir	[48]

4. Conclusions

This work reports the first application of biobased surface functionalized Spanish broom cellulose fibers to remove BPA, an endocrine disrupting chemical and priority pollutant, from water. It was found that pH significantly affects adsorption capacity with the highest adsorption rates being observed at pH 5. The functionalized cellulose fiber exhibited very good adsorption properties for BPA with 70% of the pollutant being adsorbed after 5 min of contact time. It was observed that the adsorbent system can be easily regenerated by a simple and fast washing process which allows it to recover its adsorption capacity by almost 100 % of the original one. These results indicate the potential for practical application of this technology, due to the high availability of cellulose coming from Spanish broom plants and the easily scalable process for cellulose functionalization. Other advantages of the Spanish broom fiber are: (1) its very easy extraction process [40], which gives a fiber with a high percentage of cellulose (>92%) and a relatively low lignin content (−3%) [49]; (2) its huge mechanical properties, with a tenacity of −36 cN/tex and a strain at break of −6%, which are high compared to, for instance, flax fibers [49].

Author Contributions: Data curation, A.T., E.C., F.C., A.B. and G.C.; Formal analysis, A.T., F.C. and A.B.; Funding acquisition, E.C. and G.C.; Investigation, A.T., F.C. and A.B.; Methodology, E.C.; Project administration, G.C.; Supervision, E.C. and G.C.; Validation, E.C., F.C., A.B. and G.C.; Writing—original draft, A.T.; Writing—review and editing, E.C., F.C., A.B. and G.C.

Funding: The authors are grateful to the Ministero dell’Istruzione dell’Università e della Ricerca Italiano (MIUR) and the University of Calabria for supporting this project in the framework of the ex 60% budget grant.

Conflicts of Interest: The authors declare no conflict of interest.

References

1. US Environmental Protection Agency (USEPA). Environmental protection agency—Endocrine disruptor screening program. In *Report to Congress*; USEPA: Washington, DC, USA, 2000.
2. Zeng, G.M.; Zhang, C.; Huang, G.H.; Yu, J.; Wang, Q.; Li, J.; Xi, B.; Liu, H. Adsorption behavior of bisphenol A on sediments in Xiangjiang River, Central-south China. *Chemosphere* **2006**, *65*, 1490–1499. [[CrossRef](#)] [[PubMed](#)]

3. Staples, C.A.; Dorn, P.B.; Klecka, G.M.; O'Block, S.T.; Harris, L.R. A review of the environmental fate, effects, and exposures of bisphenol A. *Chemosphere* **1998**, *36*, 2149–2173. [[CrossRef](#)]
4. Kang, J.H.; Kondo, F.; Katayama, Y. Human exposure to bisphenol A. *Toxicology* **2006**, *226*, 79–89. [[CrossRef](#)] [[PubMed](#)]
5. Huang, Y.Q.; Wong, C.K.C.; Zheng, J.S.; Bouwman, H.; Barra, R.; Wahlström, B.; Neretin, L.; Wong, M.H. Bisphenol A (BPA) in China: A review of sources, environmental levels, and potential human health impacts. *Environ. Int.* **2012**, *42*, 91–99. [[CrossRef](#)] [[PubMed](#)]
6. Yamamoto, T.; Yasuhara, A.; Shiraishi, H.; Nakasugi, O. Bisphenol A in hazardous waste landfill leachates. *Chemosphere* **2001**, *42*, 415–418. [[CrossRef](#)]
7. Fukazawa, H.; Watanabe, M.; Shiraishi, F.; Shiraishi, H.; Shiozawa, T.; Matsushita, H.; Yoshiyasu, T. Formation of chlorinated derivatives of Bisphenol A in waste paper recycling plants and their estrogenic activities. *J. Health Sci.* **2002**, *48*, 242–249. [[CrossRef](#)]
8. Heemken, O.P.; Reincke, H.; Stachel, B.; Theobald, N. The occurrence of xenoestrogens in the Elbe river and the North Sea. *Chemosphere* **2001**, *45*, 245–259. [[CrossRef](#)]
9. Lee, H.B.; Peart, T.E.; Gris, G.; Chan, J. Endocrine-disrupting chemicals in industrial wastewater samples in Toronto, Ontario. *Water Qual. Res. J. Can.* **2002**, *37*, 459–472. [[CrossRef](#)]
10. Colin, A.; Bach, C.; Rosin, C.; Munoz, J.F.; Dauchy, X. Is drinking water a major route of human exposure to alkylphenol and bisphenol contaminants in France? *Arch. Environ. Contam. Toxicol.* **2014**, *66*, 86–99. [[CrossRef](#)] [[PubMed](#)]
11. Kleywegt, S.; Pileggi, V.; Yang, P.; Hao, C.; Zhao, X.; Rocks, C.; Thach, S.; Cheung, P.; Whitehead, B. Pharmaceuticals, hormones and bisphenol A in untreated source and finished drinking water in Ontario, Canada, occurrence and treatment efficiency. *Sci. Total Environ.* **2011**, *409*, 1481–1488. [[CrossRef](#)] [[PubMed](#)]
12. Rochester, J.R. Bisphenol A and human health: A review of the literature. *Reprod. Toxicol.* **2013**, *42*, 132–155. [[CrossRef](#)] [[PubMed](#)]
13. Castoria, G.; Giovannelli, P.; Lombardi, M.; De Rosa, C.; Giraldi, T.; de Falco, A.; Barone, M.V.; Abbondanza, C.; Migliaccio, A.; Auricchio, F. Tyrosine phosphorylation of estradiol receptor by Src regulates its hormone-dependent nuclear export and cell cycle progression in breast cancer cells. *Oncogene* **2012**, *31*, 4868–4877. [[CrossRef](#)] [[PubMed](#)]
14. Di Donato, M.; Cerneria, G.; Giovannelli, P.; Galasso, G.; Bilancio, A.; Migliaccio, A.; Castoria, G. Recent advances on bisphenol-A and endocrine disruptor effects on human prostate cancer. *Mol. Cell. Endocrinol.* **2017**, *457*, 35–42. [[CrossRef](#)] [[PubMed](#)]
15. Braun, J.M.; Kalkbrenner, A.E.; Calafat, A.M.; Yolton, K.; Ye, X.; Dietrich, K.N.; Lanphear, B.P. Impact of early-life bisphenol A exposure on behavior and executive function in children. *Pediatrics* **2011**, *128*, 873–882. [[CrossRef](#)] [[PubMed](#)]
16. Rees-Clayton, E.M.; Todd, M.; Dowd, J.B.; Aiello, A.E. The impact of bisphenol A and triclosan on immune parameters in the U.S. population, NHANES 2003–2006. *Environ. Health Persp.* **2011**, *119*, 390–396. [[CrossRef](#)] [[PubMed](#)]
17. Joseph, L.; Flora, J.R.V.; Park, Y.-G.; Badawy, M.; Saleh, H.; Yoon, Y. Removal of natural organic matter from potential drinking water sources by combined coagulation and adsorption using carbon nanomaterials. *Sep. Purif. Technol.* **2012**, *95*, 64–72. [[CrossRef](#)]
18. Westerhoff, P.; Yoon, Y.; Snyder, S.; Wert, E. Fate of endocrine-disruptor, pharmaceutical, and personal care product chemicals during simulated drinking water treatment processes. *Environ. Sci. Technol.* **2005**, *39*, 6649–6663. [[CrossRef](#)] [[PubMed](#)]
19. Joseph, L.; Zaib, Q.; Khan, I.A.; Berge, N.D.; Park, Y.-G.; Saleh, N.B.; Yoon, Y. Removal of bisphenol A and 17 α -ethinyl estradiol from landfill leachate using single-walled carbon nanotubes. *Water Res.* **2011**, *45*, 4056–4068. [[CrossRef](#)] [[PubMed](#)]
20. Nam, S.W.; Jung, C.; Li, H.; Yu, M.; Flora, J.R.V.; Boateng, L.K.; Her, N.; Zoh, K.D.; Yoon, Y. Adsorption characteristics of diclofenac and sulfamethoxazole to graphene oxide in aqueous solution. *Chemosphere* **2015**, *136*, 20–26. [[CrossRef](#)] [[PubMed](#)]
21. Muhamad, M.S.; Salim, M.R.; Lau, W.J.; Yusop, Z. A review on bisphenol A occurrences, health effects and treatment process via membrane technology for drinking water. *Environ. Sci. Pollut. Res.* **2016**, *23*, 11549–11567. [[CrossRef](#)] [[PubMed](#)]

22. de Oliveira, L.K.; Moura, A.L.A.; Barbosa, V.; Parreira, R.L.T.; Banegas, R.S.; Caramori, G.F.; Ciuffi, K.J.; Molina, E.F. Removal of the emerging contaminant bisphenol A by an ureasil-PEO hybrid membrane: Experimental study and molecular dynamic simulation. *Environ. Sci. Pollut. Res.* **2017**, *24*, 18421–18433. [[CrossRef](#)] [[PubMed](#)]
23. Duan, X.D.; He, X.X.; Wang, D.; Mezyk, S.P.; Otto, S.C.; Marfil Vega, R.; Mills, M.A.; Dionysiou, D.D. Decomposition of iodinated pharmaceuticals by UV254 nm-assisted advanced oxidation processes. *J. Hazard. Mater.* **2017**, *323*, 489–499. [[CrossRef](#)] [[PubMed](#)]
24. Wang, L.; Zhao, J.; Li, Y. Removal of bisphenol A and 4-n-nonylphenol coupled to nitrate reduction using acclimated activated sludge under anaerobic conditions. *J. Chem. Technol. Biotechnol.* **2013**, *89*, 391–400. [[CrossRef](#)]
25. Wang, G.; Wu, F.; Zhang, X.; Luo, M.; Deng, N. Enhanced photodegradation of bisphenol A in the presence of β -cyclodextrin under UV light. *J. Chem. Technol. Biotechnol.* **2006**, *81*, 805–811. [[CrossRef](#)]
26. Eio, E.J.; Kawai, M.; Niwa, C.; Ito, M.; Yamamoto, S.; Toda, T. Biodegradation of bisphenol A by an algal-bacterial system. *Environ. Sci. Pollut. Res.* **2015**, *22*, 15145–15153. [[CrossRef](#)] [[PubMed](#)]
27. Davididou, K.; Hale, E.; Lane, N.; Chatzisyneon, E.; Pichavant, A.; Hochepped, J.F. Photocatalytic treatment of saccharin and bisphenol-A in the presence of TiO₂ nanocomposites tuned by Sn (IV). *Catal. Today* **2017**, *287*, 3–9. [[CrossRef](#)]
28. Outsou, A.; Frontistis, Z.; Ribeiro, R.S.; Antonopoulou, M.; Konstantinou, I.K.; Silva, A.M.T.; Faria, J.L.; Gomes, H.T.; Mantzavinos, D. Activation of sodium persulfate by magnetic carbon xerogels (C_x/CoFe) for the oxidation of bisphenol A: Process variables effects, matrix effects and reaction pathways. *Water Res.* **2017**, *124*, 97–107. [[CrossRef](#)] [[PubMed](#)]
29. Rivas, F.J.; Encinas, A.; Acedo, B.; Beltran, F.J. Mineralization of bisphenol A by advanced oxidation processes. *J. Chem. Technol. Biotechnol.* **2008**, *84*, 589–594. [[CrossRef](#)]
30. Rivero, M.J.; Alonso, E.; Dominguez, S.; Ribao, P.; Ibañez, R.; Ortiz, I.; Irabien, A. Kinetic analysis and biodegradability of the Fenton mineralization of bisphenol A. *J. Chem. Technol. Biotechnol.* **2014**, *89*, 1228–1234. [[CrossRef](#)]
31. Zacharakis, A.; Chatzisyneon, E.; Binas, V.; Frontistis, Z.; Venieri, D.; Mantzavinos, D. Solar photocatalytic degradation of bisphenol A on immobilized ZnO or TiO₂. *Int. J. Photoenergy* **2013**, *1–9*, 570–587. [[CrossRef](#)]
32. Snyder, S.A.; Adham, S.; Redding, A.M.; Cannon, F.S.; DeCarolis, J.; Oppenheimer, J.; Wert, E.C.; Yoon, Y. Role of membranes and activated carbon in the removal of endocrine disruptors and pharmaceuticals. *Desalination* **2007**, *202*, 156–181. [[CrossRef](#)]
33. Ioannou-Ttofa, L.; Foteinis, S.; Chatzisyneon, E.; Fatta-Kassinou, D. The environmental footprint of a membrane bioreactor treatment process through Life Cycle Analysis. *Sci. Total Environ.* **2016**, *568*, 306–318. [[CrossRef](#)] [[PubMed](#)]
34. Nakanishi, A.; Tamai, M.; Kawasaki, N.; Nakamura, T.; Tanada, S. Adsorption characteristics of bisphenol A onto carbonaceous materials produced from wood chips as organic waste. *J. Colloid Interface Sci.* **2002**, *252*, 393–396. [[CrossRef](#)] [[PubMed](#)]
35. Asada, T.; Oikawa, K.; Kawata, K.; Ishihara, S.; Iyobe, T. Study of removal effect of bisphenol-A and B-estradiol by porous carbon. *J. Health Sci.* **2004**, *50*, 588–593. [[CrossRef](#)]
36. Yoon, Y.; Westerhoff, P.; Snyder, S.A.; Esparza, M. HPLC fluorescence detection and adsorption of bisphenol A, 17 β -estradiol, and 17 α -ethynyl estradiol on powdered activated carbon. *Water Res.* **2003**, *37*, 3530–3537. [[CrossRef](#)]
37. Lazim, Z.M.; Hadibarata, T.; Puteh, M.H.; Yusop, Z. Adsorption characteristics of bisphenol A onto low-cost modified phyto-waste material in aqueous solution. *Water Air Soil Pollut.* **2015**, *226*, 34–45. [[CrossRef](#)]
38. Tursi, A.; Beneduci, A.; Chidichimo, F.; De Vietro, N.; Chidichimo, G. Remediation of hydrocarbons polluted water by hydrophobic functionalized cellulose. *Chemosphere* **2018**, *201*, 530–539. [[CrossRef](#)] [[PubMed](#)]
39. Arias, F.; Beneduci, A.; Chidichimo, F.; Furia, E.; Straface, S. Study of the adsorption of mercury (II) on lignocellulosic materials under static and dynamic conditions. *Chemosphere* **2017**, *180*, 11–23. [[CrossRef](#)] [[PubMed](#)]
40. Gabriele, B.; Cerchiara, T.; Salerno, G.; Chidichimo, G.; Vetere, M.V.; Alampì, C.; Gallucci, M.C.; Conidi, C.; Cassano, A. A new physical-chemical process for the efficient production of cellulose fibers from Spanish broom (*Spartium junceum* L.). *Bioresour. Technol.* **2009**, *101*, 724–729. [[CrossRef](#)] [[PubMed](#)]

41. Agenzia Nazionale per la protezione dell’Ambiente (APAT). Metodi analitici per le acque/APAT; IRSA-CNR. In *Manuali e Linee Guida 29/2003*; APAT: Roma, Italy, 2003; ISBN 8844800837.
42. Henze, M.; Comeau, Y. Wastewater characterization. In *Biological Wastewater Treatment: Principles, Modelling and Design*; Henze, M., van Loosdrecht, M.C.M., Ekama, G.A., Brdjanovic, D., Eds.; IWA Publishing: London, UK, 2008; pp. 33–52, ISBN 1843391880.
43. Boehm, H.P. Chapter thirteen—Surface chemical characterization of carbons from adsorption studies. In *Adsorption by Carbons*; Bottani, E.J., Tascón, J.M.D., Eds.; Elsevier: Amsterdam, NL, USA, 2008; pp. 301–327, ISBN 9780080444642.
44. Bismarck, A.; Aranberri-Askargorta, I.; Springer, J.; Lampke, T.; Wielage, B.; Stamboulis, A.; Limbach, H.H. Surface characterization of flax, hemp and cellulose fibers; surface properties and the water uptake behavior. *Polym. Compos.* **2002**, *23*, 872–894. [[CrossRef](#)]
45. Limousin, G.; Gaudet, J.P.; Charlet, L.; Szenknect, S.; Barthes, V.; Krimissa, M. Sorption isotherms: A review on physical bases, modeling and measurement. *Appl. Geochem.* **2007**, *22*, 249–275. [[CrossRef](#)]
46. Atkins, P.; De Paula, J. *Physical Chemistry*, 8th ed.; W. H. Freeman and Company: New York, NY, USA, 2006.
47. Chang, K.L.; Hsieh, J.F.; Ou, B.M.; Chang, M.H.; Hsieh, W.Y.; Lin, J.H.; Huang, P.J.; Wong, K.F.; Chen, S.T. Adsorption studies on the removal of an endocrine-disrupting compound (bisphenol A) using activated carbon from rice straw agricultural waste. *Sep. Sci. Technol.* **2012**, *47*, 1514–1521. [[CrossRef](#)]
48. Bautista-Toledo, I.; Ferro-Garcia, M.A.; Rivera-Utrilla, J.; Moreno-Castilla, C.; Vegas Fernandez, F.J. Bisphenol A removal from water by activated carbon. Effect of carbon characteristics and solution chemistry. *Environ. Sci. Technol.* **2005**, *39*, 6246–6250. [[CrossRef](#)] [[PubMed](#)]
49. Cerchiara, T.; Chidichimo, G.; Rondi, G.; Gallucci, M.C.; Gattuso, C.; Luppi, B.; Bigucci, F. Chemical Composition, morphology and tensile properties of Spanish broom (*Spartium junceum* L.) fibres in comparison with flax (*Linum usitatissimum* L.). *Fibres Text. East. Eur.* **2014**, *22*, 25–28.



© 2018 by the authors. Licensee MDPI, Basel, Switzerland. This article is an open access article distributed under the terms and conditions of the Creative Commons Attribution (CC BY) license (<http://creativecommons.org/licenses/by/4.0/>).

CHAPTER 7

Low pressure plasma functionalized cellulose fiber for the remediation of petroleum hydrocarbons polluted water

A. Tursi^a, N. De Vietro^{b,*}, A. Beneduci^{a,c}, A. Milella^{b,d}, F. Chidichimo^{e,c}, F. Fracassi^{b,d}, G.

Chidichimo^{a,c}

^aDepartment of Chemistry and Chemical Technologies, University of Calabria, Via P. Bucci, Cubo 15D, 87036 Arcavacata di Rende (Cs), Italy;

^bInstitute of Nanotechnology (Nanotec), National Research Council (CNR), c/o Department of Chemistry, University of Bari "Aldo Moro", Via Orabona 4, 70126 Bari, Italy;

^cSIRiA S.r.l. - Servizi Integrati e Ricerche per l'Ambiente, Spin-off of the University of Calabria, c/o Department of Chemistry and Chemical Technologies, Via P. Bucci, Cubo 15D, 87036, Arcavacata di Rende, CS, Italy

^dDepartment of Chemistry, University of Bari "Aldo Moro", Via Orabona 4, 70126 Bari, Italy;

^eDepartment of Environmental and Chemical Engineering, University of Calabria, Via P. Bucci, Cubo 41B, 87036 Arcavacata di Rende (CS), Italy.

ABSTRACT

This work reports a first example of effective purification, at laboratory level, of water polluted by petroleum hydrocarbons, by means of low pressure plasma fluorine grafted cellulose fiber extracted from Spanish Broom.

In order to improve the affinity of the cellulosic surface towards water dispersed hydrocarbons, its original hydrophilic character was turned to super-hydrophobic, by a fluorine functionalization.

Batch experiments were performed with the aim of studying kinetic and thermodynamic aspects of the adsorption process, as a function of the initial total hydrocarbon load and of the adsorbent amount. The kinetics data showed that the fiber removal efficiency ranged between 80-90% after one minute of contact time, in dependence of the initial hydrocarbon/fiber weight ratio (20-240 mg/g). A maximum adsorption capacity larger than 270 mg/g was estimated by fitting the

adsorption isotherm measurements with the Langmuir model. It turned out that the functionalized fiber is capable to perform a significant hydrocarbons removal action if compared to other cellulosic materials reported in the literature.

Finally, the efficiency of the plasma modified cellulose fiber, after iterative re-uses, was studied.

Keywords: fluorine surface functionalized cellulose fiber, total petroleum hydrocarbons, water remediation, low pressure plasma.

***Corresponding author**

Nicoletta De Vietro

Institute of Nanotechnology (Nanotec), National Research Council (CNR) c/o Department of Chemistry, University of Bari “Aldo Moro”

Via Orabona, 4

70126 – Bari (Italy)

Tel. +39.080.5443432

Fax +39.080.5443405

e-mail address: nicoletta.devietro@uniba.it

1. Introduction

The term Total Petroleum Hydrocarbons (TPHs) indicates a large family of different chemical compounds derived from petroleum. Accidental emissions of this class of petroleum products are particularly alarming for the environment and for human health [1].

A wide variety of chemicals can normally be found in TPHs such as hexane, mineral oils, benzene, toluene, xylenes, naphthalene and fluorene, as well as other crude oil products. Therefore, it is not practical to measure them separately, but it is preferable to measure the total amount of hydrocarbons in a given soil, water or air sample [2].

In recent decades, due to rapid industrialization, organic pollutants released into the environment, such as total petroleum hydrocarbons (TPHs), aliphatic hydrocarbons (AHs) and polycyclic aromatic hydrocarbons (PAHs), have increased significantly, modifying and damaging the balance of ecosystems.

Hydrocarbon components belong to the family of carcinogens and neurotoxic organic pollutants and can contaminate the environment in a widespread manner, considering their frequent use in many production processes [3].

Severe effects on marine flora and fauna and, subsequently, on human health were observed due to the strong tendency of these compounds for bioaccumulation in the food chain [4, 5]. Indeed, several studies [6, 7, 8] have demonstrated that most human cancers, such as prostate and pulmonary carcinoma, can be attributed to their presence in food. Moreover, a long exposure time to hydrocarbon components are responsible of permanent damage to the central nervous system. The ingestion of petroleum products, such as gasoline and kerosene, causes irritation of the throat and stomach, central nervous system depression, breathing difficulty and pneumonia.

When TPHs and other hydrophobic organic compounds (HOCs) accumulate into natural water reservoirs their lighter fraction floats on the surface forming thin films. The heavier fractions accumulate in the sediments, affecting fishes and other bio-organisms [9].

Currently, most of the existing technologies for the treatment and removal of this type of pollutants such as advanced oxidation techniques as ozonation (O_3/H_2O_2), photocatalysis (UV/ TiO_2) [10] and photo-Fenton [11], coagulation/flocculation [12], filtration [13], chemical precipitation, evaporation [14] are ineffective, not easy to implement and very expensive especially when the hydrocarbon concentration is very high (above 100 mg/L).

Physical adsorption is generally considered an effective method for TPHs removal in aqueous medium because of the large accessible internal and/or external surface that the common adsorbents generally have [15 - 20].

The use of modified natural fibers, for the remediation of HOCs polluted water, has been investigated by several authors in the last few years [21], in fact chemical modification can be applied to change lignocellulosic bio-sorbents properties, such as hydrophilic or hydrophobic characters, elasticity, water sorption ability. For example, experiments were carried out using hydrophobic cotton fibers, obtained by acylation of cellulose [22] or sugarcane bagasse (HOCs removal efficiency around 70%) [23], activated rice husk and straw [24] or in general with materials such as peat, sawdust, wood chips [25, 26, 27] whose hydrophobic character has been increased by treating the material at high temperatures for several hours [28].

The present work shows a novel approach for the remediation of hydrocarbon polluted water by using Spanish Broom (SB) hydrophobized cellulose fibers. It represents, as far as we know, the second case of surface modified cellulose SB fibers potentially usable to remove HOCs from water [21, 29, 30].

This plant was also investigated in several research activities, as a strengthening additive in polyurethane composites [31], for yellow dye extraction and for the design of an automated process for cellulose production [32-35].

Moreover, this plant, without any surface modification, allows the adsorption of heavy metals from water, such as mercury [36].

In this paper we propose to improve the affinity of SB fibers for TPHs, by a non-equilibrium plasma treatment of their surface, with tetrafluoromethane (CF₄) [37-41]. The non-equilibrium plasma approach is an eco-friendly versatile tool allowing the modification of the uppermost layers of flat substrates, fibers or granules [42-43], both at low or atmospheric pressure [39, 40, 44]. If the plasma is fed with fluorocarbon compounds the grafting of fluorinated functional groups or the deposition of fluoro-polymer thin films can be obtained, depending on the experimental conditions. In both cases the treated surfaces can turn hydrophobic [39] or even superhydrophobic [45-47]. On the contrary, if the plasma is fed with oxygen and acidic or basic vapours, hydrophilic surfaces can be obtained [43, 48, 49, 50]. When working with fluorine containing feed, the experimental condition must be properly evaluated since the plasma treatment of organic and of some inorganic substrates can also result in dry etching, i.e., the removal of material from the sample surface for the formation of volatile products [38, 51].

Among the different possible experimental approach, the plasma treatment of SB fibers was performed in low pressure conditions for the lower geometrical constrains which characterizes low pressure operation.

Before and after the plasma treatment, all fibers were analysed by fast Fourier transform-infrared (FT-IR) and X-ray photoelectron spectroscopy (XPS), for the chemical characterization. Morphology information were obtained by means of B.E.T. (Brunauer–Emmett–Teller) porosimetry and Scanning electron microscopy coupled to an energy dispersion X-rays spectrophotometers (SEM-EDS) for elemental analysis composition of the fiber surface. Moreover, water contact angle (WCA) measurements were used to evaluate the hydrophobicity of plasma treated fibers.

Batch experiments were performed in order to study the kinetics and thermodynamics of the adsorption process, as a function of the initial total hydrocarbon content (THC) and of the mass of adsorbent. The kinetic data, very well fitted by a pseudo second order model, showed that the equilibrium adsorption capacity was reached within an hour, with removal efficiencies as high as

99%. The equilibrium adsorption data, very well fitted by a Langmuir isotherm model, allowed to estimate maximum adsorption capacities larger than 270 mg/L.

A method for the regeneration of the plasma modified cellulose fiber was also developed and, finally, the activity of the so regenerated vegetable material, after iterative re-uses, was studied.

2. Materials and methods

2.1. SB fibers extraction process

The fibers of the vegetable, which grows naturally in the Mediterranean area, were obtained by using a pulping process in a 5% w/w NaOH solution. The vegetable was macerated for 20 minutes at a temperature of 353 K. After this treatment the cellulose fiber could be easily separated from the inner woody skeleton of the SB bushes. Lignin impurities were removed by further washing the cellulose fibers with a 0.5% w/w NaOH solution at a temperature of 353 K.

2.2. Low pressure plasma hydrophobization conditions

Low pressure plasma treatments were performed on 2.5 g of SB fiber, without any cleaning or pre-treatment, in the lab scale reactor schematized in **Fig. 1**.

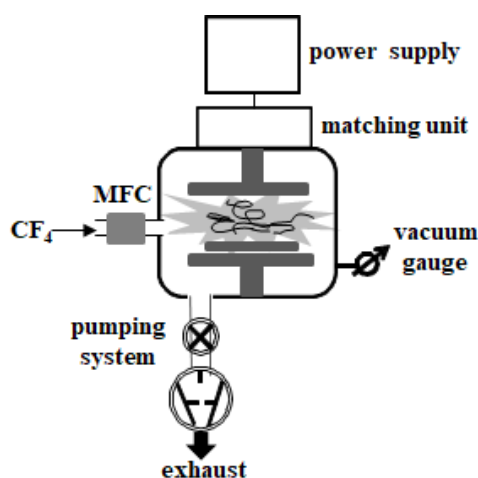


Fig. 1. Scheme of the low pressure plasma apparatus.

It consists of a cylindrical stainless steel chamber (internal diameter, 230 mm) equipped with two stainless steel electrodes (inter-electrode distance, 50 mm). The upper, circular electrode (diameter, 105 mm) is connected to a 13.56 MHz radio frequency (RF)-power supply through an automatic L-type matching network unit, while the lower square electrode (side, 95 mm), on which the SB fibers were positioned during the treatment, is grounded. The plasma was ignited at 10-70 W (below 10 W the discharge was not stable and above 70 W fiber degradation was observed) with CF₄ (*Rivoira*, purity > 99.9%) at the flow rate fixed at 20 sccm (standard cubic centimetres per minute) by means of a mass flow controller (*MKS Instruments*). During the treatments the pressure was kept constant at 13.3 Pa utilizing a rotary pump, a baratron gauge and a manual throttle valve. The plasma treatments were conducted for 10 min, in order to ensure the homogeneous treatment of the cellulosic fibers.

2.3. Chemical characterization

XPS analyses were performed with a Scanning XPS Microprobe (PHI 5000 Versa Probe II, Physical Electronics) equipped with a monochromatic Al K_α X-ray source (1486.6 eV), operated at 15 kV and 24.8 W, with a spot of 100 μm. Survey (0–1200 eV) and high resolution spectra (C1s, O1s, F1s and Ca2p) were recorded in FAT (Fixed Analyser Transmission) mode at a pass energy of 117.40 and 29.35 eV, respectively. The analyser energy resolution, evaluated on the FWHM Ag 3d_{5/2} photoemission line, was 0.7 eV for a pass energy of 29.35 eV. Surface charging was compensated using a dual beam charge neutralization, with a flux of low energy electrons (~1 eV) combined with very low energy positive Ar⁺ ions (10 eV). The hydrocarbon component of C1s spectrum was used as internal standard for charging correction and it was fixed at 285.0 eV [52]. All spectra were collected at an angle of 45° with respect to the sample surface. Best-fitting of the C1s signal was carried out with MultiPak (*Physical Electronics*) data processing software, utilizing the components reported in **Table 1** [53].

Table 1 Curve-fit data for C1s spectra of raw and plasma treated SB fibers [51, 52].

Raw SB fibers		
	Binding Energy (eV)	Peak Assignment
C1	285.0	C-C, C-H
C2	286.6±0.2	C-OH/R
C3	288.0±0.2	C=O, O-C-O
C4	289.1±0.2	COOH/R
Plasma functionalized SB fibers		
	Binding Energy (eV)	Peak Assignment
C1	285.0	C-C, C-H
C2	285.8±0.3	C-OH/R, <u>C</u> -CF, <u>CH</u> ₂ -CF ₂
C3	287.5±0.3	C=O, O-C-O, <u>C</u> =CF
C4	289.0±0.3	COOH/R, CF
C5	290.4±0.3	CF-O, <u>CF</u> ₂ -CH ₂
C6	292.1±0.3	CF ₂ , CF ₂ -O
C7	294.0±0.3	CF ₃
C8	295.2±0.3	CF ₃ O

The F1s signal of the plasma modified SB fibers was fitted, always with the MultiPak software, using two components positioned at 689.3 ± 0.1 eV and 685.6 ± 0.1 eV, due to covalent and ionic fluorine, respectively [53, 54]. The high resolution spectra were fitted with mixed Gaussian-Lorentzian peaks after a Shirley background subtraction.

Atomic concentrations were determined from the high resolution spectra after subtracting a Shirley-type background, using the Scofield sensitivity factors set in the MultiPak software. For each sample, quantitative data were averaged on 9 measurements performed on three different samples.

FT-IR analysis were carried out with a *Bruker* ALPHA FT-IR spectrometer, provided with a A241/D reflection module, in the spectral range 375-4000 cm^{-1} .

2.4. Morphological and physical characterization

A LEO 420 scanning electron microscope (SEM, *Zeiss*), operating 15 kV, was used to observe the morphological features of both pristine and plasma treated SB fibers, after metallization with sputtered gold-palladium. The EDS module was an INCAx-Sight Oxford Instruments (Vacuum conditions: 8×10^{-6} Torr, iProbe = 650 pA, Current =15 kV).

The specific surface area (SSA) of the raw and plasma modified fibers were determined employing an Autosorb IQ Chemi TCD instrument (*Quantachrome Instruments*), utilizing adsorption-desorption N_2 isotherms at 77 K.

The hydrophobic behaviour of treated SB fibers was evaluated by static water contact angle (WCA) measurements, performed with a manual goniometer (*Ramé.Hart, Inc.*), utilizing 2 μL bi-distilled water drops deposited on stretched fibers. Five fibers were analyzed for each treatment conditions, and the reported WCA values were averaged over 5 measurements on each sample.

2.5. Batch tests for water purification

In order to assess the remediation capability of the SB functionalized fibers, they were added to hydrocarbons polluted water samples, in several batch experiments. The experimental conditions were such that 5 to 15 g of fibers were used to treat 900 ml of ultrapure water ($18.2 \text{ M}\Omega \text{ cm}$) polluted with gasoline petrol in a concentration range going from 300 mg/L to 1200 mg/L. Fibers were dispersed by maintaining the system under gently stirring through a magnetic stirrer. The TPHs content was observed as a function of time (the instant at which the fibers were added to the polluted water represents the zero time), at the following instants: 1, 5, 10, 15, 30 and 60 min.

In order to study the adsorption isotherm trend, data collected after 1h of contact time at a temperature of 293 K, from the different pollutant load, have been used. The residual TPHs content

in the treated water samples were determined by using the ASTM D7678-11 (American Society for Testing and Materials procedure for TPHs in water and wastewater): after a solvent extraction of hydrocarbons, these have been quantified by Mid-IR Laser spectroscopy.

The adsorption capacity q_t , defined as the amount of adsorbed hydrocarbons per unit mass of adsorbent, were calculated according to equation (1):

$$q_t = \frac{(C_0 - C_t)V}{w} \quad (1)$$

where, C_0 is the initial TPH loads (mg/L), C_t is the one observed at time t , V is the solution volume (L) and w is the adsorbent mass (g). Once the equilibrium condition of the adsorption process is reached, $C_t = C_e$ (equilibrium concentration) and $q_t = q_e$ (equilibrium adsorption capacity).

Alternatively, data were reported in term of removal efficiency (RE%), defined with the following equation (2):

$$RE\% = \frac{(C_0 - C_t)}{C_0} \times 100 \quad (2)$$

3. Results and discussion

3.1. XPS and FTIR analyses

The surface of untreated SB fibers is composed by, approximately, 20 at.% of oxygen, 80 at.% of carbon and traces of calcium. The plasma treatment induces a fluorine uptake, which slightly decreases with the RF power (40 at. % at 10 W and 37 at.% at 70 W). Correspondingly, the carbon and oxygen concentration decrease down to 46-47 at. % and 14-16 at. %, respectively, depending on the plasma power. Under the experimental conditions utilized, the XPS atomic composition of treated surface is not considerably affected by the input power.

More details on the changes induced by the plasma treatments can be obtained by fitting the high resolution C1s spectra of the raw and treated fibers (10 W), utilizing the components of **Table 1**. The results for the pristine fibers (**Fig. 2a**) confirm the cellulosic nature of the raw fibers (peaks C1-C3) as well as the presence of carboxylic impurity (peak C4), about 2.4 % of total carbon, probably

due to lignin residues not removed by the extraction process. After the plasma treatment (**Fig. 2b**) the C1s signal broadens and additional components at higher binding energy, due to fluorine containing functional groups, appear.

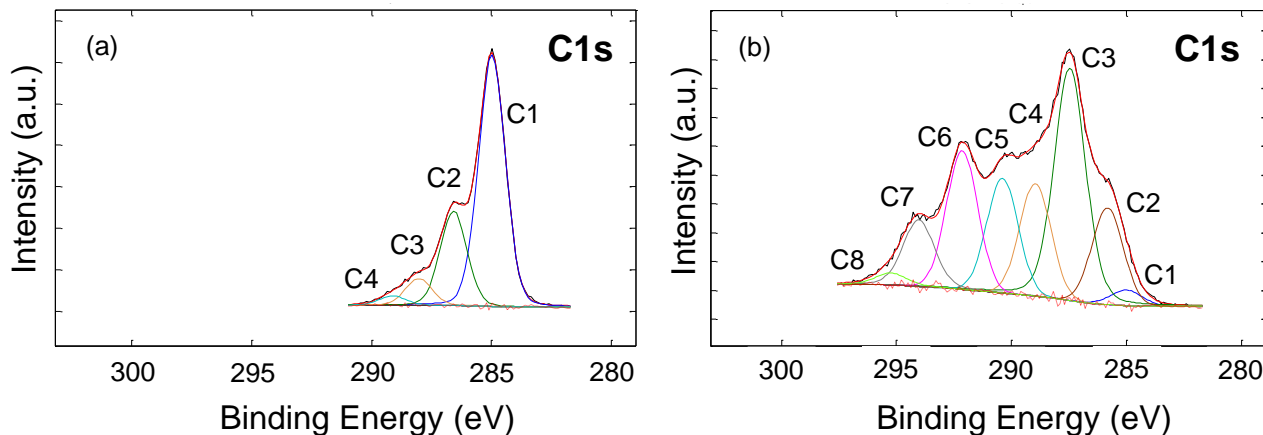


Fig. 2. High resolution C1s spectra of pristine (a) and plasma treated at 10 W SB fibers (b).

By the comparison of C1s spectra of samples treated at different input power (**Fig. 3a**) it appears that the increase of RF power induces an evident increment of the hydrocarbon component at lower binding energy (285.0 eV) and the reduction of the highly fluorinated peaks above 289 eV, (namely from C5 to C8 of Table 1). This trend can be better appreciated in **Fig. 3b**, where the total area of the highly fluorinated components is reported versus RF input power. The total area was calculated as sum of the peak areas from C5 to C8, resulting from the curve-fitting of C1s spectra for SB fibers treated at different RF powers.

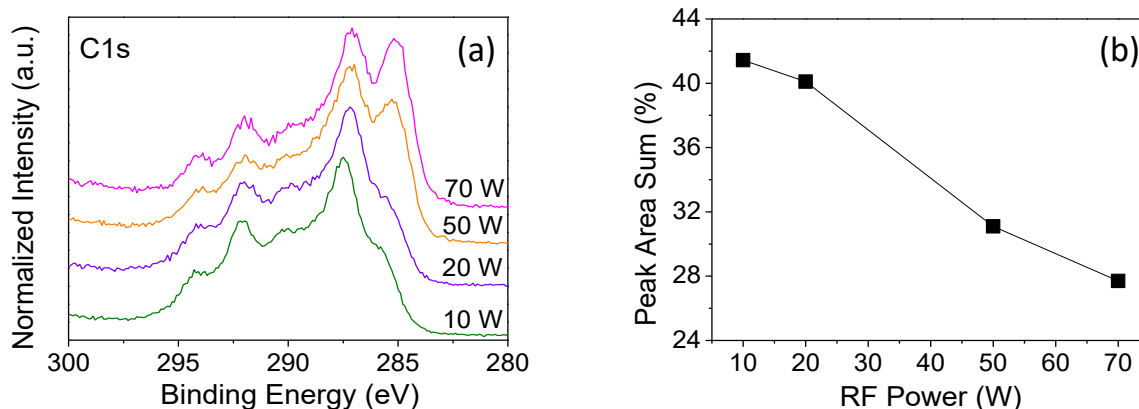


Fig. 3. (a) High resolution C1s spectra of SB fibers treated at different RF powers. Spectra were shifted for clarity. (b) Total area of highly fluorinated groups (peaks from C5-C8 of Table 1) versus RF input power.

This experimental evidence seems in disagreement with the fact that the XPS atomic composition of the treated SB fibers is not considerably affected by the input power utilized during the plasma process; the reduction of CF_x in the C1s signal at high input power, should also correspond to a more extensive decrease of atomic fluorine concentration. The high resolution F1s spectra allow to clarify this apparent discrepancy. In fact, while at 10 and 20 W the F1s signal consists only of a single peak positioned at 689.3 ± 0.1 eV, corresponding to fluorine covalently bounded to carbon, i.e., CF_x [53], at higher input power a second peak positioned at 685.6 ± 0.1 eV, assigned to calcium fluoride appears (**Fig. 4**). The intensity of this second component increases with the input power, up to about 6 at. %, and its concentration is always twice that of calcium. This would suggest the formation of calcium fluoride (CaF_2) on the fiber surfaces.

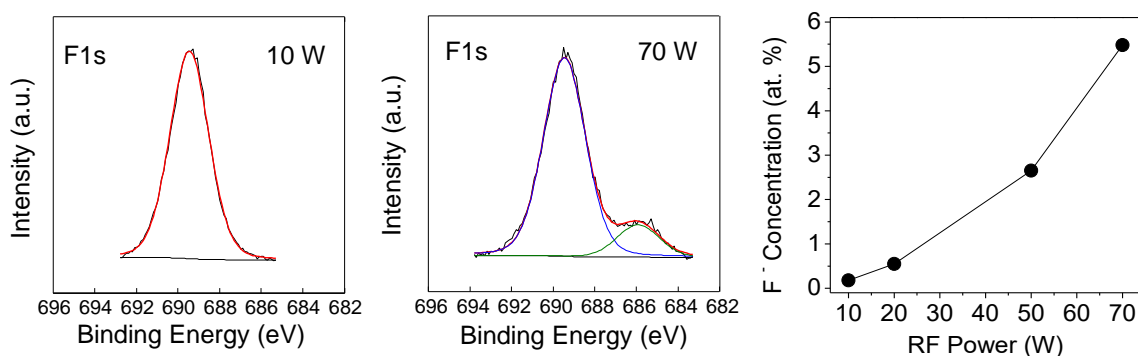


Fig. 4. High resolution F1s spectra of fibers treated at 10 W and 70 W and fluoride atomic percent at different input power.

To summarize the outcomes from XPS analyses, it is possible to conclude that milder plasma treatments allow to maximize the amount of per-fluorinated carbon groups grafted on SB fibers and then, they are expected to turn into more hydrophobic fibers with greater affinity for hydrocarbon compounds.

In order to verify the stability with time of the surface modification obtained with the plasma treatment, the ageing in air of the treated SB fibers was also investigated by XPS. It was found that, up to 3 months of storage, no changes of the surface chemical composition were registered for all the experimental plasma conditions. This was an expected result, considering the non-polar nature of the air, the storage medium [54].

The FT-IR analysis of the raw fiber confirmed its cellulosic nature (**Fig. 5**) with the characteristic vibration bands at: 668 cm^{-1} (C–O–H out-of-plane bending modes); 900 cm^{-1} (C–O–C, C–C–O and C–C–H deformation modes and stretching vibrations involving the motions of the C5 and C6); 1375 cm^{-1} (CH deformation vibration); 1430 cm^{-1} (H–C–H and O–C–H in-plane bending vibrations); 2900 cm^{-1} (C–H stretching); $4000\text{--}2995\text{ cm}^{-1}$ (hydrogen-bonded OH stretching).

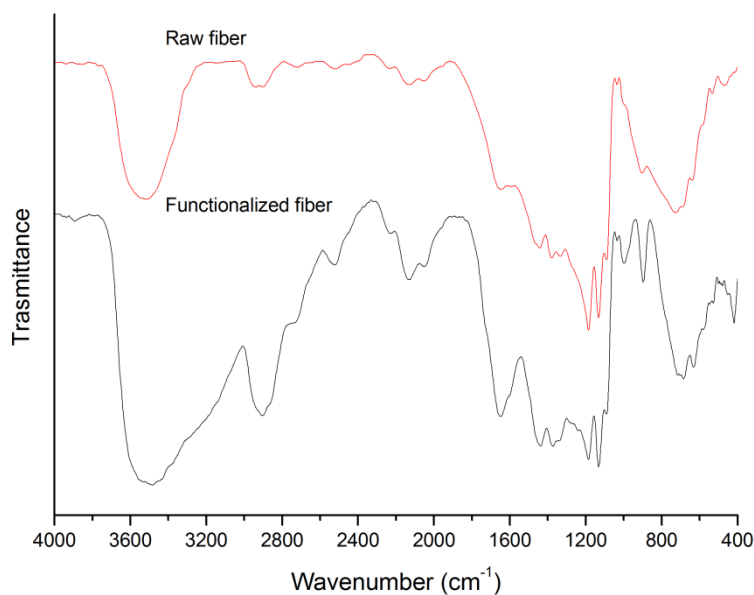


Fig. 5. FTIR spectrum of the raw SB fiber and functionalized SB fiber.

After the plasma treatments, the functionalized SB cellulose shows new adsorption bands at 1230–1570 cm^{-1} ($-\text{CF}$, $-\text{CF}_2$, and $-\text{CF}_3$) and at 570–1830 cm^{-1} ($\text{C}=\text{CF}_2$), appear in the FTIR spectra which confirmed the fiber fluorination. According to the XPS investigation, no differences were detected at different input power treatment.

3.2. WCA measurements

The pristine fiber was characterized by light hydrophilicity (static water contact angle of about 75°), for surface hydrophilic groups, e.g., hydroxyls, ethers, esters and carboxylic. After the CF_4 -plasma treatment, under all the experimental conditions explored, the fiber surface turned hydrophobic with a WCA higher than 120° and decreasing with input power (**Table 2**). The partial loss of hydrophobicity occurring at 70 W can be rationalized by taking into account the changes in the surface chemistry pointed out by the XPS analyses. Beside a slight decrease in F atomic percent, a partial conversion of covalent fluorine to ionic one was found at higher plasma power, both factors justifying the lower WCA value. The water contact angles did not show any appreciable variation after 3 months ageing in air.

Table 2. WCA values measured on plasma treated SB fibers at different input power.

RF Power (W)	WCA (°)
Raw SB fiber	75±2
10	> 160
20	148±3
50	137±8
70	131±7

3.3 SEM-EDS fiber morphology, surface elemental distribution and B.E.T. surface area measurements

SEM pictures of raw and functionalized SB fibers are shown in **Fig. 6** where the surface morphology is compared in three different cases: pristine fibers (**Fig. 6a**), fibers treated at 10W (**Fig. 6b**) and 70 W (**Fig. 6c**). It can be observed that the pristine fibers are characterized by a very smooth surface, while upon plasma treatment the surface roughness increases, likely due to etching processes associated to the plasma treatment; the effect is more pronounced at higher input power.

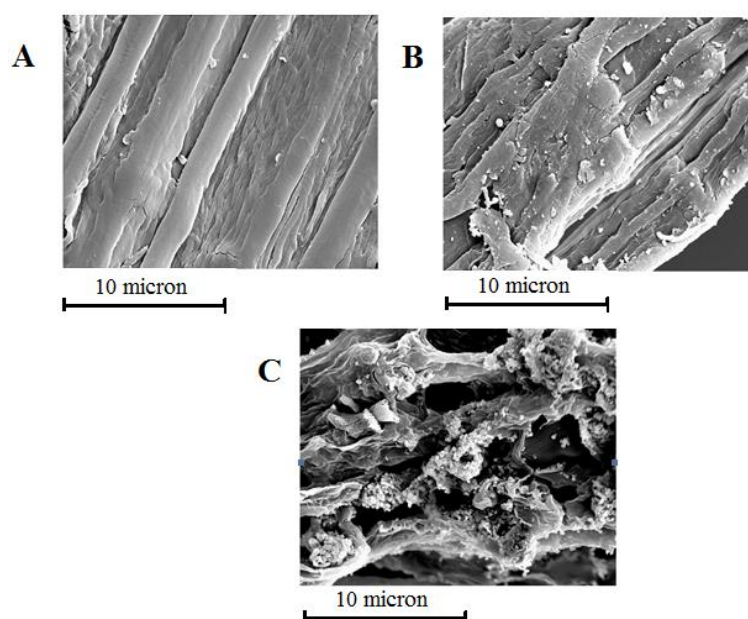


Fig. 6. SEM pictures of pristine (a) and plasma treated fibers at 10 W (b) and 70 W (c).

Complementary information on the chemical composition of the fiber treated at 70 W (**Fig. 6c**) were obtained by SEM-EDS analysis, which has a deeper sampling depth (few μm) with respect to that of XPS (less than 10 nm). **Figure 7 (Fig. 7)** represents an elemental map indicating regions with predominance of carbon (blue), fluorine (green) and calcium (red) across the fiber. Green spots are spread all over the fiber, indicating that the plasma treatment is quite homogenous. To a closer look, green spots overlapping the blue area are indicative of the perfluorinated moieties grafted with the plasma and identified by XPS. Instead, the green parts overlapping red regions identify the surface calcium fluoride. Pure red parts are, finally, representative of the calcium not modified by the treatment and likely included in the fiber as calcium oxide.

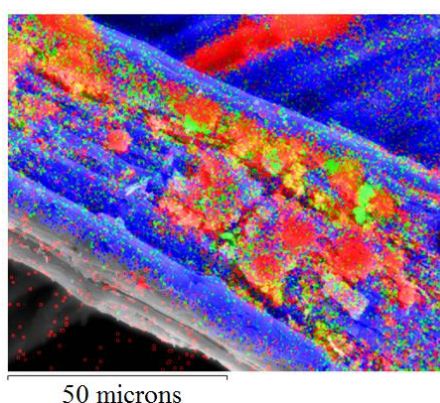


Fig. 7. Surface fibers chemical elemental spatial distribution. Blue, red, green spots are associated with carbon, calcium and fluorine predominance, respectively.

In **Table 3**, the specific surface area (SSA) of the pristine fibers is compared with the plasma treated ones. Results showed that the SSA of the fiber treated at 10 W is very close to that of the pristine broom while, for treatment performed at 70 W, a significant SSA increase was registered. This result is in agreement with the roughening of the fibers induced by harsher plasma treatment described by SEM analyses.

Table 3: B.E.T. surface area for pristine and plasma functionalized SB fibers at different input power values.

Sample	B.E.T. SSA (m ² /g)
Raw SB fiber	1.3±0.4
SB fiber treated at 10 W	1.4±0.5
SB fiber treated at 70 W	3.1±0.4

3.4. Adsorption properties of the functionalized SB fibers

Batch adsorption experiments were performed in order to study the TPHs adsorption capacity of the plasma grafted fibers, obtained at different grafting powers. In a first experimental phase, the raw fibers were investigated together with the grafted ones, by using a batch system with an initial TPHs load of 600 mg/L, was treated with 15 g of fibers in every performed experiment. Results are shown in **Figure 8 (Fig. 8)**.

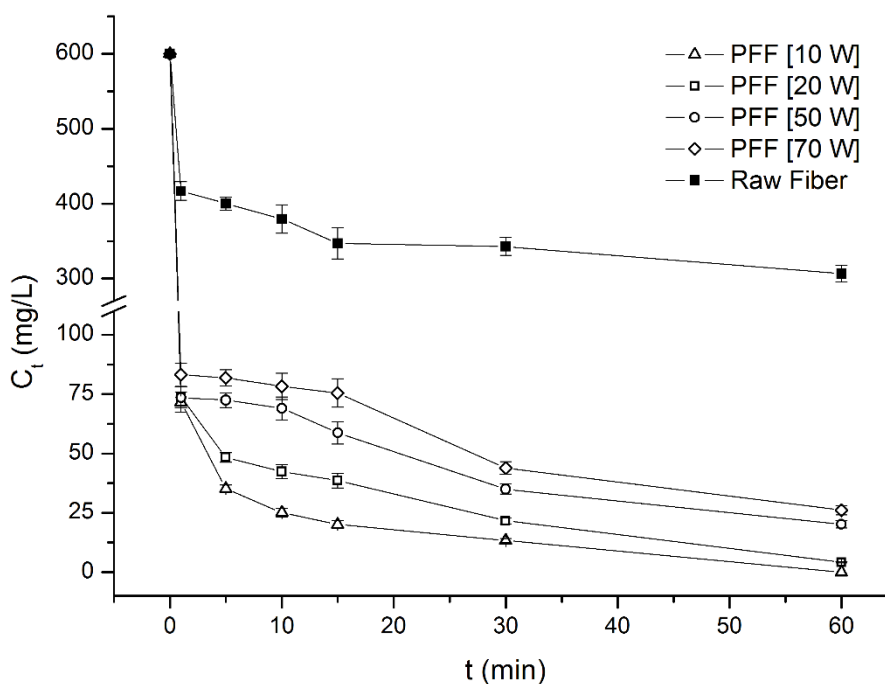


Fig. 8. Time variation of the TPHs content in polluted water, were raw and surface functionalized SB fibers were used, as pollutant adsorbers, in batch experiments.

It can be seen that the TPHs amount decreases, in all cases, very rapidly in the first 1-2 minutes, moving down to an asymptotic value as the contact time increases. For the functionalized fibers the asymptotic value is always close to zero, while it stands around the 50% of the starting TPHs content for the raw fibers. This behavior was expected because of the increased hydrophobicity of the functionalized fibers, which is fully supported, by the almost linear increase of the equilibrium adsorption capacity with the fiber hydrophobicity (WCA), as shown in **Figure 9 (Fig. 9)**.

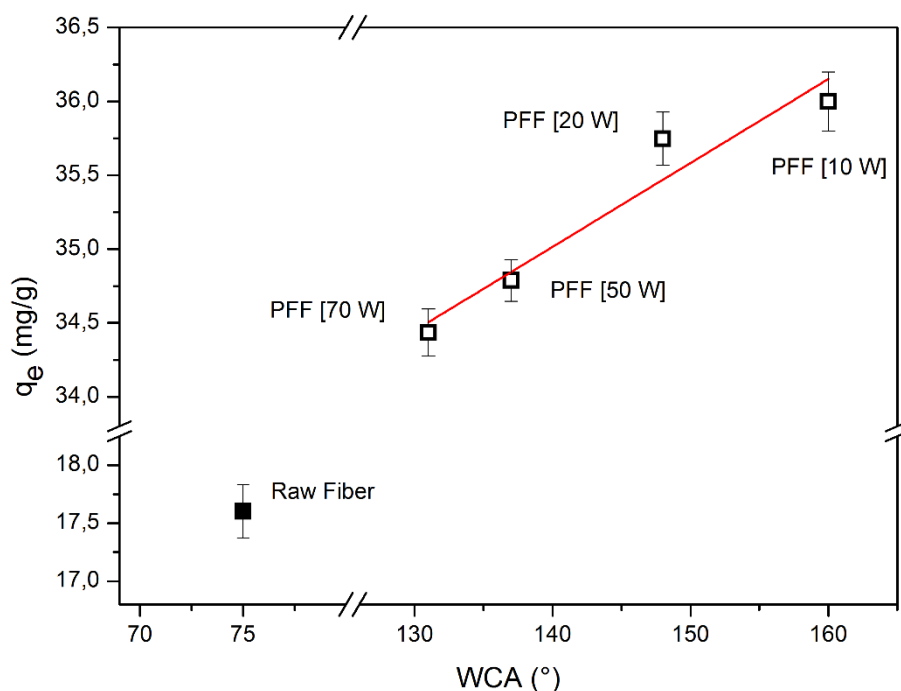


Fig. 9. Equilibrium adsorption capacity, as a function of the water contact angle (WCA), in polluted water.

This result definitely confirms that the hydrophobic effect plays the main role in the TPH adsorption. It is worth to mention that the residual pollutant concentration observed in the experiments performed with the functionalized fiber, is always close to the threshold concentration value imposed by the Italian Legislative Decree n. 152/2006 for the total hydrocarbons in wastewater (10 mg/L).

In order to gain a better insight on the kinetic and thermodynamic nature of the TPHs adsorption on the functionalized SB fibers, further batch experiments were carried out by changing the ratio

between the starting TPHs load (C_0) and the fiber mass (w) in the range from 20 to 240 (mg/L)/g. The results are shown in **Figure 10 (Fig. 10)**, where both the concentration (C_t) (**Fig. 10a**) and the removal efficiency (RE%) (**Fig. 10b**) have been reported as a function of the contact time.

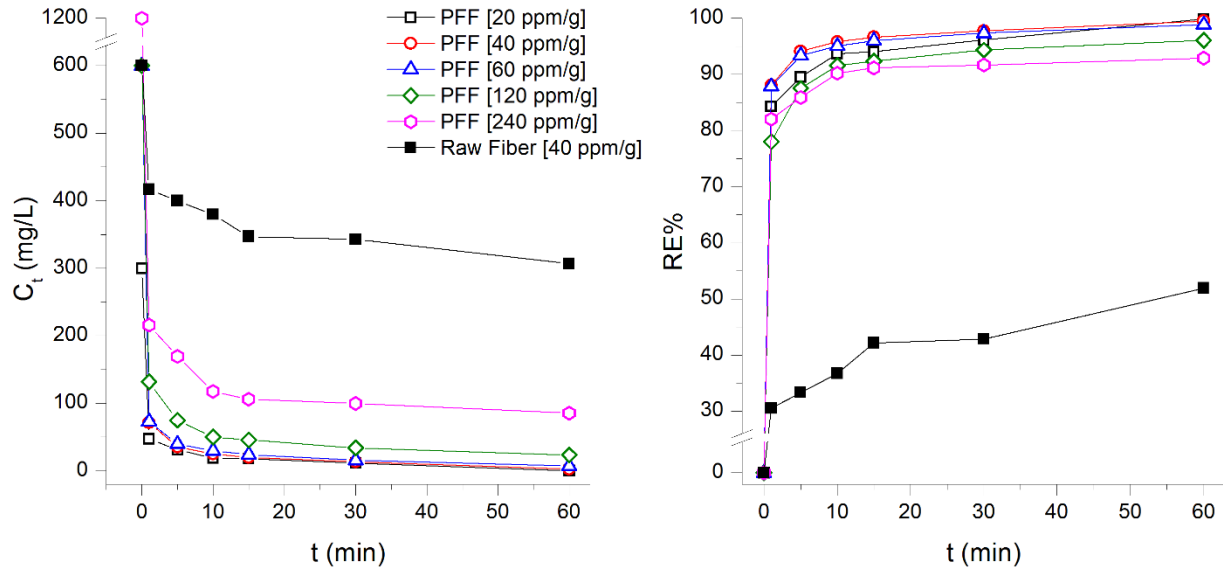


Figure 10. Raw and Functionalized SB fiber batch experiments: a) Total TPHs amount C_t and b) removal efficiency RE% as a function of the contact time.

The experimental data show that the removal efficiency of the grafted fibers, increases with the contact time up to a value of about 99%, while this parameter is close to 52% for the raw fibers [21].

The data, provided by each adsorption test, were modelled by a pseudo second order adsorption kinetic given by the equation (3) [36, 55, 56].

$$\frac{dq_t}{dt} = k_2(q_e - q_t)^2 \quad (3)$$

where, k_2 and q_e are the pseudo-second order rate constant and the equilibrium adsorption capacity, respectively. Equation (4), obtained after integration and linearization of equation (3), was used to estimate the parameters k_2 and q_e by fitting the t/q_t ratio as a function of time (**Table 4**):

$$\frac{t}{q_t} = \frac{1}{K_2 q_e^2} + \frac{1}{q_e} t \quad (4)$$

Figure 11 (Fig. 11) shows the fitting results, which are all characterized by a R^2 close to 1.

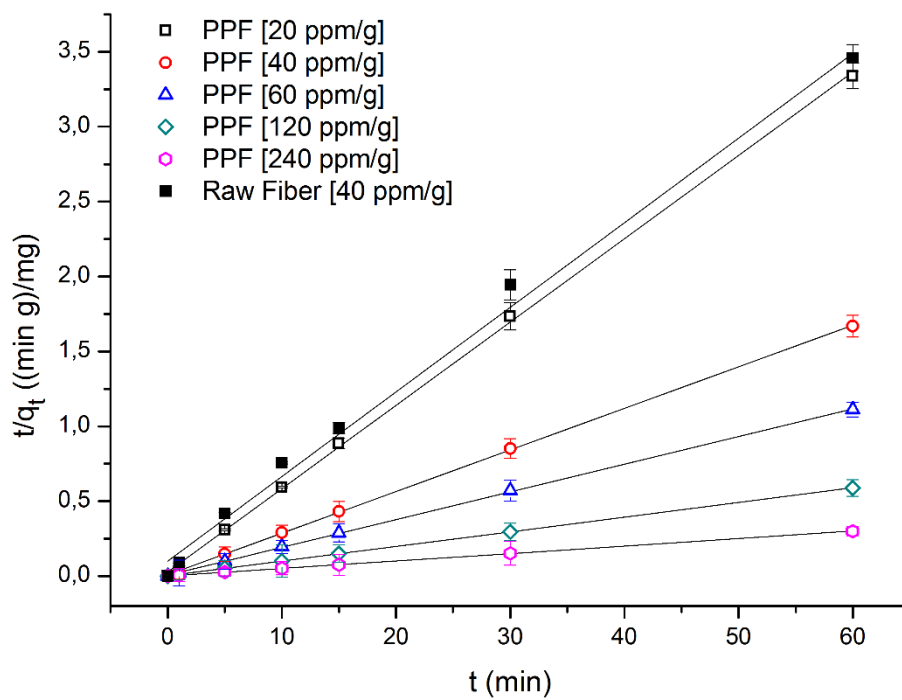


Fig. 11. Adsorption kinetic data fitted by the pseudo second order model.

The functionalized fibers show a faster adsorption kinetics than that of the raw fiber [21], with adsorption kinetic constants k_2 up to 10 times larger than that of the raw fiber. The better performance of the functionalized fibers concerns not only the kinetics aspects but also much greater values of the adsorption capacity.

Table 4

Kinetic values of plasma functionalized SB fibers at different C_0/w ratio.

C_0/w ((mg/L)/g)	k_2 (g/(mg min))	q_e (mg/g)	R^2
20	0.11 (0.05)	17.9 (0.1)	0.9995
40	0.10 (0.04)	35.8 (0.1)	0.9999
60	0.07 (0.02)	53.5 (0.2)	0.9999

120	0.024 (0.005)	104.2 (0.2)	0.9999
240	0.021 (0.006)	200.1 (0.8)	0.9999

The adsorption capacity of functionalized fibers increases with the pollutant equilibrium concentration, reaching a plateau value, representing the maximum adsorption capacity (q_m), according to the prevision of the Langmuir model, expressed by equation (5). This strongly indicates that the distribution of the adsorbed pollutants on the fiber surface can be considered a Langmuir monolayer [57, 58].

$$q_e = \frac{q_m K_L C_e}{1 + K_L C_e} \quad (5)$$

where, K_L is the Langmuir adsorption constant. The fit of data in terms of the Langmuir model, is shown in **Figure 12 (Fig. 12)**; the fit gives a quite good value of the R^2 (0.971).

Estimated value for K_L and q_m are (0.031 ± 0.009) L/g and (273 ± 32) mg/g respectively.

Such a high value of q_m indicates that the cellulose fibers surface fluorinated by cold plasma has very good pollutant uptake capacity, compared with that of other biobased sorbent matrices [59].

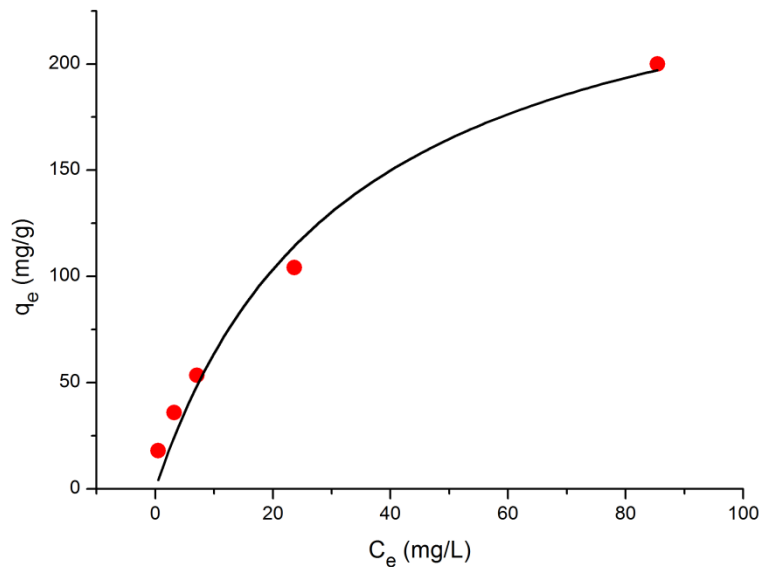


Fig. 12. Experimental adsorption isotherm and nonlinear curve fitting with the Langmuir model.

3.5. Fiber regeneration for multiple uses

One of the advantages of using surface adsorption mechanism to remove TPHs from polluted water could be, in principle, the possibility to regenerate the adsorbing filter, by washing out the adsorbed pollutant by means of an appropriate solvent. This possibility has been ascertained in the present case by studying the adsorption capacity of regenerated fluorine grafted fibers. Fibers which had already adsorbed 200.1 mg/g of TPH in a previous experiment have been washed for 1 minute with cyclohexane and then used in several adsorption/regeneration cycles to measure the progressive evolution of their Removal Efficiency. **Figure 13 (Fig. 13)** shows that the adsorption efficiency of the same functionalized fiber sample, after four applications and three regeneration processes, is retained at a value of 80%. It is probable that the removal efficiency slightly decreases because the washing procedure has not succeeded in removing all the hydrocarbons adsorbed by the fiber active sites.

This aspect requires further investigation in order to improve the regeneration stage by adopting a better washing protocol.

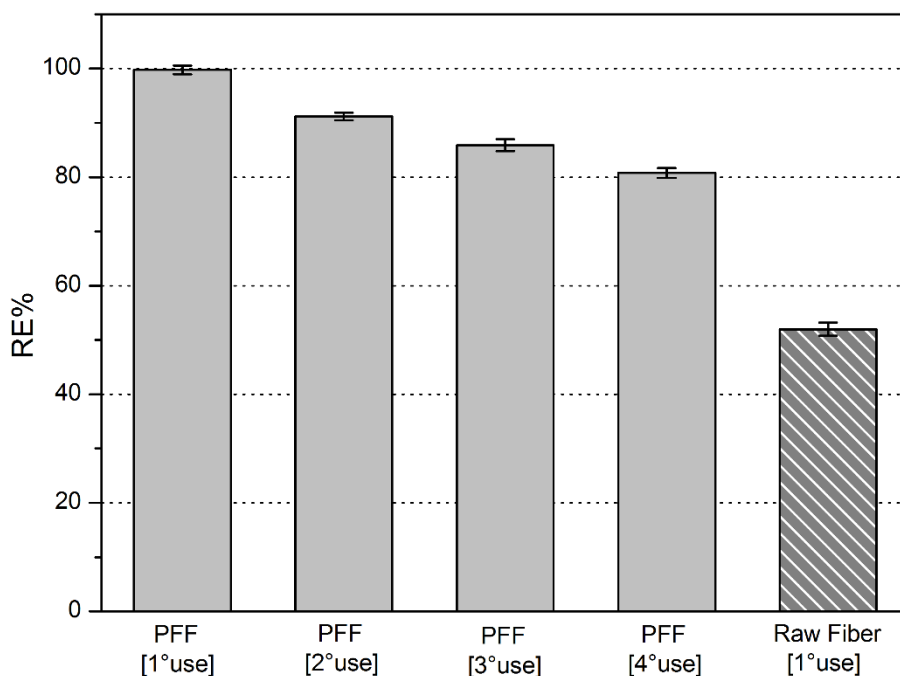


Fig. 13. Removal Efficiency as a function of the adsorption/regeneration cycles.

4. Conclusion

This work shows that fluorine grafted cellulose fibers are candidate to be very effective materials to remove hydrocarbons from polluted water. Their adsorption capacity is one of the highest ever reported in the literature. The fluorine grafting improves the hydrophobicity of the vegetable fibers in such a way that their water contact angle results to be higher than 160. As a consequence, the maximum adsorption capacity of the grafted fibers for hydrocarbons is equal to 0.273 g/g: a value which is almost thirty percent higher than that observed for analogous vegetable fibers functionalized with 4,4-MDI [21]. This important parameter, has been estimated by applying the Langmuir model which assumes that the adsorbate forms a monolayer coverage on the surface of the adsorbing material. The fluorine grafted fibers can be easily obtained by a low plasma process at a very low input power (10 W) and could be simply scaled for industrial purposes. The adsorption kinetics is fully explained in terms of a pseudo second order kinetic equation. A further advantage offered by the use of fluorine grafted vegetable fibers is that the exhausted material can be easily regenerated by washing it with an organic solvent as cyclohexane. One single washing step regenerates the adsorption capacity at a value which is comparable to the one of the fresh grafted fiber (90%).

Acknowledgments

The authors are grateful to the Ministero dell'Istruzione dell'Università e della Ricerca Italiano (MIUR) and the University of Calabria for supporting this project in the framework of the ex 60% budget grant. This research was also financially supported by Regione Puglia under grant no. 51 "Laboratorio pubblico di ricerca industrial dei plasmi, LIPP", within the Framework Programme Agreement APQ "Ricerca Scientifica", II atto integrativo - Reti di Laboratori Pubblici di Ricerca, and by MIUR

References

- [1] N. Das, P. Chandran, Microbial Degradation of Petroleum Hydrocarbon Contaminants: An Overview, *Biotechnol. Res. Int.* 2011 (2011) 1-13.
- [2] Agency for Toxic Substances and Disease Registry (ATSDR). 1999. Toxicological profile for total petroleum hydrocarbons (TPH). Atlanta, GA: U.S. Department of Health and Human Services, Public Health Service.
- [3] R. Akhbarizadeh, F. Moore, B. Keshavarzi, A. Moeinpour, Aliphatic and polycyclic aromatic hydrocarbons risk assessment in coastal water and sediments of Khark Island, SW Iran, *Mar. Pollut. Bull.* 108 (2016) 33-45.
- [4] R. Van der Oost, J. Beyer, N.P.E. Vermeulen, Fish bioaccumulation and biomarkers in environmental risk assessment: A review, *Environ. Toxicol. Pharmacol.* 13 (2003) 57-149.
- [5] G. Chen, P.A. White, The mutagenic hazards of aquatic sediments: a review, *Mutat. Res.* 567 (2-3) (2004) 151-225.
- [6] V. Dhananjayan, S. Muralidharan, V.R. Peter, Occurrence and distribution of polycyclic aromatic hydrocarbons in water and sediment collected along the Harbour Line, Mumbai, India, *Int. J. of Oceanogr.* (2012) 7-14.
- [7] D. Shen, B. Liu, Integrated urban and rural water affairs management reform in China: Affecting factors, *Phys. and Chem. of the Earth*, 33 (2008) 364–375.
- [8] N.A.A. Al-Shwafi, Total Petroleum Hydrocarbon Carcinogens in Commercial Fish in the Red Sea and Gulf of Aden – Yemen, *JKAU, Mar. Sci.* 19 (2008) 15-28.
- [9] A. Abdolali, W.S. Guo, H.H. Ngo, S.S. Chen, N.C. Nguyen, K.L. Tung, Typical lignocellulosic wastes and by-products for biosorption process in water and wastewater treatment: A critical review, *Bioresour. Technol.* 160 (2014) 57–66.
- [10] O. Lhotský, E. Krákorová, P. Mašín, R. Žebrák, T. Cajthaml, Pharmaceuticals, benzene, toluene and chlorobenzene removal from contaminated groundwater by combined UV/H₂O₂ photo-oxidation and aeration, *Water Res.* 120 (2017) 245-255.
- [11] F.J. Beltran, G. Ovejero, J.F. Garcia-Araya, J. Rivas, Oxidation of Polynuclear Aromatic Hydrocarbons in Water. 2. UV Radiation and Ozonation in the Presence of UV Radiation, *J. Ind. Eng. Chem. Res.* 34 (5) (1995) 1607–1615.
- [12] L. Joseph, J.R.V. Flora, Y.K. Park, M. Badawy, H. Saleh, Y. Yoon, Removal of natural organic matter from potential drinking water sources by combined coagulation and adsorption using carbon nanomaterials, *Sep. Purif. Technol.* 95 (2012) 64-72.
- [13] M. Farhadian, D. Duchez, C. Vachelard, C. Larroche, Monoaromatics removal from polluted water through bioreactors - A review, *Water Res.* 42 (6-7) (2008) 1325-134.

- [14] B. Doshi, M. Sillanpää, S. Kalliola, A review of bio-based materials for oil spill treatment. *Water Res.*, 135 (2018) 262-277.
- [15] G. Ersan, O.G. Apul, F. Perreault, T. Karanfil, Adsorption of organic contaminants by graphene nanosheets: A review, *Water Res.* 126 (2017) 385-398.
- [16] Y. Kalmykova, N. Moona, A.M. Strömvall, K. Björklund, Sorption and degradation of petroleum hydrocarbons, polycyclic aromatic hydrocarbons, alkylphenols, bisphenol A and phthalates in landfill leachate using sand, activated carbon and peat filters. *Water Res.* 56 (2014) 246-257.
- [17] W. Wu, K. Yang, W. Chen, W. Wang, B. Xing, Correlation and prediction of adsorption capacity and affinity of aromatic compounds on carbon nanotubes, *Water Res.* 88 (1) (2016) 492-501.
- [18] M.I. Rakowska, D. Kupryianchyk, M.P.J. Smit, A.A. Koelmans, H.H.M. Rijnaarts, Kinetics of hydrophobic organic contaminant extraction from sediment by granular activated carbon, *Water Res.* 51 (2014) 86-95.
- [19] R. Capasso, A. De Martino, polymeric and lignin, as humic acid-like sorbents from vegetable waste, for the potential remediation of waters contaminated with heavy metals, herbicides, or polycyclic aromatic hydrocarbons, *J. Agric. Food Chem.* 58 (19) (2010) 10283–10299.
- [20] R. Wahi, L.A. Chuah, T.S.Y. Choong, Z. Ngaini, M.M. Nourouzi, Oil removal from aqueous state by natural fibrous sorbent: an overview, *Sep. Purif. Technol.* 113 (2013) 51–63.
- [21] A. Tursi, A. Beneduci, F. Chidichimo, N. De Vietro, G. Chidichimo, Remediation of hydrocarbons polluted water by hydrophobic functionalized cellulose, *Chemosphere*, 201 (2018) 530-539.
- [22] G. Deschamps, H. Caruel, M.E. Borredon, C. Bonnin, C. Vignoles, Oil removal from water by selective sorption on hydrophobic cotton fibers. Study of sorption properties and comparison with other cotton fiber-based sorbents, *Environ. Sci. Technol.* 37 (5) (2003) 1013–1015.
- [23] N.S. El-Gendy, N.N. Hussein, Study on the effectiveness of spent waste sugarcane bagasse for adsorption of different petroleum hydrocarbons water pollutants: kinetic and equilibrium isotherm, *Desalin. Water Treat.* 57 (12) (2016) 5514-5528.
- [24] T. Paulauskienė, I. Jucikė, Aquatic oil spill cleanup using natural sorbents, *Environ. Sci. Pollut. Res.* 22 (2015) 14874–14881.
- [25] S.A. Younis, N.S. El-Gendy, I.E.A. Waleed, Y.M. Moustaf, Kinetic, isotherm, and thermodynamic studies of polycyclic aromatic hydrocarbons biosorption from petroleum refinery wastewater using spent waste biomass, *Desalin. Water Treat.* 56 (11) (2014) 3013-3023.

- [26] S.M. Yakout, A.A.M. Daifullah, Removal of selected polycyclic aromatic hydrocarbons from aqueous solution onto various adsorbent materials, *Desalin. Water Treat.* 51 (2013) 6711–6718.
- [27] Y. Kalmykova, N. Moona, A.M. Strömvall, K. Björklund, Sorption and degradation of petroleum hydrocarbons, polycyclic aromatic hydrocarbons, alkylphenols, bisphenol A and phthalates in landfill leachate using sand, activated carbon and peat filters, *Water Res.* 56 (2014) 246–257.
- [28] M.A. Hubbe, O.J. Rojas, M. Fingas, B.S. Gupta, Cellulosic substrates for removal of pollutants from aqueous systems: A review, *BioRes.* 8 (2013) 3038–3097.
- [29] P.G. Greco, G. La Greca, G. Larocca, S. Meduri, B. Sinopoli, D. Battaglia, A. Caseti, A. Aloise, G. Chidichimo, G. Danieli, Automatic System for fibers extraction from Brooms, 1st International Conference of IFToMM, Italy, Vicenza, 2016 December 1-2.
- [30] G. Danieli, P.F. Greco, G. La Greca, G. Larocca, G. Chidichimo, F. Chidichimo, A. Tursi, A. Beneduci, Italian Patent 102017000128798 (2017).
- [31] G. Chidichimo, A. Aloise, A. Beneduci, A. De Rango, G. Pingitore, F. Furgiuele, P. Valentino, Polyurethanes Reinforced With Spartium Junceum Fibers, *Polym. Compos.* 37 (10) (2016) 3042–3049.
- [32] T. Cerchiara, G. Chidichimo, G. Rondi, M. C. Gallucci, C. Gattuso, B. Luppi, F. Bigucci, Chemical Composition, morphology and tensile properties of spanish broom (*Spartium junceum* L.) fibres in comparison with flax (*Linum usitatissimum* L.), *Fibres Text. East. Eur.* 22 (2014) 25–28.
- [33] T. Cerchiara, G. Chidichimo, M. Ragusa, E. Belsito, A. Liguori, A. Arioli, Characterization and utilization of Spanish Broom (*Spartium junceum* L.) seed oil, *Ind. Crops Prod.* 31 (2) (2010) 423–426.
- [34] T. Cerchiara, G. Chidichimo, M. C. Gallucci, D. Vuono, Effects of extraction methods on the morphology and physico-chemical properties of Spanish Broom (*Spartium junceum* L.) fibres, *Fibres Text. East. Eur.* 18 (2) (2010) 13–16.
- [35] B. Gabriele, T. Cerchiara, G. Salerno, G. Chidichimo, M. V. Vetere, C. Alampi, M. C. Gallucci, C. Conidi, A. Cassano, A new physical-chemical process for the efficient production of cellulose fibers from Spanish broom (*Spartium junceum* L.), *Bioresour. Technol.* 101 (2009) 724–729.
- [36] F. Arias, A. Beneduci, F. Chidichimo, E. Furia, S. Straface, Study of the adsorption of mercury (II) on lignocellulosic materials under static and dynamic conditions, *Chemosphere* 180 (2017) 11–23.
- [37] R. d'Agostino, P. Favia, F. Fracassi, F. Illuzzi, The effect of power on the plasma assisted deposition of fluorinated monomer, *J. Polym. Sci. A Polym. Chem.* 28 (12) (1990) 3387–3402.

- [38] F. Fracassi, E. Occhiello, J.W. Coburn, Effect of ion bombardment on the plasma-assisted etching and deposition of plasma perfluoropolymer thin films, *J. Appl. Phys.* 62 (1987) 3980-3981.
- [39] F. Fanelli, F. Fracassi, R. d'Agostino, Fluorination of polymers by means of He/CF₄ fed atmospheric pressure glow dielectric barrier discharge, *Plasma Process. Polym.* 5 (2008) 424–432.
- [40] F. Fanelli, F. Fracassi, R. d'Agostino, Deposition and etching of fluorocarbon thin films in atmospheric pressure DBDs fed with Ar–CF₄–H₂ and Ar–CF₄–O₂ mixtures, *Surf. & Coat. Tech.* 204 (2010) 1779–1784.
- [41] L. d'Accolti, N. De Vietro, F. Fanelli, C. Fusco, A. Nacci, F. Fracassi, Heterogenization of ketone catalyst for epoxidation by low pressure plasma fluorination of silica gel supports, *Molecules* 22 (2017) 2099-2112.
- [42] N. De Vietro, C. Annese, L. d'Accolti, F. Fanelli, C. Fusco, F. Fracassi, A new synthetic approach to oxidation organocatalysts supported on Merrifield resin using plasma-enhanced chemical vapor deposition, *Appl. Catal., A* 470 (2014) 132– 139.
- [43] N. De Vietro, R. d'Agostino, F. Fracassi, Introduction of basic functionalities on the surface of granular adsorbers by low pressure plasma processes, *Plasma Process. Polym.* 9 (9) (2012) 911-918.
- [44] F. Fanelli, G. Di Renzo, F. Fracassi, R. d'Agostino, Recent advances in the atmospheric pressure PE-CVD of fluorocarbon films: influence of air and water vapour impurities, *Plasma Process. Polym.* 6 (2009) S503–S507.
- [45] A. Milella, R. Di Mundo, F. Palumbo, P. Favia, Plasma Nanostructuring of Polymers: Different Routes to Superhydrophobicity, *Plasma Process. Polym.* 6 (2009) 460–466.
- [46] F. Fanelli, A.M. Mastrangelo, N. De Vietro, F. Fracassi, Preparation of multifunctional superhydrophobic nanocomposite coatings by aerosol-assisted atmospheric cold plasma deposition, *Nanosci. Nanotech. Let.* 7(1) (2015) 84-88.
- [47] N. De Vietro, L. Belforte, V.G. Lambertini, F. Fracassi, Low pressure plasma modified polycarbonate: A transparent, low reflective and scratch resistant material for automotive applications, *Appl. Surf. Sci.* 307 (2014) 698-703.
- [48] N. De Vietro, A. Milella, F. Fracassi, Hydrophilic fluorocarbon coatings via plasma enhanced-chemical vapour co-deposition of acrylic acid and hexafluoropropylene oxide, *J. Mat. Sci. and Eng. with Adv. Tech.* 15 (2) (2017) 39-53.
- [49] P. Bosso, F. Fanelli, F. Fracassi, Deposition of water-stable coatings containing carboxylic acid groups by atmospheric pressure cold plasma jet, *Plasma Process. Polym.* 13 (2016) 217–226.
- [50] P. Favia, N. De Vietro, R. Di Mundo, F. Fracassi, R. d'Agostino, Tuning the acid/base surface character of carbonaceous materials by means of cold plasma treatments, *Plasma Process. Polym.* 3 (2006) 66–74.

- [51] F. Fracassi, R. d'Agostino, R. Lamendola, I. Mangieri, Dry etching of titanium nitride thin films in $\text{CF}_4\text{-O}_2$ plasmas, *J. Vac. Sci. Technol. A* 13 (1995) 335-342.
- [52] G. Beamson, D. Briggs, High Resolution XPS of Organic Polymers - The Scienta ESCA300 Database, Wiley & Sons, Chichester, England (1992).
- [53] C.D. Wagner, W.M. Riggs, L.E. Davis, J.F. Moulder, G.E. Muilenberg, *Handbook of X-Ray Photoelectron Spectroscopy*, Perkin-Elmer Corporation, Physical Electronics Division, Eden Prairie, Minn. 55344 (1979).
- [54] P. Favia, A. Milella, L. Iacobelli, Plasma pretreatments and treatments on polytetrafluoroethylene for reducing the hydrophobic recovery, *Plasma Process. Polym.*, R. d'Agostino, P. Favia, C. Oehr, M. R. Wertheimer Eds., WILEY-VCH Weinheim (2005).
- [55] Y.S. Ho, Review of second-order models for adsorption systems, *J. Hazard. Mater.* 136 (2006) 681–689.
- [56] K. V. Kumar, Linear and non-linear regression analysis for the sorption kinetics of methylene blue onto activated carbon, *J. Hazard. Mater. B*137 (2006) 1538–1544.
- [57] G. Limousin, J. P. Gaudet, L. Charlet, S. Szenknect, V. Barthes, M. Krimissa, Sorption isotherms: A review on physical bases, modeling and measurement, *Appl. Geochem.* 22 (2) (2007) 249–275.
- [58] P. Atkins, J. De Paula, *Physical Chemistry* (eighth edition), W. H. Freeman and Company: New York, 2006.
- [59] V. S. Tran, H. H. Ngo, W. Guo, J. Zhang, S. Liang, C. Ton-That, Typical low cost biosorbents for adsorptive removal of specific organic pollutants from water, *Bioresour. Technol.* 182 (2015) 353–363.

CHAPTER 8

Preliminary studies of the adsorption of mercury (II) in water by means of cellulosic fibers

1. Introduction

Mercury is a highly unusual natural element. At room temperature it is found in the form of a liquid with a higher density than that of lead. Mercury is classified into three forms: as inorganic salt in two ionic states: Hg^+ and Hg^{2+} , as a metallic element and organic compound in the form of methylmercury [1].

It is also a persistent bioaccumulative toxin (PBT). The World Health Organization has declared Hg as one of the most dangerous pollutants for human health [2].

Humans have extracted mercury until the end of the twentieth century to use it in the production of different and everyday products. Currently, 22% of the world's annual mercury consumption is used in electrical and electronic equipment, in numerous household products, dental fillings materials, industrial processes, in barometers, diffusion pumps, batteries and many other laboratory instruments [3]. Even today, it is used in medical equipment, data transmission equipment, telecommunications, mobile phones, mercury vapor lamps and advertising posters. The largest anthropogenic source of mercury in water is the emissions from coal-fired power plants. Approximately 6×10^3 tons of mercury are released each year into the environment as a direct result of human activities. The biggest polluters are power plants in Asia and Africa [4]. However, even the small-scale extraction of gold and silver contributes to the pollution of mercury. Other sources include inadequate disposal of mercury-containing products. Some mercury compounds have been used in agriculture, mainly as fungicides.

Although the use of mercury is reduced, high concentrations of the metal are still present in sediments related to its industrial applications, and is highly widespread in aquifer basins.

Adsorption through materials such as zeolites, activated carbon and ionic resins, represents effective alternative to conventional methods for the removal of Hg (II) in aqueous media [5, 6]. However, most of the proposed methods require expensive and energy-intensive initial pretreatments [7, 8]. Therefore, low-cost materials, to be used in an original way or with simple surface modifications to perform adsorbing action, have received great attention from scientists. Among the various natural materials produced for the different reclamation applications, the raw cellulose and the

functionalized cellulose used in the previous studies for the adsorption of petroleum hydrocarbons (TPHs) and ECDs, could represent a good adsorbent material towards the Hg (II) [9, 10].

In this regard, preliminary studies in batches with cellulosic fiber, extracted from the Spanish Broom, and cellulose fiber functionalized with fluorinated groups, through the low pressure plasma technique, have been carried out.

2. Materials and methods

SB fibers were extracted by treating the raw vegetable, alkaline solution for 20 minutes at 80 °C and further purification process by a digestion with a NaOH/water solution were performed.

The functionalization of SB cellulose fibers was performed by means of low plasma sputtering technique that allowed to obtain functionalized cellulose fiber with fluorinated groups on the surface (LP-CF). All chemical characterization and functionalization processes of the cellulosic fiber are described in the previous study concerning the removal of TPHs from water.

Spanish broom cellulose fibers (CF) and low plasma cellulose fiber (LP-CF), before their usage in the experimental tests, were first washed with distilled water and dried for two hours at 105 °C, to remove water content.

All the chemicals and reagents used for preparation and experiments had an analytical degree of purity. The aqueous solutions were prepared using ultrapure water (18.3 MΩ cm⁻¹, Ariosio- Human Corporation). The polluted solutions of Hg (II) were prepared using Hg(NO₃)₂ ·H₂O (Sigma-Aldrich, 99.99% purity).

HCl was added to the solutions in order to maintain a chloride ion concentration of 5x10⁻³ mol for the formation of HgCl₂ species. NaNO₃ was used at a concentration of 0.01 mol/L, to keep the ionic strength in solution constant. The solutions used for batch tests were prepared by serial dilutions of the Hg mother solution with a concentration of 1000 mg/L. Solutions of HNO₃ and NaOH concentrate, have been used to maintain the pH of work at 7.

Solutions were analyzed by Inductively Coupled Plasma - Mass Spectrometer (ICP/MS, iCapQ Thermofischer) to quantify the Hg(II) concentration. All samples were purified with 0.45 μm filter before ICP/MS analysis.

2.1 Adsorption experiments

In order to evaluate the Hg (II) adsorption capacity of cellulosic fiber (CF) and low plasma cellulosic fiber (LP-CF), batch experiments were conducted at different contact time: 1, 3, 7, 10, 15,

30, 45, 60, 120, 180 and 300 minutes, using the following conditions: 1) initial Hg(II) concentration = 100 mg/L, solution volume = 400 mL, mass of sorbent = 5.0 g.

Adsorption isotherms at 20 °C were obtained from similar batch experiments in which 0.5 g of biosorbent materials, were suspended in 50 mL of Hg (II) solutions with different concentrations in the range 1-180 mg/L. The suspensions, contained in 50 mL Falcons, were incubated in an oven at the set temperature for ten hours. During the incubation time, each suspension was subjected to agitations for 30 s every hour.

2.2 Adsorption properties of the cellulose fiber and low plasma functionalized cellulose fibers

Initially, the adsorption properties of the cellulosic fiber (CF) with those of the functionalized one (LP-CF) were compared, in order to evaluate if the functionalization process of the fiber surface improve the absorption capacity of the Hg (II) from polluted waters. In fact, the fluorinated groups that the LP-CF fiber exposes to the outside, could have a chelating capacity against Hg (II).

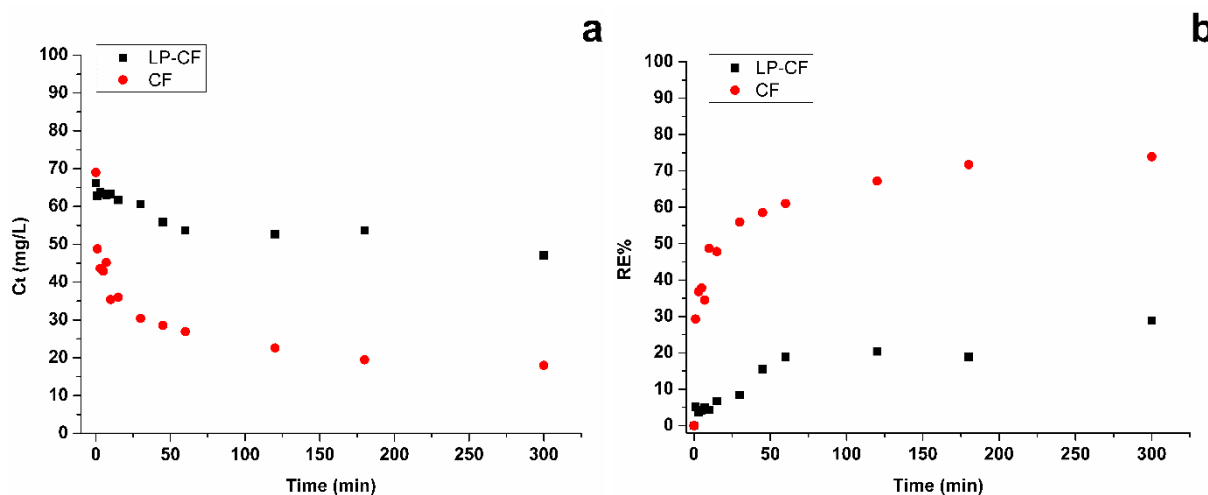


Figure 1. Hg(II) concentration (a) and removal efficiency (b) as a function of the contact time with the cellulose fiber (CF) and low plasma functionalized cellulose fiber (LP-CF).

Adsorption tests (Figure 2), show that in both cases, the concentration of Hg (II) begins to decrease after the addition of the fiber and tends to take a constant value after 45 minutes (Figure 2a). Adsorption trends are similar and there is a slight tendency to adsorb Hg (II), but the cellulose fiber (CF) allows a much higher removal efficiency than the functionalized one (LP-CF).

This is reflected in the opposite trend found for the removal efficiency (RE%), which increases with the contact time reaching a maximum value of about 74% and 29%, respectively for the CF and LP-CF (Figure 2b).

These results prove that the functionalization process did not allow to improve the adsorbing capacity of the cellulosic fiber for Hg(II), on the contrary it worsened the efficiency of removal. This behavior is probably caused by the high hydrophobicity of LP-CF. Moreover, the difference in adsorption is due to the absence of chelating groups on its surface, substituted by fluorine groups.

Since the adsorption capacity of LP-CF is lower than that of CF, further adsorption tests have been carried out to obtain only the CF isotherm, neglecting the use of LP-CF.

2.3 Adsorption isotherm

In order to better understand CF performance and the type of adsorption, experiments at different Hg (II) concentrations were conducted.

The Hg (II) maximum adsorption capacity (q_{\max}) of the cellulose fiber (CF) was assessed by the measurement of the adsorption isotherm for Hg (II) removal from water. The isotherm are shown in Figure 3, where the equilibrium adsorption capacity was plotted as a function of the equilibrium Hg (II) concentration.

The adsorption capacity shows a nonlinear increase with the equilibrium concentration and seems to approach a plateau value, corresponding to the maximum adsorption capacity (q_{\max}) of the fiber. The observed data can be modeled by a Langmuir model for which the surface of the adsorbing material is covered by a monolayer of the adsorbate [11, 12] (Limousin et al., 2007; Atkins et al., 2006).

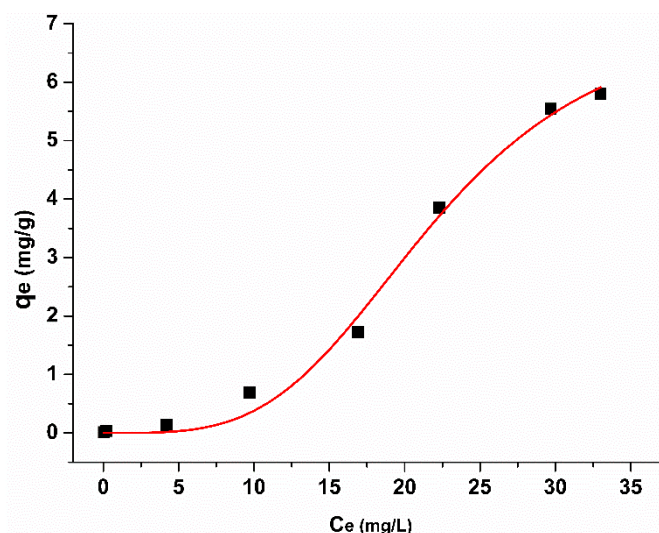


Figure 2. Hg (II) adsorption isotherm at 20 °C for the cellulose fiber and fitting with the Langmuir model (red continuous line).

The Langmuir model interprets the experimental results correctly, with an $R^2 = 0.9918$; the data relating to the fitting of the observed data show the following values: $K_L = (1.19 \pm 0.34)$ L/g and $q_{\max} = (7.25 \pm 0.99)$ mg/g.

The value of the maximum adsorption capacity is not very high when compared with other types of natural materials such as lignocellulosic fiber deriving from the same plant variety, that shown a maximum adsorption capacity close to 20 mg/g.

This experimental evidence is due to the limited presence of surface groups that could perform chelating action against Hg (II), while the lignocellulosic materials exhibit better performance, having on the surface carboxylic groups that are able to carry out the metal holding action.

Conclusion

This work reports the first application of SB cellulose fiber (CF) and SB functionalized cellulose fiber (LP-CF), extracted from Spanish broom, to remove Hg (II) pollution from water.

SB cellulose fiber (CF) showed a considerable adsorption capacity for Hg (II) heavy metal. Since it has been found that the adsorption capacity of the non-functionalized cellulose fiber to mercury is close to 74% of removal, for an aqueous system with an initial concentration of 70-100 mg/L of Hg (II), with a maximum adsorption capacity of 7.25 mg/g. The adsorption capacity of fluorinated SB fibers (low pressure plasma functionalized cellulose LP-CF) has been also studied to ascertain the chelation efficiency of fluorine groups with respect to this metal. However, this hypothesis was not found realistic, since the adsorption capacity of LP-CF is almost 29%.

References

- [1] Dopp E, Hartmann LM, Florea AM, Rettenmier AW, Hirner AV. Environmental distribution, analysis, and toxicity of organometal (loid) compounds. *Crit Rev Toxicol*. 2004;34:301–333
- [2] World Health Organ. (WHO)/UN Child. Fund (UNICEF). 2006. Meeting the MDG Drinking Water and Sanitation Target: The Urban and Rural Challenge of the Decade. Geneva, Switz./New York:WHO/UNICEF
- [3] Heavy Metals Toxicity and the Environment. Paul B Tchounwou, Clement G Yedjou, Anita K Patlolla, and Dwayne J Sutton. *EXS*. 2012 ; 101: 133–164. doi:10.1007/978-3-7643-8340-4_6.
- [4] U.S. Environmental Protection Agency (2007) Treatment Technologies for Mercury in Soil, Waste, and Water
- [5] U.S. EPA (Environmental Protection Agency) Mercury Study Report to Congress. 1997 Available at: <http://www.epa.gov/mercury/report.htm>.
- [6] Santhana A, Kumar K, Mniraj B, Puvvada S, Rajesh N. Microwave assisted preparation of glycidyl methacrylate grafted cellulose adsorbent for the effective adsorption of mercury from a coal fly ash sample. 2013 *Journal of Environmental Chemical Engineering* 1(4)
- [7] Mercury Contaminated Sites: A Review of Remedial Solutions. Jennifer Hinton, Marcello Veiga. *Proc. NIMD (National Institute for Minamata Disease) Forum 2001*. Mar. 19-20, 2001, Minamata, Japan
- [8] Tran, V. S., Ngo, H. H., Guo, W., Zhang, J., Liang, S., Ton-That, C., (2015). Typical low cost biosorbents for adsorptive removal of specific organic pollutants from water. *Bioresource Technology*, 182, 353–363.
- [9] Arias, F., Beneduci, A., Chidichimo, F., Furia, E., Straface, S., 2017. Study of the adsorption of mercury (II) on lignocellulosic materials under static and dynamic conditions. *Chemosphere* 180, 11-23.
- [10] Tursi A, Beneduci A, Chidichimo F, De Vietro N, Chidichimo G. Remediation of hydrocarbons polluted water by hydrophobic functionalized cellulose. *Chemosphere*, 2018; 201:530-539.
- [11] Limousin, G., Gaudet, J.-P., Charlet, L., Szenknect, S., Barthe`s, V., Krimissa, M., (2007). Sorption isotherms: A review on physical bases, modeling and measurement, *Appl. Geochem.*, 22, 249–275.
- [12] Atkins, P., De Paula, J., (2006). *Physical Chemistry*, Eighth ed., W. H. Freeman and Company, New York, 918-922.

CHAPTER 9

Photocatalytic inactivation of *Escherichia coli* bacteria in water using low pressure plasma deposited TiO₂ cellulose fabric

A. Tursi^{a,e}, N. De Vietro^b, A. Beneduci^a, F. Chidichimo^c, F. Dalena^a, F. Fracassi^d, E. Chatzisymeon^e, G. Chidichimo^{a*}

^aDepartment of Chemistry and Chemical Technologies, University of Calabria, Via P. Bucci, Cubo 15D, 87036 Arcavacata di Rende (Cs), Italy;

^bInstitute of Nanotechnology (Nanotec), National Research Council (CNR), c/o Department of Chemistry, University of Bari "Aldo Moro", Via Orabona 4, 70126 Bari, Italy;

^cDepartment of Environment and Chemical Engineering, University of Calabria, Via P. Bucci, Cubo 41B, 87036 Arcavacata di Rende (CS), Italy.

^dDepartment of Chemistry, University of Bari "Aldo Moro", Via Orabona 4, 70126 Bari, Italy;

^eSchool of Engineering, Institute for Infrastructure and Environment, University of Edinburgh, The King's Buildings, Edinburgh EH9 3JL, United Kingdom

Keywords: *Escherichia coli*; titania catalyst; Low pressure plasma sputtering; Titanium dioxide; water disinfection; advanced oxidation.

ABSTRACT

Fabrics obtained from cellulose spinning, extracted from Spanish broom, were coated with TiO₂ film, through the low pressure plasma sputtering technique, in order to get antibacterial activity. The obtained fabrics were used for the photocatalytic degradation of *Escherichia coli*, by irradiation with UV-light emitting diodes (UV-LED), in a batch photocatalytic reactor. Before and after functionalization treatments, cellulosic substrates were chemically characterized by X-ray photoelectron spectroscopy (XPS) analyses. Water Contact Angle (WCA) measurements allowed to obtain information about the hydrophilicity of the materials, while their antibacterial efficiency was determined at several initial concentrations (from 10³ up to 10⁸ CFU/mL) of bacteria in distilled, bottled water and synthetic wastewater. It was found that photocatalytic reactions were capable of achieving up to 100% bacterial inactivation in 1 h of treatment, following a pseudo-first order kinetic model. No bacterial regrowth was observed after photocatalytic treatments in almost all experimental conditions. In contrast, during photolytic treatment (i.e. in the absence of the TiO₂ coated fabrics) bacteria recovered their initial concentration after 3 h in the dark. Finally, the reusability of the plasma modified fibers to inactivate bacteria was studied.

1. INTRODUCTION

Safe drinking water represents the greatest need for humanity. Currently, one of the major problems that must be solved, especially in underdeveloped countries, is the decontamination of water from faecal coliform bacteria ¹. Faecal coliform bacteria are a group of bacteria that comes from faecal droppings of humans, livestock and wildlife. The most common member of this category is *Escherichia coli*.

The presence of *E. coli* is used as an indicator to monitor the possible presence of other more harmful microbes, such as *Giardia*, *Cryptosporidium* and *Shigella* ².

Many methods have been used for the inactivation of microbial pollutants, such as chlorination, ozone, filtration and photocatalytic oxidation ³. Chlorination is the most common method for the chemical disinfection of water but it also leads to the formation of carcinogenic by-products, such as trihalomethanes (THM) ^{4,5}. Therefore, it is necessary to resort to more advanced technological methods for water disinfection, overcoming the current methods of chlorination ³.

Conventional disinfection using UV mercury vapor lamps is an effective water remediation technology. But in the last few decades, UV light emitting diodes (UV-LEDs) have played an important role as an alternative to mercury vapor lamps, due to the absence of mercury, higher strength and flexibility, compact dimensions and large amounts of energy transmitted with less thermal energy production as waste. Furthermore, the UV-LEDs technology allows to adjust the working wavelengths and does not need heating periods. Nelson et al. ⁶ has demonstrated that the LEDs emitting wavelengths between 200 and 290 nm can be used for water treatment to reduce pathogens in water without formation of disinfection by-products (DBPs). In particular, experimental tests, with UV-LEDs radiation at 265 nm in ultra-pure water for 50 min exposure time, have showed a 1-2 log reduction of *E. coli* in water ⁷.

Instead, Hamamoto et al. ⁸ applied UV-A radiation with 365 nm UVA-LEDs on *E. coli* and obtained UV dose responses of 55 mJ/cm² per log inactivation.

Xiong and Hu (2013) introduced a photolytic disinfection system using 365 nm UV-LEDs, with a high UV dose response of 229 mJ/cm² per log *E. coli* inactivation, showing that 365 nm UVA-LEDs alone are not effective for bacterial inactivation ⁹.

For this reason, the use of photocatalysts is increasingly studied to improve the capacity of bacterial inactivation at different wavelengths and decrease the application/exposure times, but above all to use wavelengths closer to the visible region (such as UV-A), which require less UV light intensity and are potentially less damaging to the surrounding environment.

TiO₂, WO₃, CdS, SnO₂, ZnO₂, Fe₂O₃ can be used as photocatalysts but oxidation processes need high potentials in order to have the valence band location in a sufficiently positive state to allow the oxidation of organic compounds, such as TiO₂ and CdS^{10,11}. In these two cases, in fact, the photogenerated holes have the ability to generate ·OH radicals with sufficient energy to trigger the oxidation reactions, but CdS does not present good stability in aqueous solutions. In this regard, several studies have focused on the photocatalytic advantages of titanium oxide against bacteria¹². In recent years, several studies have shown the use of superficially modified materials with TiO₂ to increase the antibacterial activity and for a greater stability of the catalyst. Janus et al.¹³ studied the photocatalytic disinfection of *E. coli* by carbon modified TiO₂ in a pressure reactor with the use of five alcohols at 120 °C for 4 h, for modification purposes. Wu et al.¹⁴ found titanium dioxide nanoparticles co-doped with nitrogen and silver as visible light driven photocatalyst for bactericidal activity against *E. coli*. Inactivation of bacteria by nanocarbon/TiO₂ composite photocatalyst¹⁵ and titanium dioxide-coated carbon nanotubes^{16,17} were also investigated in the last decades. Dagan and Tomkiewicz¹⁸ have introduced a new method involving the use of TiO₂ aerogels for the photo-assisted oxidation of organic compounds. Sethi et al.¹⁹ have performed vanadium modified titanium (V₂O₅/TiO₂) photocatalysts, prepared by incipient wet impregnation method, using aqueous ammonium metavanadate and anatase titania for the photocatalytic destruction of *E. coli* in water.

Based on these considerations, this work presents the first application of photocatalytic bacterial inactivation using TiO₂ coated cellulose spinning, extracted from Spanish Broom (SB)²⁰. This spontaneous vegetable widely spread onto the planet, offers the possibility to easily extract either the lignocellulosic or the cellulose fibers. It has been recently shown that these fibers can be used either in the pristine form to remove inorganic contaminants from water²¹ or, after surface functionalization, organic pollutants from water by adsorption processes^{22,23}. Here we have explored the possibility to use a low pressure plasma sputtering technique for the deposition of TiO₂ on Spanish Broom cellulose surface. Generally, non-equilibrium plasma processes, both at low or atmospheric pressure, are eco-friendly, versatile and, thanks to their low temperature (near to room), allow the modification of the uppermost layers of flat substrates²⁴, fibers or granules²⁵⁻²⁹, without changing their bulk properties. Specifically, we have previously demonstrated that, feeding the discharger with metal-based precursors, anti-microbial or photocatalytic coatings can be obtained^{30,31}.

In this work several deposition processes were optimized with the aim of obtaining the highest TiO₂ mass fraction, without deterioration of the fabric substrate and needless time consumption, using surface and morphology characterization experimental results.

Before and after the plasma treatment, in fact, all fibers were analysed by X-ray photoelectron spectroscopy (XPS), for the chemical characterization of the fiber surface. Moreover, water contact angle (WCA) measurements have been performed to evaluate the hydrophilicity of plasma treated material.

The obtained fabrics were tested for the photocatalytic degradation of *E. coli*, by irradiation with 356 nm UV-LEDs in a batch photocatalytic reactor.

2. MATERIALS AND METHODS

2.1. *SB fibers extraction process and fabric preparation*

SB fibers were extracted by treating the raw vegetable, grown into the botanic garden of the University of Calabria, with a 5% w/w NaOH water solution for 20 minutes at 80 °C and, subsequently, purified by a 30 min digestion at 80 °C in a 0.5% w/w NaOH water solution, to remove lignin impurities²⁰. SB cellulose fiber obtained from the extraction process described above, followed a spinning process that began with the sorting and washing of the fiber. Subsequently, the fiber is opened and struck to remove residual dust and impurities. The fibers were arranged in a parallel manner and then wrapped on themselves. Using machines equipped with combs, the fibers were combed and prepared for "combed spinning", to obtain tops. The tops were, therefore, twisted, putting two or more threads together. The twisted yarn has consequently a greater resistance. Finally, the yarn was wound in reels and subsequently worked to obtain a fabric.

2.2 *Preparation of antimicrobial cellulosic SB fabric through plasma sputtering system*

Sputtering processes were performed on a 5 cm disk of SB fabric, without any pre-treatment, in the lab scale reactor schematized in **Figure 1**.

The experimental apparatus utilized for the deposition of the TiO₂ coatings (**Figure 1**) consists of a cylindrical low pressure plasma reactor with an asymmetric electrode configuration (70 mm inter-electrode distance), equipped by a turbomolecular-rotary pumping system. The pressure is measured and controlled in the 0 ÷ 133.32 Pa range with a baratron gauge and an automatic throttle valve. The lower stainless steel circular electrode (diameter, 190 mm), on which the SB fabrics (the substrate) were positioned during the deposition process, was thermally controlled, at 25 °C, by means of a circulating water and glycol mixture, and grounded. The upper electrode, equipped with a grounded shutter, on the other hand, is a circular balanced magnetron sputtering (MS) source (diameter, 76.2 mm), powered with 13.56 MHz radio frequency (RF) power supplies with automatic matching network units.

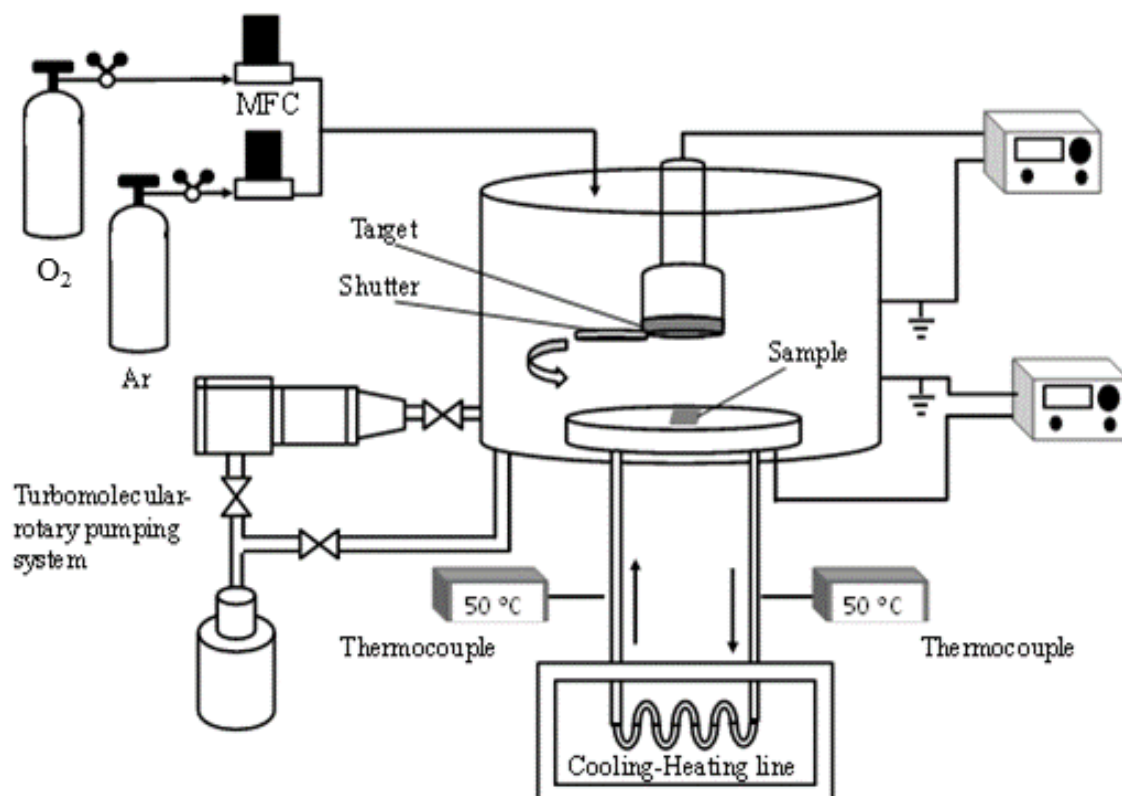


Figure 1. Scheme of the low pressure plasma reactor employed for the sputtering processes.

The magnetron source was utilized to deposit TiO₂ coatings, feeding the discharges with different argon (purity 99.999 %; *Airliquid*) and oxygen (purity 99.998 %; *Airliquid*) mixtures at 100 W of input power. Ti (purity 99.999 %; *Aja International, Inc.*) was utilized as metal target. The gas flow rate is controlled in range 1÷200 sccm by means of mass flow controllers (*MKS Instruments, Inc.*) and the feed gases were admitted in the reactor through a ring encompassing the upper electrode.

Before the TiO₂ films deposition, a sputter cleaning process with Ar (8 sccm) at 1.33 Pa for 15 min was performed, by igniting a glow discharge at 100 W between the upper magnetron electrode and the grounded shutter plate, in order to clean the metal target. At the end of this cleaning process, the reactor was fed with the selected gas mixture, the shutter was open and the substrates were coated with the TiO₂ coatings powering the discharge at 100 W. The optimized deposition conditions are resumed in **Table 1**.

It is important to stress that the input power value was set at 100 W because, under this value a too slow deposition rate (estimated by thickness measurements realized employing a *Tenchor α*-step profilometer) was registered, while over 100 W a deterioration of the SB fabric was observed.

Table 1. Low pressure plasma sputtering processes experimental conditions.

Fabric type	Gas feed mixture	Pressure	Input power	Deposition time	Film thickness	Deposition rate (Rd)
A	Ar 4 sccm; O ₂ 4 sccm	300 Pa	100 W	180 min	93±10nm	0.52±0.05 nm/min.
B	Ar 6 sccm; O ₂ 2 sccm	300 Pa	100 W	180 min	81±8nm	0.45±0.04 nm/min.
C	Ar 7 sccm; O ₂ 1 sccm	300 Pa	100 W	180 min	65±8nm	0.36±0.04 nm/min.

2.3 Chemical characterization of the SB fabric

Before and after deposition processes, SB cellulosic fabrics were chemically and morphologically characterized by XPS measurements.

XPS analyses were performed utilizing a Scanning XPS Microprobe (PHI 5000 Versa Probe II, *Physical Electronics*) equipped with a monochromatic Al K α X-ray source (1486.6 eV), operated at 15 kV and 24.8 W, with a spot of 100 μ m. Survey (0–1300 eV) and high resolution spectra (C1s, O1s and Ti2p) were recorded in FAT (fixed analyser transmission) mode at a pass energy of 117.40 and 29.35 eV, respectively. The analyser energy resolution, evaluated on the FWHM (Full Width at half maximum) Ag 3d_{5/2} photoemission line, was 0.7 eV for a pass energy of 29.35 eV. Surface charging was compensated using a dual beam charge neutralization, with a flux of low energy electrons (~1 eV) combined with very low energy positive Ar⁺ ions (10 eV). The hydrocarbon component of C1s spectrum was used as internal standard for charging correction and it was fixed at 285.0 eV³². All spectra were collected at an angle of 45° with respect to the sample surface. Atomic concentrations were determined from the high resolution spectra after subtracting a Shirley-type background, using the Scofield sensitivity factors set in the MultiPak software. For each sample, quantitative data were averaged on 9 measurements performed on three different samples. Best-fitting of the C1s signal was carried out with MultiPak (*Physical Electronics*) data processing software. High resolution spectra were fitted with mixed Gaussian-Lorentzian peaks after a Shirley background subtraction.

2.4 Study of the surface wettability

The hydrophilic behaviour of the SB fabrics, before and after plasma deposition process, was evaluated by static WCA measurements, performed with a manual goniometer (*Ramé.Hart, Inc.*), utilizing 2 μL bi-distilled water drops. The reported WCA values were averaged over 5 measurements on each fabric sample.

2.5 Photocatalytic experiments for water purification

The strain of *E. coli* ATCC 23716 (American Type Culture Collection, Rockville, MD, USA) was used. The lyophilized *E. coli* was prepared by culturing bacteria in the Brilliance *E. coli*/coliform Selective Agar (Oxoid CM1046) medium for 18-24 h at 37 °C.

Growth medium was prepared by suspending 28.1 g of Brilliance *E. coli*/coliform Selective Agar (Oxoid) in 1 L of distilled water. The medium was gently brought to a boil, to dissolve completely and autoclaved for 15 min at 121 °C. Subsequently, the medium was poured into sterile Petri dishes. Photocatalytic inactivation experiments of *E. coli* were conducted in glass beakers of 1.0 dm³, used as batch photoreactor at lab-scale, mixing by means of a plate orbital shaker, was applied during disinfection process with UV-LED lamp placed on the top of batch reactor. For LED driven photocatalysis, an indium gallium nitride (InGaN) UVA emitter ($\lambda = 365 \text{ nm}$; LZ4-00U600, LED Engin, USA) was employed and mounted onto a heat sink to prevent radiant flux decrease due to temperature rise. The LED assembly was placed directly above the reactor and a quartz protective plate was placed between them. TiO₂ fabric was immersed in 50 mL of *E. coli* solution, at the bottom of the beaker. During the experiments, samples were taken at time intervals to determine the concentration of *E. coli* in the water. The detection and quantification of bacteria, in the processing water, was performed following a standard serial dilution procedure in sterile 0.8 % (w/v %) NaCl aqueous solution and 200 μL of each dilution (including neat sample) were pipetted and spread onto Brilliance *E. coli*/Coliform Agar plates (agar plates were pre-warmed to room temperature (20 ± 5 °C) to prevent any temperature shock to the bacterial cells). Bacterial suspensions were then spread over the surface of the plate using a sterile, disposable, plastic L-shaped spreader. Agar plates were incubated at 37 °C for 18–24 h before colonies were counted. All experiments were replicated at least three times. *E. coli* colonies appeared with purple colour.

Water disinfection experiments were carried out at different initial bacterial concentrations ($10^3 - 10^8$ CFU/mL) and in different water matrices: distilled (DW), bottled (BW), 0.8% NaCl salt water (SW) and polluted water with humic acid (HA) ranging from 1 to 5 mg/L.

2.6 Photoreactivation experiments

Bacteria have the ability to repair their damaged DNA, even after their UV inactivation, through mechanisms that can occur either in the absence (dark condition) or in the presence (photo-reactivation) of light³³.

Therefore, reactivation experiments of *E. coli* in treated waters were carried out in the dark and under natural light. In order to evaluate the photoreactivation capacity, 50 mL of the treated water was transferred, after each experimental run, into a sterile conical flask and kept in continuous agitation for 3 and 24 h, under natural light conditions and in dark conditions. Samples were analysed, in terms of *E. coli* viability, with the same procedures adopted for inactivation experiments³⁴.

3. RESULTS AND DISCUSSION

3.1. Chemical and morphological characterization of the TiO₂ plasma coated SB fabrics

Survey spectra of pristine and plasma-treated SB fabric are compared in **Figure 2**. The surface of untreated SB fibers is composed by, approximately, 26 at. % of oxygen, 66 at. % of carbon, 7 at. % of silicon and 1 at. % of calcium. The spectrum of the plasma-treated SB fabric is characterized by the presence of titanium (ca. 16 at. %), oxygen (50 at. %), carbon (33 at. %) and calcium (1 at. %). The presence of calcium at the surface of the SB fabric most likely has to be ascribed to an incomplete surface coverage of the fabric by the deposited TiO_x film. In order to determine the exact film stoichiometry, i.e. the O/Ti ratio, a specific curve-fit procedure has been applied to the O1s spectra, to take into account that not all the oxygen is bound to titanium.

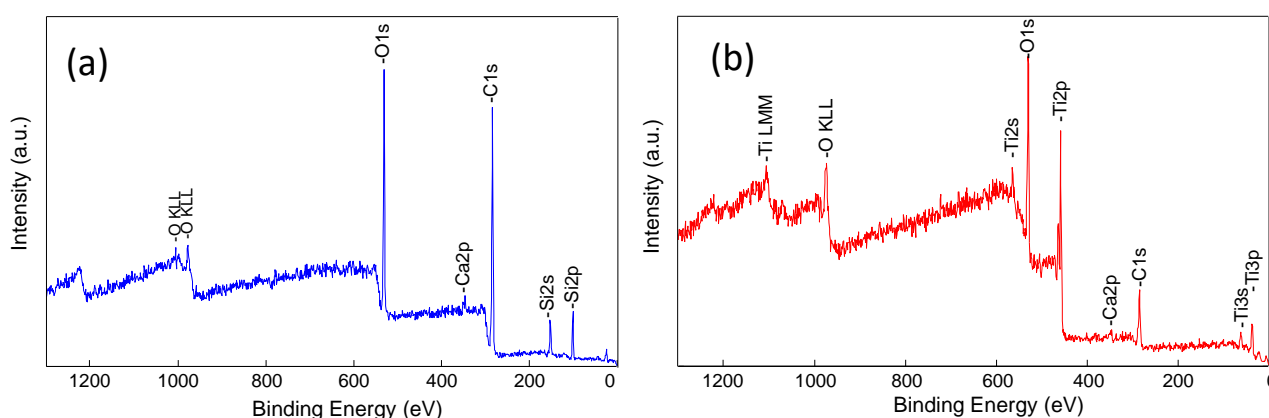


Figure 2. (a) XPS survey spectra of pristine SB fabric and (b) plasma-treated SB fabric (sample A in table 1).

Figure 3a shows a representative curve-fitting applied to sample A (table 1). The spectrum consists of three peaks. The one set at 529.9 ± 0.1 eV is assigned to titanium oxide (TiO_x), the second peak at 531.2 ± 0.1 eV is due to titanium hydroxides, defective oxides and organic oxygen, and the third one, at 532.3 ± 0.1 eV, is always due to oxygen bonded in organic functional groups^{35,36}. The film stoichiometry is then calculated from the ratio of the at. % of the peak at 529.9 eV and the at. % of Ti. For all samples analysed the ratio O/Ti was found to be nearly 2. This is further confirmed by the high resolution spectra of Ti2p, shown in **Figure 3b**. For all the samples the $\text{Ti}2p_{3/2}$ is set at 458.6 ± 0.1 eV, and the $\text{Ti}2p_{1/2} - \text{Ti}2p_{3/2}$ splitting is 5.7 ± 0.1 eV, both values typical of TiO_2 ³⁶. Furthermore, the spectra of Figure 3b have identical shape and broadening confirming the same chemical environment for all the analysed samples.

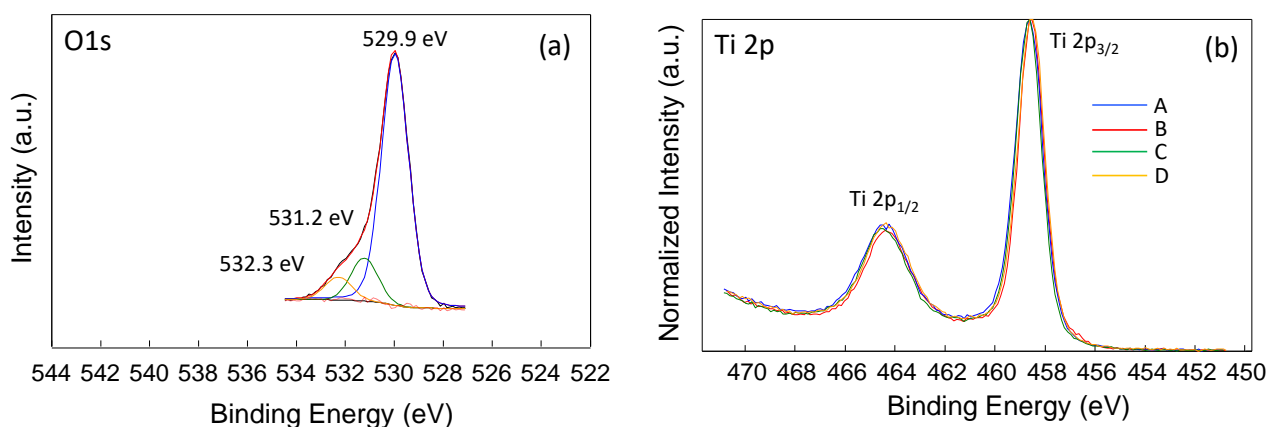


Figure 3. (a) XPS high resolution O1s spectrum for sample A and (b) Ti2p spectra for samples A-D.

In conclusion, XPS analyses showed that in all cases the plasma treatment led to the deposition of a thin TiO_2 film, even if, the coverage of the fabric surface was not complete and, presumably, directly proportional to the oxygen content in the plasma feed gas. Observing the data reported in table 1, in fact, it is evident that the sample A was covered with the highest thickness TiO_2 layer. Sample C, on the contrary, showed the thinnest coating.

WCA measurements, performed before and after plasma TiO_2 deposition process, showed an evident increasing of the hydrophilic surface character of the SB fabric, following the plasma treatment: the WCA value, in fact, passed from $75^\circ \pm 3^\circ$ (raw fabric) to $\sim 0^\circ$ (plasma TiO_2 coated sample), probably due to the grafting of oxygenated functionalities promoted by the plasma oxygen-feed glow discharges, as showed by XPS experimental results, independently by the deposition experimental conditions.

Table 2. WCA values measured on untreated and plasma treated SB fabric.

<i>SB fabric</i>	WCA (°)
Untreated	75±2
Plasma Treated	3±2

3.2 Testing the different fabric treatment for Bacterial inactivation

Bacterial degradation tests were initially carried out by maintaining the same experimental conditions, in order to identify the best grafted fabric among those prepared under different plasma conditions. The initial concentration of *E. coli* in distilled water was 10^4 CFU/mL. To evaluate the photolytic capacity of the UV-LEDs system, tests were also carried out in the absence of any antimicrobial fabric. **Figure 4** shows the kinetics of photocatalytic bacterial inactivation as a function of the UV exposure time, obtained in the presence of several TiO₂-deposited cellulose fabrics and compares them with that obtained by UV exposure only. It can be seen that UV exposure alone induces bacterial inactivation leading to a 49% reduction of the bacterial population after 90 min. However, it is a very slow process compared to the inactivation kinetics observed when the fabric photocatalyst is placed into the reactor. In this case, the 50% bacterial inactivation is achieved after about 10 min of UV irradiation, while 100% inactivation occurs after about 30-60 min, depending on the used fabric.

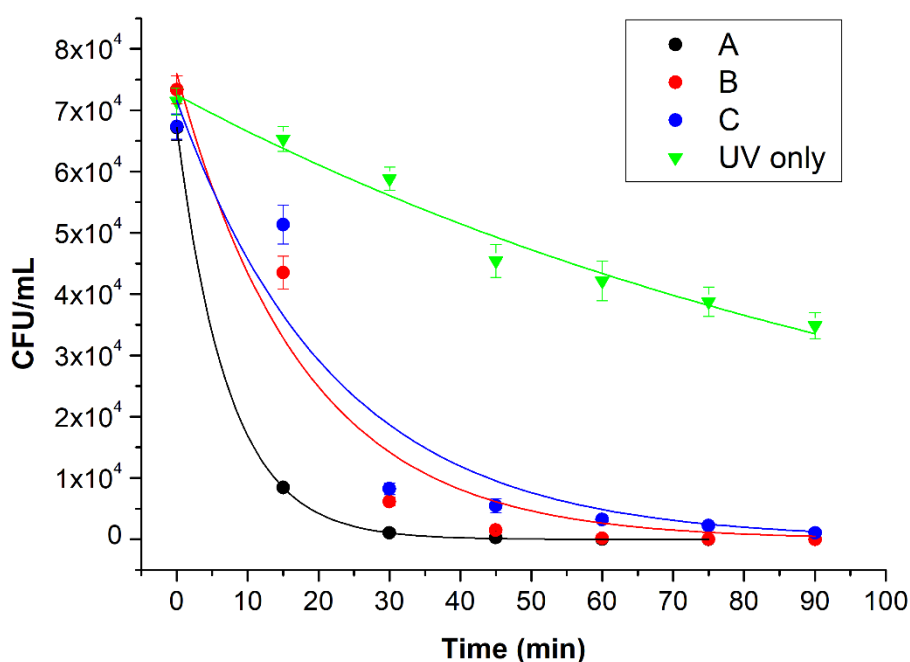


Figure 4. Kinetics of photocatalytic inactivation by different TiO₂-cellulose fabrics at a UV-LED wavelength exposure of 365 nm. Lines are the best fit of the data by a first order law.

Indeed, **Figure 4** shows that the photocatalytic inactivation kinetics significantly depends on the fabric processing (see Table 1) and increases in the following order: fabric A > fabric B ≥ fabric C. As described in the previous section, the above trend corresponds to the increase of the thickness, and probably to a more homogeneous coating, of TiO₂ film deposited on the fabric surface, passing from deposition condition A to the deposition condition C. The kinetics of *E. coli* inactivation follows a first order reaction with respect to the concentration of viable cells in the reactor as expressed by equation (1):

$$\ln \frac{N_t}{N_0} = -kt \quad (1)$$

where, N_t is the residual microbial load at a given time (CFU/mL), N_0 is the initial microbial load (CFU/mL), k is the inactivation rate constant (m²/kJ or min), t is the UV treatment time.

Figure 4 reports the fitting lines for each set of kinetic data. The fitting results, reported in **Table 3**, show that the rate constant obtained with fabric A is from 2.5 up to 3 times higher than the one observed with fabrics B and C, respectively, and more than one order of magnitude larger than that of the photolytic treatment.

Table 3. First order kinetic rate constant of the photocatalytic bactericidal activity of TiO₂-coated fabrics in various water matrices compared to photolytic treatment

Water matrix	Experiment	N ₀ (× 10 ⁴ CFU/mL)	k (s ⁻¹)	R ²
DW	photolysis	7.2	0.0090 (0.0006)	0.970
	Fabric C	7.2	0.045 (0.009)	0.903
	Fabric B	7.6	0.055 (0.009)	0.949
		6.7	0.138 (0.001)	0.99996
		4670	0.096 (0.007)	0.9939
		0.66	0.115 (0.006)	0.99815
BW	Fabric A	7.1	0.111 (0.001)	0.99989
SW		7.4	0.088 (0.002)	0.99943
1 mg/L HA			0.067 (0.002)	0.99827

2 mg/L HA	0.053 (0.003)	0.9944
5 mg/L HA	0.041 (0.003)	0.98491

Figure 5, on the other hand, puts in evidence that the first order photocatalytic inactivation mechanism holds in a wide range of initial bacterial concentration ($10^3 - 10^8$ CFU/mL), since the rate constant does not significantly change as a function of N_0 , as expected from a first order kinetic reaction (see Table 3).

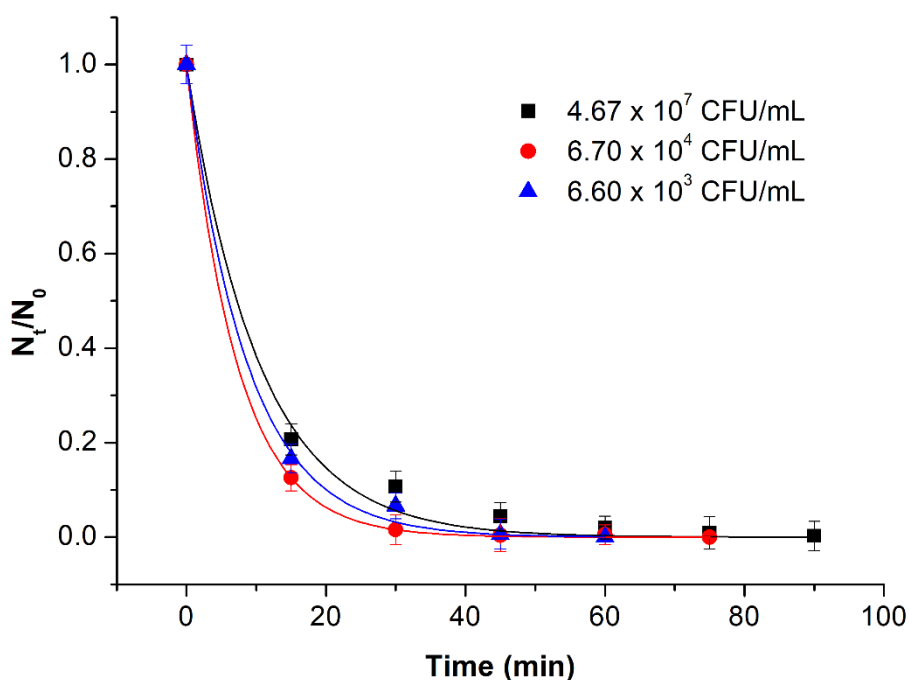


Figure 5. Effect of initial bacterial concentration.

3.3 Effect of water matrix

The photocatalytic bacterial inactivation effect has been further evaluated in different water matrices other than in distilled water (DW): bottled water (BW), 0.8% NaCl salt water (SW) and water spiked with various concentrations of humic acid (HA), ranging from 1 to 5 mg/L, in order to resemble more realistic surface water and wastewater treatment conditions.

All water matrices were spiked with an initial bacterial concentration of $6-8 \times 10^4$ CFU/mL and treated by fabric A. The inactivation kinetics measured in the different water matrices are displayed in **Figure 6**.

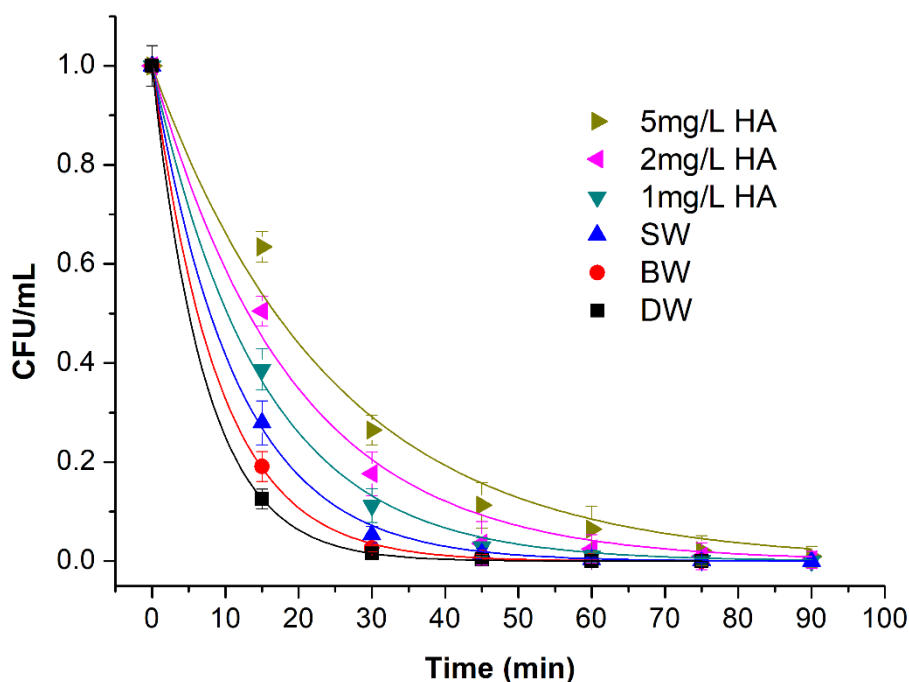


Figure 6. Kinetics of photocatalytic bacterial degradation in different water matrices.

A first order inactivation kinetics was also observed in all the water matrices under investigation, with the rate constants reported in Table 3. The kinetics of bacterial degradation is slightly reduced in BW with respect to that observed in DW. Upon addition of 0.8% of NaCl in DW, bacterial inactivation becomes slower. This may be due to the fact that bacteria are suspended in an aqueous medium with physiologic osmolarity, where they can better survive by the activation of reparatory mechanisms against the UV-induced photocatalytic degradation. Interestingly, the inactivation kinetics becomes progressively slower when *E. coli* are incubated in an aqueous medium contaminated with increasing concentration of humic acids.

3.4 Photoreactivation experiments

In order to evaluate the efficacy of UV treatment, experiments of bacterial photoreactivation were carried out on previously decontaminated aqueous matrices. The results, reported in **Table 4**, show that the reactivation of *E. Coli* is absent after 3 and 24 hours of exposure to natural light and dark condition in all matrices, except for those containing humic acid. In the case of the aqueous matrix, with a concentration of humic acid equal to 2 mg/L, the bacteria have the ability to repair their DNA, both in presence and in the absence of light after 24 h, with a value of CFU/mL lower than 100. For concentrations of humic acid of 5 mg/L, the colonies of *E. Coli* are inferior to 100 CFU/mL, after 3 h, while they increase up to a range between 100-150 CFU/mL after 24 h, in both the tested conditions. These values are indicative of the fact that the presence of humic acid in the

aqueous matrix does not allow a definitive inactivation of *E. Coli* and at the same time could provide nutrients for bacterial proliferation.

Ultimately, these results show that the UV exposure conditions used, cause irreversible biological effects on the bacteria that are no more able to repair the induced damages by the photoreactivation and dark repair mechanisms.

Table 4. *E. coli* photoreactivation experiments, under natural light and dark conditions, in UV inactivated waters

Fabric A Experiments	E. Coli initial concentration (CFU/mL)	UV treatment time for total inactivation of E. Coli (CFU/mL)	E. Coli survival after 3h of photoreactivation (CFU/mL)		E. Coli survival after 24h of photoreactivation (CFU/mL)	
			LIGHT	DARK	LIGHT	DARK
<i>Distilled water</i>	10 ³	60 min	0	0	0	0
	10 ⁴	60 min	0	0	0	0
	10 ⁸	90 min	0	0	0	0
<i>Bottled water</i>	10 ⁴	75 min	0	0	0	0
<i>Salt water</i>	10 ⁴	90 min	0	0	0	0
<i>1 mg/L HA</i>	10 ⁴	90 min	0	0	0	0
<i>2 mg/L HA</i>	10 ⁴	120 min	0	0	<100	<100
<i>5 mg/L HA</i>	10 ⁴	120 min	<100	<100	100-150	100-150

3.5 Reuse of plasma coated SB fabric

The recycling and/or re-use of photocatalytic material reduces the operating costs and the environmental impact. Therefore, reusability studies are important for assessing the potential of large-scale applications of the developed technology.

A simple regeneration process was carried out by washing the surface of the plasma TiO₂-coated SB fabrics with ultrapure water and drying it at a temperature of 90°C for 60 min before any subsequent tests. The photocatalytic effect of the regenerated fabric has been evaluated under the same experimental conditions used in the DW experiments described above. The experimental results are shown in **Figure 7**, where it can be observed that the regenerated fabric shows

satisfactory reusability, since its bacterial inactivation capacity is very close to that of the original fabric, also after the second regeneration process and the following third use.

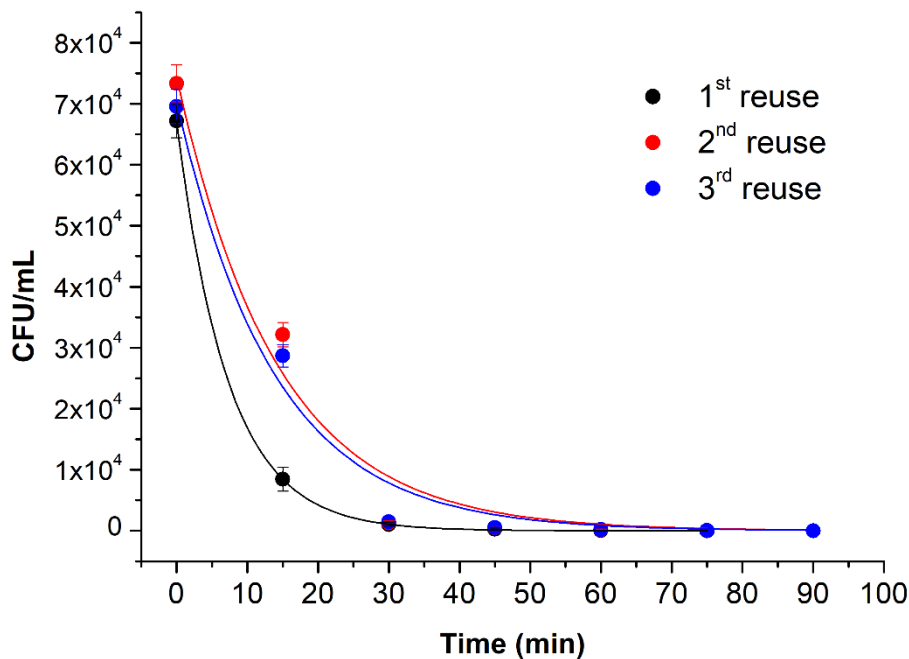


Figure 7. Bacterial degradation experiments for reuse purposes.

The only difference is found in the first few minutes of treatment, in which the bacterial inactivation performed by the reused fabrics is slower (the k goes from 0.138 for the first use, to 0.07 s^{-1} for the second and third (**Table 5**)). Nevertheless, complete inactivation of the bacteria still occurs within 90 min of treatment.

Table 5. First order kinetic rate constant of the photocatalytic bactericidal activity of TiO_2 -coated fabrics for reusability experiments.

Experiment	N_0 (CFU/mL)	k (s^{-1})	R^2
1 st use	67170 (71)	0.138 (5,467E-4)	0.999
2 nd reuse	74513 (4619)	0.07 (0,009)	0.973
3 rd reuse	70469 (3806)	0.07 (0,009)	0.979

The slight loss of the fabric catalytic activity is probably due to the regeneration method. The reduction of the bacterial inactivating capacity is ascribable to the not fully effective regeneration

and washing method, as supported by XPS analyses results performed on SB plasma modified fibers after each regeneration/use cycle. Data of **Table 6** (XPS surface atomic percent of recycled SB plasma modified samples), in fact, show that the atomic percent of titanium and oxygen decrease, while that of carbon increases.

Table 6. XPS atomic percent of plasma coated SB fiber as deposited and after different regeneration/use cycle.

Sample	C at. %	O at. %	Ti at. %
As deposited	33.3	50.5	16.2
After 1 use	48.2	44.4	7.4
After 2 use	52.1	41.3	6.6
After 3 use	59.7	36.9	3.4

This could point out to a potential leaching of the catalyst with use, but, if the elemental high resolution spectra are analyzed (**Figure 8**), it is evident that Ti chemical environment do not change with use, since the overall shape, main peak position ($Ti2p_{3/2}$) and $Ti2p_{1/2} - Ti2p_{3/2}$ splitting stay the same. Thus, it can confirm that the catalyst is stable over time.

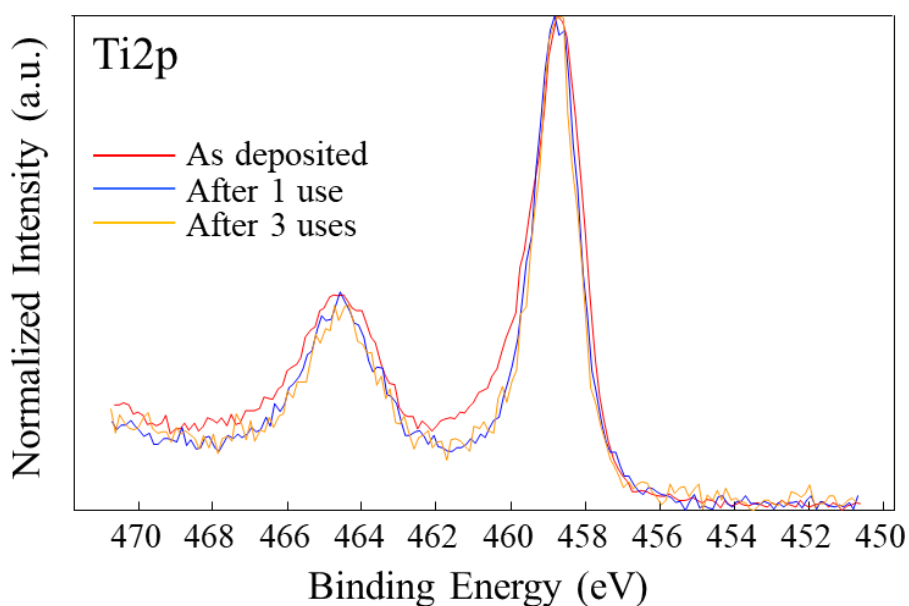


Figure 8: $Ti2p$ XPS high resolution spectra acquired after SB plasma modified fiber use.

This hypothesis was supported also by C1s spectrum analysis, which reveals some changes in the carbon chemical environment (**Figure 9**): the C1s spectrum of the as deposited sample A resembles that of untreated SB fabric. After the use, on the contrary, the spectra show that the relative contribution between 286 and 287 eV increase, likely due to the uptake from the solution environment used for testing. Therefore, it can be asserted that the decrease in titanium atomic percent is not due to a dissolution of the catalyst, but rather to a carbon uptake from the environment.

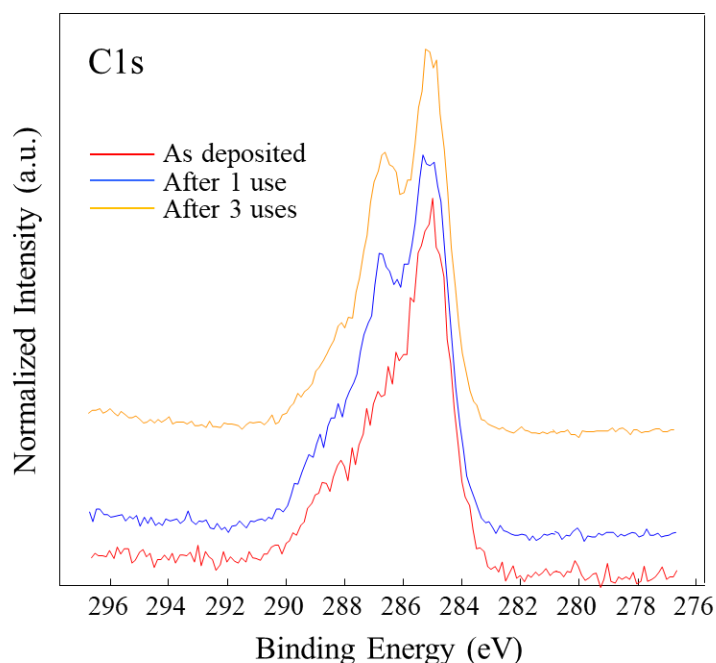


Figure 9. C1s spectra of as deposited and after recycle sample A.

Further catalyst regeneration tests could be carried out, varying the method, the solvent and the duration of the washing in order to improve the recycle protocol, totally preserving the catalytic activity of the as deposited plasma TiO₂ covered SB fabric.

4. CONCLUSION

This work reports the first application of TiO₂ plasma coated biobased fabric, obtained from Spanish broom cellulose fibers, to disinfect water from *E. coli* bacteria.

The functionalized cellulose fabric exhibited very good disinfection capacity for concentration of *E. coli* from 10³ to 10⁸ CFU/mL in water. Bacteria have been inactivated after 60-75 min of treatment time under UV-LED irradiation. First order inactivation kinetics were observed in all of the water matrices considered. The rate constant obtained with fabric A is more than one order of magnitude

larger than that obtained after photolytic treatment. It has been also observed that the photocatalysts are stable after several reuse cycles and can be easily regenerated by a simple and fast washing process which allows to maintain a disinfection capacity very close to the initial one.

In conclusion, the results obtained from this study indicate the potential disinfectant capacity of this material. The technology could be applicable on a large scale, due to the high availability of cellulose from Spanish broom plants and the low-cost scalable process of functionalization.

Moreover, unlike conventional methods of bacterial disinfection, the proposed application has the advantage of the absence of by-products during its use and the ability to perform catalytic activity through the application of lower-energy UV wavelengths.

Conflicts of interest

There are no conflicts to declare

Acknowledgements

This research was also financially supported by Regione Puglia under grant no. 51 “Laboratorio pubblico di ricerca industrial dei plasm, LIPP”, within the Framework Programme Agreement APQ “Ricerca Scientifica”, II atto integrativo - Reti di Laboratori Pubblici di Ricerca and by PON “R&C” 2007-2013 - Avviso n.254/Ric del 18 maggio 2011 PONa3_00369 “Laboratorio per lo Sviluppo Integrato delle Scienze e delle TECnologie dei Materiali Avanzati e per dispositivi innovativi (SISTEMA).

References

- 1 WHO, *Progress on Drinking Water and Sanitation*, World Health Organization and Unicef, Switzerland, 2014. ISBN 978 92 4 150724 0.
- 2 C. Regmi, B. Joshi, S. K. Ray, G. Gyawali and R. P. Pandey, Understanding Mechanism of Photocatalytic Microbial Decontamination of Environmental Wastewater, *Front. Chem.*, 2018, 6, 33.
- 3 M. N. Chong, B. Jin, H. Zhu and C. Saint, Bacterial inactivation kinetics, regrowth and synergistic competition in a photocatalytic disinfection system using anatase titanate nanofiber catalyst. *J.Photochem. and Photobio. A: Chem.*, 2010, 214, 1–9.
- 4 A. R. Rahmani, A. J. Jafari and A. H. Mahvi, Investigation of water disinfection by electrocd, *Pakistan of Biol. Sci.*, 2005, 8, 910- 913.
- 5 R. T. Bisneto and E. Bidoia, Effects of the electrolytic treatment on bacillus subtilis, *Brazilian J. Microbiol.*, 2003, 34, 48-50.

- 6 K.Y. Nelson, D. W. McMartin, C. K. Yost, K. J. Runtz and T. Ono, Point-of-use water disinfection using UV light-emitting diodes to reduce bacterial contamination, *Environ. Sci. Pollut. Res. Int.*, 2013, 20, 5441-5448.
- 7 P.O. Nyangaresi, Y. Qin, G. Chen, B. Zhang, Y. Lu and L. Shen, Effects of single and combined UV-LEDs on inactivation and subsequent reactivation of *E. coli* in water disinfection, *Water Res.*, 2018, 147, 331-341.
- 8 A. Hamamoto, M. Mori, A. Takahashi, M. Nakano, N. Wakikawa, M. Akutagawa, T. Ikehara, Y. Nakaya and Y. Kinouchi, New water disinfection system using UVA light-emitting diodes, *J. Appl. Microbiol.*, 2007, 103, 2291-2298.
- 9 P. Xiong and J. Y. Hu, Inactivation/reactivation of antibiotic-resistant bacteria by a novel UVA/LED/TiO₂ system, *Water Res.*, 2013, 47, 4547-4555.
- 10 S. Anandan, Y. Ikuma and K. Niwa, An Overview of Semi-Conductor Photocatalysis: Modification of TiO₂ Nanomaterials, *Solid State Phenom.*, 2010, 162, 239-260.
- 11 D. S. Bhatkhande, V. G. Pangarkar and A. C. M. Beenackers. Photocatalytic degradation for environmental applications – a review, *J. Chem. Technol. Biotechnol.*, 2001, **77**, 102-116.
- 12 T. V. Nguyen and J. C. S. Wu, Photoreduction of CO₂ in an optical-fiber photoreactor: Effects of metals addition and catalyst carrier, *Appl. Catalysis A: General.*, 2008, **335**, 112–120.
- 13 M. Janus, A. Markowska-Szczupak, E. Kusiak-Nejman and A. W. Morawski, Disinfection of *E. coli* by carbon modified TiO₂ photocatalysts, *Environ. Prot. Eng.*, 2012, **38**, 89–97.
- 14 P. Wu, R. Xie, K. Imlay and J. K. Shang, Visible-Light-Induced bactericidal activity of titanium Dioxide codoped with Nitrogen and Silver, *Environ. Sci. Technol.*, 2010, **44**, 6992-6997.
- 15 W. C. Oh, A. R. Jung and W. B. Ko, Characterization and relative photonic efficiencies of ZnO-coated multi-walled carbon nanotubes, *Mater. sci. eng.*, 2009, **29**, 1338-1347.
- 16 V. Krishna, S. Pumprueg, S. H. Lee, J. Zhao, W. Sigmund, B. Koopman and B. M. Moudgil, *Trans. IChemE, Proc. safety environ. prot.*, 2005, **83**, 393.
- 17 O. Akhavan, M. Abdolahad, Y. Abdi and S. Mohajerzadeh, Synthesis of titania/carbon nanotube heterojunction arrays for photoinactivation of *E. coli* in visible light irradiation, *Carbon*, 2009, **47**, 3280- 3287.
- 18 G. Dagan and M. Tomkiewicz, TiO₂ aerogels for photocatalytic decontamination of aquatic environments, *J. Phys. Chem.*, 1993, **97**, 12651-12655.
- 19 D. Sethi, N. Jada, A. Tiwari, S. Ramasamy, T. Dash and S. Pandey, Photocatalytic destruction of *Escherichia coli* in water by V₂O₅/TiO₂, *J. Photochem. Photobiol. B*, 2015, **144**, 68–74.

- 20 B. Gabriele, T. Cerchiara, G. Salerno, G. Chidichimo, M. V. Vetere, C. Alampi, M. C. Gallucci, C. Conidi and A. Cassano, A new physicochemical process for the efficient production of cellulose fibers from Spanish broom (*Spartium junceum* L.), *Bioresour. Technol.*, 2010, **101**, 724-729.
- 21 F. Arias, A. Beneduci, F. Chidichimo, E. Furia and S. Straface, Study of the adsorption of mercury (II) on lignocellulosic materials under static and dynamic conditions, *Chemosphere*, 2017, **180**, 11-23.
- 22 A. Tursi, A. Beneduci, F. Chidichimo, N. De Vietro and G. Chidichimo, Remediation of hydrocarbons polluted water by hydrophobic functionalized cellulose, *Chemosphere*, 2018, **201**, 530-539.
- 23 A. Tursi, E. Chatzisyneon, F. Chidichimo, A. Beneduci and G. Chidichimo, Removal of Endocrine Disrupting Chemicals from Water: Adsorption of Bisphenol-A by Biobased Hydrophobic Functionalized Cellulose, *Int J. Environ. Res. Public Health*, 2018, **15**, 2419.
- 24 N. De Vietro, L. Belforte, V. G. Lambertini, F. Fracassi, Low pressure plasma modified polycarbonate: A transparent, low reflective and scratch resistant material for automotive applications, *Appl. Surf. Sci.*, 2014, **307**, 698-703.
- 25 L. D'Accolti, N. De Vietro, F. Fanelli, C. Fusco, A. Nacci and F. Fracassi, Heterogenization of Ketone Catalyst for Epoxidation by Low Pressure Plasma Fluorination of Silica Gel Supports, *Molecules*, 2017, **22**, 1-14.
- 26 N. De Vietro, C. Annese, L. D'Accolti, F. Fanelli, C. Fusco and F. Fracassi, A new synthetic approach to oxidation organocatalysts supported on Merrifield resin using plasma-enhanced chemical vapor deposition, *Appl. Catal. A*, 2014, **470**, 132– 139.
- 27 N. De Vietro, R. d'Agostino and F. Fracassi, Introduction of basic functionalities on the surface of granular adsorbents by low pressure plasma processes, *Plasma Process. Polym.*, 2012, **9**, 911-918.
- 28 N. De Vietro, R. d'Agostino and F. Fracassi, Improvement of the adsorption properties of carbon black granules by means of plasma enhanced-chemical vapour deposition with acrylic acid vapours, *Carbon*, 2011, **49**, 249-255.
- 29 N. De Vietro, in *Carbon black: production, properties and uses*, ed. I. J. Sanders and T. L. Peeten, Nova Science Publishers, USA, 2011, 10, 237-262.
- 30 N. De Vietro, A. Conte, A.L. Incoronato, M.A. Del Nobile and F. Fracassi, Aerosol-assisted low pressure plasma deposition of antimicrobial hybrid organic-inorganic Cu-composite thin films for food packaging applications. *Innov. Food Sci. Emerg. Technol.*, 2017, **41**, 130–134.

- 31 F. Fanelli, A. M. Mastrangelo, N. De Vietro and F. Fracassi, Preparation of multifunctional superhydrophobic nanocomposite coatings by aerosol-assisted atmospheric cold plasma deposition, *Nanosci. Nanotechnol. Lett.*, 2015, **7**, 84-88.
- 32 G. Beamson and D. Briggs, High Resolution XPS of Organic Polymers: The Scienta ESCA300 Database, *J. Chem. Educ.*, 1993, **70**, A25.
- 33 E. Chatzisyneon, A. Droumpali, D. Mantzavinos and D. Venieri, Disinfection of water and wastewater by UV-A and UV-C irradiation: Application of real-time PCR method, *Photoch. Photobio. Sci.*, 2011, **10**, 389-95.
- 34 E. Chatzisyneon, Inactivation of bacteria in seafood processing water by means of UV treatment, *J. Food Eng.*, 2016, **173**, 1-7.
- 35 C. D. Wagner, W. M. Riggs, L. E. Davis, J. F. Moulder and G. E. Muilenberg, *Handbook of X-Ray Photoelectron Spectroscopy*, Perkin-Elmer Corporation, Minnesota, 1979.
- 36 M. C. Biesinger, L. W. M. Lau, A. R. Gerson, R. S. C. Smart, Resolving surface chemical states in XPS analysis of first row transition metals, oxides and hydroxides: Sc, Ti, V, Cu and Zn, *Appl. Surf. Sci.*, 2010, **257**, 887-898.

CONCLUSIONS

The experimental results obtained in the various researches, carried out in the frame of this thesis work, leads to conclusion that are summarized below for each pollutant of the water taken into consideration:

1. Total Petroleum Hydrocarbons (TPHs)

The **4,4'-MDI functionalized cellulose** exhibits notable adsorption properties for total petroleum hydrocarbons. Indeed, adsorption kinetics is fast and the pollutant can be removed with efficiencies larger than 90% in times of the order of 10 min, for fibers/pollutants weight ratio as low as 0.01, in samples having the volume of about 1 L. To be more clear, let us say that 0.5 kg of fibers could be sufficient to remove 100 ppm of pollutants from a ton of water in times of the order of some minute.

On the other hand, the **low pressure plasma functionalized cellulose** with fluorine groups are candidate to be very effective materials to remove hydrocarbons from polluted water. Their adsorption capacity is one of the highest ever reported in the literature. The fluorine grafting improves the hydrophobicity of the vegetables fibers in such a way that their water contact angle results to be higher than 160. As a consequence, the maximum adsorption capacity of the grafted fibers for hydrocarbons is equal to 0.273 g/g: a value which is almost thirty percent higher than that observed for analogous vegetable fibers functionalized with 4,4'-MDI.

2. Bisphenol-A

4,4'-MDI functionalized cellulose are able to remove BPA from water. It was found that pH significantly affects adsorption capacity with the highest adsorption rates being observed at pH 5. The functionalized cellulose fiber exhibited very good adsorption properties for BPA with 70% of the pollutant being adsorbed after 5 min of treatment time. It was observed that the adsorbent system can be easily regenerated by a simple and fast washing process which allows to recover its adsorption capacity by almost 100% of the original one.

3. Mercury

SB cellulose fiber (CF) showed a considerable adsorption capacity for Hg (II) heavy metal. Since it has been found that the adsorption capacity of the non-functionalized cellulose fiber to mercury is close to 74% of removal, for an aqueous system with an initial concentration of 70-100 mg/L of Hg (II), with a maximum adsorption capacity of 7.25 mg/g. The adsorption capacity of fluorinated SB fibers (**low pressure plasma functionalized cellulose LP-CF**) has been also studied to ascertain the chelation efficiency of fluorine groups with respect to this metal. However, this hypothesis was not found realistic, since the adsorption capacity of **LP-CF** is almost 29%.

4. Escherichia coli

TiO₂ coated cellulose fabric have been found very effective to remediate E. coli O157:H7 polluted water. Disinfection capacity for concentration of E. coli from 10³ to 10⁸ CFU/mL in water was very good. Bacteria have been inactivated after 60-75 min of treatment time with UV-LEDs lamp. First order inactivation kinetics was observed in all of the water matrices considered. The rate constant obtained with fabric A is more than one order of magnitude larger than that relative to the UV exposure experiment without photocatalyst. Moreover, it has been observed that the system is stable after several reuse cycles and can be easily regenerated by a simple and fast washing process which allows to maintain a disinfection capacity very close to the capacity obtained with the first use.

From the evaluation of these experimental results, it can be said that the researches carried out and reported in this thesis work open a considerable possibility for practical application of these low cost biobased materials in water remediation processes.